Biomolecules in a structured solvent

A novel formulation of nonlocal electrostatics and its numerical solution

Dissertation zur Erlangung des Grades des Doktors der Naturwissenschaften der Naturwissenschaftlich–Technischen Fakultäten der Universität des Saarlandes

vorgelegt von

Dipl. Inform. Andreas Hildebrandt

Saarbrücken im Februar 2005

Abstract

The accurate modeling of the dielectric properties of water is crucial for many applications in physics, computational chemistry, and molecular biology. In principle this becomes possible in the framework of nonlocal electrostatics, but since the complexity of the underlying equations seemed overwhelming, the approach was considered unfeasible for biomolecular purposes. In this work, we propose a novel formulation of nonlocal electrostatics which for the first time allows for numerical solutions for the nontrivial molecular geometries arising in the applications mentioned before. The approach is illustrated by its application to simple geometries, and its usefulness for the computation of solvation free energies is demonstrated for the case of monoatomic ions. In order to extend the applicability of nonlocal electrostatics to nontrivial systems like large biomolecules, a boundary element method for its numerical solution is developed and implemented. The resulting solver is then used to predict the free energies of solvation of polyatomic molecules with high accuracy. Finally, the nonlocal electrostatic potential of the protein trypsin is computed and interpreted qualitatively.

German Abstract

Die präzise Modellierung der dielektrischen Eigenschaften des Wassers ist für viele Anwendungen in Physik, Computational Chemistry und Molekularbiologie von entscheidender Bedeutung. Theoretisch ist eine solche Modellierung im Rahmen der sogenannten nichtlokalen Elektrostatik möglich, doch da die dabei auftretenden Gleichungssysteme bislang als beinahe unlösbar schwierig galten, schien dieser Zugang für biomolekulare Problemstellungen ungeeignet. In dieser Arbeit präsentieren wir eine neuartige Formulierung der nichtlokalen Elektrostatik, die zum ersten Mal die Entwicklung numerischer Methoden erlaubt, die auf die nichttrivialen molekularen Geometrien, wie sie in den oben genannten Forschungsgebieten auftreten, anwendbar sind. Wir demonstrieren unseren Zugang zunächst durch die Anwendung auf einfache Modellgeometrien und zeigen seine Nützlichkeit für die Berechnung freier Solvatationsenergien einatomiger Ionen. Um die Anwendbarkeit der nichtlokalen Elektrostatik auf nichttriviale Systeme, wie z.B. große Biomoleküle zu erweitern, wird eine Randelementmethode zur numerischen Lösung der präsentierten Gleichungen entwickelt und implementiert. Der resultierende Randelementlöser wird daraufhin zur genauen Vorhersage der freien Solvatationsenergien kleiner Moleküle verwendet. Schließlich wird das nichtlokale elektrostatische Potential des Proteins Trypsin berechnet und qualitativ interpretiert.

German Summary

Unter allen in der Natur auftretenden Wechselwirkungen spielt die Elektrodynamik eine besonders wichtige Rolle. Sie bewirkt nicht nur viele der makroskopischen Phänomene, die uns im täglichen Leben begegnen, sondern ist auch für einen großen Anteil des Verhaltens atomarer oder molekularer Systeme verantwortlich. Aus Sicht der Bioinformatik ist letzteres von größter Wichtigkeit: ein quantitatives Verständnis biologischer Prozesse auf der molekularen Ebene würde unser Wissen über die fundamentalen Prinzipien des Lebens stark erweitern und einen wichtigen Schritt in Richtung der rationalen Entwicklung medizinischer Therapien darstellen. Auf diese Weise könnte der Wirkstoffentwurfsprozess nicht nur erheblich beschleunigt und verbilligt, sondern auch die Entwicklung weit wirksamerer Medikamente ermöglicht werden.

Da das Verhalten molekularer Systeme letztendlich durch die in ihnen auftretenden Wechselwirkungen bestimmt ist, ist eine akkurate und verlässliche Vorhersage der zugehörigen Energetik eine unvermeidliche Vorbedingung für die oben angesprochenen Ziele. Die Fortschritte in der modernen theoretischen Physik und Chemie mögen zwar den Anschein erwecken, dass dies schon heute zur Zufriedenheit möglich wäre – mit Hilfe der Gesetze der Quantenmechanik sollten sich alle benötigten Größen hochpräzise bestimmen lassen, in der Realität ist der benötigte Rechenaufwand für die meisten interessanten Anwendungen heutzutage jedoch noch viel zu hoch. Daraus erklärt sich der große Bedarf nach approximativen aber dennoch akkuraten Theorien der zwischen Biomolekülen auftretenden Wechselwirkungen. Auf *makroskopischer* Ebene ist dies für die Elektrostatik in Form der sogenannten makroskopischen Maxwell-Gleichungen gelungen. Doch auf Systeme auf *mikroskopischer* Ebene lassen sich diese leider nicht ohne Genauigkeitsverluste anwenden [Sim01]. Im Falle biomolekularer Systeme lassen sich die hierbei auftretenden Probleme in erster Linie auf einen einzigen Faktor zurückführen: den Einfluss des beinahe immer vorhandenen umgebenden Wassers. Dieses ist aufgrund seiner hohen Polarität in der Lage, die elektrostatischen Felder und Potentiale im Vergleich zum Vakuumfall auf drastische Weise zu verändern.

Leider ist es andererseits für die meisten Anwendungen auch unmöglich, das ein Biomolekül umgebende Wasser explizit zu modellieren – schon in unmittelbarer Umgebung des Proteins befinden sich dafür viel zu viele Wassermoleküle. Daher basieren heutzutage beinahe alle Elektrostatikberechnungen für biomolekulare Systeme auf sogenannten *Kontinuumsnäherungen* wie zum Beispiel den oben angeführten makroskopischen Maxwell-Gleichungen. In diesen wird der Einfluss des Wassers auf das System als makroskopischer Effekt beschrieben, der über die individuellen Beiträge einzelner Wassermoleküle gemittelt wird. In seiner einfachsten Form vernachlässigt dieser Mittelungsprozess jegliche Korrelationen oder Wechselwirkungen zwischen den beteiligten Wassermolekülen. Genau diese Näherung bricht zusammen, sobald Systeme auf atomaren Skalen betrachtet werden: Wassermoleküle sind in realen Systemen aufgrund des hochdynamischen Wasserstoffbrückennetzwerks stark miteinander korreliert.

Im Prinzip existiert seit etwa 1970 ein theoretischer Rahmen, der die Integration solcher struktureller Effekte in die Elektrostatik ermöglicht: Rezav Dogonadze's *nichtlokale Elektrostatik*, die von Alexei Kornyshev, Mikhail Vorotyntsev und anderen weiterentwickelt wurde. In der klassischen Formulierung der nichtlokalen Elektrostatik werden dabei die partiellen Differentialgleichungen der lokalen Elektrostatik durch partielle integro–Differentialgleichungen ersetzt, in denen eine Volumenintegration über

den kompletten Außenraum durchgeführt werden muss. Doch obwohl die nichtlokale Elektrostatik für geometrisch triviale Systeme wie zum Beispiel sphärische Ionen beachtliche Erfolge erzielen konnte, schien die Anwendung auf große Systeme mit komplizierter Geometrie, wie zum Beispiel auf Biomoleküle, bislang aufgrund der hohen Komplexität der Gleichungen unmöglich.

In dieser Arbeit präsentieren wir eine neuartige, vollständig differentielle Formulierung der nichtlokalen Elektrostatik, die auf viele Modelle der Wasser–Wasser Korrelation anwendbar ist. Die daraus resultierenden Gleichungen haben im wesentlichen den selben Komplexitätsgrad wie diejenigen der klassischen lokalen Elektrostatik. Um die allgemeinen Eigenschaften der nichtlokalen Theorie genauer zu untersuchen, haben wir zunächst analytische Lösungen für geometrisch handhabbare Situationen entwickelt, die es uns erlauben, die freie Solvatationsenergie einatomiger Ionen zu bestimmen. Vergleicht man die berechneten Werte mit experimentellen Daten, so zeigt sich eine hervorragende Übereinstimmung, die die Entwicklung eines effizienten und genauen numerischen Lösungsverfahrens motiviert. Dabei entschieden wir uns für eine Randelementmethode, die zwar nur unter hohem analytischen Aufwand entwickelt werden kann, dafür jedoch große Verlässlichkeit und gute Laufzeiteigenschaften aufweist. Diese Arbeit mündete in der Erstellung eines Randelementlösers der Gleichungen der nichtlokalen Elektrostatik unter Verwendung des sogenannten Lorentz-Modells für die Wasser–Wasser–Korrelation, der es uns zum ersten Mal ermöglicht, diese Theorie auf komplexe Systeme wie kleine Moleküle und sogar Proteine anzuwenden.

Der erstellte Löser wurde daraufhin ausführlich gegen analytische Resultate für einfache Geometrien getestet und erwies sich als hochpräzise. Daher war es uns möglich, das nichtlokale elektrostatische Potential und die freie Solvatationsenergie einiger kleiner sowohl geladener als auch neutraler Moleküle zu bestimmen, und auch diese Ergebnisse mit experimentellen Daten zu vergleichen. Dies ist unseres Wissens nach die erste Anwendung der nichtlokalen Theorie auf solch komplizierte Systeme, und die Resultate sind in der Tat sehr vielversprechend: die berechneten Werte der freien Solvatationsenergie sind von sehr hoher Qualität. Für mögliche biologische Anwendungen jedoch muss zunächst die Anwendbarkeit auf große Systeme – in erster Linie auf Proteine – sichergestellt werden. Diese bringt jedoch ganz eigene Schwierigkeiten für die Numerik mit sich, die sich hauptsächlich aus den extremen Speicheranforderungen der aktuellen Implementierung ergeben[1]. Um dennoch schon heute in der Lage zu sein, unsere Theorie anhand eines Beispielproteins zu testen und ihre prinzipielle Anwendbarkeit auf Systeme dieser Größe zu beweisen, entschieden wir uns dafür, die Eingabedaten – eine Triangulierung der Oberfläche des Moleküls, in unserem Fall des Proteins Trypsin – von Hand so aufzubereiten, dass eine vergleichsweise kleine Eingabegröße ermöglicht werden kann. Leider existiert für eine solche Berechnung keine einfache Vergleichsmöglichkeit mit experimentellen Daten – eine solche werden wir in der Zukunft mit Hilfe von pK_a–Berechnungen schaffen – doch die resultierenden Potentiale lassen sich qualitativ interpretieren und ermöglichen so neue Einblicke in die Natur des nichtlokalen Effektes. Wie erwartet zeigt sich dabei in erster Linie eine im Vergleich zum lokalen Fall deutlich erhöhte elektrostatische Sichtbarkeit des Enzyms, die den Prozess der molekularen Erkennung deutlich vereinfachen könnte: das Potential reicht erheblich weiter in den Raum um das Protein hinein, als dies in der lokalen Näherung der Fall ist. Unter der Annahme, dass sich dieser Effekt in zukünftigen Studien bestätigt, glauben wir, so zeigen zu können, dass die nichtlokale Elektrostatik zum tieferen Verständnis einiger Aspekte der molekularen Erkennung, die bislang nicht zur Zufriedenheit erklärt werden können, beitragen kann.

---

1 Diese werden in einer zukünftigen Implementierung mit Hilfe eines Approximationsverfahrens drastisch verringert werden.

Danksagung

German Summary

x

Contents

Contents

Contents

4

1. Introduction

Among all interactions we encounter in nature, electrodynamics plays a particularly important role. Not only does it account for many of the macroscopic phenomena we experience every day, but it also governs much of the behaviour of systems at a molecular or atomic level. From a bioinformatics perspective, the latter is of the utmost importance: a quantitative understanding of biological processes at the molecular level would greatly influence our knowledge about the fundamental principles of life, and would provide an important step to the development of rational medical therapies. Being able to accurately predict biochemical interactions, we might for example study the binding of disease–related proteins like viral enzymes, to their targets, thus gaining insight into the mechanisms of the particular illness. In this way, we would achieve an important step toward a rational computer–aided drug design process, where the binding strength of the complex between a drug target and a potential inhibitor can be accurately assessed without the need for time–consuming and expensive experiments. Such a first–principles approach would not only have the potential to reduce the amount of time and money needed for the development process, but should also allow the design of much more potent drugs than those currently known.

Since the behaviour of biomolecular systems is in the end determined by their interactions, an accurate and reliable prediction of their energetics is an inevitable prerequisite to the goals mentioned above. But while it might seem that the advances in modern theoretical physics and chemistry already provide the solution to this problem – a full–scale application of the laws of quantum mechanics should allow us to compute the required quantities with the needed accuracy – the involved computational complexity currently forbids their application to most of the systems of interest. There is thus a high demand for an approximate, but nonetheless accurate, theoretical description of the interactions of biomolecules. But while such a theory has been found for *macroscopic* systems in the form of the so–called macroscopic Maxwell equations, the same can not be said for systems on a microscopic scale: the macroscopic formulation has been shown to become inaccurate when looking at properties at the atomic scale [Sim01]. The failure of methods known to work well for large–scale problems can be attributed mostly to one important factor: the inevitable presence of solvent water in all biomolecular systems of interest. It is well–known that the presence of water dramatically changes the magnitude of electrostatic fields and potentials when compared to the vacuum case, an effect that is due to water's highly polar nature.

Since the number of water molecules immediately surrounding the biomolecules of interest is typically forbiddingly large, an explicit representation of each individual water molecule is often infeasible. This is why most approaches to electrostatics calculations in an aqueous environment are based on so–called *continuum approximations* – the macroscopic Maxwell theory mentioned above – where the influence of solvent water on the field is represented as a macroscopic effect, averaged over the contributions of many individual water molecules. In its most simple form, this averaging process completely neglects correlations or interactions among the water molecules themselves. It is this approximation that breaks down when looking at systems at atomic detail: water molecules are strongly correlated through a highly dynamic hydrogen bonding network, responsible for many of water's properties.

In principle at least, a theoretical framework for the inclusion of these structural effects of the solvent is available since the 1970's in the form of Rezav Dogonadze's *nonlocal electrostatics* which was further developed by Alexei Kornyshev, Mikhail Vorotyntsev, and others. In its classical formulation, the

partial differential equations of simple local electrostatics are replaced by partial integro–differential equations, where the integration is performed over the complex geometry of the exterior of the solute. But while nonlocal electrostatics has achieved considerable successes in studies of geometrically trivial systems like spherical ions, an application to the large and complicated geometries of biomolecules seemed completely unfeasible due to the inherent complexity of the integro–differential formulation.

In this thesis we present a novel and entirely differential formulation of nonlocal electrostatics for a wide class of models for the water–water correlation, including the most important Lorentzian one. In essence, the resulting set of equations is of very similar complexity than the system of conventional local electrostatics, and in fact it turns out that the problem of its numerical solution lies in the same complexity class than that of the local theory. To investigate the properties of nonlocal electrostatics, we have derived analytical solutions for geometrically feasible situations, most importantly for the electrostatic potential and the free energy of solvation for monoatomic ions. Comparison of the results to experimental data shows excellent agreement, and motivates the development of an efficient and accurate numerical solver. After careful consideration we decided upon a boundary element based approach, which requires a significant amount of extensive analytical manipulations of the equations to be solved, since we expected that the work invested into these computations would pay off in terms of reliability and runtime in the final implementation. This work culminated in a boundary element solver for nonlocal electrostatics using the Lorentzian model, which for the first time allows to apply this theory to geometrically complex real–world problems, like small polyatomic molecules or even proteins. The implementation was thoroughly tested against known analytical results for simple geometries and was found to be highly accurate. We were thus in a position to compute the nonlocal electrostatic potential and the free energy of solvation for a number of polyatomic molecules, both ions and neutrals, and to compare the results to experimental data. To our knowledge, this is the first successful application of the full theory of nonlocal electrostatics to geometrically complex systems, and the results are highly promising: the computed values for the free energy of solvation for these molecules can be considered highly precise. For the purposes of computational biology, though, the ultimate goal would be the application to large biomolecular systems like proteins. This poses severe difficulties for the numerical implementation, mostly due to extreme memory requirements, which will be addressed in a more space–efficient implementation in the near future. To be still able to prove the applicability of the nonlocal theory in our novel formulation to proteins, we chose to carefully process the input data – the triangulation of the molecular surface – for a protein of manageable size, trypsin. In this way, we were able to compute the nonlocal potential of trypsin and compare the results to the local potential[1], yielding interesting insights into the nature of the nonlocal effect. As expected, the most notable feature of the nonlocal electrostatic potential of trypsin is a greatly enhanced visibility, simplifying molecular recognition – the potential extends much farther into space than in the local case. Assuming that this effect will be confirmed by future studies on a variety of proteins, we believe that nonlocal electrostatics might help to shed some light on aspects of molecular recognition that can not be quantitatively understood in the framework of classical local electrostatics.

1.1. Outline of this work

The derivation of the novel formulation of nonlocal electrostatics derived in this work requires considerable familiarity with the conventional local theory, and with the older integro–differential formulation of nonlocal electrostatics. Chapter 2 is thus devoted to an introduction to those concepts of local electrostatics that will become important in our later considerations, and can be skipped by readers already familiar with the field. From this background, Chapter 3 then develops the fundamentals of

---

1 Unfortunately, there is no simple experimental reference data like the free energy of solvation we had for the polyatomic molecules to compare the numerical results to in the case of proteins.

the classical integro–differential formulation of nonlocal electrostatics, describes the process of determining a suitable model for the water–water correlation, and presents a first successful application – the computation of the free energy of solvation of monoatomic ions with very high precision.

Having thus shown the principal ability of the theory to accurately account for electrostatic solvation effects, we derive our central result – the novel and purely differential formulation, suitable for numerical solutions, in Chapter 4. The results presented there allow for the development of a boundary element solver, the fundamentals of which are described in Chapter 5. There, we give a brief introduction into boundary element methods, and derive the necessary set of boundary integral equations and representation formulae for the system of nonlocal cavity electrostatics, providing the necessary mathematical results for a reimplementation of the boundary element solver.

The current implementation of a solver of the boundary integral equations derived in Chapter 5 is then discussed in Chapter 6, and the results of the application to several test cases of small polyatomic molecules and the enzyme trypsin are discussed in detail in Chapter 7.

Finally, the appendices contain brief introductions to some necessary concepts from mathematics and theoretical physics required throughout this work.

1. Introduction

2. Local electrostatics

In this chapter we will give a short introduction into the classical theory of local electrostatics of a charge distribution immersed in a medium. This theory dates back to James Clerk Maxwell [Max64] who was able to describe the seemingly very different phenomena observed for charged bodies together with all aspects of magnetism in a unified framework. This framework is commonly called the *theory of electrodynamics*, which is governed by a set of four equations, the so-called *Maxwell equations*, combined with a set of *material laws*, describing the influence of the medium on the electromagnetic field.

Since most of the material found in this chapter is contained in all classical textbooks and monographs on electrodynamics, the treatment here is deliberately concise, and derivations are only given when they are later needed for the generalization to the nonlocal setting. For a more detailed treatment, the reader is referred to the excellent monographs of Jackson [Jac98] or Landau–Lifshitz [LL87, LL84].

2.1. The electromagnetic field

The central entity in electrodynamics is the electromagnetic field. Its fundamental importance can easily be explained from the following argument: it is well known that charged bodies interact over large distances. While opposite charges attract each other, like charges are repelled. This empirical fact seems to imply a certain *action at a distance*: the charges feel their mutual presence even over large distances and react to it instantaneously. This on the other hand would require an arbitrarily fast transmission of information, which of course conflicts with special relativity from which we have learned that the maximal velocity for any kind of information is bounded from above by the speed of light in vacuum. This problem is elegantly circumvented by the introduction of the electromagnetic field: any charge distribution creates a field everywhere in space, which tells any other charge distribution about its presence. This electromagnetic field propagates with the speed of light, but as soon as it has been established at a certain point in space, any other charge visiting that point can instantaneously react *with the field of the original charge distribution*. Thus, the paradox action at a distance is replaced by a local *action at a point* principle fully compatible with special relativity.

This hand–waving introduction tells us two important things:

1. charges are the sources of the electromagnetic field

2. charges react to electromagnetic fields

Therefore, electrodynamics answers two questions:

1. What does the field of a given charge distribution look like?

2. How does a charge distribution react to a given field?

Conceptually at least, the second question is easy to answer: assume that a charge q is situated at a certain point $r \in \mathbb{R}^3$ in three–dimensional space, and is travelling with the velocity $v \in \mathbb{R}^3$. Let $E(r)$ denote the electric component of the electromagnetic field at position r, and $B(r)$ the magnetic

component. If the charge q is sufficiently small that its presence does not disturb the field (such a charge is called a *test charge*), then it feels a force given by the so-called *Lorentz force law*:

$$\boldsymbol{F}(\boldsymbol{r}) = q\left(\boldsymbol{E}(\boldsymbol{r}) + \boldsymbol{v}(\boldsymbol{r}) \times \boldsymbol{B}(\boldsymbol{r})\right) \tag{2.1}$$

In our case, the magnetic component can be neglected, since we are dealing only with *electrostatic* effects, and equation (2.1) thus simplifies to:

$$\boldsymbol{F}(\boldsymbol{r}) = q\boldsymbol{E}(\boldsymbol{r}) \tag{2.2}$$

Answering the first question, i. e. how to compute the electromagnetic field for a given charge distribution, turns out to be more complicated.

2.2. The Maxwell equations in vacuum

For the important special case of a charge distribution $\rho(\boldsymbol{r})$ and a current distribution $\boldsymbol{j}(\boldsymbol{r})$ immersed in vacuum, this problem was first solved by James Clerk Maxwell in 1864 [Max64], when he discovered the equations of motion of the electromagnetic field. In his original formulation, Maxwell proposed a set of 20 equations in 20 scalar variables, which was significantly simplified and reduced by choosing more convenient vector valued variables. In the classical notation[1], and formulated in the SI system of units[2], the Maxwell equations take the following famous form:

$$\begin{aligned} \boldsymbol{\nabla}\cdot\boldsymbol{E} &= \frac{\rho}{\varepsilon_0} & \boldsymbol{\nabla}\cdot\boldsymbol{B} &= 0 \\ \boldsymbol{\nabla}\times\boldsymbol{E} &= -\frac{\partial\boldsymbol{B}}{\partial t} & \boldsymbol{\nabla}\times\boldsymbol{B} &= \mu_0\boldsymbol{j} + \varepsilon_0\mu_0\frac{\partial\boldsymbol{E}}{\partial t} \end{aligned} \tag{2.3}$$

where $\varepsilon_0 \approx 8.854 \times 10^{-12}$ F/m is the so–called *vacuum permittivity*. In these equations we have made use of the convenient *nabla–operator notation*, where the i–th component of the vectorial operator $\boldsymbol{\nabla}$ (*"nabla"*) is given by the partial derivative with respect to dimension x_i. Thus, in three–dimensional space, $\boldsymbol{\nabla}$ can be written as

$$\boldsymbol{\nabla} := (\partial_x, \partial_y, \partial_z) \tag{2.4}$$

Application of $\boldsymbol{\nabla}$ to a scalar function $\varphi(\boldsymbol{r})$ yields the *gradient* $\boldsymbol{\nabla}\varphi(\boldsymbol{r})$ of $\varphi(\boldsymbol{r})$, the scalar product of $\boldsymbol{\nabla}$ with a vector valued function $\boldsymbol{A}(\boldsymbol{r})$ the *divergence* $\boldsymbol{\nabla}\cdot\boldsymbol{A}(\boldsymbol{r})$ of $\boldsymbol{A}(\boldsymbol{r})$, and the cross product of $\boldsymbol{\nabla}$ with $\boldsymbol{A}(\boldsymbol{r})$ the *curl* $\boldsymbol{\nabla}\times\boldsymbol{A}(\boldsymbol{r})$ of $\boldsymbol{A}(\boldsymbol{r})$.

If the geometry of the system of charges and currents is more delicate than that of euclidean $\mathbb{R}^3$, e.g. if the charge distribution is surrounded by a conducting or insulated sphere, the Maxwell equations have to be supplemented by a set of *boundary* or, to be more precise, *transmission conditions*, from which we can deduce the behaviour of the electromagnetic field on any boundary we impose on our system.

2.2.1. Boundary conditions in vacuum electrostatics

Since we are only concerned with electrostatic situations, i.e. systems in which we can neglect the magnetic contributions, we will only derive suitable boundary conditions for the electric field $\boldsymbol{E}(\boldsymbol{r})$. In

---

[1] In the modern language of differential forms (the Cartan calculus), the Maxwell equations reduce to $dF = 0$ and $d{*}F = j$, where $*$ is the Hodge operator. While this is probably the most elegant formulation of these important equations, the classical notation (formulated in the so-called Ricci calculus) is usually still employed for computational purposes. Therefore, we will use the classical Ricci calculus for all computations in this work

[2] For a discussion of the different systems of units commonly employed in electrostatics today, please refer to Appendix E

this case, equations (2.3) reduce to

$$\boldsymbol{\nabla}\!\cdot\!\boldsymbol{E} = \frac{\rho}{\varepsilon_0} \tag{2.5}$$

$$\boldsymbol{\nabla}\!\times\!\boldsymbol{E} = 0 \tag{2.6}$$

Let us first take a closer look at equation (2.5). Obviously, any sensible charge distribution $\rho(\boldsymbol{r})$ is in $\mathcal{L}^1(\mathbb{R}^n)$, and therefore we can take the integral of (2.5) over an arbitrary volume Ω to yield:

$$\int_\Omega \boldsymbol{\nabla}\!\cdot\!\boldsymbol{E}(\boldsymbol{r})\, d\boldsymbol{r} = \int_\Omega \rho(\boldsymbol{r})\, d\boldsymbol{r} = Q_\Omega \tag{2.7}$$

where Q_Ω denotes the total charge contained inside Ω. To rewrite this equation, we will now make use of the remarkable identity known as *Gauss's law* or as the *divergence theorem*:

Theorem 2.2.1 (Gauss's divergence theorem). *Let $A(\boldsymbol{r})$ be a differentiable vector field, and let Ω be a bounded domain in $\mathbb{R}^n$ with piecewise smooth boundary[3] $\partial\Omega \in \mathcal{C}^{0,1}$. For all $\boldsymbol{r} \in \partial\Omega$, let $\hat{\boldsymbol{n}}(\boldsymbol{r})$ denote the unit outward normal vector of $\partial\Omega$ at position $\boldsymbol{r}$, let $d\Gamma$ denote the infinitesimal surface element of $\partial\Omega$, and let[4] $\gamma_0^{int} : H^s(\Omega) \to H^{s-\frac{1}{2}}(\Gamma)$, $\frac{1}{2} < s \le 1$ denote the internal Dirichlet trace operator*

$$\gamma_0^{int} f(\boldsymbol{r}) := \lim_{\Omega \ni \tilde{\boldsymbol{r}} \to \boldsymbol{r} \in \Gamma} f(\tilde{\boldsymbol{r}}), \quad \boldsymbol{r} \in \Gamma$$

Then,

$$\boxed{\int_\Omega \boldsymbol{\nabla}\!\cdot\!\boldsymbol{A}(\boldsymbol{r})\, d\boldsymbol{r} = \oint_{\partial\Omega} \left(\gamma_0^{int} \boldsymbol{A}\right) \!\cdot\! \hat{\boldsymbol{n}}\, d\Gamma} \tag{2.8}$$

The internal trace operator denotes the restriction of a function that is defined inside the domain to the boundary by taking a continuous path that lies completely inside Ω, and from the fact that it is a mapping from $H^s(\Omega)$ to $H^{s-\frac{1}{2}}(\Gamma)$ we can conclude that by this operation, we lose half a Sobolev index in smoothness. In this chapter, it will usually be clear from context if we talk about a function f in the domain Ω or its restriction $\gamma_0^{int} f$ to Γ, and thus we will drop the explicit mentioning of the trace operator in this chapter. In this shorthand notation, where we use the same sign for the function and its trace, Gauss' theorem (2.8) becomes

$$\int_\Omega \boldsymbol{\nabla}\!\cdot\!\boldsymbol{A}(\boldsymbol{r})\, d\boldsymbol{r} = \oint_{\partial\Omega} \boldsymbol{A}\!\cdot\!\hat{\boldsymbol{n}}\, d\Gamma$$

Applying this shorthand form of equation (2.8) to (2.7), we arrive at

$$\oint_{\partial\Omega} \boldsymbol{E}\!\cdot\!\hat{\boldsymbol{n}}\, d\Gamma = \int_\Omega \rho(\boldsymbol{r})\, d\boldsymbol{r} \tag{2.9}$$

Now assume that the system under consideration contains at least one boundary surface Γ, separating two regions with different electromagnetic properties. Equation (2.9) is valid for any arbitrary Lipshitz domain Ω, and therefore we are free to choose Ω in a way that crosses the boundary Γ, for example a very small cylinder with top and bottom situated at different sides of Γ, oriented such that its axis is parallel to the surface normal at that point (c.f. Fig. 2.1). If we now consider a limiting process

---

3 Intuitively, the space $\mathcal{C}^{0,1}$ contains those hypersurfaces in $\mathbb{R}^{n-1}$, that are smooth except for a finite number of corners and edges, and that have no zero–angle corners. A precise mathematical definition is outside the scope of this work, but it should be noted that this is an astonishingly weak requirement on the properties of the boundary. For a rigorous definition, see Section D.3

4 For a discussion of the *Sobolev spaces H^s*, see Appendix D.
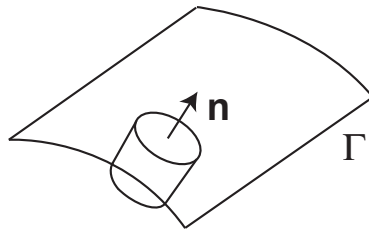
Figure 2.1.: Geometry of the boundary Γ and the domain Ω as described in the derivation of the boundary conditions for the normal components of vectorial quantities.

in which we let the height of the cylinder shrink to zero, it is obvious that the mantle of the cylinder does not contribute to the integrals in equation (2.9). If we chose the radius of the cylinder small enough that $\boldsymbol{E}$ can be considered constant inside the disk at the top and at the bottom respectively, and if we denote by $\boldsymbol{E}_2$ the value of $\boldsymbol{E}$ at the top, by $\boldsymbol{E}_1$ the value at the bottom, and by Δa the area of the disks at top and bottom, we arrive at:

$$\oint_{\partial\Omega} \boldsymbol{E}\cdot\hat{\boldsymbol{n}}\, d\Gamma = (\boldsymbol{E}_2 - \boldsymbol{E}_1)\cdot\hat{\boldsymbol{n}}\, \Delta a \tag{2.10}$$

Now we can consider the right hand side of equation (2.9). Since the volume of integration approaches zero with the height of the cylinder Ω, the integral $\int_\Omega \rho(\boldsymbol{r})\, d\boldsymbol{r}$ can only take on a non–zero value if the charge distribution ρ is singular on the boundary surface Γ, thus producing a *surface charge distribution* σ on Γ. If ρ is well–behaved and continuous on the interface, then $\sigma \equiv 0$. With this definition, the integral on the right hand side of equation (2.9) can be evaluated:

$$\int_\Omega \rho(\boldsymbol{r})\, d\boldsymbol{r} = \sigma\, \Delta a \tag{2.11}$$

Finally, putting equations (2.10) and (2.11) together, we arrive at a boundary condition for the quantity $\boldsymbol{E}$ on Γ:

$$(\boldsymbol{E}_2 - \boldsymbol{E}_1)\cdot\hat{\boldsymbol{n}} = \sigma \tag{2.12}$$

which tells us that the normal component of any vectorial quantity $\boldsymbol{E}$ fulfilling a divergence equation $\boldsymbol{\nabla}\cdot\boldsymbol{E} = \rho$ has a jump across any surface Γ that is equal to the surface charge distribution on that surface. This also means that the normal component is continuous across any surface not carrying surface charges.

Remark 2.2.1. In the derivation of the boundary condition (2.12), we did not make use of the fact that Γ is the boundary between different regions of space. Therefore, this condition is in fact valid everywhere in space, and is therefore often called a *transmission condition* rather than a boundary condition.

In equation (2.12), we have found our first boundary condition for the Maxwell equations in vacuum. A second condition can be derived from the curl equation (2.6). In order to transfer this equation, we will make use of another important theorem from vector analysis, namely Stokes's theorem:[5]

---

[5] In a more precise treatment of this theorem, we would again have to include explicitly a corresponding trace operator for the field $\boldsymbol{A}$, restricting $\boldsymbol{A}$ from the surface S to its boundary ∂S. Since in this chapter, it will be always clear from context if we are talking about the function or its trace, and since we will not need the more explicit form anywhere in this work, we drop the trace operators from the notation.

Theorem 2.2.2 (Stokes's theorem). *Let $\boldsymbol{A}(\boldsymbol{r})$ be a differentiable vector field, let S be a bounded flat two dimensional surface in $\mathbb{R}^3$ with surface element $d\Gamma$, and let ∂S be the contour bounding S with line element $d\boldsymbol{l}$. Let S be oriented by choosing $\hat{\boldsymbol{n}}$ in the direction corresponding to a right–handed screw relating to the sense of integration along ∂S. Then:*

$$\int_S (\boldsymbol{\nabla} \times \boldsymbol{A}) \cdot \hat{\boldsymbol{n}} \, d\Gamma = \oint_{\partial S} \boldsymbol{A} \cdot d\boldsymbol{l} \tag{2.13}$$

Similar to the derivation of the boundary condition for the normal components, let us now consider a rectangular surface S crossing the boundary surface Γ such that its long sides are tangent to the surface in the midpoint of S (c.f. Fig. 2.2). Multiplying the second Maxwell equation (2.6) by $\hat{\boldsymbol{n}}$,
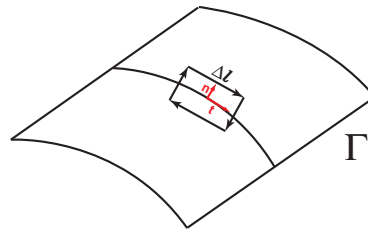
Figure 2.2.: Geometry of the boundary Γ and the surface S as described in the derivation of the boundary conditions for the tangential components of vectorial quantities.

integrating the result over S, and applying equation (2.13), we arrive at

$$0 = \int_S (\boldsymbol{\nabla} \times \boldsymbol{E}) \cdot \hat{\boldsymbol{n}} = \oint_{\partial S} \boldsymbol{E} \cdot d\boldsymbol{l} \tag{2.14}$$

If we let the height of the rectangle S approach zero, only the sides parallel to the surface contribute to the integral on the right hand side of equation (2.14), and therefore we have, if we choose the length Δl of the parallel sides small enough that $\boldsymbol{E}(\boldsymbol{r})$ can be considered constant along $\Delta \boldsymbol{l}$:

$$\oint_{\partial S} \boldsymbol{E} \cdot d\boldsymbol{l} = (\boldsymbol{E}_2 - \boldsymbol{E}_1) \cdot \Delta \boldsymbol{l} \underset{(2.14)}{=} 0 \tag{2.15}$$

Of course, equation (2.15) holds for *any* direction $\Delta \boldsymbol{l}$ in the tangent space of Γ at the point under consideration, and therefore we can conclude:

$$(\boldsymbol{E}_2 - \boldsymbol{E}_1) \times \hat{\boldsymbol{n}} = 0 \tag{2.16}$$

Equation (2.16) tells us that the tangential component of the electric field $\boldsymbol{E}$ is continuous everywhere in space, even across boundaries between different media, and therefore constitutes the second boundary condition for the Maxwell equations.

2.2.2. The electrostatic potential, the Laplace– and Poisson–equation

Equation (2.6) tells us that in the case of electrostatics, the electric field $\boldsymbol{E}(\boldsymbol{r})$ is curl free or *irrotational*. It is a well–known mathematical fact that any irrotational field can be written as the gradient of a

scalar potential field, and therefore we can introduce a new scalar quantity, the so–called *electrostatic potential* $\varphi(\boldsymbol{r})$ with the property

$$\boldsymbol{E}(\boldsymbol{r}) =: -\boldsymbol{\nabla}\varphi(\boldsymbol{r}) \tag{2.17}$$

The meaning of the electrostatic potential can easily be deduced by remembering that in the case of electrostatics, the force on a test charge is given by $\boldsymbol{F}(\boldsymbol{r}) = q\boldsymbol{E}(\boldsymbol{r})$. Inserting equation (2.17), we find that

$$\boldsymbol{F}(\boldsymbol{r}) = -q\boldsymbol{\nabla}\varphi(\boldsymbol{r})$$

Therefore, $q\varphi(\boldsymbol{r})$ can be interpreted as the potential of a test charge of magnitude q in the electrostatic field $\boldsymbol{E}(\boldsymbol{r})$. From this identification, we can directly deduce a necessary boundary condition for φ: clearly, the potential energy on a test charge q should be a continuous quantity, since otherwise the force acting on q when passing through a region of discontinuity would experience infinite forces. This hand–waving motivation can also be made precise by virtue of equation (2.16): consider a point $\boldsymbol{r}^- \in \Omega$ infinitesimally close to the boundary Γ and the corresponding point $\boldsymbol{r}^+ \in \Sigma$ along the surface normal $\hat{\boldsymbol{n}}$ in $\boldsymbol{r} \in \Gamma$. Let $\hat{\boldsymbol{t}}$ be any unit vector in the tangential space on Γ in $\boldsymbol{r}$, and let ϵ be small enough that $\boldsymbol{r}^- + \epsilon\hat{\boldsymbol{t}} \in \Omega$, $\boldsymbol{r}^+ + \epsilon\hat{\boldsymbol{t}} \in \Sigma$, and that both points are again infinitesimally close to the boundary Γ. From equation (2.15), we have

$$\left(\boldsymbol{E}^+ - \boldsymbol{E}^-\right)\cdot\hat{\boldsymbol{t}} = 0$$

and with (2.17), this becomes

$$\left(\boldsymbol{\nabla}\varphi(\boldsymbol{r}^-) - \boldsymbol{\nabla}\varphi(\boldsymbol{r}^+)\right)\cdot\hat{\boldsymbol{t}} = 0 \tag{2.18}$$
$$\Leftrightarrow \boldsymbol{\nabla}\varphi(\boldsymbol{r}^-)\cdot\hat{\boldsymbol{t}} - \boldsymbol{\nabla}\varphi(\boldsymbol{r}^+)\cdot\hat{\boldsymbol{t}} = 0 \tag{2.19}$$
$$\Leftrightarrow \partial_t\varphi(\boldsymbol{r}^-) - \partial_t\varphi(\boldsymbol{r}^+) = 0 \tag{2.20}$$

The directional derivatives ∂_t appearing in this equation can be approximated for sufficiently small ϵ by the finite differences

$$\partial_t\varphi(\boldsymbol{r}^-) = \frac{1}{\epsilon}\left(\varphi(\boldsymbol{r}^-) - \varphi(\boldsymbol{r}^- + \epsilon\hat{\boldsymbol{t}})\right)$$
$$\partial_t\varphi(\boldsymbol{r}^+) = \frac{1}{\epsilon}\left(\varphi(\boldsymbol{r}^+) - \varphi(\boldsymbol{r}^+ + \epsilon\hat{\boldsymbol{t}})\right)$$

Inserting this into equation (2.20), and reordering the terms, we arrive at

$$\left[\varphi(\boldsymbol{r}^-) - \varphi(\boldsymbol{r}^+)\right] = \left[\varphi(\boldsymbol{r}^- + \epsilon\hat{\boldsymbol{t}}) - \varphi(\boldsymbol{r}^+ + \epsilon\hat{\boldsymbol{t}})\right] \tag{2.21}$$

Since this holds for *any* direction $\hat{\boldsymbol{t}}$ in the tangential space in $\boldsymbol{r}$ on Γ, and since we can apply the same argument at the point $\boldsymbol{r} + \epsilon\hat{\boldsymbol{t}}$, we thus have that

$$\varphi(\boldsymbol{r}^-) - \varphi(\boldsymbol{r}^+) = \text{const}$$

on Γ. Freedom of gauge of the electrostatic potential allows us to fix this constant to zero, and we indeed arrive at the *continuity condition*

$$\varphi(\boldsymbol{r}^-) - \varphi(\boldsymbol{r}^+) = 0 \quad \text{on } \Gamma \tag{2.22}$$

Inserting the definition of φ, equation (2.17) into (2.5), we obtain the famous *Poisson equation* for the electrostatic potential φ:

$$\Delta\varphi(\boldsymbol{r}) = -\frac{\rho(\boldsymbol{r})}{\varepsilon_0} \tag{2.23}$$

with the *Laplace operator* Δ:

$$\Delta\varphi = \operatorname{div}(\operatorname{grad}\varphi) \tag{2.24}$$

$$= \boldsymbol{\nabla}\cdot(\boldsymbol{\nabla}\varphi) \tag{2.25}$$

$$= \sum_{i=1}^{3} \partial_{x_i}^2 \varphi(\boldsymbol{r}) \tag{2.26}$$

The Poisson equation (2.23) is of enormous practical importance, since we have reduced the vectorial partial differential equation of first order, i.e. a set of three scalar partial differential equations, (2.5), to a single scalar partial differential equation of second order. This equation is in general easier to solve and to analyse than the original equation (2.5), and in fact a rich theory of the existence, uniqueness and the properties of solutions to equation (2.23) has been developed [Tay96a, Tay96b, Tay96c].

An important special case of the Poisson equation (2.23) arises when $\rho(\boldsymbol{r}) \equiv 0$ in the region of interest. In that case, the Poisson equation reduces to the well-known *Laplace equation*:

$$\Delta\varphi(\boldsymbol{r}) = 0 \tag{2.27}$$

Definition 2.2.1 (Harmonic function). A function fulfilling the Laplace equation (2.27) in a domain $\Omega \in \mathbb{R}^3$ is said to be *harmonic* in Ω.

Using the fundamental solution for the Poisson equation (c.f. Appendix C), which is given by

$$\mathcal{G}^p(\boldsymbol{r}-\boldsymbol{r}') = -\frac{1}{4\pi}\frac{1}{|\boldsymbol{r}-\boldsymbol{r}'|}$$

we can finally conclude that if there are no boundaries in the system, we can compute the electrostatic potential for a charge distribution $\rho(\boldsymbol{r})$ as the solution to the Poisson equation $\Delta\varphi(\boldsymbol{r}) = -\frac{\rho(\boldsymbol{r})}{\varepsilon_0}$ from

$$\varphi(\boldsymbol{r}) = -\frac{1}{4\pi\varepsilon_0}\int_{\mathbb{R}^3} \mathcal{G}^p(\boldsymbol{r}-\boldsymbol{r}')\rho(\boldsymbol{r}')\,d\boldsymbol{r}' \tag{2.28}$$

$$= \frac{1}{4\pi\varepsilon_0}\int_{\mathbb{R}^3} \frac{\rho(\boldsymbol{r}')}{|\boldsymbol{r}-\boldsymbol{r}'|}\,d\boldsymbol{r}' \tag{2.29}$$

2.2.3. The multipole expansion

The most simple charge distribution possible is that of a point charge q at position $\bar{\boldsymbol{r}}$. This charge distribution can be easily modeled using Dirac's δ–distribution[6] (c.f. Appendix B):

$$\rho(\boldsymbol{r}) = q\delta(\boldsymbol{r}-\bar{\boldsymbol{r}})$$

Such a charge distribution that concentrates all the charge in a single point is called a *monopole*.

In fact, it turns out that each charge distribution, no matter how complicated, can be assigned a certain *monopole moment*, that describes "how much it behaves like a monopole with all charge concentrated in a single point". This monopole moment just corresponds to the total charge

$$Q = \int \rho(\boldsymbol{r})d\boldsymbol{r}$$

This monopole moment is the first term of an expansion valid for arbitrary charge distributions, that often captures the important features of even complicated distributions in just a few terms, the so

---

6 Here, $\delta(\boldsymbol{r}-\bar{\boldsymbol{r}})$ is used as a convenient alias for $\delta^{\bar{\boldsymbol{r}}}[\boldsymbol{r}]$

called *multipole expansion*. The multipole expansion is an expansion of the electrostatic potential in terms of spherical harmonics Y_{lm}, and assumes – in spherical coordinates (r, θ, ϕ) – the form (see e.f. [Jac98]):

$$\varphi(\boldsymbol{r}) = \frac{1}{4\pi\varepsilon_0} \sum_{l=0}^{\infty} \sum_{m=-l}^{l} \frac{4\pi}{2l+1} q_{lm} \frac{Y_{lm}(\theta, \phi)}{r^{l+1}}$$

where the coefficients q_{lm}, the so–called *multipole moments*, are determined from

$$q_{lm} = \int Y_{lm}^*(\theta', \phi') r'^l \rho(\boldsymbol{r}') d\boldsymbol{r}'$$

Remark 2.2.2. The monopole moment $Q = \int \rho(\boldsymbol{r}) d\boldsymbol{r}$ is related to the q_{00} multipole moment by $Q = \sqrt{4\pi}\, q_{00}$.

The moments q_{10} and q_{11} can be used to form a more convenient expression, the so–called *dipole vector* $\boldsymbol{p}$. This leads to:

$$\boldsymbol{p} = \int \boldsymbol{r}\rho(\boldsymbol{r}) d\boldsymbol{r}$$

The length $p = |\boldsymbol{p}|$ is often called the dipole moment.
Very important for the theory of continuum electrostatics, as we will see soon, is the ideal electric *dipole*, i.e., a charge distribution with nonvanishing dipole moment but all other moments equal to zero. This can only be realized by arranging two opposite charges of equal magnitude an infinitesimal distance apart from each other. In any *real* dipole of course, the charges will be separated by a small but finite distance vector $\boldsymbol{d}$. If $d = |\boldsymbol{d}|$ is small enough, all higher moments are negligible compared to the dipole moment, and therefore the dipole can be considered an ideal dipole. The charge distribution of such a real dipole centered around the origin can be written as[7]

$$\rho(\boldsymbol{r}) = q \left[\delta(\boldsymbol{r} - \frac{1}{2}\boldsymbol{d}) - \delta(\boldsymbol{r} + \frac{1}{2}\boldsymbol{d}) \right]$$

where $\boldsymbol{d}$ points from the negative to the positive charge, leading to

$$\boldsymbol{p} = q\boldsymbol{d}$$

As a charge distribution, the dipole itself leads to an electrostatic field. If all higher moments can be
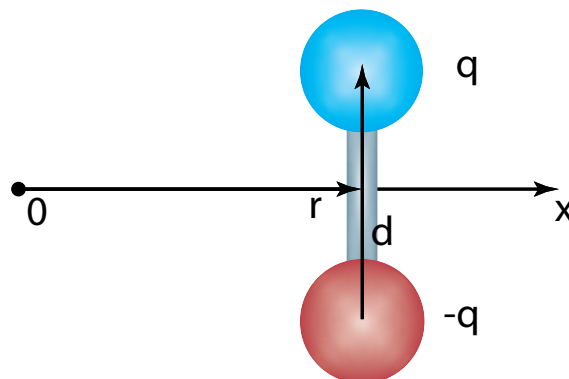
Figure 2.3.: Geometry of the dipole charge distribution.

---

[7] For the definition of the Dirac δ–distribution occurring in this expression, please refer to Appendix B

neglected (i.e. if the dipole can be considered a real dipole, which is usually the case for small d), and if we choose a coordinate system in which the p is oriented along the z axis and situated at position r', the electric potential of the dipole at a point r reads

$$\varphi(r) = \frac{1}{4\pi\epsilon_0} \frac{p \cdot (r - r')}{|r - r'|^3} \tag{2.30}$$

leading to an electric field equal to

$$E(r) = \frac{3\hat{n}(p \cdot \hat{n}) - p}{4\pi\epsilon_0 |r - r'|^3}$$

where

$$\hat{n} := \frac{r - r'}{|r - r'|}$$

is the unit vector pointing from r' to r.

On the other hand, if the dipole is brought into an external electric field, and if its own electric dipole field is small compared to the external field, it can be considered as a test particle, feeling the influence of the external field. For an ideal dipole situated at position r, the potential energy can be computed from a series expansion of the potential around its center, yielding:

$$E_{\text{pot}} = -p \cdot E(r)$$

If the external field $E(r)$ is homogeneous, i.e. it does not depend on the position r: $E(r) = E \, \forall r$, then the resulting force on the dipole $F = -\nabla E_{\text{pot}}$ vanishes. This is easy to understand, since the forces acting on both charges of the dipole cancel exactly in a homogeneous field. But while the net *force* on the ideal dipole in a homogeneous field vanishes, the *torque* does not, and can be easily computed to yield

$$N = p \times E \tag{2.31}$$

This can be interpreted as well: of course, the external field E can be interpreted as the field of an external charge distribution ρ_{ext}. The field lines of E are by definition pointing away from the positive and to the negative external charges, while the dipole vector is pointing from the negative to the positive side of the dipole. Since the dipole in the external field will try to arrange his positive side close to the negative external charge, and the negative side close to the positive external charge, it will rotate until the dipole vector p and the external field E are parallel, and therefore leading to a vanishing N.

This behaviour does *not* change qualitatively when the applied field is inhomogeneous, and in fact the hand–waving explanation for the orientation of the dipole in the external field is still valid. But in an inhomogeneous field, the dipole will feel a resulting net force, pulling it as a whole into a certain direction, and possible also an additional torque acting in the center of mass of the dipole, leading to the rotation of the dipole as a whole about the origin. But in all cases, **a dipole that is free to rotate and put into an external electrostatic field will orient its dipole vector parallel to the external field at the position of its origin.**

2.2.4. The local Maxwell equations for ponderable media

In principle, the Maxwell equations, supplemented by the corresponding boundary conditions, suffice to solve all problems occurring in classical (as opposed to quantum mechanical) electrodynamics, including the case of a charge distribution in water. In practice, however, this turns out to be infeasible,
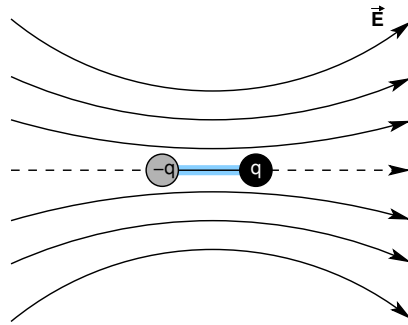
Figure 2.4.: Alignment of the dipole with an external electric field.

since the enormous complexity of the charge distribution of a highly structured medium like water, combined with the huge number of individual water molecules that would have to be taken into account prohibit any such low–level computational approach. Integrating the effects of a ponderable medium into electrodynamics calculations will therefore only be possible by accepting certain approximations. Several approximations are possible, and are used in different fields of science. It is, e.g. possible to approximately simulate a large number of water molecules by integrating their equations of motion and obtain their effect on an electric field by assigning partial charges to the positions of the hydrogen and oxygen atoms. Of course, the computational complexity of this approach is huge, especially for large systems. The other common approach consists in separating the charge distribution $\rho(\boldsymbol{r})$ into two parts: one *free* part, that is due to the charges brought into the system (this part corresponds to our earlier definition of ρ) and a *bound* part, due to the surrounding medium. Then, the difficult microscopic charge distribution for the bound charges is averaged out into a macroscopic material property, and the Maxwell equations are carefully adjusted to work with the new, macroscopic quantities instead of the complicated microscopic ones.

Classically, this averaging process leads to the well–established local macroscopic Maxwell equations, an average continuum theory for the electrodynamic field in a medium that is considered as a featureless continuum. Later, we will see how the same averaging process can be used to describe a "structured continuum" in the framework of nonlocal electrodynamics.

Local continuum electrostatics

Let us assume that a certain charge distribution $\rho(\boldsymbol{r})$ is brought into a region of space filled with a medium consisting of a large number of electrically neutral molecules. Since each individual molecule is electrically neutral as a whole, i.e. its *monopole moment* (c.f. Section 2.2.3) vanishes, the *dominating* multipole moment of a medium is typically the dipole moment. In particular this is true for *water*, which can be considered as an ideal dipole for most applications.

If the medium is "left alone" or undisturbed by any free charge distributions, its constituents will try to arrange themselves in a way that the average field vanishes, which means that all multipoles, averaged over many medium molecules, vanish. This changes drastically as soon as the external charge distribution $\rho(\boldsymbol{r})$ is brought into the medium. This charge distribution leads mainly to two effects in the medium: first, the charge distribution of the medium molecules is distorted by the external charge distribution, since the partial charges in the molecule are effected by the external charges, and rearrange inside the molecule. This typically increases the dipole moment of the constituent molecules, and therefore, a resulting net dipole moment is created (*influenced*) in the medium. This effect is of course dependent on the medium and is governed by the molecular polarizability of the substance. As

a second effect, the resulting dipole moment – the combination of any a priori dipole moment and the influenced one – interacts with the electrostatic field of the charge distribution $\rho(\boldsymbol{r})$, and as we know from the discussion of the electric dipole[8] in Section 2.2.3, the medium molecules will try to align their individual dipole vectors with the electric field due to $\rho(\boldsymbol{r})$. Compared to the free medium without any external charge distribution, where all dipole vectors point in any random direction, leading to a vanishing averaged dipole moment, the individual molecules now orient with the external field. This means that we will find many molecules pointing in the same direction in a small area of space, and therefore, the averaged dipole moment of the medium is now a finite quantity. This effect is known as the *orientational polarization* of the medium.

From Section 2.2.3, we know that each individual dipole in the medium creates its own electric field according to

$$\boldsymbol{E}_{\text{dipole}}(\boldsymbol{r}) = \frac{3\hat{\boldsymbol{n}}(\boldsymbol{p}{\cdot}\hat{\boldsymbol{n}}) - \boldsymbol{p}}{4\pi\epsilon_0|\boldsymbol{r} - \boldsymbol{r}'|^3}$$

with

$$\hat{\boldsymbol{n}} := \frac{\boldsymbol{r} - \boldsymbol{r}'}{|\boldsymbol{r} - \boldsymbol{r}'|}$$

Evaluating this expression infinitesimally close to the position of the dipole $\boldsymbol{r}$ and on its axis, it is easy to see that the dipole field is oriented *antiparallel* to the dipole vector $\boldsymbol{p}$. Since each individual dipole is oriented parallel to the external electric field $\boldsymbol{E}(\boldsymbol{r})$, and since electric fields are additive, we can conclude that **the external field is reduced by the dipole fields in the medium.** Thus, the presence of a medium effectively *shields* any applied electric field, and thus reduces all electrostatic interactions as compared to the vacuum case.

We will now try to quantify this effect approximately by averaging all the microscopic quantities over a volume ΔV that is considered to be macroscopically small ("almost infinitesimal") but large enough that a statistically relevant number of medium molecules is contained inside. This leads to the *macroscopic electric polarization vector $\boldsymbol{P}(\boldsymbol{r})$*, which gives the average dipole moment per unit volume at position $\boldsymbol{r}$. Assuming again that all other multipole moments of the medium charge distribution vanish, we can compute the electrostatic potential of a *free* or *excess* charge distribution $\rho(\boldsymbol{r})$ introduced into the medium by adding up the effects of the excess charges and the medium polarization, which creates a potential according to equation (2.30). For this computation, we build up the potential by linearly superimposing the contributions from each volume $\Delta V(\boldsymbol{r})$ used in the averaging process. Since the net free charge contained in $\Delta V(\boldsymbol{r})$ is $\rho(\boldsymbol{r})\Delta V(\boldsymbol{r})$ and the dipole moment in $\Delta V(\boldsymbol{r})$ is given by $\boldsymbol{P}(\boldsymbol{r})\Delta V(\boldsymbol{r})$, we can write down the electrostatic potential at position $\boldsymbol{r}$ due to the volume element $\Delta V(\boldsymbol{r}')$ at position $\boldsymbol{r}'$ as

$$\Delta\varphi(\boldsymbol{r}, \boldsymbol{r}') = \frac{1}{4\pi\epsilon_0}\left[\frac{\rho(\boldsymbol{r}')}{|\boldsymbol{r} - \boldsymbol{r}'|}\Delta V(\boldsymbol{r}') + \frac{\boldsymbol{P}(\boldsymbol{r}'){\cdot}(\boldsymbol{r} - \boldsymbol{r}')}{|\boldsymbol{r} - \boldsymbol{r}'|^3}\Delta V(\boldsymbol{r}')\right]$$

Since we assume $\Delta V(\boldsymbol{r}')$ to be "almost infinitesimal", we can replace it by the volume element $d\boldsymbol{r}'$ and integrate over the averaged contributions at each $\boldsymbol{r}'$ to yield the electrostatic potential of the charge distribution $\rho(\boldsymbol{r})$ in all of space:

$$\varphi(\boldsymbol{r}) = \frac{1}{4\pi\varepsilon_0}\int\left\{\frac{\rho(\boldsymbol{r}')}{|\boldsymbol{r} - \boldsymbol{r}'|} + \frac{\boldsymbol{P}(\boldsymbol{r}'){\cdot}(\boldsymbol{r} - \boldsymbol{r}')}{|\boldsymbol{r} - \boldsymbol{r}'|^3}\right\}d\boldsymbol{r}' \tag{2.32}$$

$$= \frac{1}{4\pi\varepsilon_0}\int\left\{\frac{\rho(\boldsymbol{r}')}{|\boldsymbol{r} - \boldsymbol{r}'|} + \boldsymbol{P}(\boldsymbol{r}'){\cdot}\boldsymbol{\nabla}'\left(\frac{1}{|\boldsymbol{r} - \boldsymbol{r}'|}\right)\right\}d\boldsymbol{r}' \tag{2.33}$$

---

[8] In all practical situations, higher multipole moments in the medium can be neglected

This result can be significantly simplified by shifting the gradient in the second term from the $\frac{1}{r}$–term to the polarization vector $\boldsymbol{P}$. This can easily be achieved by an integration by parts of the second term, using the property that

$$\lim_{r \to \infty} \frac{\boldsymbol{P}(r)}{r} = 0$$

This yields

$$\varphi(\boldsymbol{r}) = \frac{1}{4\pi\varepsilon_0} \int \{\rho(\boldsymbol{r}') - \boldsymbol{\nabla}'\!\cdot\!\boldsymbol{P}(\boldsymbol{r}')\} \frac{1}{|\boldsymbol{r}-\boldsymbol{r}'|} d\boldsymbol{r}' \tag{2.34}$$

Comparing this result to the free–space solution of the Poisson equation (2.28), we see that the quantity in braces in the integral in equation (2.34) can be identified with an *effective charge distribution* $\bar{\rho}(\boldsymbol{r})$, capturing the effects of the free charges and the medium polarization in a single quantity. We can therefore conclude from the first Maxwell equation of electrostatics (2.5), that

$$\boldsymbol{\nabla}\!\cdot\!\boldsymbol{E}(\boldsymbol{r}) = \frac{1}{\epsilon_0}\bar{\rho}(\boldsymbol{r}) \tag{2.35}$$

$$= \frac{1}{\epsilon_0}\{\rho(\boldsymbol{r}) - \boldsymbol{\nabla}\!\cdot\!\boldsymbol{P}(\boldsymbol{r})\} \tag{2.36}$$

This equation motivates the definition of a new, macroscopic electric quantity, the *dielectric displacement field* $\boldsymbol{D}(\boldsymbol{r})$:

$$\boldsymbol{D}(\boldsymbol{r}) = \varepsilon_0\boldsymbol{E}(\boldsymbol{r}) + \boldsymbol{P}(\boldsymbol{r}) \tag{2.37}$$

With this definition, equation (2.36) becomes

$$\boldsymbol{\nabla}\!\cdot\!\boldsymbol{D}(\boldsymbol{r}) = \rho(\boldsymbol{r}) \tag{2.38}$$

which is the macroscopic analogue of the first microscopic Maxwell equation of electrostatics, equation (2.5). Equation (2.38) immediately tells us that the normal component of the dielectric displacement field $\boldsymbol{D}(\boldsymbol{r})$ obeys the same boundary condition (2.12) as the normal component of the electric field in vacuum, i.e.

$$(\boldsymbol{D}_2 - \boldsymbol{D}_1)\!\cdot\!\hat{\boldsymbol{n}} = \sigma \tag{2.39}$$

across any surface Γ, where σ is a possible surface charge density on Γ.

2.2.5. The material equations

Since the polarization can in general not be determined microscopically, the basic idea in continuum electrostatics consists in proposing so–called *material equations*, coupling the field $\boldsymbol{D}(\boldsymbol{r})$ to $\boldsymbol{E}(\boldsymbol{r})$, and therefore approximately describing the macroscopic effect of the medium on the electrostatic field. The quality of this approximation depends on the complexity of the material equations, and the level of detail at which the different effects of the medium on the fields are modeled.

The first approximation commonly applied is the use of *linear* material equations. This is the crucial approximation we will use throughout this work, which significantly simplifies the handling of the equations of electrostatics. Fortunately, this approximation is no real restriction, since in all applications in bioinformatics we have in mind (and in most typical other applications of electrostatics in water), the field strengths are sufficiently small to justify this approach. From the linearity, we can conclude that the electric field $\boldsymbol{E}(\boldsymbol{r})$ and the dielectric displacement field $\boldsymbol{D}(\boldsymbol{r})$ are related through a linear operator $\mathcal{E}$:

$$\boldsymbol{D}(\boldsymbol{r}) = \mathcal{E}(\boldsymbol{E}(\boldsymbol{r})) \tag{2.40}$$

The second common approximation which we will also apply in our treatment of nonlocal electrostatics is the *isotropy assumption*, which means that the dielectric response of the medium is assumed to be

independent of *direction*. Under this assumption, the medium "looks the same" in every direction, and no direction is preferred by the system. While this assumption typically breaks down e.g. in crystals, it seems very reasonable for liquid media like water. On the other hand, close to a boundary, like that of a protein for example, preference or selection of certain directions might possibly occur [KRV78a], and might thus be included in future treatments of electrostatic effects in solution.

The classical approximation typically made at this point now leads to the so–called *local theory of electrostatics*. This can be achieved by assuming complete *independence* of the individual medium molecules from each other. This assumption is obviously very restrictive: since the medium molecules have at least non–vanishing dipole moments, they necessarily interact with each other, therefore inducing correlation effects in between them. In the local continuum description of electrostatics, all these effects are completely neglected, as well as other structure inducing interactions in the medium, like the important hydrogen bonding network in the case of water. The huge advantage of the local approach leading to its enormous popularity is of course its simplicity. If all medium molecules are uncorrelated, their effect on the electrostatic field can be described by a function that only depends on the position, the so–called *dielectric response function* or just *dielectric function* $\varepsilon(\boldsymbol{r})$, leading to[9]

$$\boldsymbol{D}(\boldsymbol{r}) = \varepsilon_0 \varepsilon(\boldsymbol{r}) \boldsymbol{E}(\boldsymbol{r}) \tag{2.41}$$

Combining equations (2.37) and (2.41), we can conclude that there is also a linear dependence of the polarization $\boldsymbol{P}(\boldsymbol{r})$ on the electric field $\boldsymbol{E}(\boldsymbol{r})$. The proportionality function between the two is commonly called the *dielectric response* $\chi_e(\boldsymbol{r})$. Using the dielectric response, equation (2.37) takes the form

$$\boldsymbol{D}(\boldsymbol{r}) = \epsilon_0 \boldsymbol{E}(\boldsymbol{r}) + \epsilon_0 \chi_e(\boldsymbol{r}) \boldsymbol{E}(\boldsymbol{r}) \tag{2.42}$$

$$= \epsilon_0 \left(1 + \chi_e(\boldsymbol{r}) \right) \boldsymbol{E}(\boldsymbol{r}) \tag{2.43}$$

We can therefore conclude from equations (2.37) and (2.43), that

$$\varepsilon(\boldsymbol{r}) = 1 + \chi_e(\boldsymbol{r}) \tag{2.44}$$

These equations form the basis of local electrostatics, and in the next section we will present briefly how this theory can be applied to biomolecular problems, before we will develop our nonlocal extension.

2.3. Local electrostatics for biomolecules – the cavity model

To solve electrostatic problems in a biomolecular setting, e.g. the potential of a protein immersed in water, it is common to employ the *cavity model:* the biomolecule is modeled as a bounded open domain $\Omega \subset \mathbb{R}^3$, the remainder of euclidean space $\Sigma := \mathbb{R}^3 \setminus \bar{\Omega}$ is supposed to be filled with water. This seemingly simple step hides one of the most problematic points in biomolecular electrostatics: the definition of the molecular surface. At this point, we will just assume that a suitable definition has been found and later discuss this problem in more detail, but the reader should keep in mind that no "natural" infinitely sharp boundary surface can be found in general. For reasons of simplicity, we will assume that Σ does not contain any free charges[10], i.e. the charge distribution $\rho(\boldsymbol{r})$ is strictly confined within Ω, and that the protein does not carry a singular surface charge distribution layer σ. This last approximation is no real restriction for biomolecular situations: since molecules in reality do not possess a really sharp interface with the surrounding water, singular charge layers can not be built up. The charge distribution $\rho(\boldsymbol{r})$ is then usually determined by positioning the constituent atoms of

---

9 Factoring out ε_0 has the advantage that $\varepsilon(\boldsymbol{r})$ and $\chi_e(\boldsymbol{r})$ become dimensionless quantities.

10 We will later briefly discuss how a large number of freely movable charged particles inside Σ can be included in the equations. This leads to the so–called *Poisson–Boltzmann theory*.
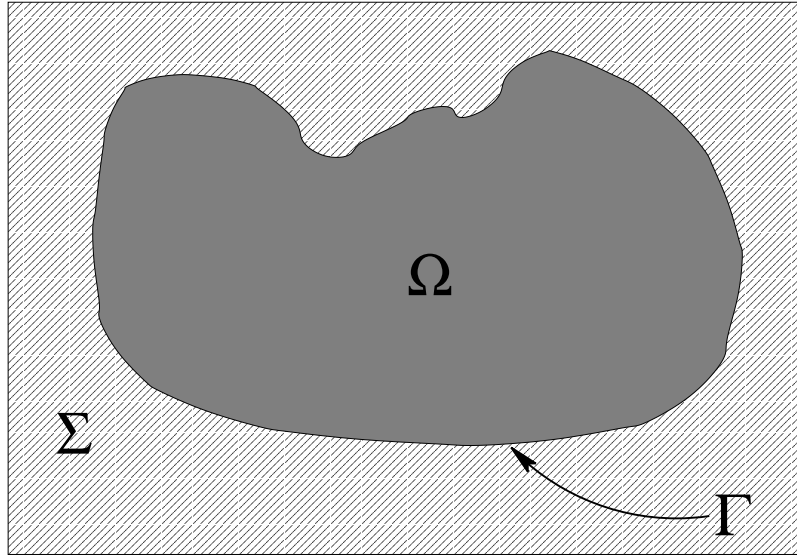
Figure 2.5.: The geometry of the cavity model of protein electrostatics. The protein is modeled as the open domain $\Omega \subset \mathbb{R}^3$, while the outside $\Sigma := \mathbb{R}^3 \setminus \bar{\Omega}$ is supposed to be filled with water, and Γ is the protein–water interface.

the molecules in their equilibrium positions, assigning – e.g. through quantum mechanical electronic structure calculations – partial charges to those atoms, and finally replacing the atoms by point or spherical charges situated at the center of the atom. The protein is typically assigned a dielectric constant of $\varepsilon_\Omega \approx 2 - 4$ [SP92, PFvG01], and the surrounding water a dielectric constant of about $\varepsilon_\Sigma \approx 78$, which is the experimentally measured *macroscopic* value of the dielectric constant of water. This value can be taken as a good approximation, when the length scales of the system under consideration are very large compared to the correlation length scales in the water. In this case, correlation effects can be neglected, but obviously, this does not hold when describing molecular systems.

The large jump of the dielectric constant from the value of $2 - 4$ inside the protein to the value of 78 outside poses several problems when solving the equations, and in fact it is generally not sensible to assume that such a large jump really takes place: as has been explained above, there is no sharp interface between the two media. Therefore, some intermediate transition region is often assumed, in which the dielectric function $\varepsilon(\boldsymbol{r})$ rises smoothly from the value inside to the dielectric constant of water. Unfortunately, no well posed theory for the behaviour and the functional form of $\varepsilon(\boldsymbol{r})$ exists today, and therefore, empirical approximations are usually assumed.

When all these preparations have been made, the task to solve the resulting system of equations[11]

$$
\left.
\begin{aligned}
\Delta \varphi_\Omega(\boldsymbol{r}) &= \frac{-\rho(\boldsymbol{r})}{\varepsilon_0 \varepsilon_\Omega} & \boldsymbol{r} &\in \Omega \\
\boldsymbol{\nabla}_{\boldsymbol{r}} \left(\varepsilon_\Sigma(\boldsymbol{r}) \boldsymbol{\nabla}_{\boldsymbol{r}} \varphi_\Sigma(\boldsymbol{r}) \right) &= 0 & \boldsymbol{r} &\in \Sigma \\
[\partial_n(\varepsilon_\Omega \varphi_\Omega) - \partial_n(\varepsilon_\Sigma(\boldsymbol{r}) \varphi_\Sigma)] &= 0 & \boldsymbol{r} &\in \Gamma \\
[\varphi_\Omega(\boldsymbol{r}) - \varphi_\Sigma(\boldsymbol{r})] &= 0 & \boldsymbol{r} &\in \Gamma
\end{aligned}
\right\}
\tag{2.45}
$$

still remains. Due to the complexity of the geometry of typical biomolecules and of the charge distributions, analytical solutions are in all practical cases infeasible. Therefore, some numerical method

---

11 The curl equation $\boldsymbol{\nabla} \times \boldsymbol{E}(\boldsymbol{r}) = 0$ is automatically fulfilled by setting $\boldsymbol{E}(\boldsymbol{r}) = -\boldsymbol{\nabla}\varphi(\boldsymbol{r})$

for the solution of systems of coupled partial differential equations has to be chosen, and the simplest – and therefore by far the most common – numerical approach is the *finite difference approach*. For a finite difference method, the interesting quantities are projected onto a grid by approximating them as piecewise constant functions. The differential operators occurring in the system are then replaced by *finite difference operators* of varying degree of sophistication, reducing the system of partial differential equations to a system of linear algebraic equations, which is usually solved iteratively.

While the appealing simplicity of this kind of method and the comparably low computational costs might explain their undiminished popularity, they are known to have serious drawbacks concerning the accuracy of the acquired solutions[BWS+95], and tend to ignore the boundary conditions prescribed by the theory.

2.4. The energy content of the electrostatic field and the reaction field method

In the last section, we have derived a setting suitable for considerations in the field of local biomolecular electrostatics. The equations derived there will allow us to compute the electrostatic potential in space, and from this the fields $E(r)$ and $D(r)$, and thus in principle yield all forces acting on a test charge distribution. But for many applications in the field of bioinformatics, the fields and the electrostatic potential are not the main quantities of interest. Usually, the more important quantity is the *potential energy* of this charge distribution in the fields at hand. This energy is for example needed for the computation of binding free energies or solubilities, which are in turn important inputs for common drug design related algorithms. In this section we will thus develop the required techniques to compute electrostatic energies *as soon as the electrostatic potential is known.* And since the theory of nonlocal electrostatics we will derive later will – just as the local theory, but in a much better approximation and much more realistic model – enable us to compute the electrostatic potential of a biomolecule in water, the results of this section can be directly applied to the solution of local as well as nonlocal problems. The presentation in this section is based on the excellent treatment in [Jac98]

In Section 2.1, we have seen that the force on a test point charge q located at position r in an electric field $E(r)$ is given by the Lorentz force (2.1), which for the case of vanishing magnetic field reduces to the simple equation (2.2)

$$F(r) = qE(r) \tag{2.46}$$

which we transformed in Section 2.2.2 by inserting the definition of the electrostatic potential φ into

$$F(r) = -q\boldsymbol{\nabla}\varphi(r) \tag{2.47}$$

From classical mechanics, we know that the work done in moving the charge from a position $\boldsymbol{\alpha}$ to a point $\boldsymbol{\beta}$ is given by the integral over minus one times the force times the infinitesimal line element of the path taken from $\boldsymbol{\alpha}$ to $\boldsymbol{\beta}$, where the minus appears since we are calculating the work that is done *on* the charge, not *by* the charge. Thus, the work $W_{es}^{pc}(\boldsymbol{\alpha}, \boldsymbol{\beta})$ is given by

$$W_{es}^{pc}(\boldsymbol{\alpha}, \boldsymbol{\beta}) = -\int_{\boldsymbol{\alpha}}^{\boldsymbol{\beta}} F \cdot dl = -q \int_{\boldsymbol{\alpha}}^{\boldsymbol{\beta}} E \cdot dl \tag{2.48}$$

$$= q \int_{\boldsymbol{\alpha}}^{\boldsymbol{\beta}} \boldsymbol{\nabla}\varphi \cdot dl \tag{2.49}$$

$$= q \int_{\boldsymbol{\alpha}}^{\boldsymbol{\beta}} d\varphi \tag{2.50}$$

$$= q \left\{ \varphi(\boldsymbol{\beta}) - \varphi(\boldsymbol{\alpha}) \right\} \tag{2.51}$$

Thus, the quantity $q\varphi$ can indeed be interpreted as the *potential energy* of the test point charge in the external electrostatic field. It is also worth noting that the fact that the electric field is rotation free means that the force field $q\boldsymbol{F}$ is *conservative*, i.e. the work is independent of the path taken and only depends on its endpoints.

Since the potential energy W of a charge q at position $\boldsymbol{r}$ in the electrostatic field $\boldsymbol{E}(\boldsymbol{r})$ can be interpreted as the work required to bring q from infinity to $\boldsymbol{r}$ under the action of $\boldsymbol{E}(\boldsymbol{r})$, we can conclude from (2.51)

$$W = q \lim_{\|\boldsymbol{\alpha}\| \to \infty} \left\{ \varphi(\boldsymbol{r}) - \varphi(\boldsymbol{\alpha}) \right\} \tag{2.52}$$

and since the energy content of the electrostatic field must be finite, we can conclude that

$$\lim_{\|\boldsymbol{\alpha}\| \to \infty} \varphi(\boldsymbol{\alpha}) = 0$$

and thus

$$W = q\varphi(\boldsymbol{r}) \tag{2.53}$$

Of course, this equation lends itself to a straightforward generalization: suppose that the system consists of a number of n point charges q_i **in vacuum** at positions $\boldsymbol{r}_i$. Then, the electrostatic potential of this charge distribution is given by

$$\varphi(\boldsymbol{r}) = \frac{1}{4\pi\varepsilon_0} \sum_{i=1}^{n} \frac{q_i}{|\boldsymbol{r} - \boldsymbol{r}_i|} \tag{2.54}$$

and thus the potential energy of one of those charges q_j is given by

$$W_j = q_j \varphi(\boldsymbol{r}) = \frac{q_j}{4\pi\varepsilon_0} \sum_{i=1}^{n} \frac{q_i}{|\boldsymbol{r} - \boldsymbol{r}_i|} \tag{2.55}$$

where each term i in the sum gives the contribution to the potential energy of q_j due to the interaction with the charge q_i. To compute the total potential energy of the system, we have to add up the contributions due to each individual point charge q_j. At this point we have to be careful not to count a contribution twice: for each charge q_i we account for the interaction with each charge q_j, and by just summing up all contributions, we would count this interaction again when considering all interactions of q_j. Thus, the electrostatic potential of this charge distribution is given by

$$W = \frac{1}{4\pi\varepsilon_0} \sum_{i=1}^{n} \sum_{j \leq i} \frac{q_i q_j}{|\boldsymbol{r}_i - \boldsymbol{r}_j|} \tag{2.56}$$

This can be written in a more symmetric fashion by remembering that in a *unrestricted* summation, we would count each interaction term exactly twice, and thus, we can replace equation (2.56) by

$$W = \frac{1}{8\pi\varepsilon_0} \sum_{i=1}^{n} \sum_{j=1}^{n} \frac{q_i q_j}{|\boldsymbol{r}_i - \boldsymbol{r}_j|} \tag{2.57}$$

By analogy to equation (2.57), we thus conclude that for a general – possibly continuous – charge distribution $\rho(\boldsymbol{r})$, the potential energy in its own electrostatic field is given by

$$W = \frac{1}{2} \int \rho(\boldsymbol{r}) \varphi(\boldsymbol{r}) \, d\boldsymbol{r} \tag{2.58}$$

where the factor $\frac{1}{2}$ is included to avoid counting interactions twice, just as in equation (2.57), and is thus due to the fact that we are computing the energy of the charge distribution in its *own* field. If φ was considered as an *external* field and ρ as a *test charge distribution*, small enough that it would not alter φ significantly, this prefactor would **not** occur, which is a common reason for confusion.

In this derivation, we gracefully passed over a deeply rooted problem in equations (2.56) and (2.57): in the second summation, we had to include the $i = j$ term for each value of i, since each charge will also interact with its own field. But as can be seen from the $|\boldsymbol{r}_i - \boldsymbol{r}_j|^{-1}$ – dependence of the individual terms, this so–called *self energy* terms are all *infinite*. Thus, the potential energy of a number of point charges in an external field is itself always *infinite*, which is of course completely unphysical. It can be shown that this effect is in essence due to the idealized notion of Dirac δ – like point charges, which is typically an unrealistic approximation in itself. This problem can be addressed by a certain *renormalization process*. To this end, we will first decompose the sum in equation (2.57) into two components:

$$W = \frac{1}{8\pi\varepsilon_0} \sum_{i=1}^{n} \sum_{j=1}^{n} \frac{q_i q_j}{|\boldsymbol{r}_i - \boldsymbol{r}_j|} \tag{2.59}$$

$$= \frac{1}{8\pi\varepsilon_0} \sum_{i=1}^{n} \left\{ \frac{q_i^2}{|\boldsymbol{r}_i - \boldsymbol{r}_i|} + \sum_{\substack{j=1 \\ j \neq i}}^{n} \frac{q_i q_j}{|\boldsymbol{r}_i - \boldsymbol{r}_j|} \right\} \tag{2.60}$$

$$= \underbrace{\frac{1}{8\pi\varepsilon_0} \sum_{i=1}^{n} \frac{q_i^2}{|\boldsymbol{r}_i - \boldsymbol{r}_i|}}_{\text{infinite self energy } W_{\text{self}}} + \underbrace{\frac{1}{8\pi\varepsilon_0} \sum_{i=1}^{n} \sum_{\substack{j=1 \\ j \neq i}}^{n} \frac{q_i q_j}{|\boldsymbol{r}_i - \boldsymbol{r}_j|}}_{\text{finite energy contribution } W_{\text{inter}}} \tag{2.61}$$

The main idea of the renormalization process now consists in considering the *infinite* quantity W_{self} as just an additive *gauge constant*, and since potential energies are *always* gauge–invariant for additive constants – those terms vanish when computing the derivative of the potential, which leads to the "physical" fields – they can be "renormalized away", or, more loosely speaking, just ignored, for many purposes. In particular, this self energy term can be neglected when we are computing *differences* of the electrostatic energy for the same charge distribution e.g. in different media, since the same term appears twice but with opposite signs. While this might seem like a violation of mathematics – in principle we have just computed $\infty - \infty = 0$, this technique can be strictly justified. We will soon see how this technique can be used to compute electrostatic contributions to energetic solvation quantities.

The derivations leading to equation (2.58) have interpreted the potential energy of an electrostatic field as being due to the work that had to be done against the field during the building process of the charge distribution, and as being stored in the interactions between charges at different positions. An alternative point of view consists in imagining the energy to be stored in the electric field surrounding the charge distribution. This is often especially fruitful, since it for example allows to compute the energy content of a given external electric field without having to know the charge distribution that lead to its creation. Such a setting can be easily obtained by eliminating the charge distribution from equation (2.58). Remembering that we are still considering only charge distributions **in vacuum**, we

can replace the charge distribution in equation (2.58) by making use of the vacuum Poisson equation (2.23),

$$\varepsilon_0 \Delta \varphi = -\rho$$

to yield

$$W = \frac{1}{2} \int \rho(\boldsymbol{r})\varphi(\boldsymbol{r})\, d\boldsymbol{r} \tag{2.62}$$

$$= -\frac{\varepsilon_0}{2} \int \varphi \Delta \varphi \, d\boldsymbol{r} \tag{2.63}$$

which can in turn be integrated by parts to yield

$$W = -\frac{\varepsilon_0}{2} \int |\boldsymbol{\nabla}\varphi|^2 \, d\boldsymbol{r} \tag{2.64}$$

$$= \frac{\varepsilon_0}{2} \int |\boldsymbol{E}|^2 \, d\boldsymbol{r} \tag{2.65}$$

and thus, in vacuum electrostatics, we can interpret the quantity

$$\omega := \frac{\varepsilon_0}{2}|E|^2 \tag{2.66}$$

as the *energy density* of the electrostatic field $\boldsymbol{E}(\boldsymbol{r})$.

Leaving now the simple vacuum case, we notice that defining a suitable energy functional for ponderable media is considerably more involved for the following reason: in vacuum, we can imagine that the whole work that is done on the system is spent for building up the charge distribution, since "nothing else is present in the system". A ponderable medium on the other hand is *polarized* by the electric field as we saw in Section 2.2.4. This polarization has to be "paid for" somehow, and thus, additional work is done to maintain the polarizational effect in the medium. Assuming for reasons of generality neither linearity nor locality nor any other restrictive property of the dielectric response, we can only state that the *change* of the electrostatic energy δW due to a small change $\delta\rho$ of the charge distribution will be effected by an equal amount δW of work that is done against the *currently present and unperturbed* electrostatic potential φ. This can be written as

$$\delta W = \int \delta\rho(\boldsymbol{r})\varphi(\boldsymbol{r})\, d\boldsymbol{r} \tag{2.67}$$

and with the help of equation (2.38)

$$\boldsymbol{\nabla}\cdot\boldsymbol{D}(\boldsymbol{r}) = \rho(\boldsymbol{r})$$

we can replace the infinitesimal change in the charge distribution, $\delta\rho$, by the equivalent resulting change in the displacement field via

$$\delta\rho = \boldsymbol{\nabla}\cdot(\delta\boldsymbol{D}) \tag{2.68}$$

and thus we arrive at

$$\delta W = \int (\delta\boldsymbol{D}(\boldsymbol{r}))\,\varphi(\boldsymbol{r})\, d\boldsymbol{r} \tag{2.69}$$

Assuming that $\rho(\boldsymbol{r})$ is localized in space, i.e. that ρ has compact support in $\mathbb{R}^3$, we can integrate by parts with vanishing boundary terms, leading to

$$\delta W = -\int (\boldsymbol{\nabla}\varphi(\boldsymbol{r}))\cdot\delta\boldsymbol{D}(\boldsymbol{r})\, d\boldsymbol{r} \tag{2.70}$$

$$= \int \boldsymbol{E}(\boldsymbol{r})\cdot\delta\boldsymbol{D}(\boldsymbol{r})\, d\boldsymbol{r} \tag{2.71}$$

The total electrostatic potential energy in the medium can now found from this equation by integrating over the infinitesimal change in the displacement field $\delta \boldsymbol{D}(\boldsymbol{r})$, thus building it up from zero to its final value $\boldsymbol{D}(\boldsymbol{r})$. Formally, we can thus write

$$W = \int d\boldsymbol{r} \int_0^{\boldsymbol{D}} \langle \boldsymbol{E}(\boldsymbol{r}), \delta \boldsymbol{D}(\boldsymbol{r}) \rangle \tag{2.72}$$

In the remainder of this work, we will always assume a *linear* relationship between the fields $\boldsymbol{E}(\boldsymbol{r})$ and $\boldsymbol{D}(\boldsymbol{r})$ – even though it might be nonlocal – which allows us to write the scalar product appearing in this integral in a more symmetric fashion:

$$\langle \boldsymbol{E}(\boldsymbol{r}), \delta \boldsymbol{D}(\boldsymbol{r}) \rangle = \frac{1}{2} \delta \langle \boldsymbol{E}(\boldsymbol{r}), \boldsymbol{D}(\boldsymbol{r}) \rangle \tag{2.73}$$

and thus the integral becomes

$$W = \frac{1}{2} \int d\boldsymbol{r} \int_0^{\boldsymbol{E}(\boldsymbol{r}) \cdot \boldsymbol{D}(\boldsymbol{r})} \delta \left(\langle \boldsymbol{E}(\boldsymbol{r}), \boldsymbol{D}(\boldsymbol{r}) \rangle \right) \tag{2.74}$$

the second integral over the differential form $\delta \langle \boldsymbol{E}(\boldsymbol{r}), \boldsymbol{D}(\boldsymbol{r}) \rangle$ can be trivially replaced by the values of $\langle \boldsymbol{E}(\boldsymbol{r}), \boldsymbol{D}(\boldsymbol{r}) \rangle$ at the integration boundaries, and since the lower boundary is zero and the upper just the final value of this product, we can finally conclude for the electrostatic potential energy of a charge distribution ρ in its own field embedded in a medium

$$\boxed{W = \frac{1}{2} \int \langle \boldsymbol{E}(\boldsymbol{r}), \boldsymbol{D}(\boldsymbol{r}) \rangle \, d\boldsymbol{r}} \tag{2.75}$$

and with the help of $\boldsymbol{D}(\boldsymbol{r}) = -\boldsymbol{\nabla}\varphi(\boldsymbol{r})$ and $\boldsymbol{\nabla}\boldsymbol{D}(\boldsymbol{r}) = \rho(\boldsymbol{r})$ and another integration by parts, we again obtain the equivalent representation of W, just as in the vacuum case:

$$\boxed{W = \frac{1}{2} \int \rho(\boldsymbol{r}) \varphi(\boldsymbol{r}) \, d\boldsymbol{r}} \tag{2.76}$$

which has now been shown to be valid in a medium as well as in vacuum. Thus, the energy density of the electrostatic field in medium is given by

$$\omega = \frac{1}{2} \langle \boldsymbol{E}(\boldsymbol{r}), \boldsymbol{D}(\boldsymbol{r}) \rangle \tag{2.77}$$

At this point we want to stress that we did **not** make use of the assumption of locality in the relation between $\boldsymbol{E}(\boldsymbol{r})$ and $\boldsymbol{D}(\boldsymbol{r})$, and thus, the results we have just obtained will readily apply to the nonlocal setting we will develop in the next chapter. For a *nonlinear relationship* – which we can typically neglect in the case of biomolecular electrostatics – the computation of the electrostatic potential energy will have to make use of the more general equation (2.74).

We have already mentioned that the electrostatic energy in the medium can be decomposed into a contribution that is due to the charge distribution "feeling" its own field and one that is due to the polarization of the medium. Assuming that the charge distribution describes a molecular system, this motivates the introduction of a decomposition of the electrostatic potential into the *molecular* and the *reaction field* potential, where the first term describes the energetic contribution due to the charge distribution itself, and the second the reaction of its surroundings. We thus write

$$\boxed{\varphi(\boldsymbol{r}) = \varphi_{\mathsf{mol}}(\boldsymbol{r}) + \varphi^*(\boldsymbol{r})} \tag{2.78}$$

where $\varphi_{\text{mol}}(\boldsymbol{r})$ is the potential of the charge distribution *without* the presence of the dielectric boundary, i.e. the potential of the charges embedded in an infinitely spread out molecule, and $\varphi^*(\boldsymbol{r})$ is the reaction field potential, i.e. change in the potential that is induced by the presence of the dielectric boundary [VS96, Boe73]. The above definition of the molecular potential is a common and subtle source of confusion: the molecular potential as defined above is in general **not** the potential of the same charge distribution embedded in vacuum. To see this, let us assume that the molecular is modelled as having a dielectric constant of ε_Ω. Then, the molecular potential φ_{mol} is the potential of the given charge distribution, embedded in an *infinite domain with dielectric constant ε_Ω*. Thus, the molecular potential equals the vacuum potential for nonvanishing charge distribution if and only if $\varepsilon_\Omega \equiv 1$, in which case the vacuum reaction field potential vanishes. For $\varepsilon_\Omega \neq 1$ on the other hand, the reaction field potential does **not** vanish, even if the molecule is embedded in vacuum.

The decomposition into molecular potential and reaction field potential has several desirable properties, e.g. it is typically possible – at least in linear local electrostatics – to attribute the reaction field potential to a virtual polarization surface charge distribution on the boundary of the system. But for us, the most important advantage is the fact that the *singular behaviour* of the potential e.g. at the locations of point charges is *completely covered* by the molecular potential, while the reaction field potential is a nonsingular quantity, so it is in general much easier to work with. In addition, the definition of the molecular potential φ_{mol} as the potential of a charge distribution in an unbounded domain typically allows for the derivation of *analytical expressions* for φ_{mol}, for example in the probably most common case where ρ is given as a number of point charges centered at the positions of the individual atoms. In this case, we can directly conclude that

$$\varphi_{\text{mol}}(\boldsymbol{r}) = \frac{1}{4\pi\varepsilon_0\varepsilon_\Omega} \sum_{i=1}^{n} \frac{q_i}{|\boldsymbol{r} - \boldsymbol{r}_i|} \tag{2.79}$$

In addition, the fact that the molecular potential is defined independent of the surroundings of the charge distribution allows to *avoid* its computation completely if we are interested in *differences* of potential energies, as is for example the case when computing solvation related quantities. In this case, we typically have to consider quantities like

$$\Delta W = W^{\text{water}} - W^{\text{vacuum}} \tag{2.80}$$

$$= \frac{1}{2} \left\{ \int \rho(\boldsymbol{r}) \varphi^{\text{water}}(\boldsymbol{r}) \, d\boldsymbol{r} - \int \rho(\boldsymbol{r}) \varphi^{\text{vacuum}}(\boldsymbol{r}) \, d\boldsymbol{r} \right\} \tag{2.81}$$

$$= \frac{1}{2} \int \rho(\boldsymbol{r}) \left\{ (\varphi_{\text{mol}}(\boldsymbol{r}) + \varphi^*_{\text{water}}(\boldsymbol{r})) - (\varphi_{\text{mol}}(\boldsymbol{r}) + \varphi^*_{\text{vacuum}}(\boldsymbol{r})) \right\} d\boldsymbol{r} \tag{2.82}$$

$$= \frac{1}{2} \int \rho(\boldsymbol{r}) \left\{ \varphi^*_{\text{water}}(\boldsymbol{r}) - \varphi^*_{\text{vacuum}}(\boldsymbol{r}) \right\} d\boldsymbol{r} \tag{2.83}$$

and thus a computation of solvation energies can be performed with the help of the nonsingular reaction field potential alone, avoiding the problems related to the infinite self energy of point charges. In particular, for a charge distribution made up of a number of point charges, the last equation becomes:

$$\Delta W = \frac{1}{2} \sum_{i=1}^{n} q_i \left(\varphi^*_{\text{water}}(\boldsymbol{r}_i) - \varphi^*_{\text{water}}(\boldsymbol{r}_i) \right) \tag{2.84}$$

$$= \frac{1}{2} \sum_{i=1}^{n} q_i \varphi^*_{\text{water}}(\boldsymbol{r}_i) - \frac{1}{2} \sum_{i=1}^{n} q_i \varphi^*_{\text{vacuum}}(\boldsymbol{r}_i) \tag{2.85}$$

$$=: W^*_{\text{water}} - W^*_{\text{vacuum}} \tag{2.86}$$

2.5. The free energy of solvation

Probably the most important solvation quantity for applications in bioinformatics is the *free energy of solvation*, and in fact, its computation was the reason for our engagement in the field of nonlocal electrostatics. In this chapter, we want to briefly introduce its properties and discuss ways to compute it.

Following Ben–Naim [BN87], we can define the term *solvation* as follows:

Definition 2.5.1. The solvation of a solute *M* in a solvent *S* is the process of transferring *M* from a fixed position in an ideal gas phase into a fixed position in the liquid phase *S* while pressure, temperature and composition of the system remain unchanged.

This process is connected with a change in some kind of *energy*, i.e. in the language of thermodynamics, energy is stored in or retrieved from some *thermodynamic potential* (in this case, the so-called *Gibbs free energy* or *free enthalpy* G). For a detailed discussion how this Gibbs free energy is defined, and how this relates to the theory of electrostatics, the interested reader is referred to [Hil02]. For this work, it is sufficient to know that the difference in the Gibbs free energy ΔG

$$\Delta G := G_{\text{water}} - G_{\text{vacuum}} \tag{2.87}$$

contains the all necessary information about the energetics of the solvated system, and is thus termed the *free energy of solvation*. It can be shown that for the process of solvation, the equilibrium state – the state that the system will assume if it is *left alone* for a sufficient amount of time – is a state of minimal free energy of solvation, and thus, the equilibrium of a system undergoing solvation can be determined from a minimization of ΔG, and thus ΔG can be considered a valuable term in high–quality scoring functions for applications in structural bioinformatics, like protein docking.

A variety of interactions is able to influence the free energy of solvation – in principle, each interaction that is "changed" in some way by the presence of the solvent will lead to a contribution to ΔG. Following the approach by Jackson and Sternberg [JS94, JS95], we will use the following decomposition:

$$\Delta G^{\text{solv}} = \Delta G^{\text{polar}} + \underbrace{\Delta G^{\text{cav}} + \Delta G^{\text{conf}} + \Delta G^{\text{vdW}}}_{\Delta G^{\text{nonpolar}}}$$

This work is exclusively concerned with electrostatic interactions, and thus, the methods developed in this thesis will provide methods for the accurate and efficient determination of the term ΔG^{polar}, and in fact, this term is often the dominant one. But when we will be comparing our results to experimental values in later chapters, we will need to compute the *full* ΔG^{solv}. For this purpose, we will use existing and well–established models for the nonpolar contributions, and we will take special care to chose validation systems – most notably the small ions – for which $\Delta G^{\text{polar}} \gg \Delta G^{\text{nonpolar}}$ so that the results will not be clouded by possible errors induced by the computation of the nonpolar contribution.

The nonpolar contribution

The nonpolar contribution to the free energy of solvation includes all the effects that are not already covered by the electrostatic interactions. This includes [HC72, JS94, JS95] the effects of dispersion and repulsion (ΔG^{vdW}), the formation of a cavity in the solvent that accommodates the solute (the solute covers a certain amount of space that the solvent molecules are now denied; therefore, one first has to "drag" some solvent molecules to make room for the solute, and this leads to the energetic contribution ΔG^{cav}) and terms that cover explicitly entropic effects due to the change in conformation

of the solute (ΔG^{conf}). For nonpolar molecules, like e.g. the alkanes, this nonpolar part of the free energy of solvation is the only significant contribution, and therefore electrostatic interactions can be neglected. But in general – e.g. for large proteins which contain many highly charged regions – ΔG^{polar} typically dominates or at least equals $\Delta G^{nonpolar}$.

The polar contribution

In the last section we have seen that the origin of the polar or *electrostatic* contribution to the free energy of solvation lies in the polarization effects that are due to the dielectric boundary. The difference of the energy associated with this effect – ΔW – will then yield a measure for the gain in energy a certain molecule will acquire when being brought from the gas phase (i.e. from an embedding in vacuum) into the solvent. In can be shown that the *free energy of solvation ΔG* is related to ΔW by a simple change of units: while ΔW is the difference in the potential energy of a single molecule, ΔG is a *macroscopic thermodynamical quantity*, and should thus be measured in molar units rather than in molecular ones. In the system of units employed in this work, we will simply set

$$\Delta G^{\mathsf{polar}} = \mathcal{N}_a \Delta W \tag{2.88}$$

where $\mathcal{N}_a \approx 6.022 \times 10^{23} \mathrm{mol}^{-1}$

Since the dipoles in the medium tend to shield any applied electrostatic field, less energy is needed to maintain it in a solvent than in vacuum. Therefore, for a given charge distribution the energy difference of its electric fields in the solvent and in vacuum

$$\Delta G = G_{\mathsf{water}} - G_{\mathsf{vacuum}}$$

should be negative. If this gain in energy is bigger than the possible loss through nonpolar contributions, the state of solution is advantageous for the system.

2.6. The free energy of binding

Another important quantity that has direct use for docking applications and similar techniques is the *free energy of binding*, which predicts the strength with which a biomolecular complex is kept together. In [JS95], Jackson and Sternberg have shown how to compute the difference in the free energy of binding when changing from the gaseous to the solvated state from the knowledge of the free energy of solvation using the procedure schematically described in Fig. 2.6.

The change in the free energy of a system due to the binding of the proteins in presence of the solvent ΔG^{bind} is then given by:

$$\Delta G^{\mathsf{bind}} = \Delta \Delta G^A_{\mathsf{sol}} + \Delta \Delta G^B_{\mathsf{sol}} + \Delta G^{A-B}_{\mathsf{int}}.$$

$\Delta G^{A-B}_{\mathsf{int}}$ contains the energy that is stored in the bonds between both protein, and contains again polar and nonpolar contributions. Of course, the calculation of the polar contribution can also profit from an improved theory of solvent electrostatics like the one that is developed in this work.

2.7. Shortcomings of local continuum electrostatics

Comparing the results of local electrostatics computations for biomolecules to experimentally obtained data, e.g. computed and measured data for the free energy of solvation, it becomes painfully clear that some of the approximations made in the last chapter seems to break down when looking at systems at a molecular scale [Sim01, LG98].
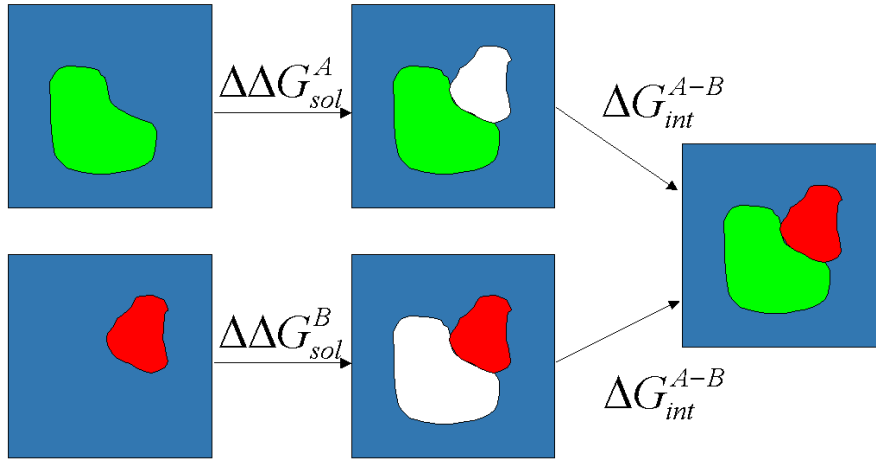
Figure 2.6.: Thermodynamical process used for calculating the change in the free energy of binding ΔG^{bind} due to the agglomeration of two proteins. First, we compute the loss of interaction between solvent and protein A $\Delta\Delta G^A_{\text{sol}}$ and solvent and protein B $\Delta\Delta G^B_{\text{sol}}$. Then, we calculate the contribution due to the interaction of A and B in the presence of the solvent, $\Delta G^{A-B}_{\text{int}}$

In our opinion, the assumption that cannot be maintained when dealing with systems the size of typical biomolecules is the independence assumption of the water molecules, leading to a correlationless local dielectric function $\varepsilon(\boldsymbol{r})$, and thus to a complete neglect of the solvent structure around the solute.

The consequences of this neglect can be demonstrated by computing the electrostatic contribution to the free energy of solvation around a simple charge distribution immersed in water. For reasons of simplicity, we choose a very simple but nonetheless important model to illustrate the problem, namely that of a sphere immersed in water with radius a and total charge Q distributed over its surface. This charge distribution is a commonly employed model for an ion solvated in water, and is called the *Born model*.

It is very easy to show that the electric field $\boldsymbol{E}(\boldsymbol{r})$ of this charge distribution outside the sphere, i.e. for all $\boldsymbol{r}$ with $|\boldsymbol{r}| > a$ is given by

$$\boldsymbol{E}(\boldsymbol{r}) = \frac{Q}{4\pi\varepsilon_0\varepsilon r^2}\,\hat{\boldsymbol{e}}_r \tag{2.89}$$

where $\hat{\boldsymbol{e}}_r$ is the normalized vector $\frac{\boldsymbol{r}}{|\boldsymbol{r}|}$ pointing in the direction of $\boldsymbol{r}$. From this expression, we can now compute the energy contained in the electric field surrounding the charge distribution using equation (2.75)

$$W_{\text{el}} = \frac{1}{2}\int \langle \boldsymbol{E}(\boldsymbol{r}), \boldsymbol{D}(\boldsymbol{r})\rangle \, d\boldsymbol{r} \tag{2.90}$$

$$= \frac{1}{2}\varepsilon_0\varepsilon \int \langle \boldsymbol{E}(\boldsymbol{r}), \boldsymbol{E}(\boldsymbol{r})\rangle \, d\boldsymbol{r} \tag{2.91}$$

$$= \frac{1}{2}\varepsilon_0\varepsilon \int \boldsymbol{E}^2(\boldsymbol{r}) \, d\boldsymbol{r} \tag{2.92}$$

$$\underset{(2.89)}{=} \frac{1}{2}\varepsilon_0\varepsilon \int_a^\infty \frac{Q^2}{(4\pi\varepsilon_0\varepsilon r^2)^2} 4\pi r^2 \, dr \tag{2.93}$$

2. Local electrostatics

$$= \frac{Q^2}{8\pi\varepsilon_0\varepsilon a} \tag{2.94}$$

In this derivation we have computed the electrostatic energy from an integration over the whole space surrounding the sphere, and we can conclude that the energy associated with a charge distribution is spread out over a large (in principle infinite) volume.

This has direct consequences for the quality of the approximation made in local electrostatics: describing the water as a featureless continuum can only be valid, if the effects of the discrete nature of the solvent can be averaged out. This means that the field should be spread out "as evenly as possible" over large volumes, such that we can separate the surrounding space into volume elements small enough that the field is nearly constant inside the volume but large enough that a statistically relevant number of molecules is contained inside. If, on the other hand, the typical length scales of the variation of the electric field is so small that any box in which the field can be considered constant contains only a small number of individual water molecules, the effects of the solvent structure can no longer be ignored.

In our model system we can easily test this proposition. From equation (2.93) we can conclude that the energy content in the spherical shell of radius R around the ion is simply given by

$$W_{\mathrm{el}}^R = \frac{1}{2}\varepsilon_0\varepsilon \int\limits_a^R \frac{Q^2}{(4\pi\varepsilon_0\varepsilon r^2)^2} 4\pi r^2 \, dr \tag{2.95}$$

$$= \frac{-Q^2}{8\pi\varepsilon_0\varepsilon}\left[\frac{1}{a} - \frac{1}{R}\right] \tag{2.96}$$

Taking a typical ion radii of $a = 1\text{Å}$, which is close to the observed radius for Na^+, equation (2.96) tells us that 50% of the energy is contained within the spherical shell from $r = a = 1\text{Å}$ to $r = R = 2\text{Å}$, and in a shell ranging to $R = 10\text{Å}$, 90% of the ion's energy will be concentrated. Obviously, there is not much room for water molecules inside these shells, so the averaging process that was done to yield a structureless solvent continuum should be suspected to break down.

To illustrate this further, it is instructive to look at a so–called *radial distribution function (RDF)* for a sodium ion solvated in water. This function $g(r)$ can be interpreted as the probability that, if the ion is located at $r = 0$, there is a water molecule centered at position r. Figure 2.7 shows such a function that has been derived from a molecular dynamics simulation. In this figure, the region shaded in dark gray corresponds to a sphere of radius 2Å around the ion, i.e. a spherical shell of size 1Å around its surface. From the above computations, we know that in this shell, 50% of the electrostatic energy is concentrated, while looking at the radial distribution function clearly shows that this region does not contain a single water molecule. Since in the local continuum approach depicted in Section 2.2.4, assumes that in this case there is a continuum of water molecules starting at radius $r = 1$ Å, leading to a 78–fold shielding, we should be prepared to expect large deviations in energy computations for this kind of system: the local continuum approach completely fails to describe the system at least in a region responsible for about 50% of the result. From the rdf in Fig. 2.7 we can also conclude that the distribution of water molecules in about 2 to 3 shells around the ion shows a more or less rich structure, again disallowing a simple homogeneous continuum description. That this is not a purely academic question can e.g. be illustrated by looking at the electrostatic contribution to the free energy of solvation of ions. This quantity can easily be computed[12] from the electrostatic field around the

---

12 The question of how to determine the *radii* for the individual ions will be covered in detail in a later section.

ion, and is also − at least to a certain degree − experimentally available. From equation (2.94) and from equation (2.88) we have

$$\Delta G^{\text{polar}} = -\mathcal{N}_a \left(W^{\text{polar}}_{\text{vacuum}} - W^{\text{polar}}_{\text{water}} \right) \tag{2.97}$$

$$= -\mathcal{N}_a \frac{Q^2}{8\pi\epsilon_0 a} \left[1 - \frac{1}{\epsilon} \right] \tag{2.98}$$

The plot shown in Fig. 2.8 compares values computed from equation (2.98) to experimental data, and obviously, the deviation in the results is huge. We will later see how this problem can be resolved by including information about the solvent structure with the help of nonlocal electrostatics.
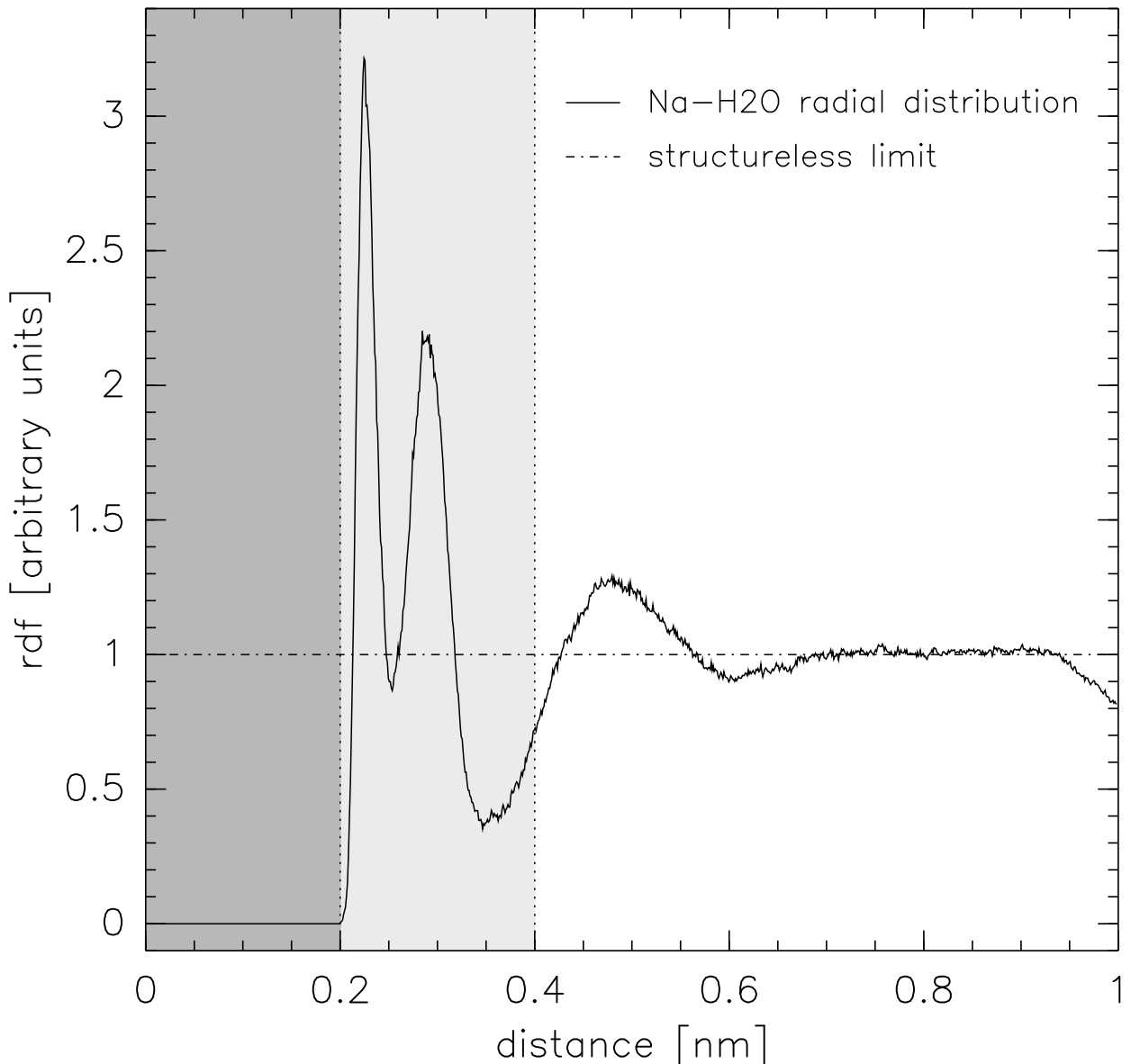
Figure 2.7.: A radial distribution function obtained from a molecular dynamics simulation of a sodium ion in water.

Free Energy of Solvation using Born's Formula

Comparison with Experiment
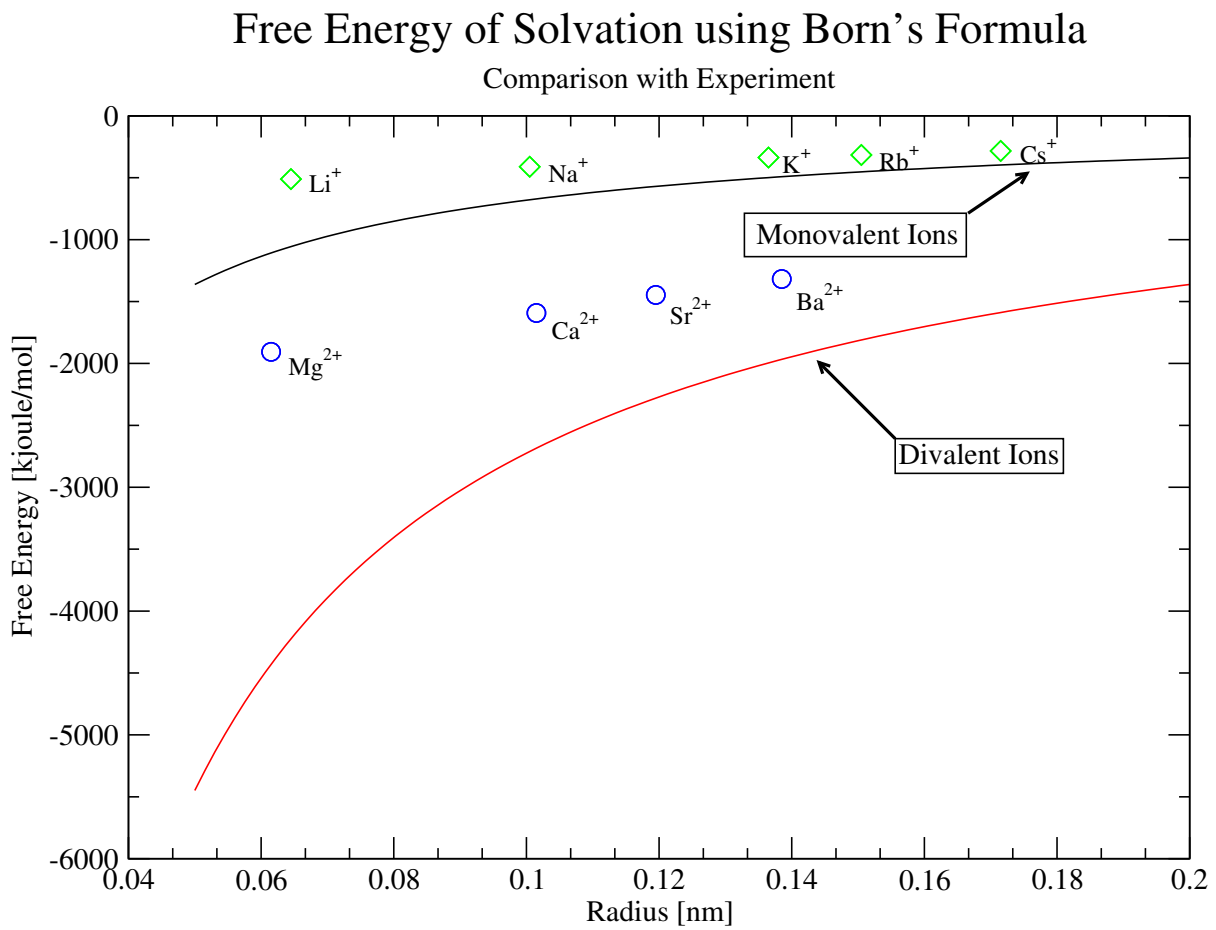
Figure 2.8.: The free energy of solvation in the Born approach. In this plot, symbols are used for experimental values and the curves show the behavior of equation (2.98)

3. The theory of nonlocal electrostatics

In this chapter we will develop the fundamentals of the theory of nonlocal electrostatics. We will show how it arises as a natural extension of local electrostatics, and investigate its classical formulation. We will demonstrate how nonlocal electrostatics is able to resolve several of the deficiencies of a local approach for the computation of electrostatic quantities in water, but we will also explore the computational difficulties the nonlocal approach poses in its well–established form, motivating the need for a novel formulation.

3.1. Water as a structured continuum

In Section 2.7 we have seen that a featureless continuum description of water fails to accurately describe electrostatic systems in solution, and that this might lead to unsatisfying results in solvation computations, therefore posing an obstacle for many possible applications e.g. in bioinformatics. From this problem one could be lead to suppose that the only accurate molecular scale description of electrostatic systems solvated in water would consist in an explicit simulation of the charge distribution and all surrounding water molecules in the area of interest. Unfortunately, the computational complexity of such an approach usually disallows this alternative in many relevant applications. In our opinion, the remedy to this problem is given by combining structural information with the simplicity of a continuum approach into something we call the *structured continuum model*. To this end, it is imperative to understand how structural properties of a solvent influence an electrostatic field.

The water network

Despite the intriguing simplicity of its constituents, water is known to show a very rich structure. The individual water molecules are not independent from each other; instead, they interact via hydrogen bonds and dipole–dipole interactions. Especially the hydrogen bonds lead to a characteristic effect: the formation of the so–called *hydrogen bond network*. Since each hydrogen bond is energetically favorable for the donor and the acceptor of the bond, each water molecule tries to participate in as many bonds as possible simultaneously, acting as a donor (via its hydrogens) and an acceptor (via its oxygen) at the same time. Hydrogen bonds are highly angle– and distance selective, and therefore, because of the random thermal movement of the solvent molecules, the hydrogen bond network is highly dynamic in the sense that individual bonds break, reconnect, or are replaced by others at small time scales.

Neighbouring water molecules in this network "communicate" with each other through their hydrogen bond and, to a smaller degree, through their dipole–dipole interactions. Therefore, rotating one water molecule at position r, its neighbours will feel the urge to rotate as well in order to keep the hydrogen bonds alive and to keep their dipoles aligned. These water molecules in the first shell around the original molecule will now in turn influence *their* neighbours, and thus, the information about the original orientation propagates through the network. It is clear that this information propagation has to decay on a certain characteristic length scale λ: water molecules at opposite sides of an ocean will not feel their mutual presence. But it is well–established that the correlation of water molecules due to the hydrogen bond networks covers several molecule "layers", and therefore, the *correlation length*
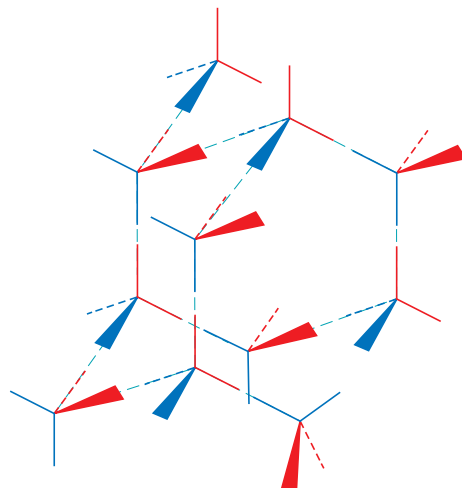
Figure 3.1.: Symbolical picture of the hydrogen bonding network in water.

λ ca be assumed to be on the order of several Ångstroms.

Recalling Section 2.2.5, we can conclude the following: under the influence of an external electric field, the water molecule at position r will try to align its dipole vector with $E(r)$ according to equation (2.31). Through the water network it will try to force the surrounding water to follow its rotation, and this information will propagate through the network, therefore perturbing the orientation of all water molecules in a ball around r with the radius on the order of magnitude λ. But of course, all those water molecules want to align their individual dipole vectors with the external field as well, in turn trying to influence the orientation of their neighbours. The system becomes *frustrated*, since the water molecules are caught between satisfying the hydrogen bonds and dipole–dipole interactions and aligning with the electric field. Keeping the network undisturbed would cost energy through the interactions with the electric field, and aligning all dipoles with the field would in general cost energy because of the loss of hydrogen bonds and unfavorable dipole–dipole interactions, so the system will try to assume an intermediate state between those two extremes.

If the typical length scales of the variation of the electric field are much larger than the correlation length λ, the effect will more or less average out. In this case, the system can be decomposed into several averaging domains in which the field is approximately constant. These domains have of course an average dipole moment, and can turn into the electric field as a whole, aligning their average dipole vector with the external field. Since these domains are large compared to individual molecules, the effects at the domain boundaries can be ignored. In this case, we will recover the large scale local continuum description, with a dielectric shielding of about 78 everywhere in the water.

If on the other hand the electric field varies on length scales on the order of magnitude of λ, as is the case for example for typical biomolecular fields in solution, the frustration effect can not be left out of our considerations. The individual water molecules will no longer be free to rotate as much as they would have to align with the applied field, and therefore the resulting shielding should be lower than the customary 78. To be more precise, the possible degree of rotation for any water molecule at position r is determined by the current state of any other water molecule it interacts with, i.e. all molecules at any other position r', with an interaction strength decaying on the order of λ. Therefore,

a theory including polarization correlations into continuum electrostatics should be what is called a *nonlocal theory*: the properties of the solvent are no longer describable by a simple local function of one spatial argument. Rather, the influences of all other positions r' have to be summed up. Such a theory will therefore be centered around integrals over a quantity of *two* spatial variables r and r'.

It is also clear, which of the functions appearing in electrostatics has to carry the nonlocality. The charge distribution $\rho(r)$, the potential $\varphi(r)$ and the fields $E(r)$ and $D(r)$ are of course *local* quantities. The charge e.g. is either situated at a certain point or not; it does not depend on any other point in the system. The only quantity we have left is the dielectric function $\varepsilon(r)$, which is ideally suited for our task, since it is supposed to describe the response of the medium to an applied field. We can therefore formally denote the transition from local to nonlocal electrostatics by replacing $\varepsilon(r) \mapsto \int_{\mathbb{R}^3} \varepsilon(r, r') dr'$.

3.2. The classical formulation of nonlocal electrostatics

The nonlocal material equations

In Section 2.2.5, we have derived the macroscopic quantity $D(r)$ under the assumption of a linear response of the medium to the applied field $E(r)$, an assumption that still holds in the case of nonlocal electrostatics. We can therefore start with the linear response operator equation (2.40)

$$D(r) = \mathcal{E}(E(r))$$

in order to derive a material equation for nonlocal electrostatics. Recalling that in Section 2.2.5 we replaced the operator $\mathcal{E}$ with the *function* $\varepsilon(r)$, we will now use the identification

$$\mathcal{E}(E(r)) \equiv \varepsilon_0 \int_{\mathbb{R}^3} \varepsilon(r, r') E(r') \, dr'$$

leading to the *material equation of nonlocal electrostatics:*

$$D(r) = \varepsilon_0 \int_{\mathbb{R}^3} \varepsilon(r, r') E(r') \, dr' \tag{3.1}$$

$$= -\varepsilon_0 \int_{\mathbb{R}^3} \varepsilon(r, r') \nabla_{r'} \varphi(r') \, dr' \tag{3.2}$$

The nonlocal Maxwell equations

The role that is played by the fields $E(r)$ and $D(r)$ in nonlocal electrostatics is completely analogous to that in the local framework, and therefore, Maxwell's equations of electrostatics remain unchanged when expressed in terms of these fields:

$$\nabla \cdot D = \rho \tag{3.3}$$

$$\nabla \times E = 0 \tag{3.4}$$

Inserting the nonlocal material equation (3.2) into equation (3.3), we obtain the *nonlocal Poisson equation*:

$$\varepsilon_0 \nabla_r \int_{\mathbb{R}^3} \varepsilon(r, r') \nabla_{r'} \varphi(r') \, dr' = -\rho(r) \tag{3.5}$$

This equation is the nonlocal generalization of the local Poisson equation, equation (2.23).

Boundary conditions for nonlocal electrostatics

Remembering the derivation of the boundary conditions for local electrostatics in Section 2.2.1, we can conclude that all arguments in the derivation of the boundary conditions still hold. Meaning and definition of the field $\boldsymbol{E}(\boldsymbol{r})$ are completely unchanged in nonlocal electrostatics, and in particular, the Maxwell equation (2.6),

$$\boldsymbol{\nabla} \times \boldsymbol{E}(\boldsymbol{r}) = 0$$

still holds. Therefore, the boundary or transmission condition for the tangential component of $\boldsymbol{E}(\boldsymbol{r})$, equation (2.16),

$$(\boldsymbol{E}_2 - \boldsymbol{E}_1) \times \hat{\boldsymbol{n}} = 0 \tag{3.6}$$

must be fulfilled everywhere, which, as we have shown in Section 2.2.2, implies the continuity of the electrostatic potential φ

$$(\varphi_2 - \varphi_1) = 0 \tag{3.7}$$

Similarly, the computations in Section 2.2.4, which established the displacement field $\boldsymbol{D}(\boldsymbol{r})$, deliberately made no use of the local formulation, and since the meaning of $\boldsymbol{D}(\boldsymbol{r})$ is again unchanged in nonlocal electrostatics, we can reuse the results from 2.2.4 and 2.2.1. From equation (3.3),

$$\boldsymbol{\nabla} \cdot \boldsymbol{D} = \rho$$

therefore follows

$$(\boldsymbol{D}_2 - \boldsymbol{D}_1) \cdot \hat{\boldsymbol{n}} = \sigma \tag{3.8}$$

across any surface Γ, where σ is the surface charge density[1] on Γ.

3.3. Nonlocal electrostatics for biomolecules – the nonlocal cavity model

With the equations derived in Section 3.2, we are now able to generalize the cavity model derived in Section 2.3, leading to a description of nonlocal electrostatic phenomena in solution for biomolecules. Using the same notation as in Section 2.3, we model the molecule as a bounded open domain $\Omega \in \mathbb{R}^3$, the surrounding water as $\Sigma := \mathbb{R}^3 \setminus \bar{\Omega}$, and the boundary of the molecule as $\Gamma := \partial\Omega \in \mathcal{C}^{0,1}$, where we assume as in Section 2.3 that the surface charge distribution σ vanishes for all biomolecules, since the molecular surface as such can not be considered an infinitely sharp interface between different media, and therefore the concept of a singular surface charge distribution on Γ could not be justified. We want to emphasize that this assumption of a vanishing charge distribution is no restriction to the generality of the method, and that a given nonvanishing σ can be taken into account without any practical or theoretical difficulties in all further equations.

An important approximation that is always made in the field of nonlocal electrostatics, and that is also in effect in the remainder of this work, is to assume that the interior of the molecule, the domain Ω, can be described by using the classical *local* electrostatics approach[2] (see e.g. [BP96]). This is justified, since the contribution of orientational polarization to the dielectric constant inside the protein can usually be neglected, which can be seen from the fact that ε_Ω for proteins is usually of the order

---

1 It should be kept in mind that ρ and σ only contain the *free* parts of the charge distribution, not the possible influenced multipoles, that are by definition "hidden" in the displacement field $\boldsymbol{D}(\boldsymbol{r})$.

2 In principle at least, a nonlocal interior can be taken into account without additional theoretical complications, but at larger computational cost.

of 2–4, a magnitude that is virtually entirely explained by the dipoles induced in the protein due to its polarizability, without a significant orientational polarization contribution. It is important to realize that this does **not** mean that the potential on the inside would not be influenced by the nonlocal effects on the outside, since the potentials in Ω and Σ are tightly coupled through the boundary conditions (3.8) and (3.6). The nonlocal effects due to the water structure therefore propagate into the protein through the coupling on Γ.

With these conventions we can now assemble the system of equations for the electrostatic potential $\varphi(\boldsymbol{r})$ in the *nonlocal cavity model* that take the role of the *local* system of equations (2.45)

$$
\left.
\begin{aligned}
\Delta\varphi_\Omega(\boldsymbol{r}) &= \frac{-\rho(\boldsymbol{r})}{\varepsilon_0\varepsilon_\Omega} & \boldsymbol{r} &\in \Omega \\[2mm]
\boldsymbol{\nabla}_{\boldsymbol{r}}\int_\Sigma \varepsilon(\boldsymbol{r},\boldsymbol{r}')\boldsymbol{\nabla}_{\boldsymbol{r}'}\varphi_\Sigma(\boldsymbol{r}')\,d\boldsymbol{r}' &= 0 & \boldsymbol{r} &\in \Sigma \\[2mm]
\left[\boldsymbol{\nabla}_{\boldsymbol{r}}(\varepsilon_\Omega\varphi_\Omega(\boldsymbol{r})) - \int_\Sigma \varepsilon(\boldsymbol{r},\boldsymbol{r}')\boldsymbol{\nabla}_{\boldsymbol{r}'}\varphi_\Sigma(\boldsymbol{r}')\,d\boldsymbol{r}'\right]\cdot\hat{\boldsymbol{n}} &= 0 & \boldsymbol{r} &\in \Gamma \\[2mm]
[\varphi_\Omega(\boldsymbol{r}) - \varphi_\Sigma(\boldsymbol{r})] &= 0 & \boldsymbol{r} &\in \Gamma
\end{aligned}
\right\}
\tag{3.9}
$$

For any choice of $\varepsilon(\boldsymbol{r},\boldsymbol{r}')$ other than a single Dirac δ distribution (reducing system (3.9) to the local system (2.45)) or a finite sum of Dirac δ distributions centered at different positions (meaning that the water molecules are correlated only over a discrete set of positions – a clearly useless assumption), equations (3.9) constitute a system of partial integro–differential equations of at least[3] second order, where the integration is performed over a complex domain, with a complicated integro–differential boundary condition. These kinds of systems are in general extremely hard to interpret, understand, and solve.

Considerable efforts have been put into the study of nonlocal electrostatics in this classical formulation, and in the investigation of system (3.9) [DKKU85, BP96, BP98a, BP98b, KRV78a, KRV78b, Sut99, Hil02]. Due to the enormous complexity of system (3.9), and due to the overwhelming challenges arising when looking for analytical or numerical solutions, all previous approaches have only been applied successfully to trivial geometries, i.e. to domains Ω of a simple form. The most important examples include spherical domains, cylindrical domains, and the semi–infinite halfspace. Since even in those cases, solving equations (3.9) is highly involved, several researchers have proposed approximations that were designed to turn the system into something more accessible to mathematical means, but none of these was able to extend the range of possible model domains Ω. Due to these seemingly fundamental problems, the field of nonlocal electrostatics lay dormant for several years, the latest important contribution probably being the paper by Basilevsky and Parsons [BP98b], which appeared in 1998. In the remainder of this work, we will present an equivalent reformulation of system (3.9) much more suited for analytical *and* numerical treatment as well as for physical interpretation, and a numerical scheme for its efficient solution. This numerical method will allow to consider all domains Ω whose boundary can be described by a finite set of *boundary elements*, meaning in our case flat triangles. In practice, the limit of applicability is only determined by memory constraints due to the current non–optimal handling of the system matrices, which will be greatly improved in the near future, and by some quality requirements on the surface like the non–degeneracy of all triangles. But before we can present this main result of our work, we will have to address a question we previously left out deliberately, namely that of a sensible choice for $\varepsilon(\boldsymbol{r},\boldsymbol{r}')$.

---

3 Depending on the exact choice of $\varepsilon(\boldsymbol{r},\boldsymbol{r}')$.

3.4. The nonlocal dielectric function of water

The nonlocal dielectric function of water describes – by definition – the correlation between water molecules situated at position r and r', respectively, and is therefore in a way the basis for any nonlocal treatment of structurally related electrostatic effects in water. Consequently, a considerable amount of work has been devoted to elucidating its characteristics and to developing a – possibly approximate – functional expression for $\varepsilon(r, r')$ as a function of r, r', and the correlation length λ, of which we know from our considerations in Section 3.1 that it has to enter the description. This fundamental question has not been solved completely yet, and in the literature, differing functions have been proposed.

Far from the boundary of the domain Ω, the dielectric response $\varepsilon(r, r')$ of the system will be isotropic in nature since there are no preferred directions in the bulk medium. To simplify further computations, it is thus typically assumed that this isotropy of the dielectric function holds everywhere in Σ, and thus, $\varepsilon(r, r') \equiv \varepsilon(r - r')$. While we will adopt this common approximation throughout this thesis, we want to point out that the use of more general expressions for $\varepsilon(r, r')$ is still possible in our approach, and will only lead to a different set of final equations. In a series of papers, and in the PhD–thesis of Godehard Sutmann [Sut99], Alexei Kornyshev and collaborators tried to derive $\varepsilon(r, r')$ – or the Fourier transform $\hat{\varepsilon}(k)$ of this function with respect to $r - r'$ – from molecular dynamics simulations by virtue of the *theorem of fluctuations and dissipations*, coupling correlation functions to the dynamical behaviour of a system [Sut99, KS99, BKS96, KS97]. The results of these considerations led them to propose an $\hat{\varepsilon}(k)$, showing two divergences at wavelengths $k_1 \approx 1$ Å and $k_2 \approx 12.5$ Å, and $\hat{\varepsilon}(k) < -1.0 \,\forall\, k_1 < k < k_2$. That the Fourier transform of the dielectric function in this model is negative in a certain wave vector interval has a severe consequence: individual Fourier components of the electrostatic potential acquire a sign opposite to that in a local setting, and therefore, the electrostatic potential φ of an external charge distribution $\rho(r)$ will show *oscillations about zero* when regarded as a function of distance $r := \|r\|$, and these oscillations depend sensitively on the details of the Fourier transform $\rho(k)$ of the charge distribution. This astonishing result has been termed the *overscreening effect*, and leads to clearly unphysical results for the potential of point charges [Sut99].

This overscreening effect and the occurrence of divergences in the dielectric function seem to contradict traditionally held beliefs about any dielectric response, and might therefore be an unphysical artifact of the computational techniques involved in its determination. This assumption is supported e.g. by the details of the molecular dynamics simulations that were used to compute $\hat{\varepsilon}(k)$ by means of the theorem of fluctuations and dissipations: according to [Sut99], the simulations that were carried out covered only 200 water molecules in a box with 18.1 Å long edges, since simulations on a larger scale were infeasible at the time. This is problematic at least, since the correlation length we typically observed, and which seems consistent with experimental data[4] is on the order of 15–22 Å, and therefore the simulation would be expected to yield erroneous results by "cutting off" correlations. Another point of discussion has been the employed water model – the so–called BJH water [BJH83, JBH84] – which even seems to fail to reproduce some of the large–scale behaviour of the dielectric response function, and it is not clear a–priori whether it can be trusted on a microscopic scale. For an investigation of the dielectric properties of BJH water see for example [THH93].

For these reasons, most researchers prefer different, simpler models consistent with the physical intuition. The effects proposed by Kornyshev and collaborators are either ignored as unphysical artifacts, or considered as higher order effects, either not playing a role in real applications or being in turn suppressed by other effects neglected by Kornyshev et al. Such higher order effects could in principle be in-

---

[4] We will discuss this point in more detail in a later section.

cluded in such simpler models, should the need arise. The basic model ubiquitous in most articles is the *Lorentzian model*, for which $\hat{\varepsilon}(\boldsymbol{k})$ is based on a Lorentzian curve (see e.g. [THH93, RWRG92, BP96]). In [Net99], a field–theoretic approach is used to derive a different model for the nonlocal dielectric function showing very similar behaviour[5] to the Lorentzian model.

In [Hil02], we have discussed the model building process for $\varepsilon(\boldsymbol{r}, \boldsymbol{r}')$ in detail. In this work, we have proposed a number of constraints that should be fulfilled by any physically sound model for $\varepsilon(\boldsymbol{r}, \boldsymbol{r}')$, and have provided a class of functions consistent with them, including a special Lorentzian curve, very similar to those appearing in earlier work. In the following, we will briefly introduce those constraints and will derive the Lorentzian model for $\varepsilon(\boldsymbol{r}, \boldsymbol{r}')$.

3.4.1. Constraints on the nonlocal dielectric function

The classes of possible models for the dielectric function of water can be restricted to those consistent with fundamental physical principles, like the laws of causality. We will now shortly discuss a small set of such constraints which we consider elementary for all models for $\varepsilon(\boldsymbol{r}, \boldsymbol{r}')$.

Causality of the response function

In full generality, the Fourier transform $\hat{\varepsilon}(\boldsymbol{k})$ of the dielectric function might be complex valued, and have an additional dependency on frequency ω: $\varepsilon = \hat{\varepsilon}(\boldsymbol{k}, \omega)$. In this case, the *real part* $\Re(\hat{\varepsilon}(\boldsymbol{k}))$ is responsible for the dielectric shielding effect discussed in Section 2.2.4, while the *imaginary part* $\Im(\hat{\varepsilon}(\boldsymbol{k}))$ is related to an effect we did not discuss yet, since it typically can be ignored in static situations and is only of importance for fields varying in time, namely the excitation of internal degrees of freedom in the solvent. Of course, this excitation requires a source of energy, and this source is the electric field of the charge distribution. This loss of energy can easily be computed from the imaginary part of $\hat{\varepsilon}(\boldsymbol{k})$ (see e.g. [Rei80]), and is found to be given by the *dielectric susceptibility*:[6]

$$\hat{\chi}(\boldsymbol{k}, \omega) := 1 - \frac{1}{\sqrt{2\pi}^3 \hat{\varepsilon}(\boldsymbol{k}, \omega)}$$

The frequency dependence will not be used in our considerations, since we are only dealing with static electric fields, such that in all computations $\hat{\varepsilon}(\boldsymbol{k}, \omega)$ reduces to $\hat{\varepsilon}(\boldsymbol{k}, \omega = 0) =: \hat{\varepsilon}(\boldsymbol{k})$. This also means that we will be able to neglect the dielectric loss effects, and will therefore work with dielectric functions $\hat{\varepsilon}(\boldsymbol{k})$ having only *real* Fourier components, which is our first constraint.

Nonetheless, the hypothetical existence of *any* frequency dependence of the dielectric function, whether or not we make use of it, astonishingly has another important consequence. Any dielectric function has to be consistent with the fundamental *law of causality*, which – roughly speaking – states that effects do not happen before their cause. The remarkable theorem of Kramers [Kra26] and Kronig [Kro26] establishes a relationship between the real and the imaginary part of the Fourier transform of any linear causal function (see e.g. [Rei80]), and in our case yields [Sut99]:

$$\Re(\hat{\chi}(\boldsymbol{k}, \omega)) = 1 - \frac{\Re(\hat{\varepsilon}(\boldsymbol{k}, \omega))}{|\hat{\varepsilon}(\boldsymbol{k}, \omega)|^2} = \frac{2}{\pi} \int_0^\infty \frac{\omega'}{\omega'^2 - \omega^2} \frac{\Im(\hat{\varepsilon}(\boldsymbol{k}, \omega'))}{|\hat{\varepsilon}(\boldsymbol{k}, \omega')|^2} \, d\omega' \tag{3.10}$$

---

5 While this model and the Lorentzian one differ for large Fourier components, the behaviour is similar enough that the Lorentzian model can at least be seen as a good approximation of the model of Netz.

6 This quantity should not be confused with the *dielectric response* χ_e introduced in Section 2.2.5

3. The theory of nonlocal electrostatics

In the static case, $\hat{\varepsilon}(\boldsymbol{k}) = \hat{\varepsilon}(\boldsymbol{k}, \omega = 0)$, the corresponding relation can be found by frequency integration of the imaginary part [Sut99]:

$$\hat{\chi}(\boldsymbol{k}) = 1 - \frac{1}{\sqrt{2\pi}^3 \hat{\varepsilon}(\boldsymbol{k})} = \frac{2}{\pi} \int\limits_0^\infty \frac{d\omega}{\omega} \frac{\Im(\hat{\varepsilon}(\boldsymbol{k}, \omega))}{|\hat{\varepsilon}(\boldsymbol{k}, \omega)|^2} \tag{3.11}$$

Thermodynamic stability

Thermodynamic stability demands, that the energy loss is positive semi definite, since otherwise, energy could be created, and the system would keep producing energy without ever reaching a stable state. From the right hand side of equation (3.11), it can be concluded [DKM81] that this requires $\chi(\boldsymbol{k}) > 0$, which, in conjunction with equation (3.11) implies that thermodynamic stability can only be achieved for $\hat{\varepsilon}(\boldsymbol{k}) > \frac{1}{\sqrt{2\pi}^3}$ or $\hat{\varepsilon}(\boldsymbol{k}) < 0$. This is the second constraint on any dielectric function.

Behaviour for high wave numbers

For electric fields with fast spatial oscillations, i.e. significant components of $\boldsymbol{E}(\boldsymbol{k})$ for large values of $\|\boldsymbol{k}\|$, the solvent molecules will not be able to follow the external excitation, and therefore, the rotational polarization should be lost in the limit[7]

$$\varepsilon_\infty := \frac{1}{\sqrt{2\pi}^3} \lim_{\|\boldsymbol{k}\| \to \infty} \hat{\varepsilon}(\boldsymbol{k})$$

It has often been argued that in this limit of infinitely "fast" oscillations, the solvent will show no reaction whatsoever to the applied field, since it "has no time to react[8]", and consequently, many authors set $\varepsilon_\infty = 1$ [LL84]. Especially in later works it has been argued, though, that internal degrees of freedom of the water molecules will still lead to a finite reaction, even for $\|k\| \to \infty$. In those cases, $\varepsilon_\infty \neq 1$. Usually, ε_∞ is then taken to be equal to the square of the refractive index: $\varepsilon_\infty \approx 1.33^2 \approx 1.8$ [Sut99, Has73]. We will therefore demand that any model for the dielectric function of water reduces to a finite constant ε_∞ in the limit $\|k\| \to \infty$, and will allow both choices.

Dependence on the correlation length

In Section 3.1, we have argued the existence of a typical length scale λ for the polarization correlations. Of course, this length scale must be reflected somehow in the functional expression for $\varepsilon(\boldsymbol{r}, \boldsymbol{r}')$. We therefore demand that $\varepsilon = \varepsilon(\boldsymbol{r}, \boldsymbol{r}', \lambda)$, but will in the following usually suppress the explicit dependence on λ in the notation, since the correlation length is not assumed to be a variable quantity.

Reproduction of the local limit

Local continuum electrostatics is a very successful and well–established theory for many applications, that just breaks down when the length scales of the system under consideration are comparable to the correlation length. Since the correlation length describes the range of the polarization correlations that lead to the deviation from the local results, we would expect to recover the local behaviour in the limit of $\lambda \to 0$, i.e. in the limit when there is no correlation between different molecules. If this is realized in the model, it is easy to see that the local theory of electrostatics is in fact contained in our theory, since for length scales large compared to the correlation length, the system behaves as in the limit $\lambda \to 0$. Therefore we have proposed in [Hil02] to include this reduction to the local limit into our

---

7 The appearance of the factor $\sqrt{2\pi}^{-3}$ is due to the symmetric normalization of the Fourier transform employed in this work.

8 These arguments have been put in apostrophes since the oscillations are spatial, not temporal in nature.

set of constraints: any model for $\varepsilon(\boldsymbol{r}, \boldsymbol{r}', \lambda)$ should reduce to the limit of local electrostatics for $\lambda \to 0$.

So what does it mean for a dielectric function to *reduce to the local limit*? In the equations of nonlocal electrostatics, $\varepsilon(\boldsymbol{r}, \boldsymbol{r}')$ appears as a spatial integral kernel, while in the local equations, no integrals are present. The local limit can therefore only be obtained from the nonlocal equations, if, for $\lambda \to 0$, $\varepsilon(\boldsymbol{r}, \boldsymbol{r}', \lambda)$ reduces integrals to the value of the integrand at a single point. Exactly this behaviour is what is commonly used to define the Dirac δ–distribution. For a concise treatment and for its definition, please refer to Appendix B.

To illustrate this, we will have a look at equation (3.2),

$$\boldsymbol{D}^{\mathrm{nl}}(\boldsymbol{r}) = -\varepsilon_0 \int_{\mathbb{R}^3} \varepsilon(\boldsymbol{r}, \boldsymbol{r}', \lambda) \boldsymbol{\nabla}_{\boldsymbol{r}'} \varphi(\boldsymbol{r}') \, d\boldsymbol{r}'$$

which is the nonlocal equivalent of

$$\boldsymbol{D}^{\mathrm{loc}}(\boldsymbol{r}) = \varepsilon_0 \varepsilon(\boldsymbol{r}) \boldsymbol{E}(\boldsymbol{r}) = -\varepsilon_0 \varepsilon_\Sigma \boldsymbol{\nabla}_{\boldsymbol{r}} \varphi(\boldsymbol{r})$$

where ε_Σ is the macroscopic dielectric constant of water. Using equation (B.2),

$$\int_\Sigma \delta(\boldsymbol{r} - \boldsymbol{r}') \varphi(\boldsymbol{r}') \, dx' = \varphi(\boldsymbol{r}) \quad \text{iff } \boldsymbol{r} \in \Sigma$$

we see that, in order to recover the local limit for $\lambda \to 0$, $\varepsilon(\boldsymbol{r}, \boldsymbol{r}', \lambda)$ must reduce to a Dirac δ–distribution times the macroscopic dielectric constant[9]. Therefore, our last requirement on any nonlocal dielectric function $\varepsilon(\boldsymbol{r}, \boldsymbol{r}', \lambda)$ is that it needs to fulfill

$$\lim_{\lambda \to 0} \varepsilon(\boldsymbol{r}, \boldsymbol{r}', \lambda) = \varepsilon_\Sigma \delta(\boldsymbol{r} - \boldsymbol{r}') \tag{3.12}$$

Assumptions on the dielectric constant – homogeneity and isotropy

In full generality, the nonlocal dielectric response might be a very complicated function of both spatial arguments $\boldsymbol{r}$ and $\boldsymbol{r}'$, that can in principle even depend on *direction*. In that case, $\varepsilon(\boldsymbol{r}, \boldsymbol{r}')$ will be a *tensorial quantity* with components $\varepsilon_{ij}(\boldsymbol{r}, \boldsymbol{r}')$. Fortunately, in the case of the electrostatics of biomolecules it is possible to assume homogeneity as well as isotropy, meaning that the *correlation properties* of the water, the way the water molecules communicate with each other, do not depend on position and direction. It does **not** mean, though, that this is equivalent to assuming that water was an isotropic and homogeneous medium as in the case of local electrostatics: the mere existence of the nonlocal dielectric response leads to an inhomogeneous behaviour.

Homogeneity of the nonlocal dielectric function amounts to the statement, that the correlation of two water molecules anywhere in the system only depends on their *distance vector* $\boldsymbol{r} - \boldsymbol{r}'$, not on their *absolute position* inside Σ: $\varepsilon(\boldsymbol{r}, \boldsymbol{r}') = \varepsilon(\boldsymbol{r} - \boldsymbol{r}')$. Isotropy of $\varepsilon(\boldsymbol{r}, \boldsymbol{r}')$ tells us, that we can reduce the tensorial quantity $\varepsilon_{ij}(\boldsymbol{r} - \boldsymbol{r}')$ to a scalar function $\varepsilon(\boldsymbol{r} - \boldsymbol{r}')$, since the correlation does not depend on the direction. For nonmagnetic media and electro*static* situations we can also conclude that the direction of the distance vector between two molecules $\boldsymbol{r} - \boldsymbol{r}'$ will not affect their correlation, and therefore we can further assume $\varepsilon(\boldsymbol{r} - \boldsymbol{r}') = \varepsilon(|(\boldsymbol{r} - \boldsymbol{r}')|)$.

---

9 The generalization to the case of a local dielectric *function* instead of a *constant*, equation (2.41), is straightforward: we just have to replace the constant ε_Σ by the function $\varepsilon(\boldsymbol{r})$.

These conditions might not be strictly fulfilled e.g. close to the boundary Γ, but for the remainder of this work we can assume all inhomogeneous and anisotropic effects as negligible higher order terms, and therefore will only consider dielectric functions of the form $\varepsilon(|\boldsymbol{r} - \boldsymbol{r}'|)$. An introduction into the discussion of the validity of this approach can e.g. be found in [Sut99] and [KRV78a].

3.4.2. The Lorentzian model for the nonlocal dielectric function of water

In [Hil02], we have provided a class of several functions fulfilling all of the constraints derived in Section 3.4.1. In this section, we will briefly show how to derive the most important member of this class, which will be the model we will use in the remainder of this work, and which – with slightly modified details – was also proposed by other researchers because of different considerations [DKKU85, RWRG92, BP96]: the so–called *Lorentzian model*. This model has its name from the functional expression of its Fourier transform $\hat{\varepsilon}(\boldsymbol{k})$, and is one of the simplest possible models consistent with all the requirements of Section 3.4.1.

Since maintaining the correlations over a distance costs energy, the dielectric function $\varepsilon(|\boldsymbol{r} - \boldsymbol{r}'|)$ necessarily has to decay on a certain characteristic length scale λ, the correlation length of the system. One of the simplest and most important types of decay in physics – especially in screened electrostatics – is of so–called *Yukawa*–type, with a functional expression of the form $\propto \dfrac{e^{-\frac{|\boldsymbol{r}-\boldsymbol{r}'|}{\lambda}}}{|\boldsymbol{r}-\boldsymbol{r}'|}$.

In order to derive the complete expression for the exponential model, we first have to remember that the local limit should be recovered for $\lambda \to 0$, or for the case where the relevant length scales of the system are much greater than λ. For this to hold, the integral over $\varepsilon(|\boldsymbol{r} - \boldsymbol{r}'|)$ must equal the macroscopic value of the dielectric constant, ε_Σ, i.e. with $\varrho := |\boldsymbol{r} - \boldsymbol{r}'|$:

$$\int_\Sigma \varepsilon(\varrho)d\varrho = \varepsilon_\Sigma \tag{3.13}$$

This must hold for *arbitrary* choices of Σ fulfilling the smoothness conditions on Γ, and therefore also for $\Sigma := \mathbb{R}^3$. In this case, we have (c.f. Appendix A):

$$\int_{\mathbb{R}^3} \varepsilon(\varrho)d\varrho = \int_{\mathbb{R}^3} \varepsilon(\varrho)e^0 d\varrho \tag{3.14}$$

$$= \int_{\mathbb{R}^3} \varepsilon(\varrho)e^{i(\boldsymbol{0}\cdot\boldsymbol{\varrho})}d\varrho \tag{3.15}$$

$$= \sqrt{2\pi}^3 \hat{\varepsilon}(k=0) \tag{3.16}$$

$$\underset{(3.13)}{=} \varepsilon_\Sigma \tag{3.17}$$

From this computation we therefore obtain for any model $\varepsilon(|\boldsymbol{r} - \boldsymbol{r}'|)$ with Fourier transform $\hat{\varepsilon}(k)$:

$$\hat{\varepsilon}(k=0) = \frac{\varepsilon_\Sigma}{\sqrt{2\pi}^3} \tag{3.18}$$

According to Appendix A, the Fourier transform of $f(r) := \dfrac{e^{-\frac{r}{\lambda}}}{r}$ can be computed – due to its radial symmetry – from equation (A.12):

$$\hat{f}(k) = \sqrt{\frac{2}{\pi}} \int_0^\infty dr\, r^2 f(r) \frac{\sin(kr)}{kr}$$

And therefore we have

$$\mathcal{FT}[f(r)] = \hat{f}(k) \tag{3.19}$$

$$= \sqrt{\frac{2}{\pi}} \int\limits_{0}^{\infty} dr \, r^2 f(r) \frac{\sin(kr)}{kr}$$

$$= \sqrt{\frac{2}{\pi}} \int\limits_{0}^{\infty} dr \, \not{r}^2 \frac{e^{-\frac{r}{\lambda}}}{\not{r}} \frac{\sin(kr)}{k\not{r}}$$

$$= \sqrt{\frac{2}{\pi}} \frac{1}{k} \int\limits_{0}^{\infty} dr \, \underbrace{e^{-\frac{r}{\lambda}}}_{v'} \underbrace{\sin(kr)}_{u}$$

$$\overset{\text{P.I.}}{=} \sqrt{\frac{2}{\pi}} \frac{\lambda}{k} \left\{ - \left[e^{-\frac{r}{\lambda}} \sin(kr) \right]_0^\infty + k \int\limits_{0}^{\infty} dr \, \underbrace{e^{-\frac{r}{\lambda}}}_{v'} \underbrace{\cos(kr)}_{u} \right\}$$

$$\overset{\text{P.I.}}{=} -\sqrt{\frac{2}{\pi}} \frac{\lambda}{k} \left\{ \left[e^{-\frac{r}{\lambda}} \sin(kr) \right]_0^\infty + k\lambda \left[e^{-\frac{r}{\lambda}} \cos(kr) \right]_0^\infty \right.$$

$$\left. + k^2 \lambda \int\limits_{0}^{\infty} dr \, e^{-\frac{r}{\lambda}} \sin(kr) \right\}$$

$$= -\sqrt{\frac{2}{\pi}} \frac{\lambda}{k} \left\{ \left[e^{-\frac{r}{\lambda}} \left\{ \sin(kr) + (k\lambda) \cos(kr) \right\} \right]_0^\infty \right.$$

$$\left. + k^2 \lambda \int\limits_{0}^{\infty} dr \, e^{-\frac{r}{\lambda}} \sin(kr) \right\}$$

$$\Leftrightarrow \quad \sqrt{\frac{2}{\pi}} \frac{1}{k} \int\limits_{0}^{\infty} dr \, e^{-\frac{r}{\lambda}} \sin(kr) = -\sqrt{\frac{2}{\pi}} \frac{1}{k} k^2 \lambda^2 \int\limits_{0}^{\infty} dr \, e^{-\frac{r}{\lambda}} \sin(kr)$$

$$- \sqrt{\frac{2}{\pi}} \frac{\lambda}{k} \left[e^{-\frac{r}{\lambda}} \left\{ \sin(kr) + (k\lambda) \cos(kr) \right\} \right]_0^\infty$$

$$\Leftrightarrow \left(1 + (k\lambda)^2 \right) \sqrt{\frac{2}{\pi}} \frac{1}{k} \int\limits_{0}^{\infty} dr \, e^{-\frac{r}{\lambda}} \sin(kr) = -\sqrt{\frac{2}{\pi}} \frac{\lambda}{k} \left[e^{-\frac{r}{\lambda}} \left\{ \sin(kr) + (k\lambda) \cos(kr) \right\} \right]_0^\infty$$

$$\Leftrightarrow \quad \sqrt{\frac{2}{\pi}} \frac{1}{k} \int\limits_{0}^{\infty} dr \, e^{-\frac{r}{\lambda}} \sin(kr) = \sqrt{\frac{2}{\pi}} \frac{-\lambda}{k(1 + \lambda^2 k^2)} \times \left\{ \lim_{r \to \infty} \underbrace{e^{-\frac{r}{\lambda}} \sin(kr)}_{\to 0} \right.$$

$$+ \lim_{r \to \infty} \underbrace{e^{-\frac{r}{\lambda}} (k\lambda) \cos(kr)}_{\to 0}$$

$$- \lim_{r \to 0} \underbrace{e^{-\frac{r}{\lambda}} \sin(kr)}_{\to 0}$$

$$\left. + \lim_{r \to 0} \underbrace{e^{-\frac{r}{\lambda}} (k\lambda) \cos(kr)}_{\to -(k\lambda)} \right\}$$

45

3. The theory of nonlocal electrostatics

$$\Leftrightarrow \qquad \sqrt{\frac{2}{\pi}}\frac{1}{k}\int\limits_0^\infty dr\, e^{-\frac{r}{\lambda}}\sin(kr) \;=\; \sqrt{\frac{2}{\pi}}\frac{\lambda^2}{1+\lambda^2 k^2}$$

And thus, according to equation (3.19), we obtain

$$\mathcal{FT}\left[f(r)\right] = \hat{f}(k) = \sqrt{\frac{2}{\pi}}\frac{\lambda^2}{1+\lambda^2 k^2} \tag{3.20}$$

From equation (3.20), we can easily figure out how to fulfill requirement (3.18) for the Lorentzian model. Since

$$f(k=0) = \sqrt{\frac{2}{\pi}}\lambda^2$$

and

$$\varepsilon(k=0) \overset{!}{=} \frac{\varepsilon_\Sigma}{\sqrt{2\pi}^3}$$

our first guess for a Lorentzian–type model for $\varepsilon(|\boldsymbol{r}-\boldsymbol{r}'|)$ is given by

$$\begin{aligned}
\varepsilon(|\boldsymbol{r}-\boldsymbol{r}'|) &= f(|\boldsymbol{r}-\boldsymbol{r}'|)\frac{1}{\lambda^2}\sqrt{\frac{\pi}{2}}\frac{\varepsilon_\Sigma}{\sqrt{2\pi}^3} \\
&= f(|\boldsymbol{r}-\boldsymbol{r}'|)\frac{\varepsilon_\Sigma}{4\pi}\frac{1}{\lambda^2} \\
&= \frac{\varepsilon_\Sigma}{4\pi\lambda^2}\frac{e^{-\frac{|\boldsymbol{r}-\boldsymbol{r}'|}{\lambda}}}{|\boldsymbol{r}-\boldsymbol{r}'|}
\end{aligned} \tag{3.21}$$

While equation (3.21) in fact fulfills requirement (3.18), and therefore also the constraint of the reduction to the local limit for $\lambda \to 0$ (to see this, just remember that for $\lambda \to 0$, $\hat{\varepsilon}(k) = \frac{\varepsilon_\Sigma}{\sqrt{2\pi}^3}\frac{1}{1+\lambda^2 k^2}$ is a constant, and therefore $\lim_{\lambda\to 0}\varepsilon(|\boldsymbol{r}-\boldsymbol{r}'|) = \varepsilon_\Sigma\delta(\boldsymbol{r}-\boldsymbol{r}')$). Unfortunately, the behaviour for high wave vectors $k \to \infty$ is not yet consistent with our constraints, since

$$\lim_{k\to\infty}\frac{\varepsilon_\Sigma}{\sqrt{2\pi}^3}\frac{1}{1+\lambda^2 k^2} = 0 \neq \frac{\varepsilon_\infty}{\sqrt{2\pi}^3}$$

Of course the high–k limit can easily be corrected to yield ε_∞ by just adding the term $\frac{\varepsilon_\infty}{\sqrt{2\pi}^3}$ to the Fourier transform $\hat{\varepsilon}(k)$ of $\varepsilon(|\boldsymbol{r}-\boldsymbol{r}'|)$, which is equivalent of adding the term $\varepsilon_\infty\delta(\boldsymbol{r}-\boldsymbol{r}')$ to $\varepsilon(|\boldsymbol{r}-\boldsymbol{r}'|)$, but it is easy to see that this term breaks the correct low–λ behaviour, since

$$\lim_{\lambda\to 0}\left(\frac{\varepsilon_\infty}{\sqrt{2\pi}^3} + \frac{\varepsilon_\Sigma}{\sqrt{2\pi}^3}\frac{1}{1+\lambda^2 k^2}\right) = \frac{\varepsilon_\infty + \varepsilon_\Sigma}{\sqrt{2\pi}^3} \neq \frac{\varepsilon_\Sigma}{\sqrt{2\pi}^3}$$

This in turn can be repaired without touching the high–k limit by making the replacement $\varepsilon_\Sigma \to \varepsilon_\Sigma - \varepsilon_\infty$.

Theorem 3.4.1 (Validity of the Lorentzian model). *The Lorentzian model for the nonlocal dielectric function of water given by*

$$\hat{\varepsilon}(k) = \frac{1}{\sqrt{2\pi}^3}\left\{\varepsilon_\infty + \frac{\varepsilon_\Sigma - \varepsilon_\infty}{1+\lambda^2 k^2}\right\} \tag{3.22}$$

$$\varepsilon(|\boldsymbol{r}-\boldsymbol{r}'|) = \varepsilon_\infty\delta(\boldsymbol{r}-\boldsymbol{r}') + \frac{\varepsilon_\Sigma - \varepsilon_\infty}{4\pi\lambda^2}\frac{e^{-\frac{|\boldsymbol{r}-\boldsymbol{r}'|}{\lambda}}}{|\boldsymbol{r}-\boldsymbol{r}'|} \tag{3.23}$$

is a valid model in the sense that is consistent with all constraints developed in Section 3.4.1.

Proof.

- As can be seen from equation (3.22), the Lorentzian model obviously has only real Fourier coefficients as demanded by the first constraint (no loss of energy in the medium).

- Since $\varepsilon_\infty \geq 1$, and since $\frac{\varepsilon_\Sigma - \varepsilon_\infty}{1+\lambda^2 k^2} > 0$ for finite k, $\hat{\varepsilon}(k) > \frac{1}{\sqrt{2\pi}^3}$ as demanded by the second constraint (thermodynamic stability).

- $\lim_{k \to \infty} \hat{\varepsilon}(k) = \frac{\varepsilon_\infty}{\sqrt{2\pi}^3}$ as demanded by the third constraint (high–k behaviour).

- The correlation length λ is included as a parameter in $\varepsilon(|\boldsymbol{r} - \boldsymbol{r}'|)$ (dependence on the correlation length).

- The fourth constraint, equivalent to equation (3.18), is obviously fulfilled (reproduction of the local limit). □

Remark 3.4.1 *(Nonlocal electrostatics for the Lorentzian model).* For the Lorentzian model (3.23) of the nonlocal dielectric function of water, and with the definition

$$\tilde{\varepsilon} := \frac{\varepsilon_\Sigma - \varepsilon_\infty}{\lambda^2}$$

the classical formulation of the equations of nonlocal electrostatics, (3.9), become:

$$\left. \begin{aligned} \varepsilon_0 \varepsilon_\Omega \Delta \varphi_\Omega(\boldsymbol{r}) + \rho(\boldsymbol{r}) = 0 \quad & \boldsymbol{r} \in \Omega \\ \varepsilon_\infty \Delta \varphi_\Sigma(\boldsymbol{r}) + \tilde{\varepsilon} \, \boldsymbol{\nabla}_{\boldsymbol{r}} \int_\Sigma \frac{1}{4\pi} \frac{e^{-\frac{|\boldsymbol{r}-\boldsymbol{r}'|}{\lambda}}}{|\boldsymbol{r}-\boldsymbol{r}'|} \boldsymbol{\nabla}_{\boldsymbol{r}'} \varphi_\Sigma(\boldsymbol{r}') \, d\boldsymbol{r}' = 0 \quad & \boldsymbol{r} \in \Sigma \\ \left[\varepsilon_\Omega \boldsymbol{\nabla} \varphi_\Omega(\boldsymbol{r}) - \varepsilon_\infty \boldsymbol{\nabla} \varphi_\Sigma(\boldsymbol{r}) - \tilde{\varepsilon} \int_\Sigma \frac{1}{4\pi} \frac{e^{-\frac{|\boldsymbol{r}-\boldsymbol{r}'|}{\lambda}}}{|\boldsymbol{r}-\boldsymbol{r}'|} \boldsymbol{\nabla}_{\boldsymbol{r}'} \varphi_\Sigma(\boldsymbol{r}') \, d\boldsymbol{r}' \right] \cdot \hat{\boldsymbol{n}} = 0 \quad & \boldsymbol{r} \in \Gamma \\ [\varphi_\Omega(\boldsymbol{r}) - \varphi_\Sigma(\boldsymbol{r})] = 0 \quad & \boldsymbol{r} \in \Gamma \end{aligned} \right\} \tag{3.24}$$

3.5. Spherically symmetric systems

In this section, we will demonstrate how nonlocal electrostatics and our Lorentzian model for the nonlocal dielectric function of water can be applied to the case of spherically symmetric systems, one of the few geometries for which we can find analytical solutions in the classical formulation of the equations. Systems possessing spherical symmetry can serve as models for ions, and therefore we will be able to compute the free energy of solvation of simple ions, and thus provide a first comparison of results obtained from nonlocal electrostatics with experiment.

3.5.1. Monoatomic ions

In a way, monoatomic ions are very complicated systems, since a detailed understanding is only possible in the framework of quantum mechanics. For the purposes of solvation computations, though, it turns out that a very simple model is usually sufficiently accurate, namely that of a spherical domain with a point charge located at its center, or, equivalently, a charged conducting spherical shell. Since there is no medium *inside* the ion, its dielectric constant ε_Ω is equal to that of vacuum: $\varepsilon_\Omega = 1$. This model is called the *Born model*.

3. The theory of nonlocal electrostatics

The Born model for monoatomic ions

Let

$$\mathcal{B}_R(\boldsymbol{r}) := \left\{ \boldsymbol{r}' \in \mathbb{R}^3 \ \middle| \ \|\boldsymbol{r} - \boldsymbol{r}'\| < R \right\} \tag{3.25}$$

denote the *open ball* of radius R centered around $\boldsymbol{r}' \in \mathbb{R}^3$, and let

$$\mathcal{S}_R^2(\boldsymbol{r}) := \left\{ \boldsymbol{r}' \in \mathbb{R}^3 \ \middle| \ \|\boldsymbol{r} - \boldsymbol{r}'\| = R \right\} \tag{3.26}$$

the *sphere* of radius R, also centered around $\boldsymbol{r}' \in \mathbb{R}^3$. Then we obviously have

$$\partial \mathcal{B}_R(\boldsymbol{r}) = \mathcal{S}_R^2(\boldsymbol{r})$$

With these definitions, a simple *cavity model* for a monoatomic ion with charge q and radius a, which is centered at position $\boldsymbol{r} = \boldsymbol{0} \in \mathbb{R}^3$, and which is surrounded by water, is given by:

$$\rho(\boldsymbol{r}) = q\delta(\boldsymbol{r}) \tag{3.27}$$
$$\varepsilon_\Omega = 1 \tag{3.28}$$
$$\Omega = \mathcal{B}_a(\boldsymbol{0}) =: \mathcal{B}_a^0 \tag{3.29}$$
$$\Gamma = \partial \mathcal{B}_a^0 = \mathcal{S}_a^2(\boldsymbol{0}) =: \mathcal{S}_a^2 \tag{3.30}$$
$$\Sigma = \mathbb{R}^3 \setminus \mathcal{B}_a^0 \tag{3.31}$$

and thus, the classical formulation for the equations of nonlocal electrostatics with the Lorentzian model for the nonlocal dielectric function of water (3.24), becomes:

$$\left. \begin{aligned} \varepsilon_0 \Delta \varphi_{\mathcal{B}_a^0}(\boldsymbol{r}) + q\delta(\boldsymbol{r}) &= 0 & \boldsymbol{r} &\in \mathcal{B}_a^0 \\ \varepsilon_\infty \Delta \varphi_\Sigma(\boldsymbol{r}) + \tilde{\varepsilon}\, \boldsymbol{\nabla}_{\boldsymbol{r}} \int_\Sigma \frac{1}{4\pi} \frac{e^{-\frac{|\boldsymbol{r}-\boldsymbol{r}'|}{\lambda}}}{|\boldsymbol{r} - \boldsymbol{r}'|} \boldsymbol{\nabla}_{\boldsymbol{r}'} \varphi_\Sigma(\boldsymbol{r}')\, d\boldsymbol{r}' &= 0 & \boldsymbol{r} &\in \Sigma \\ \left[\boldsymbol{\nabla}\varphi_\Omega(\boldsymbol{r}) - \varepsilon_\infty \boldsymbol{\nabla}\varphi_\Sigma(\boldsymbol{r}) - \tilde{\varepsilon} \int_\Sigma \frac{1}{4\pi} \frac{e^{-\frac{|\boldsymbol{r}-\boldsymbol{r}'|}{\lambda}}}{|\boldsymbol{r} - \boldsymbol{r}'|} \boldsymbol{\nabla}_{\boldsymbol{r}'} \varphi_\Sigma(\boldsymbol{r}')\, d\boldsymbol{r}' \right] \cdot \hat{\boldsymbol{n}} &= 0 & \boldsymbol{r} &\in \mathcal{S}_a^2 \\ \left[\varphi_\Omega(\boldsymbol{r}) - \varphi_\Sigma(\boldsymbol{r}) \right] &= 0 & \boldsymbol{r} &\in \mathcal{S}_a^2 \end{aligned} \right\} \tag{3.32}$$

While this system is – due to the spherical symmetry – considerably simpler than system (3.24), it is still not obvious how to solve it. To this end, it is useful to notice that for our purposes, a point charge located in the middle of a sphere with $\varepsilon_\Omega = 1$ is equivalent to a *conducting sphere* containing only vacuum, carrying a surface charge equivalent to the point charge of the original model. Both models behave equivalently *outside* the sphere, as can be seen by computing their respective electrostatic potentials in a local setting.

To compute the *local* electrostatic potential of the Born model, we have to solve the following system of equations:

$$\left. \begin{aligned} \varepsilon_0 \Delta \varphi_{\mathcal{B}_a^0}(\boldsymbol{r}) &= -q\delta(\boldsymbol{r}) & \boldsymbol{r} &\in \mathcal{B}_a^0 \\ \Delta \varphi_\Sigma(\boldsymbol{r}) &= 0 & \boldsymbol{r} &\in \Sigma \\ \left[\partial_n \varphi_{\mathcal{B}_a^0}(\boldsymbol{r}) - \varepsilon_\Sigma \partial_n \varphi_\Sigma(\boldsymbol{r}) \right] &= 0 & \boldsymbol{r} &\in \mathcal{S}_a^2 \\ \left[\varphi_{\mathcal{B}_a^0}(\boldsymbol{r}) - \varphi_\Sigma(\boldsymbol{r}) \right] &= 0 & \boldsymbol{r} &\in \mathcal{S}_a^2 \end{aligned} \right\} \tag{3.33}$$

The first equation is solved by (with $r := \|\boldsymbol{r}\|$)

$$\varphi_{\mathcal{B}_a^0}(r) = \frac{q}{4\pi\varepsilon_0}\frac{1}{r} + \mathcal{C}$$

Continuity of the potentials, the fourth equation in (3.33), then tells us that for $r = a$

$$\varphi_{\mathcal{B}_a^0}(r = a) = \frac{q}{4\pi\varepsilon_0}\frac{1}{a} + \mathcal{C} = \varphi_\Sigma(r = a) \tag{3.34}$$

While from the equation for the normal derivatives, the third equation in (3.33), we can deduce

$$\partial_n\varphi_{\mathcal{B}_a^0}(r = a) = -\frac{q}{4\pi\varepsilon_0}\frac{1}{a^2}$$

$$= \varepsilon_\Sigma \partial_n\varphi_\Sigma(r = a)$$

$$\Rightarrow \qquad \varphi_\Sigma(r) = \frac{q}{4\pi\varepsilon_0\varepsilon_\Sigma}\frac{1}{r} + \mathcal{C}' \tag{3.35}$$

Combining (3.34) and (3.35), we arrive at

$$\varphi_\Sigma(a) = \frac{q}{4\pi\varepsilon_0\varepsilon_\Sigma}\frac{1}{a} + \mathcal{C}'$$

$$= \frac{q}{4\pi\varepsilon_0}\frac{1}{a} + \mathcal{C}$$

$$\Rightarrow \qquad \mathcal{C} = \mathcal{C}' + \frac{q}{4\pi\varepsilon_0 a}\left\{\frac{1}{\varepsilon_\Sigma} - 1\right\} \tag{3.36}$$

Since potentials are only defined up to an additive constant [Jac98], we can always gauge transform our system such that $\mathcal{C}' = 0$ and therefore arrive at the result:

$$\varphi_{\mathcal{B}_a^0}^{\text{Born}}(r) = \frac{q}{4\pi\varepsilon_0}\left\{\frac{1}{r} + \frac{1}{a}\left(\frac{1}{\varepsilon_\Sigma} - 1\right)\right\} \tag{3.37}$$

$$\varphi_\Sigma^{\text{Born}}(r) = \frac{q}{4\pi\varepsilon_0\varepsilon_\Sigma}\frac{1}{r} \tag{3.38}$$

To show that the model of a conducting spherical shell carrying a surface charge is in fact equivalent to that of the Born ion *outside* the sphere, we will now compute *its* electrostatic potential. The charge distribution used in this model will have to reflect the fact that the point charge q is now spread over the sphere of radius a. This can be achieved by taking as charge distribution a Dirac δ–distribution for the *radius*:

$$\rho^{\text{SS}}(\|\boldsymbol{r}\|) = \frac{q}{4\pi a^2}\delta(\|\boldsymbol{r}\| - a) \tag{3.39}$$

$$\rightsquigarrow \int_V d\boldsymbol{r}\,\rho^{\text{SS}}(\|\boldsymbol{r}\|) = \int_V \frac{q}{4\pi a^2}\delta(\|\boldsymbol{r}\| - a)d\boldsymbol{r}$$

$$= 4\pi\int_0^\infty dr\, r^2 \frac{q}{4\pi a^2}\delta(\|\boldsymbol{r}\| - a)$$

$$= 4\pi a^2 \frac{q}{4\pi a^2}$$

$$= q$$

So the total amount of charge in this model is in fact q, just as in the corresponding Born model. The field of this charge distribution is computed easily when working in Fourier space, and therefore we first need to compute $\hat{\rho}(k)$ for which we employ equation (A.12):

$$
\begin{aligned}
\hat{\rho}(k) &= \sqrt{\frac{2}{\pi}} \int_0^\infty dr \, \frac{q}{4\pi r^2} r^2 \frac{\sin(kr)}{kr} \delta(r-a) \\
&= \sqrt{\frac{2}{\pi}} \frac{q}{4\pi} \frac{\sin(ka)}{ka} \\
&= \frac{2}{\sqrt{2\pi}^3} \frac{\sin(ka)}{ka}
\end{aligned}
$$
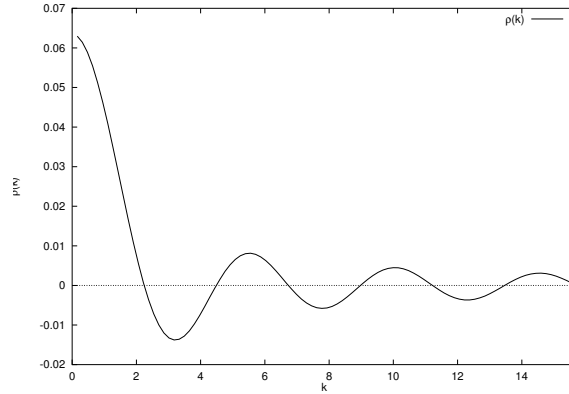
Figure 3.2.: $\rho_{BS}(k)$ for an ion with radius 1.4 Å and unit charge.

In order to compute the electrostatic potential of this model, we will in a first step assume that the sphere is also filled with water, and therefore $\varepsilon_\Omega \equiv \varepsilon_\Sigma$. In this case the corresponding Poisson equation for the spherical shell can be easily solved by remembering that the Fourier transform transfers linear differential equations into algebraic ones (c.f. Appendix A):

$$
\begin{aligned}
\Delta\varphi(r) &= -\frac{\rho(r)}{\varepsilon_\Sigma \varepsilon_0} \\
\overset{\mathcal{FT}}{\rightsquigarrow} -k^2 \hat{\varphi}(k) &= -\frac{q}{\sqrt{2\pi}^3} \frac{\sin(ka)}{ka} \frac{1}{\varepsilon_0 \varepsilon_\Sigma} \\
\Leftrightarrow \quad \hat{\varphi}(k) &= \frac{q}{\varepsilon_0 \varepsilon_\Sigma} \frac{1}{\sqrt{2\pi}^3} \frac{\sin(ka)}{k^3 a} \\
\overset{\mathcal{FT}}{\rightsquigarrow} \quad \varphi(r) &= \sqrt{\frac{2}{\pi}} \frac{q}{\varepsilon_0 \varepsilon_\Sigma} \frac{1}{\sqrt{2\pi}^3} \int_0^\infty dk \frac{\sin(kr)}{kr} \frac{\sin(ka)}{ka} \\
&= \frac{q}{2\pi^2 \varepsilon_0 \varepsilon_\Sigma} \frac{1}{ra} \left(\frac{\pi}{4} \left\{ (r-a)\sigma(a-r) + (a+r) \right\} \right) \\
&= \frac{q}{4\pi\varepsilon_0\varepsilon_\Sigma} \frac{1}{ra} \begin{cases} r, & a > r \\ a, & a < r \end{cases} \\
&= \frac{q}{4\pi\varepsilon_0\varepsilon_\Sigma} \begin{cases} \frac{1}{a}, & a > r \\ \frac{1}{r}, & a < r \end{cases}
\end{aligned}
$$

(3.40)

(3.41)

where $\sigma(a - r)$ is the *signum* of $(a - r)$, i.e.

$$\sigma(a - r) = \begin{cases} 1, & a > r \\ -1, & a < r \end{cases}$$

In the next step we can now assume that the *interior* of the sphere is filled with vacuum instead of water. It is easy to see that the qualitative behaviour of the potential as derived in equation (3.41) does not change. The only change is the value of the constant potential inside the sphere.

Expressing the gradient vector $\boldsymbol{\nabla}$ in spherical coordinates [Jac98]

$$\boldsymbol{\nabla}\psi = \frac{\partial \psi}{\partial r}\hat{\boldsymbol{e}}_r + \frac{1}{r}\frac{\partial \psi}{\partial \theta}\hat{\boldsymbol{e}}_\theta + \frac{1}{r \sin \theta}\frac{\partial \psi}{\partial \phi}\hat{\boldsymbol{e}}_\phi$$

We can therefore conclude:

$$\begin{aligned} \boldsymbol{E}(r) &= -\boldsymbol{\nabla}\varphi(r) \\ &= -\frac{\partial \varphi}{\partial r}\hat{\boldsymbol{e}}_r \\ &= -\frac{q}{4\pi\varepsilon_0\varepsilon_\Sigma}\hat{\boldsymbol{e}}_r \begin{cases} \frac{\partial}{\partial r}\frac{1}{a}, & a > r \\ \frac{\partial}{\partial r}\frac{1}{r}, & a < r \end{cases} \\ &= \frac{q}{4\pi\varepsilon_0\varepsilon_\Sigma}\hat{\boldsymbol{e}}_r \begin{cases} 0, & a > r \\ \frac{1}{r^2}, & a < r \end{cases} \\ &= \frac{q}{4\pi\varepsilon_0\varepsilon_\Sigma}\frac{1}{r^2}\theta(r - a)\hat{\boldsymbol{e}}_r \end{aligned} \tag{3.42}$$

Remark 3.5.1. The electrostatic potential of a spherical shell as defined by equation (3.39) for $r > a$ is the same as that of the equivalent Born sphere (3.27):

$$\varphi(r) = \frac{q}{4\pi\varepsilon_0\varepsilon_\Sigma}\frac{1}{r} \quad r > a$$

For $r < a$, the potential of the spherical shell model is constant, and therefore, the electric field inside the sphere, $\boldsymbol{E}(r)$, vanishes:

$$\boldsymbol{E}(r) = 0 \quad r < a$$

These two observations explain why the spherical shell model is advantageous for our considerations: we can expect that the field on the outside is the same as for the "real" Born model, and the field on the inside vanishes. This means that in the nonlocal integrals of the form

$$\int_\Sigma d\boldsymbol{r}'\varepsilon(\boldsymbol{r} - \boldsymbol{r}')\boldsymbol{\nabla}_{\boldsymbol{r}'}\varphi(\boldsymbol{r}') = -\int_\Sigma d\boldsymbol{r}'\varepsilon(\boldsymbol{r} - \boldsymbol{r}')\boldsymbol{E}(\boldsymbol{r}')$$

the domain of integration can be extended to the whole $\mathbb{R}^3$, since $\boldsymbol{E}(\boldsymbol{r}) \equiv 0$ inside Ω. The integrals therefore become *convolutions* (c.f. B.5), and thus can be easily computed in Fourier space (c.f. Appendix A.1.3):

$$\boldsymbol{D}(\boldsymbol{r}) = -\varepsilon_0\int_{\mathbb{R}^3} d\boldsymbol{r}'\,\varepsilon(\boldsymbol{r} - \boldsymbol{r}')\boldsymbol{\nabla}_{\boldsymbol{r}'}\varphi(\boldsymbol{r}') = -\varepsilon_0\varepsilon*(\boldsymbol{\nabla}\varphi) = -\sqrt{2\pi}^3\varepsilon_0\mathfrak{FT}^{-1}\left[\hat{\varepsilon}(\boldsymbol{k})\left(-\imath\boldsymbol{k}\hat{\varphi}(\boldsymbol{k})\right)\right]$$

and thus

$$\hat{\boldsymbol{D}}(\boldsymbol{k}) = \mathfrak{FT}\left[\boldsymbol{D}(\boldsymbol{r})\right] = -\imath\sqrt{2\pi}^3\varepsilon_0\boldsymbol{k}\hat{\varepsilon}(\boldsymbol{k})\hat{\varphi}(\boldsymbol{k}) = \sqrt{2\pi}^3\varepsilon_0\hat{\varepsilon}(\boldsymbol{k})\hat{\boldsymbol{E}}(\boldsymbol{k}) \tag{3.43}$$
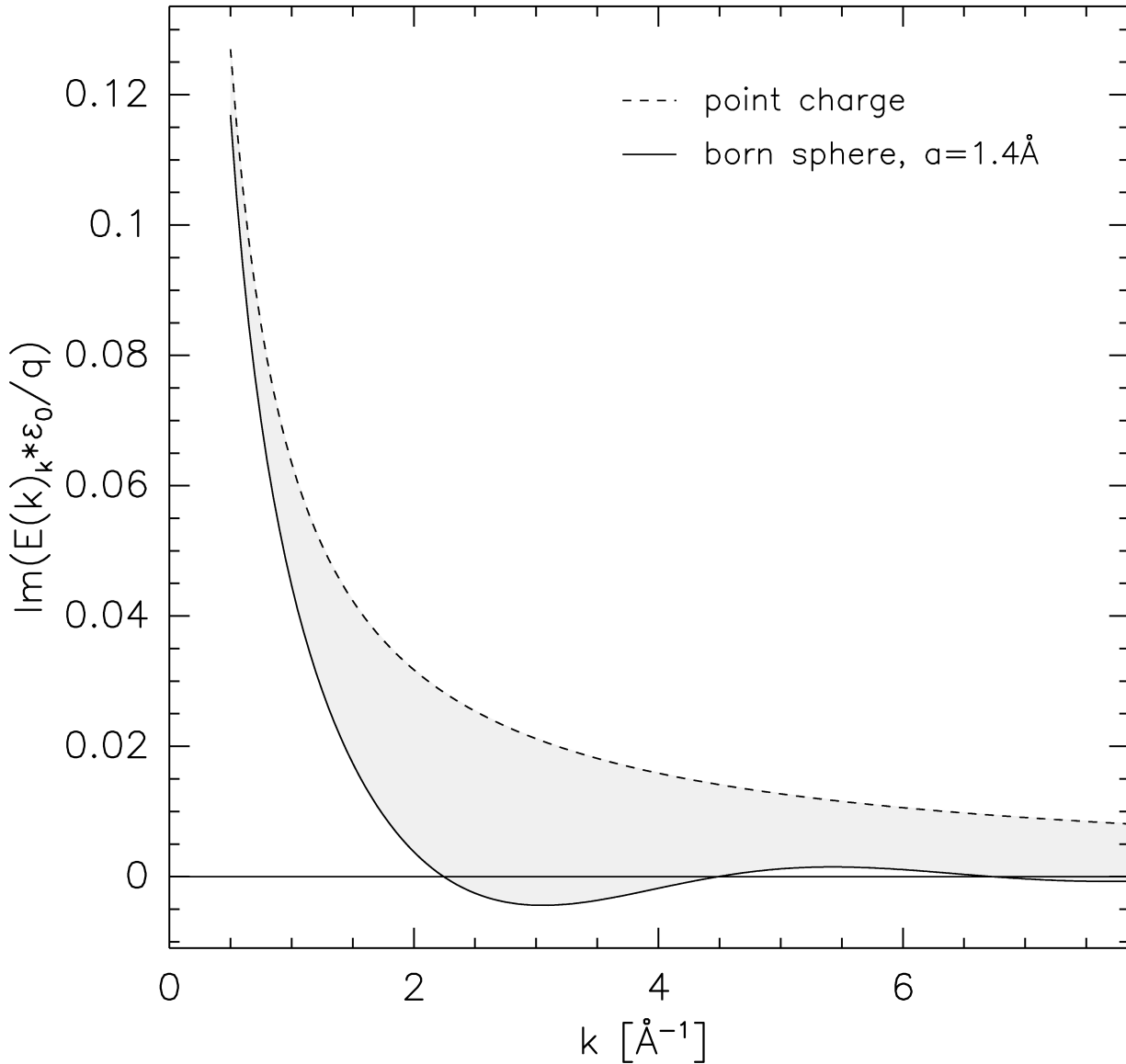
Figure 3.3.: Comparison of the fields of a Born ion and a simple point charge. The fields are imaginary and directed along the $\boldsymbol{k}$-vector in Fourier space since in physical space they have only a symmetric component along the antisymmetric radius vector $\hat{e}_r$ (c.f. Appendix A.1.5). In this plot we have set $\frac{q}{\varepsilon_0} = 1$. The upper curve corresponds to the field of a point charge $(a = 0)$, the lower curve to a Born sphere of radius $a = 1.4$ Å.

To compute the polar contribution to the free energy of solvation

$$\Delta G^{\text{polar}} \stackrel{(2.88)}{=} \mathcal{N}_a \Delta W = \mathcal{N}_a \left(W^{\text{water}} - W^{\text{vacuum}} \right)$$

where, according to equation (2.75),

$$W = \frac{1}{2} \int\limits_{\mathbb{R}^3} d\boldsymbol{r} \, \boldsymbol{E}(\boldsymbol{r}) \cdot \boldsymbol{D}(\boldsymbol{r})$$

we now have to compute

$$\Delta G^{\text{polar}} = \frac{1}{2} \left(\int\limits_{\mathbb{R}^3} d\boldsymbol{r} \left\{ \boldsymbol{E}^{\text{water}} \cdot \boldsymbol{D} - \boldsymbol{E}^{\text{vacuum}} \cdot \boldsymbol{D} \right\} \right) \tag{3.44}$$

$$= \frac{1}{2} \left(\int\limits_{\mathbb{R}^3} d\boldsymbol{r} \left\{ \boldsymbol{E}^{\text{water}} \cdot \boldsymbol{D} - \frac{1}{\varepsilon_0} \boldsymbol{D} \cdot \boldsymbol{D} \right\} \right) \tag{3.45}$$

Parseval's theorem − equation (A.13) − allows us to perform this computation in Fourier space:

$$\Delta G^{\text{polar}} = \frac{1}{2} \left(\int\limits_{\mathbb{R}^3} d\boldsymbol{r} \left\{ \boldsymbol{E}^{\text{water}} \cdot \boldsymbol{D} - \frac{1}{\varepsilon_0} \boldsymbol{D} \cdot \boldsymbol{D} \right\} \right) \tag{3.46}$$

$$= \frac{1}{2} \left(\int\limits_{\mathbb{R}^3} d\boldsymbol{k} \left\{ \hat{\boldsymbol{E}}(\boldsymbol{k})^{\text{water}} \cdot \hat{\boldsymbol{D}}(\boldsymbol{k}) - \frac{1}{\varepsilon_0} \hat{\boldsymbol{D}}^2(\boldsymbol{k}) \right\} \right) \tag{3.47}$$

$$\stackrel{(3.43)}{=} \frac{1}{2} \left(\int\limits_{\mathbb{R}^3} d\boldsymbol{k} \left\{ \frac{1}{\sqrt{2\pi}^3} \frac{1}{\varepsilon_0 \hat{\varepsilon}(\boldsymbol{k})} \hat{\boldsymbol{D}}^2(\boldsymbol{k}) - \frac{1}{\varepsilon_0} \hat{\boldsymbol{D}}^2(\boldsymbol{k}) \right\} \right) \tag{3.48}$$

$$= -\frac{1}{2\varepsilon_0} \int\limits_{\mathbb{R}^3} d\boldsymbol{k} \left\{ 1 - \frac{1}{\sqrt{2\pi}^3} \frac{1}{\hat{\varepsilon}(\boldsymbol{k})} \right\} \hat{\boldsymbol{D}}^2(\boldsymbol{k}) \tag{3.49}$$

so that we can conclude from equation (3.43)

$$\Delta G^{\text{polar}} = \frac{(2\pi)^3}{2\varepsilon_0} \int\limits_{\mathbb{R}^3} d\boldsymbol{k} \left\{ 1 - \frac{1}{\sqrt{2\pi}^3} \frac{1}{\hat{\varepsilon}(\boldsymbol{k})} \right\} k^2 \hat{\varepsilon}^2(\boldsymbol{k}) \hat{\varphi}^2(\boldsymbol{k}) \tag{3.50}$$

In [Hil02] and [HKBL02], we have devised and demonstrated a stable and efficient numerical scheme to solve equation (3.50). Since then, however, we have been able to compute ΔG^{polar} for the Born model and the Lorentzian nonlocal dielectric function (3.23) analytically. To this end, we first observe that the displacement field $\boldsymbol{D}(\boldsymbol{r})$ fulfills − in the nonlocal as well as in the local setting − the same equation as the electric field of the same charge distribution in vacuum, as long as no boundary conditions have to be taken into account. Since by replacing the Born model by the spherical shell model, we effectively extended the equations from Σ into the whole $\mathbb{R}^3$, circumventing the necessity of the boundary conditions for the computation of the nonlocal fields. We can therefore conclude that the field $\boldsymbol{D}(\boldsymbol{r})$ can be found from equation (3.42). Since (3.42) is the solution to

$$\boldsymbol{\nabla} \cdot \boldsymbol{E}^{\text{local}}(\boldsymbol{r}) = \frac{\rho(\boldsymbol{r})}{\varepsilon_0 \varepsilon_\Sigma}$$

3. The theory of nonlocal electrostatics

and the sought $\boldsymbol{D}(\boldsymbol{r})$ fulfills

$$\nabla\cdot\boldsymbol{D}(\boldsymbol{r}) = \rho(\boldsymbol{r})$$

and since all boundary conditions can be neglected, we obtain:

$$
\begin{aligned}
\boldsymbol{D}(\boldsymbol{r}) &= \varepsilon_0\varepsilon_\Sigma\boldsymbol{E}^{\mathrm{local}}(\boldsymbol{r}) \\
&\overset{(3.41)}{=} -\varepsilon_0\varepsilon_\Sigma\nabla\varphi^{\mathrm{local}}(\boldsymbol{r}) \\
&= -\nabla\frac{q}{4\pi}
\begin{cases}
\frac{1}{a}, & a > r \\
\frac{1}{r}, & a < r
\end{cases}
\end{aligned}
$$

To obtain the Fourier transform of this expression, we make use of the already computed Fourier transform of the local electrostatic potential of the shell model $\varphi^{\mathrm{local}}(\boldsymbol{r})$:

$$\hat{\boldsymbol{D}}(\boldsymbol{k}) \overset{(3.40)}{=} -\imath\boldsymbol{k}\frac{q}{\sqrt{2\pi}^3}\frac{\sin(ka)}{k^3 a}$$

Plugging this equation and the expression for the Fourier transform of the Lorentzian model (3.22) into expression (3.43), we arrive at

$$-\imath\boldsymbol{k}\frac{q}{\sqrt{2\pi}^3}\frac{\sin(ka)}{k^3 a} = -\imath\sqrt{2\pi}^3\varepsilon_0\boldsymbol{k}\frac{1}{\sqrt{2\pi}^3}\left\{\varepsilon_\infty + \frac{\varepsilon_\Sigma - \varepsilon_\infty}{1 + \lambda^2 k^2}\right\}\hat{\varphi}(\boldsymbol{k}) \tag{3.51}$$

and thus

$$\hat{\varphi}(\boldsymbol{k}) = \frac{q}{\sqrt{2\pi}^3}\frac{\sin(ka)}{k^3 a}\frac{1}{\varepsilon_0}\left\{\varepsilon_\infty + \frac{\varepsilon_\Sigma - \varepsilon_\infty}{1 + \lambda^2 k^2}\right\}^{-1} \tag{3.52}$$

$$= \frac{q}{\sqrt{2\pi}^3}\frac{\sin(ka)}{k^3 a}\frac{1}{\varepsilon_0}\left\{\frac{1 + \lambda^2 k^2}{\lambda^2 k^2\varepsilon_\infty + \varepsilon_\Sigma}\right\} \tag{3.53}$$

Being radially symmetric, $\hat{\varphi}(\boldsymbol{k}) \equiv \hat{\varphi}(k)$ can again be Fourier backtransformed using

$$
\begin{aligned}
\varphi(r) &= \sqrt{\frac{2}{\pi}}\int_0^\infty dk\, k^2\frac{\sin(kr)}{kr}\hat{\varphi}(k) \\
&= \sqrt{\frac{2}{\pi}}\int_0^\infty dk\, k^2\frac{\sin(kr)}{kr}\frac{q}{\sqrt{2\pi}^3}\frac{\sin(ka)}{k^3 a}\frac{1}{\varepsilon_0}\left\{\frac{1 + \lambda^2 k^2}{\lambda^2 k^2\varepsilon_\infty + \varepsilon_\Sigma}\right\} \\
&= \frac{q}{2\pi^2\varepsilon_0}\int_0^\infty dk\,\frac{\sin(kr)}{kr}\frac{\sin(ka)}{ka}\left\{\frac{1 + \lambda^2 k^2}{\lambda^2 k^2\varepsilon_\infty + \varepsilon_\Sigma}\right\} \tag{3.54}
\end{aligned}
$$

The computation of the integral appearing in equation (3.54) is tedious and lengthy, requiring recurring and rather technical manipulations of trigonometric functions. Therefore, we will only state the result, yielding the nonlocal expression for the electrostatic potential of the spherical shell using the Lorentzian model for the dielectric function of water. With the definition of the dimensionless quantity

$$\nu := \sqrt{\frac{\varepsilon_\Sigma}{\varepsilon_\infty}}\frac{a}{\lambda}$$

the electrostatic potential is given by

$$\boxed{\varphi(r) = \frac{q}{4\pi\varepsilon_0\varepsilon_\Sigma}\frac{1}{r}\left\{1 + \frac{\varepsilon_\Sigma - \varepsilon_\infty}{\varepsilon_\infty}\frac{\sinh\nu}{\nu}e^{-\frac{\nu}{a}r}\right\}} \tag{3.55}$$

Equation (3.55), the nonlocal electrostatic potential of a charged conducting spherical shell in the Lorentzian model, allows a very interesting decomposition: the first term on the right hand side of equation (3.55) is exactly the same as the *local* potential of this charge distribution, while the second term contains the *nonlocal corrections* to the local structureless bulk.

$$\varphi(r) = \underbrace{\frac{q}{4\pi\varepsilon_0\varepsilon_\Sigma}\frac{1}{r}}_{\text{Local potential}}\left\{1 + \underbrace{\frac{\varepsilon_\Sigma - \varepsilon_\infty}{\varepsilon_\infty}\frac{\sinh\nu}{\nu}e^{-\frac{\nu}{a}r}}_{\text{Nonlocal corrections}}\right\} \tag{3.56}$$

Obviously, the second term in the braces, corresponding to the nonlocal effect, is positive definite. Therefore, the nonlocality *increases* the absolute value of the electrostatic potential as compared to a local computation in vacuum, just as we had hoped, since due to the correlations between the water molecules, the shielding effect of the solvent is clearly overestimated in the local setting. We also find that this nonlocal effect decays exponentially on a scale $\frac{r}{\lambda}$, such that for $r \gg \lambda$ all nonlocal corrections vanish and the local behaviour is recovered, just as we demanded in Section 3.4.1.

While these properties of our result are very satisfying and promising, real confirmation for the nonlocal theory of electrostatics can only come from a comparison to experimental data. The quantity that seems ideally suited for such a comparison is the electrostatic contribution to the free energy of solvation for monoatomic ions. For these systems, the solvation free energy is clearly dominated by electrostatic effects and any nonpolar contributions can be neglected. We can therefore easily compare our results to measured values for ionic solvation. To this end, we first have to compute the reaction field energy of the Born ion in the nonlocal setting, which can be easily obtained by remembering that the field *outside* the ion $\varphi_\Sigma(r)$ is the same than that for the spherical conducting charged shell, which we have just computed. We therefore have

$$\varphi_\Sigma(r = a) = \frac{q}{4\pi\varepsilon_0\varepsilon_\Sigma}\frac{1}{a}\left\{1 + \frac{\varepsilon_\Sigma - \varepsilon_\infty}{\varepsilon_\infty}\frac{\sinh\nu}{\nu}e^{-\nu}\right\}$$

and with the same arguments used to derive the potential in the local setting (c.f. equations (3.33) – (3.38)), we obtain

$$\varphi_{\mathcal{B}_a^0}^{\text{Born}}(r) = \frac{q}{4\pi\varepsilon_0}\left\{\frac{1}{r} + \frac{1}{a\varepsilon_\Sigma}\left(1 - \varepsilon_\Sigma + \frac{\varepsilon_\Sigma - \varepsilon_\infty}{\varepsilon_\infty}\frac{\sinh\nu}{\nu}e^{-\nu}\right)\right\} \tag{3.57}$$

$$\varphi_\Sigma^{\text{Born}}(r) = \frac{q}{4\pi\varepsilon_0\varepsilon_\Sigma}\frac{1}{r}\left\{1 + \frac{\varepsilon_\Sigma - \varepsilon_\infty}{\varepsilon_\infty}\frac{\sinh\nu}{\nu}e^{-\nu\frac{r}{a}}\right\} \tag{3.58}$$

Since the first term in equation (3.57) is just the local vacuum potential of the Born ion, and since the solvation free energy is defined as the difference between the electric field energy in the solvent and in vacuum (c.f. Section 2.4), we can easily read off the electrostatic contribution to the free energy of solvation of the Born ion in the nonlocal setting using the Lorentzian model:

Theorem 3.5.1 (Free energy of solvation for monoatomic ions). *The electrostatic contribution to the free energy of solvation of a monoatomic ion of charge q and radius a in the Lorentzian model for the nonlocal dielectric function of water* (3.23) *is given by*

$$\boxed{\Delta G^{polar} = \frac{-q^2}{8\pi\varepsilon_0\varepsilon_\Sigma a}\left\{\frac{\varepsilon_\Sigma - \varepsilon_\infty}{\varepsilon_\infty}\frac{\sinh\nu}{\nu}e^{-\nu} - (\varepsilon_\Sigma - 1)\right\}} \tag{3.59}$$

Proof. According to equation (2.87) and equation (2.76) the electrostatic contribution to the free

energy of solvation ΔG^{polar} is given by

$$
\begin{aligned}
\Delta G^{\text{polar}} &= G^{\text{polar}}_{\text{solvent}} - G^{\text{polar}}_{\text{vacuum}} \\
&= -\frac{1}{2} \int\limits_{\mathbb{R}^3} \rho(\boldsymbol{r})\varphi^{\text{solvent}}(\boldsymbol{r})d\boldsymbol{r} + \frac{1}{2} \int\limits_{\mathbb{R}^3} \rho(\boldsymbol{r})\varphi^{\text{vacuum}}(\boldsymbol{r})d\boldsymbol{r} \\
&= -\frac{1}{2} \int\limits_{\mathbb{R}^3} q\delta(\boldsymbol{r}) \left(\varphi^{\text{solvent}}(\boldsymbol{r}) - \varphi^{\text{vacuum}}(\boldsymbol{r}) \right) d\boldsymbol{r} \\
&= -\frac{q}{2} \left(\varphi^{\text{solvent}}(0) - \varphi^{\text{vacuum}}(0) \right) \\
&= -\frac{q}{2} \frac{q}{4\pi\varepsilon_0\varepsilon_\Sigma a} \left\{ \frac{\varepsilon_\Sigma - \varepsilon_\infty}{\varepsilon_\infty} \frac{\sinh\nu}{\nu} e^{-\nu} - (\varepsilon_\Sigma - 1) \right\} \\
&= \frac{-q^2}{8\pi\varepsilon_0\varepsilon_\Sigma a} \left\{ \frac{\varepsilon_\Sigma - \varepsilon_\infty}{\varepsilon_\infty} \frac{\sinh\nu}{\nu} e^{-\nu} - (\varepsilon_\Sigma - 1) \right\}
\end{aligned}
$$

$\square$

Before we can finally compare this to experimental data, two more questions have to be addressed: we have to choose values for the *radii* of the monoatomic ions, and we have to decide on the value of the correlation length λ.

3.5.2. Physically motivated radii for monoatomic ions

The Born ion, i.e. a point charge located in the center of a vacuum filled sphere, is only an approximate description for monoatomic ions. In reality, these are highly complex systems governed by the laws of quantum mechanics and quantum field theory, and not necessarily strictly spherically symmetric. While these effects can be neglected for the sake of solvation computations, it is clear that in reality, there is no canonic notion of the *radius* of such a system. In fact, in quantum mechanics, the atom itself is spread out over all of space with a strongly decaying probability around its center. While it might be possible to define a set of ion radii based on this quantum mechanical probability distribution, e.g. by taking the radius of the contour surface of a certain probability value, but in practice, such an approach turns out to be infeasible.

For this reason, many approaches to the computation of the free energy of solvation for monoatomic ions therefore use the radii as a *fit parameter* [LSJBI02]. Since then the theory contains at least one fit parameter per data point, this is in our opinion of no use for assessing the quality of a novel theory. Another approach consists in studying the properties of the lattice structure in the ion's crystalline state [SP69, Sha76]. Unfortunately, there is no reason to believe that the properties of the ion are the same in the crystalline and in the solvated state, and since therefore, such a radii set might contain a systematic error, we prefer a different approach that is due to Johan Åqvist [Å90]. The idea of this approach is to make use of the radial distribution function $g(r)$ (c.f. 2.7), which yields the probability that, given a particle at the origin of the system, there is another particle situated at position r. A solvated ion is surrounded by several shells of water molecules (this effect is known as *hydration*), and the first of these shells will in general be "as close as possible" to the ion, with its oxygens "touching its boundary",

The ion radius in the Åqvist model can therefore be obtained from a two–fold process. First, we somehow have to determine the oxygen–oxygen rdf, i.e. the probability that, given an oxygen at $r = 0$, there is another oxygen at position r. The position of the first peak r_1 in this oxygen–oxygen rdf corresponds to the distance of the oxygens closest to the one in the center, i.e. to the ones that

"touch" it. Therefore, the oxygen radius r_O in the Åqvist model can be determined by $r_O = \frac{1}{2}r_1$.

In the second step, we consider the ion–oxygen rdf, where the position of the first peak r_1 corresponds to the distance of the centers of the ion and the oxygens in the first solvation shell. The ion radius in the Åqvist model is therefore obtained from $r_I = r_1 - r_O$.

While the radial distribution functions needed for this approach can in principle be determined from e.g. neutron diffraction experiments, the quality of the data typically obtained forbids such a microscopic examination. Åqvist therefore proposed a different technique for obtaining the rdfs [Å90]: in a first step, he performed a free energy perturbation, a technique for obtaining free energies from molecular dynamics simulations, of a system composed of an ion in a water box. This energy is compared to experimental data, and in an iterative process, the parameters of the force field are optimized with respect to this energy. The resulting parameter set guarantees to reproduce the free energy of solvation accurately, and with these parameters, another simulation of the ion in the water box is performed. From this simulation, in turn, the radial distribution functions can be computed by an angular and temporal integration over the distance vectors of all oxygens from the ion. The ion radii obtained in this way are known as the *Åqvist–radii*.

In [Å90], Åqvist chose the GROMOS force field [vGB87] and employed several different water models (flexible and rigid SPC [BPvGH81, TJE87] and TIP3P [JCM$^+$83]). He found only a slight dependence on the water model, but it should be noted that none of the employed models contains intramolecular degrees of freedom, or molecular polarizability, and thus $\varepsilon_\infty = 1$. The expected effects on the radial distribution functions and thus on the ion radii though is very small, but might be noticeable for small and highly charged ions. In fact, Åqvist remarks:

> "However, the value of R_{I-w}^{calc} for Mg^{2+} show a less good agreement with the observed distance than for any of the other ions and appears to be slightly too small. It seems, in fact, rather difficult to obtain a larger Mg^{2+} radius while maintaining a value of $\Delta G_{\text{hydr}}^{\text{calc}}$ close to the observed one. One reason for this problem may be the use of a rigid un-polarizable water model. That is, for the first solvation shell ligands one might expect a significant increase of the dipole moment due to the strong interaction with the ion, which is suppressed by the use of a rigid water model. This effect would be more pronounced for Mg^{2+} than for any of the other ions, since it is the smallest divalent one treated here."

To our knowledge, there has been no complete investigation of effects of the polarizability of the water model on the quality of the free energy perturbation, but results from a comparison of hydration simulations of the chloride ions with the non–polarizable TIP4P [MJ00] and the polarizable TIP4P–FQ [Ric01] performed by Stuart and Berne [SB96] seem to suggest that a slight dependence exists. Therefore, repeating Åqvist's experiments with a modern water model might lead to slight corrections to the radii of the smallest ions.

Also, it is well–known that the experimental data used in the parameter fitting process in Åqvist's approach, and which will be used by us to compare our results to experimental data, cannot be measured to an arbitrary degree of precision, because, as has been shown by Rashim and Honig[10] [RH85], the ion cannot be completely separated from its counter ion in a real physical system. Thus, the experimental data also carries a certain but fortunately small error margin.

---

10 Here we have given the most current publications on the TIP4P and TIP4P–FQ models, and thus it is no contradiction that these articles are more recent than the one by Rashim and Honig.

Nonetheless, the radii obtained by Åqvist seem to be of a very high quality, and are consistent with experimentally observed margins[11] found in for ion radii, as can be seen in table 3.4.

Ion	Radius [Å] (calc)	Radius [Å] (observed)
Li^+	0.645	0.615-0.695
Na^+	1.005	0.965-1.035
K^+	1.365	1.345-1.415
Rb^+	1.505	1.504
Cs^+	1.715	1.705-1.765
Mg^{2+}	0.615	0.665-0.715
Ca^{2+}	1.015	1.005-1.035
Sr^{2+}	1.195	1.145
Ba^{2+}	1.385	1.365

Figure 3.4.: Ion radii for some monovalent and divalent ions, taken from [Å90]

3.5.3. The correlation length

The remaining quantity we have to consider before we can do our comparison to experimental data is the correlation length λ. Obviously, λ can be used as a *fit parameter* in these comparisons, and in fact we will follow this approach in this work. On the other hand, it would be much more convincing if the value for λ thus found could be somehow confirmed by independent experimental data. In [Hil02] we have shown how this can be accomplished for a certain class of models for $\varepsilon(\boldsymbol{r}, \boldsymbol{r}')$, including the Lorentzian (3.23) model employed in this work. The idea outlined in [Hil02] consists in taking the nonlocal electrostatic potential in water and comparing this to the local electrostatic potential of the same charge distribution in vacuum. From this, an effective local shielding of the vacuum potential can be derived, which might be considered as an *effective local dielectric function* $\varepsilon^{\text{eff}}(\boldsymbol{r})$. Since the polarization correlations leading to the nonlocal effect are clearly dependent on the geometry and to a lesser extent on the charge distribution of the system, this effective local dielectric function will feature the same dependence. But for a given choice of system, again the Born ion, the results obtained can in fact be compared to experimental data, or to well–established models for a local dielectric function for spherical systems that in turn have been fitted to experimental data. Such dielectric functions for the Born ion[12] have been published e.g. by Conway [CBA51] and Mehler and Eichele [ME84], who have derived slightly different models and fitted them to experimental data.

A complete derivation of the effective local dielectric function for the Born ion using the Lorentzian model at this place seems out of the scope of this work, and the interested reader is referred to [Hil02]. Here, we will only state the main result of that examination, which is that the Lorentzian model accurately reproduces the Mehler and Eichele data for a choice of $\lambda \approx 20$ Å, while the data from Conway can be reproduced for $\lambda \approx 15$ Å. In anticipation of the next section we would like to mention at this point, that the value of λ that is obtained from a fit against the experimental values for the free energy of solvation is given by $\lambda \approx 23$ Å, while for $\lambda \approx 15$ Å, the free energy results are only slightly worse. We therefore conclude that the only free parameter of our model, the correlation length λ, can be fixed in at least two completely independent ways, i.e. by looking at an effective local shielding or by comparing to free energies of solvation, and in both cases this fitting leads – within

---

11 According to [Å90], the lower margin is the Pauling radius, taken from [Pau60], the higher one – if available – from experimentally determined RDF peaks, found in [Mag83] and the references therein.

12 For a detailed discussion of the choice of charge distribution and geometry for the comparison, see [Hil02].

the error margin of the computations and the experimental data – to the same results, which in our opinion strongly supports our model.

3.5.4. Comparison to experimental data

Having finally assembled everything that is needed to compute the electrostatic contribution to the free energy of solvation in a nonlocal setting, we can now easily compare our results to experimental data. Being such a small system, the nonpolar contributions to the free energy of solvation, like the cavity formation term, can conveniently be neglected, and thus we can directly compare the results obtained from equation (3.59) to the experimental data, which was taken from [Mar85]. A natural and common choice of units for these energies is kJ/mol, which can directly be obtained by replacing equation (3.59) with:

$$\Delta G^{\mathrm{polar}} = \frac{\mathcal{N}_a}{1000} \frac{-q^2}{8\pi\varepsilon_0\varepsilon_\Sigma a} \left\{ \frac{\varepsilon_\Sigma - \varepsilon_\infty}{\varepsilon_\infty} \frac{\sinh\nu}{\nu} e^{-\nu} - (\varepsilon_\Sigma - 1) \right\} \tag{3.60}$$

where $\mathcal{N}_a \approx 6.022\times10^{23}$ is is the *Avogadro constant*. A comparison of our results to experimental data and to a purely local computation can be found in Fig. 3.5. As can be clearly seen from that figure, the nonlocal approach predicts the free energy of solvation of monoatomic ions with an extremely high accuracy, and the results are considerably better than that of the corresponding local computation.
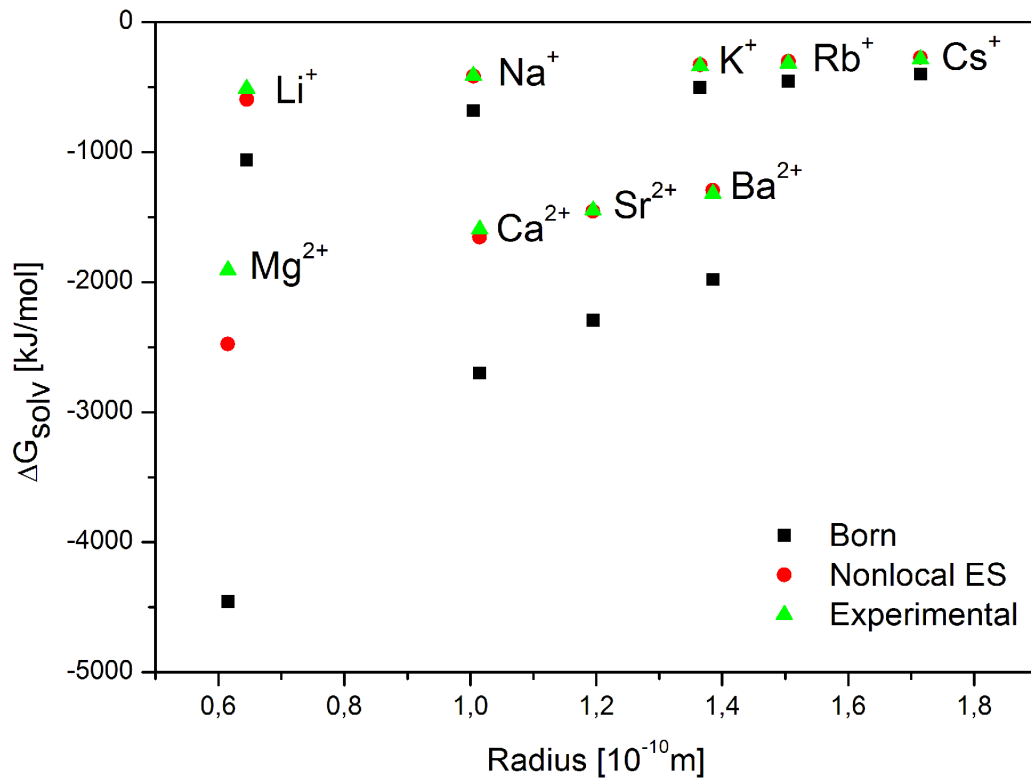
Figure 3.5.: The free energy of solvation of monoatomic ions. In this plot, the green triangles denote experimental values [Mar85], the red spheres the nonlocal results, computed with $\lambda \approx 23$ Å, and the black boxes the local ones.

3. The theory of nonlocal electrostatics

4. A novel formulation of nonlocal electrostatics

In Section 3.5 we have seen that the theory of nonlocal electrostatics really seems to capture the behaviour of solvated molecular systems much better than the local approach, if the typical length scales of the system under consideration are comparable to the correlation length of the water molecules, which turned out to be roughly of the order of 15–25 Å. Applying this method to more delicate geometries and charge distributions, especially those of biomolecules like proteins, seems therefore a highly desirable aim. The derivation of our results for monoatomic ions, though, relied much on the simple model geometry we chose, and in particular could only be obtained since we were able to replace the Born ion model with the spherical shell model, for which in turn we could replace the nonlocal integrals over Σ by those over $\mathbb{R}^3$. This allowed the interpretation of the nonlocal integrals over the dielectric function and the electric field as a convolution of those two quantities, which could be evaluated since the Fourier transforms of both were known.

For a general geometry and an arbitrary charge distribution, of course, this extension of integration domains is not possible, and even if it was, we would still need an analytical expression for the vacuum potential and its Fourier transform – both of which can typically not be obtained – in order to perform our calculations.

A numerical solution to the problem in its classical formulation also seems infeasible: the integro–differential equations appearing can e.g. not be solved by simply discretising the differential operators as is usually done in finite difference computations for the local setting, since the integral operators would require different and expensive techniques.

In this section we will develop a novel equivalent reformulation of the equations of nonlocal electrostatics for a certain class of nonlocal dielectric functions that fortunately contains the Lorentzian model. This reformulation has the astonishing property, that the integro–differential operators appearing in the classical formulation (3.9) are replaced by purely *differential* equations, that – at least for the Lorentzian model – are still *linear, elliptic, and of second order*, i.e. they are of the same class of equations as the original *local* equations of electrostatics, and therefore "not much harder" to solve or to interpret. In our opinion, this reformulation allows for the first time to exactly apply the theory of nonlocal electrostatics to geometries relevant for applications in bioinformatics. The results described in this chapter have been published in [HBR$^+$04].

4.1. The Helmholtz decomposition

In order to simplify manipulations of the vectorial quantity $\boldsymbol{D}(\boldsymbol{r})$, the displacement field, the *Helmholtz decomposition theorem* provides an invaluable tool. While in its most simple formulation this theorem can be found in most standard textbooks on theoretical or mathematical physics (see e.g. [Arf85, GR00]), a precise treatment including the range of validity and necessary conditions for its applicability turns out to be highly involved [Fra04, Whi60].

In the commonly quoted form, the Helmholtz theorem reads as follows:

Theorem 4.1.1 (Helmholtz decomposition). *Any sufficiently smooth vector field $v(r)$ that decays sufficiently fast in the sense that*

$$\lim_{\|r\|\to\infty} \nabla\cdot v(r) = 0$$

$$\lim_{\|r\|\to\infty} \nabla\times v(r) = 0$$

may be uniquely decomposed into a sum of an irrotational part $-\nabla\psi(r)$ with $\nabla\times(-\nabla\psi(r)) = 0$ and a solenoidal part $\nabla\times\xi(r)$ with $\nabla\cdot(\nabla\times\xi(r)) = 0$:

$$v(r) = -\nabla\psi(r) + \nabla\times\xi(r) \tag{4.1}$$

Remark 4.1.1. In full generality, the field $v(r)$ can be decomposed into *three* terms, an irrotational part, a solenoidal part, and a third part that is irrotational as well as solenoidal, i.e. a term $w(r)$ with vanishing divergence and curl. In the following we will always suppose that such a term $w(r)$ is contained in the irrotational term $\nabla\psi(r)$, which is possible since $w(r)$ is irrotational itself.

Remark 4.1.2. Theorem 4.1.1 is a special case of the celebrated *Kodaira–Hodge–De Rham* decomposition theorem [AP95], which is probably the best starting point for a detailed discussion of the delicate points of validity, uniqueness and the required smoothness conditions of theorem 4.1.1.

By virtue of the Helmholtz decomposition (4.1), we can write

$$D(r) = -\nabla\psi(r) + \nabla\times\xi(r) \tag{4.2}$$

where

$$D(r) = \begin{cases} D_\Omega(r), & r \in \Omega \\ D_\Sigma(r), & r \in \Sigma \end{cases}$$

$$\psi(r) = \begin{cases} \psi_\Omega(r), & r \in \Omega \\ \psi_\Sigma(r), & r \in \Sigma \end{cases}$$

$$\xi(r) = \begin{cases} \xi_\Omega(r), & r \in \Omega \\ \xi_\Sigma(r), & r \in \Sigma \end{cases}$$

With these definitions, $\nabla\cdot D(r) = \rho(r)$ everywhere, which leads to

$$\begin{aligned} \nabla\cdot D(r) &= \nabla\cdot(-\nabla\psi(r) + \nabla\times\xi(r)) \\ &= -\Delta\psi(r) + \underbrace{\nabla\cdot(\nabla\times\xi(r))}_{=0} \\ &= -\Delta\psi(r) \\ &= \rho(r) \end{aligned}$$

and thus

$$\Delta\psi_\Omega = -\rho, \quad r \in \Omega \tag{4.3}$$
$$\Delta\psi_\Sigma = 0, \quad r \in \Sigma \tag{4.4}$$

Remembering that we assumed that $\rho \equiv 0$ in a finite neighbourhood of the boundary Γ, and thus the non–existence of apparent surface charges on the protein surface, the arguments from Section 2.2.1 imply:

$$[\partial_n\psi_\Sigma - \partial_n\psi_\Omega]|_\Gamma = 0 \tag{4.5}$$

While this might already seem like a reduction to a purely local setting, since ψ is governed by the same laws as φ in local vacuum electrostatics, it is important to keep in mind that the quantity we are ultimately interested in is φ, not ψ, since only φ can be used to compute the forces and energies for the system. Inside Ω this is unproblematic, since due to the relationship

$$\boldsymbol{D}_\Omega(\boldsymbol{r}) = \varepsilon_0\varepsilon_\Omega\boldsymbol{E}(\boldsymbol{r})$$

we can conclude

$$\psi_\Omega = \varepsilon_0\varepsilon_\Omega\varphi_\Omega \tag{4.6}$$

but φ_Σ and ψ_Σ are still related through the complex nonlocal integro–differential equation

$$\boldsymbol{D}_\Sigma(\boldsymbol{r}) = -\varepsilon_0\int_\Sigma d\boldsymbol{r}'\,\varepsilon(\boldsymbol{r},\boldsymbol{r}')\boldsymbol{\nabla}_{\boldsymbol{r}'}\varphi_\Sigma(\boldsymbol{r}') = -\boldsymbol{\nabla}\psi(\boldsymbol{r}) + \boldsymbol{\nabla}\times\xi(\boldsymbol{r}) \tag{4.7}$$

4.2. Fundamental solutions as dielectric functions

We have repeatedly stated in this work that the main difficulties in solving and interpreting the system of equations (3.9) stems from the mixture of integral and differential operators. The obvious remedy of course would be "to get rid" of the integrals, i.e. more precisely, replacing the integral operators by the integrands, evaluated at a single point. But this is only possible without changing the solutions to the equation, if the integrand contains a Dirac δ–distribution as a prefactor. Since the integrands are products of the electric field with the nonlocal dielectric function, this seems to be impossible to achieve: Dirac–like fields are clearly unphysical and will therefore not occur, and the dielectric function also differs remarkably from a δ–distribution for finite λ.

Our novel reformulation of nonlocal electrostatics now is based on an interesting observation: if the dielectric function was the fundamental solution (c.f. Appendix C) of a differential operator, then, since in our case, integration and differentiation commute, the dielectric function is transformed into a δ–distribution and the integrals should vanish. In the following, we will consider how this relates to the Lorentzian model for the nonlocal dielectric function of water.

4.2.1. The Yukawa–operator and its fundamental solution

The Lorentzian model for the nonlocal dielectric function of water (3.23) has a very peculiar structure: it is obviously the sum of two quite different terms: a δ–distribution, and a $e^{-\frac{r}{\lambda}}r^{-1}$–like function. A decomposition of the following kind therefore seems in order:

$$\varepsilon(\boldsymbol{r} - \boldsymbol{r}') = \varepsilon_\infty\delta(\boldsymbol{r} - \boldsymbol{r}') + \frac{\varepsilon_\Sigma - \varepsilon_\infty}{4\pi\lambda^2}\frac{e^{-\frac{|\boldsymbol{r}-\boldsymbol{r}'|}{\lambda}}}{|\boldsymbol{r} - \boldsymbol{r}'|}$$
$$= \varepsilon_\infty\delta(\boldsymbol{r} - \boldsymbol{r}') + \tilde{\varepsilon}\mathcal{G}(\boldsymbol{r} - \boldsymbol{r}') \tag{4.8}$$

where we have introduced the abbreviations

$$\tilde{\varepsilon} := \frac{\varepsilon_\Sigma - \varepsilon_\infty}{\lambda^2} \tag{4.9}$$

$$\mathcal{G}(\boldsymbol{r} - \boldsymbol{r}') := \frac{1}{4\pi}\frac{e^{-\frac{|\boldsymbol{r}-\boldsymbol{r}'|}{\lambda}}}{|\boldsymbol{r} - \boldsymbol{r}'|} \tag{4.10}$$

The outstanding importance of this decomposition for our considerations stems from the following theorem:

4. A novel formulation of nonlocal electrostatics

Theorem 4.2.1 (Fundamental solution of the Yukawa equation). *The function $-\mathcal{G}(r-r')$ defined by equation* (4.10),

$$-\mathcal{G}(r - r') := \frac{-1}{4\pi} \frac{e^{-\frac{|r-r'|}{\lambda}}}{|r - r'|}$$

is the fundamental solution (c.f. Appendix C) of the Yukawa operator

$$\mathcal{L}_\lambda := \Delta - \frac{1}{\lambda^2} \tag{4.11}$$

i.e.

$$\boxed{\mathcal{L}_\lambda \mathcal{G}(r - r') = -\delta(r - r')} \tag{4.12}$$

Proof. With the definition of the Yukawa operator[1] (4.11), (4.12) yields:

$$\left(\Delta_r - \frac{1}{\lambda^2}\right) \mathcal{G}(r - r') = -\delta(r - r') \tag{4.13}$$

To simplify the following computations, we choose – without loss of generality – a coordinate system with origin in r', and since the Laplacian appearing in the Yukawa operator is a translation invariant operator – this can be seen easily by e.g. expressing Δ in spherical coordinates – it is left unchanged by this transformation. We can therefore write

$$\mathcal{G}(r - r') \mapsto \mathcal{G}(r)$$

and have to solve for

$$\left(\Delta_r - \frac{1}{\lambda^2}\right) \mathcal{G}(r) = -\delta(r)$$

Fourier transforming this expression and utilising equations (A.24) and (B.12) yields:

$$\left(\Delta_r - \frac{1}{\lambda^2}\right) \mathcal{G}(r) = -\delta(r)$$

$$\stackrel{\mathscr{FT}}{\rightsquigarrow} \left((-\imath k)^2 - \frac{1}{\lambda^2}\right) \hat{\mathcal{G}}(k) = -\frac{1}{\sqrt{2\pi}^3}$$

$$\Leftrightarrow \quad \left(k^2 + \frac{1}{\lambda^2}\right) \hat{\mathcal{G}}(k) = \frac{1}{\sqrt{2\pi}^3}$$

$$\Leftrightarrow \quad \hat{\mathcal{G}}(k) = \frac{1}{\sqrt{2\pi}^3} \frac{1}{k^2 + \frac{1}{\lambda^2}} \tag{4.14}$$

$\mathcal{G}(r)$ can now be computed by backtransforming equation (4.14) into physical space:

$$\mathcal{G}(r) = \frac{1}{(2\pi)^3} \int_{\mathbb{R}^3} \frac{e^{-\imath k \cdot r}}{k^2 + \frac{1}{\lambda^2}} \, dk$$

$$= \frac{1}{(2\pi)^3} \frac{4\pi}{|r|} \int_0^\infty \frac{k}{k^2 + \frac{1}{\lambda^2}} \sin(kr) \, dk \qquad \left(\hat{\mathcal{G}}(k) = \hat{\mathcal{G}}(|k|)\right)$$

$$= \frac{4\pi}{(2\pi)^3} \frac{1}{2|r|} \int_{-\infty}^\infty \frac{k}{k^2 + \frac{1}{\lambda^2}} \sin(kr) \, dk \qquad \text{(Integrand is even)}$$

---

1 The index r of the Laplacian operator denotes the variable with respect to which the second derivatives are taken.

$$= \frac{1}{(2\pi)^2} \frac{1}{|\boldsymbol{r}|} \int\limits_{-\infty}^{\infty} \frac{k}{k^2 + \frac{1}{\lambda^2}} \left\{ \frac{e^{\imath kr} - e^{-\imath kr}}{2\imath} \right\} dk$$

$$= \frac{1}{(2\pi)^2} \frac{1}{2\imath |\boldsymbol{r}|} \left\{ \underbrace{\int\limits_{-\infty}^{\infty} \frac{ke^{\imath kr}}{\left(k + \frac{\imath}{\lambda}\right)\left(k - \frac{\imath}{\lambda}\right)} dk}_{\mathcal{I}_1} - \underbrace{\int\limits_{-\infty}^{\infty} \frac{ke^{-\imath kr}}{\left(k + \frac{\imath}{\lambda}\right)\left(k - \frac{\imath}{\lambda}\right)} dk}_{\mathcal{I}_2} \right\} \tag{4.15}$$

To solve the integral $\mathcal{I}_1$, we notice that the integrand has two simple poles in the complex plane, both situated at the imaginary axis:
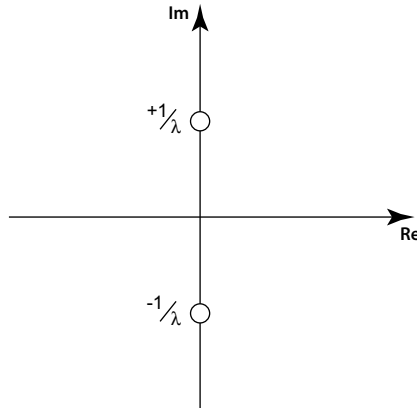
We will solve this integral using Cauchy's remarkable *residue theorem*, which we will just state here without giving a proof, since it can be found in any textbook on complex analysis (see for example [Kno96, Kra99]).

Definition 4.2.1 (Complex residue). Let $f(z), z \in \mathbb{C}$ be a complex analytic function, whose *Laurent series expansion* about the point $z_0 \in \mathbb{C}$ is given by:

$$f(z) = \sum_{n=-\infty}^{\infty} a_n (z - z_0)^n \tag{4.16}$$

$$= a_0 + a_1(z - z_0) + a_2(z - z_0)^2 + \cdots + \frac{a_{-1}}{(z - z_0)} + \frac{a_{-2}}{(z - z_0)^2} + \ldots \tag{4.17}$$

a_{-1} is called the *complex residue* of the function $f(z)$ in z_0:

$$\operatorname*{Res}_{z=z_0} f(z) := a_{-1}$$

where the subscript $z = z_0$ denotes that the coefficient a_{-1} was taken from the expansion about the point z_0.

Definition 4.2.2 (Pole of order m). Let $f(z), z \in \mathbb{C}$ be complex analytic with Laurent expansion (4.17). The point z_0 is called a *pole of order m of f*, **iff** in (4.17), $a_{-m} \neq 0$ and $a_{-k} = 0 \quad \forall k > m$.

Lemma 4.2.1 (Residues of functions with poles). *Let $f(z), z \in \mathbb{C}$ be complex analytic, and let f possess a pole of order m in the point $z = z_0$. Then, the complex residue of f in z_0 is given by:*

$$\operatorname*{Res}_{z=z_0} f(z) = \begin{cases} \lim\limits_{z \to z_0} (z - z_0)f(z) & m = 1 \\ \lim\limits_{z \to z_0} \frac{(z-z_0)^m}{(m-1)!} f(z) & m \geq 2 \end{cases} \tag{4.18}$$

Theorem 4.2.2 (The residue theorem of complex integration). *Let $f : U \subseteq \mathbb{C} \to \mathbb{C}$ be complex analytic on the open set U up to a finite set of poles Z, let γ be a closed C^1 positively oriented Jordan contour in U, and let $A \subseteq Z$ denote the subset of the poles of f that are enclosed by γ. Then*

$$\oint_{\gamma} f(z)\, dz = 2\pi\imath \sum_{z_i \in A} \operatorname{Res}_{z=z_i} f(z) \tag{4.19}$$

Formally extending the integrand $\mathcal{D}_1(k)$ into the complex plane to define a suitable contour that can be used to solve the integral $\mathcal{I}_1$

$$\mathcal{I}_1 = \int_{-\infty}^{\infty} \underbrace{\frac{ke^{\imath kr}}{\left(k + \frac{\imath}{\lambda}\right)\left(k - \frac{\imath}{\lambda}\right)}}_{\mathcal{D}_1(k)}\, dk \tag{4.20}$$

we notice that for k with large imaginary part, $\mathcal{D}_1(k)$ vanishes for *real valued* $r \in \mathbb{R}$, since with

$$k = \Re(k) + \imath\, \Im(k) =: u + \imath\, v$$

we have

$$e^{\imath kr} = e^{-vr} e^{\imath ur}$$

which in fact vanishes for $v \to \infty$. We can thus replace the integration over the real axis by an integration over a semi circle with infinite radius in the upper half of the complex plane, since the integration over the arc will not contribute to the integral:
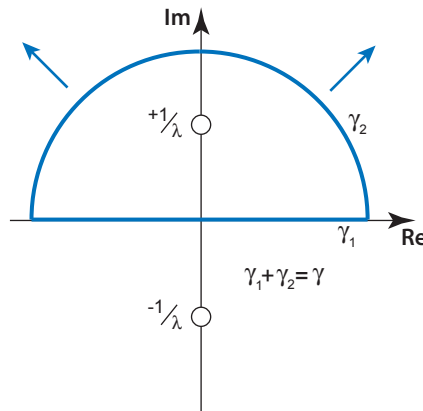
$$
\begin{aligned}
\int_{-\infty}^{\infty} \mathcal{D}_1(k)\, dk &= \int_{\gamma_1} \mathcal{D}_1(k)\, dk \\
&= \int_{\gamma_1} \mathcal{D}_1(k)\, dk + \underbrace{\int_{\gamma_2} \mathcal{D}_1(k)\, dk}_{=0} \\
&= \int_{\gamma_1 + \gamma_2} \mathcal{D}_1(k)\, dk \\
&= \oint_{\gamma} \mathcal{D}_1(k)\, dk
\end{aligned}
$$

$$\overset{(4.19)}{=} 2\pi\imath \sum_{\substack{k_j \in \mathcal{P}(\mathcal{D}_1) \\ \Im(k_i) \geq 0}} \operatorname{Res}_{k=k_i} \mathcal{D}_1(k)$$

where $\mathcal{P}(\mathcal{D}_1)$ denotes the set of poles of $\mathcal{D}_1(k)$. Since $\mathcal{D}_1(k)$ possesses two simple poles at the points

$$k_{1,2} = \pm\frac{\imath}{\lambda}$$

we have

$$\mathcal{P}(\mathcal{D}_1) = \left\{ \frac{+\imath}{\lambda}, \frac{-\imath}{\lambda} \right\}$$

and thus, according to Lemma 4.2.1, the two residues of $\mathcal{D}_1(\boldsymbol{k})$ are given by

$$\begin{aligned}
\operatorname{Res}_{k=k_1} \mathcal{D}_1(k) &= \lim_{k \to \frac{\imath}{\lambda}} \frac{\left(k - \frac{\imath}{\lambda}\right) k e^{\imath k r}}{\left(k + \frac{\imath}{\lambda}\right)\left(k - \frac{\imath}{\lambda}\right)} \\
&= \frac{\frac{\imath}{\lambda} e^{-\frac{r}{\lambda}}}{2\frac{\imath}{\lambda}} \\
&= \frac{1}{2} e^{-\frac{r}{\lambda}}
\end{aligned}$$ (4.21)

$$\begin{aligned}
\operatorname{Res}_{k=k_2} \mathcal{D}_1(k) &= \lim_{k \to \frac{-\imath}{\lambda}} \frac{\left(k + \frac{\imath}{\lambda}\right) k e^{\imath k r}}{\left(k + \frac{\imath}{\lambda}\right)\left(k - \frac{\imath}{\lambda}\right)} \\
&= \frac{\frac{\imath}{\lambda} e^{+\frac{r}{\lambda}}}{2\frac{\imath}{\lambda}} \\
&= \frac{1}{2} e^{+\frac{r}{\lambda}}
\end{aligned}$$ (4.22)

Since $\Im(k_2) = -\lambda^{-1} < 0$, k_2 lies *outside* the contour of integration γ, and thus does not contribute to the integral $\mathcal{I}_1$. We therefore obtain

$$\begin{aligned}
\mathcal{I}_1 &= \int_{-\infty}^{\infty} \frac{k e^{\imath k r}}{\left(k + \frac{\imath}{\lambda}\right)\left(k - \frac{\imath}{\lambda}\right)} \, dk \\
&= 2\pi\imath \operatorname{Res}_{k=k_1} \mathcal{D}_1(k) \\
&= 2\pi\imath \frac{1}{2} e^{-\frac{r}{\lambda}} \\
&= \pi\imath e^{-\frac{r}{\lambda}}
\end{aligned}$$ (4.23)

A completely analogous computation for the integral $\mathcal{I}_2$, using a contour in the lower complex semi plane shows that only $\operatorname{Res}_{k=k_2}$ contributes to $\mathcal{I}_2$, and leads to

$$\mathcal{I}_2 = -\pi\imath e^{-\frac{r}{\lambda}}$$ (4.24)

Inserting $\mathcal{I}_1$ and $\mathcal{I}_2$ into equation (4.15)

$$\mathcal{G}(\boldsymbol{r}) = \frac{1}{(2\pi)^2} \frac{1}{2\imath|\boldsymbol{r}|} \left\{ \underbrace{\int_{-\infty}^{\infty} \frac{k e^{\imath k r}}{\left(k + \frac{\imath}{\lambda}\right)\left(k - \frac{\imath}{\lambda}\right)} \, dk}_{\mathcal{I}_1} - \underbrace{\int_{-\infty}^{\infty} \frac{k e^{-\imath k r}}{\left(k + \frac{\imath}{\lambda}\right)\left(k - \frac{\imath}{\lambda}\right)} \, dk}_{\mathcal{I}_2} \right\}$$

yields

$$\begin{aligned}
\mathcal{G}(\boldsymbol{r}) &= \frac{1}{(2\pi)^2}\frac{1}{2\imath r}\left\{\pi\imath e^{-\frac{r}{\lambda}} - (-\pi\imath)e^{-\frac{r}{\lambda}}\right\} \\
&= \frac{2\pi}{(2\pi)^2}\frac{\imath}{2\imath r}e^{-\frac{r}{\lambda}} \\
&= \frac{1}{4\pi}\frac{e^{-\frac{r}{\lambda}}}{r} \qquad\qquad\qquad\qquad\qquad\quad \square
\end{aligned}$$

4.2.2. Reformulation of the equations of nonlocal electrostatics

In this chapter, we will show how we can make use of the special structure of dielectric functions of a general form shared by the Lorentzian model (3.23) in conjunction with the Helmholtz decomposition (4.7) of the displacement field in order to reduce the integro–differential equations of system (3.9) to a set of purely *differential equations*. The common feature of these dielectric functions will be the general form apparent in equation (4.8), i.e. the decomposition of the dielectric function into the sum

$$\varepsilon(\boldsymbol{r}-\boldsymbol{r}') = \varepsilon_\infty\delta(\boldsymbol{r}-\boldsymbol{r}') + \tilde{\varepsilon}\mathcal{G}(\boldsymbol{r}-\boldsymbol{r}')$$

where $\mathcal{G}(\boldsymbol{r}-\boldsymbol{r}')$ is the fundamental solution of a certain linear differential operator $-\mathcal{L}$, i.e.

$$\mathcal{L}\mathcal{G} = -\delta$$

in the distributional sense (c.f. Appendix C.1).

The general case

The original system of the equations of nonlocal electrostatics for the cavity model (3.9)

$$\left.\begin{aligned}
\Delta\varphi_\Omega(\boldsymbol{r}) &= \frac{-\rho(\boldsymbol{r})}{\varepsilon_0\varepsilon_\Omega} & \boldsymbol{r}\in\Omega \\
\boldsymbol{\nabla}_{\boldsymbol{r}}\int_\Sigma \varepsilon(\boldsymbol{r},\boldsymbol{r}')\boldsymbol{\nabla}_{\boldsymbol{r}'}\varphi_\Sigma(\boldsymbol{r}')\,d\boldsymbol{r}' &= 0 & \boldsymbol{r}\in\Sigma \\
\left[\boldsymbol{\nabla}_{\boldsymbol{r}}(\varepsilon_\Omega\varphi_\Omega(\boldsymbol{r})) - \int_\Sigma \varepsilon(\boldsymbol{r},\boldsymbol{r}')\boldsymbol{\nabla}_{\boldsymbol{r}'}\varphi_\Sigma(\boldsymbol{r}')\,d\boldsymbol{r}'\right]\cdot\hat{\boldsymbol{n}} &= 0 & \boldsymbol{r}\in\Gamma \\
\left[\varphi_\Omega(\boldsymbol{r}) - \varphi_\Sigma(\boldsymbol{r})\right] &= 0 & \boldsymbol{r}\in\Gamma
\end{aligned}\right\} \tag{4.25}$$

can formally be derived by inserting the nonlocal *material equation* (3.2) for Σ

$$\boldsymbol{D}_\Sigma(\boldsymbol{r}) = -\varepsilon_0\int_\Sigma \varepsilon(\boldsymbol{r},\boldsymbol{r}')\boldsymbol{\nabla}_{\boldsymbol{r}'}\varphi(\boldsymbol{r}')\,d\boldsymbol{r}'$$

and the local material equation (2.41) inside Ω

$$\boldsymbol{D}_\Omega(\boldsymbol{r}) = \varepsilon_0\varepsilon(\boldsymbol{r})\boldsymbol{E}_\Omega(\boldsymbol{r}) = -\varepsilon_0\varepsilon_\Omega\boldsymbol{\nabla}\varphi_\Omega(\boldsymbol{r})$$

into the system of cavity electrostatics for the displacement field, formulated independent of the choice of a local or nonlocal description:

$$\left.\begin{aligned}
\Delta\varphi_\Omega(\boldsymbol{r}) &= \frac{-\rho(\boldsymbol{r})}{\varepsilon_0\varepsilon_\Omega} & \boldsymbol{r}\in\Omega \\
\boldsymbol{\nabla}\cdot\boldsymbol{D}_\Sigma(\boldsymbol{r}) &= 0 & \boldsymbol{r}\in\Sigma \\
[\boldsymbol{D}_\Omega(\boldsymbol{r})) - \boldsymbol{D}_\Sigma(\boldsymbol{r})]\cdot\hat{\boldsymbol{n}} &= 0 & \boldsymbol{r}\in\Gamma \\
[\varphi_\Omega(\boldsymbol{r}) - \varphi_\Sigma(\boldsymbol{r})] \quad &= 0 & \boldsymbol{r}\in\Gamma
\end{aligned}\right\} \tag{4.26}$$

Combining these equations with their corresponding material equations, and using the considerations from Section 4.1, especially the Helmholtz decomposition (4.7), we can rewrite this to yield

$$\left.\begin{aligned}
\Delta\psi_\Omega &= -\rho & \boldsymbol{r} &\in \Omega \\
\Delta\psi_\Sigma &= 0 & \boldsymbol{r} &\in \Sigma \\
[\partial_n\psi_\Sigma - \partial_n\psi_\Omega] &= 0 & \boldsymbol{r} &\in \Gamma \\
[\varphi_\Omega - \varphi_\Sigma] &= 0 & \boldsymbol{r} &\in \Gamma \\
\varepsilon_0\varepsilon_\Omega\varphi_\Omega &= \psi_\Omega & \boldsymbol{r} &\in \Omega \\
-\varepsilon_0\int\limits_\Sigma d\boldsymbol{r}'\,\varepsilon(\boldsymbol{r},\boldsymbol{r}')\boldsymbol{\nabla}_{\boldsymbol{r}'}\varphi_\Sigma(\boldsymbol{r}') &= -\boldsymbol{\nabla}\psi(\boldsymbol{r}) + \boldsymbol{\nabla}\times\xi(\boldsymbol{r}) & \boldsymbol{r} &\in \Sigma
\end{aligned}\right\}$$ (4.27)

From now on, we will assume that the nonlocal dielectric function is of the particular form

$$\varepsilon(\boldsymbol{r}-\boldsymbol{r}') = \varepsilon_\infty\delta(\boldsymbol{r}-\boldsymbol{r}') + \tilde{\varepsilon}\mathcal{G}(\boldsymbol{r}-\boldsymbol{r}')$$ (4.28)

with $-\mathcal{G}$ being the fundamental solution of a linear differential operator $\mathcal{L}$, just as discussed above. With equation (4.28), the last equation in system (4.27) becomes

$$\varepsilon_0\int\limits_\Sigma d\boldsymbol{r}'\,\varepsilon(\boldsymbol{r},\boldsymbol{r}')\boldsymbol{\nabla}_{\boldsymbol{r}'}\varphi_\Sigma(\boldsymbol{r}') = \varepsilon_0\left\{\varepsilon_\infty\int\limits_\Sigma d\boldsymbol{r}'\,\delta(\boldsymbol{r}-\boldsymbol{r}')\boldsymbol{\nabla}_{\boldsymbol{r}'}\varphi_\Sigma(\boldsymbol{r}')\right.$$

$$\left.+\,\tilde{\varepsilon}\int\limits_\Sigma d\boldsymbol{r}'\,\mathcal{G}(\boldsymbol{r}-\boldsymbol{r}')\boldsymbol{\nabla}_{\boldsymbol{r}'}\varphi_\Sigma(\boldsymbol{r}')\right\}$$

$$= \varepsilon_0\varepsilon_\infty\boldsymbol{\nabla}\varphi_\Sigma(\boldsymbol{r}) + \varepsilon_0\tilde{\varepsilon}\int\limits_\Sigma d\boldsymbol{r}'\,\mathcal{G}(\boldsymbol{r}-\boldsymbol{r}')\boldsymbol{\nabla}_{\boldsymbol{r}'}\varphi_\Sigma(\boldsymbol{r}')$$

$$= \boldsymbol{\nabla}\psi(\boldsymbol{r}) - \boldsymbol{\nabla}\times\xi(\boldsymbol{r})$$

It is worthwhile to investigate the result of this computation

$$\boxed{\varepsilon_0\varepsilon_\infty\boldsymbol{\nabla}\varphi_\Sigma(\boldsymbol{r}) + \varepsilon_0\tilde{\varepsilon}\int\limits_\Sigma d\boldsymbol{r}'\,\mathcal{G}(\boldsymbol{r}-\boldsymbol{r}')\boldsymbol{\nabla}_{\boldsymbol{r}'}\varphi_\Sigma(\boldsymbol{r}') = \boldsymbol{\nabla}\psi(\boldsymbol{r}) - \boldsymbol{\nabla}\times\xi(\boldsymbol{r})}$$ (4.29)

closely. Apparently, the second term on the left hand side of equation (4.29) is an integral operator with the fundamental solution $\mathcal{G}$ of the differential operator $\mathcal{L}$ as its kernel function, and this is the only integral appearing. Integration commutes with $\mathcal{L}$, and thus we can hope to simplify equation (4.29) by letting $\mathcal{L}$ act on both sides:[2]

$$\varepsilon_0\varepsilon_\infty\mathcal{L}\left(\boldsymbol{\nabla}\varphi_\Sigma(\boldsymbol{r})\right) + \varepsilon_0\tilde{\varepsilon}\int\limits_\Sigma d\boldsymbol{r}'\,\left[\mathcal{L}_{\boldsymbol{r}}\mathcal{G}(\boldsymbol{r}-\boldsymbol{r}')\right]\boldsymbol{\nabla}_{\boldsymbol{r}'}\varphi_\Sigma(\boldsymbol{r}') = \mathcal{L}\left(\boldsymbol{\nabla}\psi(\boldsymbol{r})\right) - \mathcal{L}\left(\boldsymbol{\nabla}\times\xi(\boldsymbol{r})\right)$$

and since $\mathcal{G}$ is the fundamental solution of $-\mathcal{L}$, i.e. $\mathcal{L}\mathcal{G} = -\delta$, this becomes

$$\varepsilon_0\varepsilon_\infty\mathcal{L}\left(\boldsymbol{\nabla}\varphi_\Sigma(\boldsymbol{r})\right) - \mathcal{L}\left(\boldsymbol{\nabla}\psi(\boldsymbol{r})\right) + \mathcal{L}\left(\boldsymbol{\nabla}\times\xi(\boldsymbol{r})\right) = \varepsilon_0\tilde{\varepsilon}\int\limits_\Sigma d\boldsymbol{r}'\,\delta(\boldsymbol{r}-\boldsymbol{r}')\boldsymbol{\nabla}_{\boldsymbol{r}'}\varphi_\Sigma(\boldsymbol{r}')$$ (4.30)

$$= \varepsilon_0\tilde{\varepsilon}\boldsymbol{\nabla}\varphi_\Sigma(\boldsymbol{r})$$ (4.31)

---

2 As usual, $\mathcal{L}_{\boldsymbol{r}}$ denotes that the differentiation is taken with respect to the argument $\boldsymbol{r}$.

4. A novel formulation of nonlocal electrostatics

rearranging the terms in this last equation yields

$$\varepsilon_0 \left\{ \varepsilon_\infty \mathcal{L} - \tilde{\varepsilon} \right\} \boldsymbol{\nabla} \varphi_\Sigma(\boldsymbol{r}) - \mathcal{L}\left(\boldsymbol{\nabla} \psi(\boldsymbol{r}) \right) = -\mathcal{L}\left(\boldsymbol{\nabla} \times \xi(\boldsymbol{r}) \right) \tag{4.32}$$

We will now further assume that the differential operator $\mathcal{L}$ commutes with the gradient and curl operators:

$$[\mathcal{L}, \boldsymbol{\nabla}] = 0 \tag{4.33}$$

$$[\mathcal{L}, \boldsymbol{\nabla} \times] = 0 \tag{4.34}$$

This is no real restriction, since typically, fundamental solutions for operators with non–constant coefficients can only be found, if the variability of the coefficients is merely an artifact of the parametrization, i.e. if there exists a suitable coordinate system in which the coefficients are constant. This effect is most easily understood when remembering that e.g. the clearly variable coefficients of the Laplacian expressed in spherical coordinates

$$\Delta \psi(r, \theta, \phi) = \frac{1}{r^2} \frac{\partial}{\partial r} \left(r^2 \frac{\partial \psi}{\partial r} \right) + \frac{1}{r^2 \sin(\theta)} \frac{\partial}{\partial \theta} \left(\sin(\theta) \frac{\partial \psi}{\partial \theta} \right) + \frac{1}{r^2 \sin^2(\theta)} \frac{\partial^2 \psi}{\partial \phi^2}$$

become constant when expressed in a Cartesian frame of reference

$$\Delta \psi(x, y, z) = \frac{\partial^2 \psi}{\partial x^2} + \frac{\partial^2 \psi}{\partial y^2} + \frac{\partial^2 \psi}{\partial z^2}$$

and thus it is no contradiction that a fundamental solution for the Laplacian is known. We can therefore restrict our considerations to differential operators whose coefficients can be made trivial, i.e. constant, in a certain coordinate system, and assuming that $\mathcal{L}$ and equation (4.32) are expressed in this coordinate system, the commutation relations (4.33) and (4.34) are unproblematic, and we can assume that they hold for our differential operator. We can therefore push the gradient and curl operators in equation (4.32) to the left to yield

$$\boldsymbol{\nabla} \left[\varepsilon_0 \left\{ \varepsilon_\infty \mathcal{L} - \tilde{\varepsilon} \right\} \varphi_\Sigma(\boldsymbol{r}) - \mathcal{L} \psi_\Sigma(\boldsymbol{r}) \right] = -\boldsymbol{\nabla} \times \left(\mathcal{L} \xi(\boldsymbol{r}) \right) \tag{4.35}$$

Equation (4.35) is equivalent to

$$\boldsymbol{\nabla} \left[\varepsilon_0 \left\{ \varepsilon_\infty \mathcal{L} - \tilde{\varepsilon} \right\} \varphi_\Sigma - \mathcal{L} \psi_\Sigma \right] + \boldsymbol{\nabla} \times \left(\mathcal{L} \xi \right) \equiv \boldsymbol{0} \quad \text{in } \Sigma \tag{4.36}$$

i.e. a decomposition of the trivial field $\boldsymbol{0}$ into an irrotational and a solenoidal part, which motivates the following theorem:

Theorem 4.2.3. *For the displacement field $\boldsymbol{D}_\Sigma(\boldsymbol{r})$ of the nonlocal cavity model, the following equations hold for $\boldsymbol{r} \in \Sigma$:*

$$\boldsymbol{\nabla} \left[\varepsilon_0 \left\{ \varepsilon_\infty \mathcal{L} - \tilde{\varepsilon} \right\} \varphi_\Sigma(\boldsymbol{r}) - \mathcal{L} \psi_\Sigma(\boldsymbol{r}) \right] = \boldsymbol{0} \tag{4.37}$$

$$\boldsymbol{\nabla} \times \left(\mathcal{L} \xi(\boldsymbol{r}) \right) = \boldsymbol{0} \tag{4.38}$$

Proof. We will prove theorem 4.2.3 by showing that the two terms in

$$\boldsymbol{\nabla} \left[\varepsilon_0 \left\{ \varepsilon_\infty \mathcal{L} - \tilde{\varepsilon} \right\} \varphi_\Sigma - \mathcal{L} \psi_\Sigma \right] + \boldsymbol{\nabla} \times \left(\mathcal{L} \xi \right) \equiv \boldsymbol{0} \quad \text{in } \Sigma$$

are orthogonal in Σ, and since the sum of two orthogonal vectors can only vanish when both terms vanish independently of each other, this will complete the proof. Orthogonality of two fields $\boldsymbol{\nabla} \varphi$ and $\boldsymbol{\nabla} \times \boldsymbol{A}$, with $\boldsymbol{A} \in \mathcal{C}^2(\Sigma)$ and $\varphi \in \mathcal{C}^1(\Sigma)$, is equivalent to

$$\int_\Sigma \left(\boldsymbol{\nabla} \varphi(\boldsymbol{r}) \right) \cdot \left(\boldsymbol{\nabla} \times \boldsymbol{A}(\boldsymbol{r}) \right) d\boldsymbol{r} = 0$$

With Gauss's divergence theorem 2.2.1, this becomes

$$\oint_{\Gamma} \varphi(\boldsymbol{r}) \left(\boldsymbol{\nabla} \times \boldsymbol{A}(\boldsymbol{r})\right)_n \, d\boldsymbol{r} = 0 \tag{4.39}$$

The field $\boldsymbol{\nabla} \times \boldsymbol{A}(\boldsymbol{r})$ is obviously divergence–free, and with the considerations from Section 2.2.1, in particular equation (2.12), we can conclude that its normal component $\left(\boldsymbol{\nabla} \times \boldsymbol{A}(\boldsymbol{r})\right)_n$ is continuous along the interface Γ. In the equation we want to prove, $\boldsymbol{A} \equiv \mathcal{L}\xi_\Sigma$. Since we know that inside Ω, classical local electrostatics holds, where $\boldsymbol{E}_\Omega(\boldsymbol{r})$ and $\boldsymbol{D}_\Omega(\boldsymbol{r})$ are proportional, and since $\boldsymbol{\nabla} \times \boldsymbol{E}(\boldsymbol{r}) = 0$ everywhere, the solenoidal component in the decomposition of $\boldsymbol{D}_\Omega(\boldsymbol{r})$ must vanish:

$$\xi_\Omega \equiv 0$$

This of course implies that

$$\mathcal{L}\xi_\Omega \equiv 0$$

and thus

$$\left(\boldsymbol{\nabla} \times \mathcal{L}\xi_\Omega\right)_n \equiv 0$$

which finally, due to continuity of the normal components of solenoidal quantities leads to

$$\left(\boldsymbol{\nabla} \times \mathcal{L}\xi_\Sigma\right)_n \equiv 0$$

With the help of equation (4.39), it thus follows that the quantities $\boldsymbol{\nabla}\varphi_\Sigma$ and $\boldsymbol{\nabla} \times (\mathcal{L}\xi_\Sigma)$ are indeed orthogonal, and thus must vanish independently of each other everywhere in Σ. $\qquad\square$

With the help of theorem 4.2.3 we have been able to decouple the fields ψ_Σ and φ_Σ from ξ_Σ, and from inspection of system (4.27) we see that ξ_Σ is not needed to determine any other quantity of interest. Since it does also not occur in any of the boundary conditions, we can ignore ξ_Σ in all our further considerations.[3] The only equation we have left as a replacement for the nonlocal material equation is now, according to theorem 4.2.3 given by

$$\boldsymbol{\nabla} \left[\varepsilon_0 \left\{\varepsilon_\infty \mathcal{L} - \tilde{\varepsilon}\right\} \varphi_\Sigma(\boldsymbol{r}) - \mathcal{L}\psi_\Sigma(\boldsymbol{r})\right] = \boldsymbol{0} \tag{4.40}$$

The main quantities appearing in this equation, φ_Σ and ψ_Σ, are potentials, and as such they are only defined up to an additive gauge constant. But equation (4.40) equates the *gradients* of functions of those fields, and equality of the gradients implies equality of the functions up to an additive constant. The freedom of choice for an additive constant for the potentials φ_Σ and ψ_Σ allows us to "gauge this difference away", enabling us to finally drop the gradient operator in equation (4.40), yielding the *scalar* equation

$$\boxed{\varepsilon_0 \left\{\varepsilon_\infty \mathcal{L} - \tilde{\varepsilon}\right\} \varphi_\Sigma(\boldsymbol{r}) = \mathcal{L}\psi_\Sigma(\boldsymbol{r})} \tag{4.41}$$

This equation is the *purely differential equivalent* of the nonlocal integro–differential material equation for nonlocal electrostatics

$$\boldsymbol{D}_\Sigma(\boldsymbol{r}) = -\varepsilon_0 \int_\Sigma \varepsilon(\boldsymbol{r}, \boldsymbol{r}') \boldsymbol{\nabla}_{\boldsymbol{r}'} \varphi(\boldsymbol{r}') \, d\boldsymbol{r}'$$

for dielectric functions of the form (4.28). We can gather these results into our novel set of equations for nonlocal cavity electrostatics

$$\left.\begin{array}{rl}
\Delta\psi_\Omega = -\rho & \boldsymbol{r} \in \Omega \\
\Delta\psi_\Sigma = 0 & \boldsymbol{r} \in \Sigma \\
\left[\partial_n\psi_\Sigma - \partial_n\psi_\Omega\right] = 0 & \boldsymbol{r} \in \Gamma \\
\left[\varphi_\Omega - \varphi_\Sigma\right] = 0 & \boldsymbol{r} \in \Gamma \\
\varepsilon_0\varepsilon_\Omega\varphi_\Omega = \psi_\Omega & \boldsymbol{r} \in \Omega \\
\varepsilon_0 \left\{\varepsilon_\infty \mathcal{L} - \tilde{\varepsilon}\right\} \varphi_\Sigma(\boldsymbol{r}) = \mathcal{L}\psi_\Sigma(\boldsymbol{r}) & \boldsymbol{r} \in \Sigma
\end{array}\right\}$$

---

3 Note that the choice of $\xi_\Sigma \equiv \boldsymbol{0}$ would also be valid and consistent.

from which we can further eliminate the field ψ_Ω, since it is trivially related to φ_Ω, to yield

$$
\left.
\begin{aligned}
\varepsilon_0 \varepsilon_\Omega \Delta \varphi_\Omega &= -\rho & \boldsymbol{r} &\in \Omega \\
\Delta \psi_\Sigma &= 0 & \boldsymbol{r} &\in \Sigma \\
[\varepsilon_0 \varepsilon_\Omega \partial_n \varphi_\Omega - \partial_n \psi_\Sigma] &= 0 & \boldsymbol{r} &\in \Gamma \\
[\varphi_\Omega - \varphi_\Sigma] &= 0 & \boldsymbol{r} &\in \Gamma \\
\varepsilon_0 \left\{ \varepsilon_\infty \mathcal{L} - \tilde{\varepsilon} \right\} \varphi_\Sigma(\boldsymbol{r}) &= \mathcal{L} \psi_\Sigma(\boldsymbol{r}) & \boldsymbol{r} &\in \Sigma
\end{aligned}
\right\}
\tag{4.42}
$$

This system is purely differential, still linear by virtue of the linearity of the differential operator $\mathcal{L}$, and in general much easier to solve and interpret than the original system of equations (4.27). Last but not least, its formulation enables the use of efficient numerical techniques to solve for the electrostatic potential, as we will see in a later chapter.

Most importantly, for all nonlocal dielectric models of the proposed form, i.e. the sum of a Dirac δ distribution and a fundamental solution, and thus in particular for the Lorentzian model, system (4.42) is *exactly equivalent* to the classical formulation, and even though it is much more amenable to analytical, theoretical, and numerical means than the original system, and thus in particular invaluable for nontrivial geometries, it is *not an approximation* of the classical theory, as typical former approaches to the simplification of nonlocal electrostatics (e.g. [BP96]). It provides instead an *equivalent reformulation* for a wide class of models, including the by far most important one: the Lorentzian model (3.23).

Application to the Lorentzian model

For the special case where the nonlocal dielectric function of water $\varepsilon(\boldsymbol{r}, \boldsymbol{r}')$ is given by the Lorentzian model (3.23), the system (4.42) simplifies further. In this case, we have

$$
\begin{aligned}
\varepsilon(|\boldsymbol{r} - \boldsymbol{r}'|) &= \varepsilon_\infty \delta(\boldsymbol{r} - \boldsymbol{r}') + \frac{\varepsilon_\Sigma - \varepsilon_\infty}{4\pi\lambda^2} \frac{e^{-\frac{|\boldsymbol{r} - \boldsymbol{r}'|}{\lambda}}}{|\boldsymbol{r} - \boldsymbol{r}'|} \\
&= \varepsilon_\infty \delta(\boldsymbol{r} - \boldsymbol{r}') + \tilde{\varepsilon} \mathcal{G}(\boldsymbol{r} - \boldsymbol{r}')
\end{aligned}
$$

where

$$
\tilde{\varepsilon} := \frac{\varepsilon_\Sigma - \varepsilon_\infty}{\lambda^2}
$$

and

$$
\mathcal{G}(\boldsymbol{r} - \boldsymbol{r}') := \frac{1}{4\pi} \frac{e^{-\frac{|\boldsymbol{r} - \boldsymbol{r}'|}{\lambda}}}{|\boldsymbol{r} - \boldsymbol{r}'|}
$$

As we have seen in Section 4.2.1, $-\mathcal{G}$ is the fundamental solution of the Yukawa operator $-\mathcal{L}_\lambda$ with

$$
\mathcal{L}_\lambda := \Delta - \frac{1}{\lambda^2}
$$

such that – according to theorem 4.2.1 –

$$
\mathcal{L}_\lambda \mathcal{G} = -\delta
$$

in the distributional sense. With these definitions, the last equation in system (4.42) becomes:

$$
\varepsilon_0 \left\{ \varepsilon_\infty \mathcal{L}_\lambda - \tilde{\varepsilon} \right\} \varphi_\Sigma(\boldsymbol{r}) = \mathcal{L}_\lambda \psi_\Sigma(\boldsymbol{r})
\tag{4.43}
$$

$$
\Leftrightarrow \qquad \varepsilon_0 \left\{ \varepsilon_\infty \left(\Delta - \frac{1}{\lambda^2} \right) - \tilde{\varepsilon} \right\} \varphi_\Sigma(\boldsymbol{r}) = \left(\Delta - \frac{1}{\lambda^2} \right) \psi(\boldsymbol{r})
\tag{4.44}
$$

$$\Leftrightarrow \qquad \left\{ \varepsilon_\infty \Delta - \frac{\varepsilon_\infty}{\lambda^2} - \frac{\varepsilon_\Sigma - \varepsilon_\infty}{\lambda^2} \right\} \varphi_\Sigma(\boldsymbol{r}) = \frac{1}{\varepsilon_0} \left(\Delta - \frac{1}{\lambda^2} \right) \psi(\boldsymbol{r}) \qquad (4.45)$$

$$\Leftrightarrow \qquad \left\{ \Delta - \frac{\varepsilon_\Sigma}{\varepsilon_\infty \lambda^2} \right\} \varphi_\Sigma(\boldsymbol{r}) = \frac{1}{\varepsilon_0 \varepsilon_\infty} \left(\Delta \psi(\boldsymbol{r}) - \frac{1}{\lambda^2} \psi(\boldsymbol{r}) \right) \qquad (4.46)$$

Where we have used that according to (4.42), ψ_Σ is *harmonic* in Σ. The term in braces on the left hand side of equation (4.46) is again a Yukawa–operator, but with the *rescaled correlation length*

$$\Lambda := \lambda \sqrt{\frac{\varepsilon_\infty}{\varepsilon_\Sigma}}$$

and we can thus rewrite the last equation in (4.42) to yield

$$\boxed{\varepsilon_0 \varepsilon_\infty \mathcal{L}_\Lambda \varphi_\Sigma = -\frac{1}{\lambda^2} \psi_\Sigma} \qquad (4.47)$$

This is an *inhomogeneous Yukawa–equation*

$$\mathcal{L}_\Lambda \varphi_\Sigma = \varrho$$

with *correlation length*

$$\Lambda := \lambda \sqrt{\frac{\varepsilon_\infty}{\varepsilon_\Sigma}}$$

and *source term*

$$\rho \equiv -\frac{1}{\lambda^2 \varepsilon_0 \varepsilon_\infty} \psi_\Sigma$$

The appearance of a Yukawa–equation is interesting for a number of different reasons, the least important of which is the striking coincidence that it was a Yukawa–equation we started with. The reproduction of the structure of the equation is a highly nontrivial result, that of course does not hold for general differential operators $\mathcal{L}$.

More importantly, the nature of the nonlocal effect in the Lorentzian model can be studied by carefully investigating the structure of equation (4.47). The first question we will address is the behaviour in the local limit, and the way the nonlocal effects arise when λ is smoothly varied from zero to a finite value. To this end, we multiply equation (4.47) by λ^2, and take the local limit of vanishing correlation, to yield

$$0 = \lim_{\lambda \to 0} \left\{ \varepsilon_0 \varepsilon_\infty \lambda^2 \Delta \varphi_\Sigma - \varepsilon_0 \varepsilon_\Sigma \varphi_\Sigma + \psi_\Sigma \right\} \qquad (4.48)$$

$$= -\varepsilon_0 \varepsilon_\Sigma \varphi_\Sigma + \psi_\Sigma \qquad (4.49)$$

$$\Rightarrow \quad \psi_\Sigma = \varepsilon_0 \varepsilon_\Sigma \varphi_\Sigma \qquad (4.50)$$

This is exactly the local material equation for the coupling of the potentials ψ_Σ and φ_Σ as can e.g. be seen from the system (4.27), which again tells us that the local limit is exactly recovered in our novel formulation of nonlocal electrostatics, just as we demanded in the beginning. We also observe that with λ the nonlocal effect is switched on smoothly, by perturbing the local material equation into an operator equation, where the contribution of the differential operator Δ is weighted by the correlation length λ, more and more dominating the local effects when λ increases.

In order to study the nonlocal effect in the Lorentzian model further, it is invaluable to notice that under a different name, the inhomogeneous Yukawa equation became enormously popular in a different field of biomolecular electrostatics: the potential of a charge distribution immersed in an *electrolyte*. We will therefore now undertake a small digression into the field of *electrostatic screening in ionic solutions*.

4. A novel formulation of nonlocal electrostatics

The local theory of ionic screening

Let us assume that our charge distribution ρ is immersed in a solvent, which in addition contains a certain large number of mobile anions and cations, which arise due to salt dissociation in the solvent. Typically, the solvent as a whole has vanishing monopole moment, which means that the number of positive elementary charges in the bulk solvent equals the number of negative ones, and since we are dealing only with neutral solvent molecules, this means that the anion charges exactly counter the cation charges. For the sake of clarity, we will only consider the case where only two species of ions exist: anions and cations of the valence Z, i.e. anions with charge. For a detailed review of the general case the reader is referred to the excellent monographs of Lamm [Lam03] and Holst [Hol94]. More concise introductions can be found in a variety of standard textbooks, like [Isr98, BR98, RN61, Dav62, Hil86, McQ76] and many more. The number of ions in such a system is typically very large, and thus a description in the framework of statistical mechanics is necessary. Using a field theoretical approach, it can be shown[NO00] that if correlation effects for the ions can be neglected, the probability distribution for the ions follows a Maxwell–Boltzmann law[McQ76, Hil86, Rei80], which means that the local ion concentration for the cations is proportional to

$$e^{-eZ\frac{\varphi(\boldsymbol{r})}{k_B T}}$$

and the local ion concentration of the anions to

$$e^{+eZ\frac{\varphi(\boldsymbol{r})}{k_B T}}$$

where k_B is the Boltzmann constant and T the temperature of the solution. This can be combined with the external charge density ρ^{ex} to a local charge density

$$\rho(\boldsymbol{r}) = \rho^{\text{ex}}(\boldsymbol{r}) + eZc_s \left\{ e^{-eZ\frac{\varphi(\boldsymbol{r})}{k_B T}} - e^{+eZ\frac{\varphi(\boldsymbol{r})}{k_B T}} \right\}$$

where c_s is the salt concentration for the case of vanishing potential. With the trigonometric identity

$$\sinh z \equiv \frac{1}{2} \left(e^z - e^{-z} \right)$$

the charge density can be simplified to

$$\rho(\boldsymbol{r}) = \rho^{\text{ex}}(\boldsymbol{r}) - 2eZc_s \sinh \left[eZ\frac{\varphi(\boldsymbol{r})}{k_B T} \right] \tag{4.51}$$

which can be inserted into the local Poisson equation for the electrostatic potential, yielding the famous *local Poisson–Boltzmann equation*.

$$\boxed{\Delta\varphi(\boldsymbol{r}) = \frac{1}{\varepsilon_0 \varepsilon_\Sigma} \left\{ -\rho^{\text{ex}}(\boldsymbol{r}) + 2eZc_s \sinh \left[eZ\frac{\varphi(\boldsymbol{r})}{k_B T} \right] \right\}} \tag{4.52}$$

The Debye–Hückel equation

For small values of the local electrostatic potential,

$$\frac{eZ\varphi}{k_B T} \lesssim 1$$

the hyperbolic sine in equation (4.52) can be expanded in a Taylor series

$$\sinh(x) = x + \frac{1}{6}x^3 + \frac{1}{120}x^5 + \mathcal{O}(x^6)$$

which yields to the lowest order with the definition of the *Debye screening length*

$$\kappa = \sqrt{\frac{2Z^2e^2c_s}{\varepsilon_0\varepsilon_\Sigma k_B T}}$$

the famous *Debye–Hückel equation*[DH23a, DH23b, Deb54]

$$\Delta\varphi(\boldsymbol{r}) = \frac{1}{\varepsilon_0\varepsilon_\Sigma}\left\{-\rho^{\mathsf{ex}}(\boldsymbol{r}) + \kappa^2\varphi(\boldsymbol{r})\right\} \tag{4.53}$$

which is nothing but our inhomogeneous Yukawa equation with a correlation length $\Lambda = \kappa^{-1}$ and source term $-\frac{1}{\varepsilon_0\varepsilon_\Sigma}\rho^{\mathsf{ex}}(\boldsymbol{r})$:

$$\mathcal{L}_{\kappa^{-1}}\varphi(\boldsymbol{r}) = -\frac{1}{\varepsilon_0\varepsilon_\Sigma}\rho^{\mathsf{ex}}(\boldsymbol{r})$$

This is of course a very interesting result, since it tells us that in the Lorentzian model for the nonlocal dielectric function, the water acts – up to nonlinear corrections – like a cloud of counterions screening the "polarization charge distribution" $\frac{\psi_\Sigma}{\lambda^2}$! We also learn from this considerations something very remarkable: in order to include linear counterion effects into nonlocal electrostatics, we only have to *shift the correlation length* by adding to the conventional Λ from equation (4.47) a term $\bar{\Lambda} = \kappa^{-1}$. Thus, linear counterion effects seem to be already included "for free" in our formulation of nonlocal electrostatics for the Lorentzian model, without causing any extra computational costs. This should be compared with the situation in the classical formulation (4.27), where any counterion term would increase the complexity of the equations even further.

The novel equations of cavity electrostatics for the Lorentzian model

We will conclude this section by combining the computations made so far into our novel formulation for the cavity model of nonlocal electrostatics using the Lorentzian model. The complete set of equations, which has all the convenient properties mentioned in the discussion of the more general system (4.42), and in addition *only* contains well–known and – much more important – *elliptic* differential equations, namely the *Poisson–, Laplace–,* and *inhomogeneous Yukawa–/Debye–Hückel equation*, looks as follows:

$$\left.\begin{aligned}
\varepsilon_0\varepsilon_\Omega\Delta\varphi_\Omega &= -\rho & \boldsymbol{r} &\in \Omega \\
\Delta\psi_\Sigma &= 0 & \boldsymbol{r} &\in \Sigma \\
[\varepsilon_0\varepsilon_\Omega\partial_n\varphi_\Omega - \partial_n\psi_\Sigma] &= 0 & \boldsymbol{r} &\in \Gamma \\
[\varphi_\Omega - \varphi_\Sigma] &= 0 & \boldsymbol{r} &\in \Gamma \\
\varepsilon_0\varepsilon_\infty\mathcal{L}_\Lambda\varphi_\Sigma &= -\frac{1}{\lambda^2}\psi_\Sigma & \boldsymbol{r} &\in \Sigma
\end{aligned}\right\} \tag{4.54}$$

4.2.3. Spherical systems revisited

To demonstrate how computations in this novel framework can be performed, we will now rederive the electrostatic potential for the Born model, equations (3.57) and (3.58) without having to use the equivalence with the spherical shell model, which was crucial for our derivations in Section 3.5.1. For

the Born model, the system (4.54) assumes the form

$$
\left.
\begin{aligned}
\varepsilon_0 \Delta \varphi_{\mathcal{B}_a^0} &= -q\delta & \boldsymbol{r} &\in \mathcal{B}_a^0 \\
\Delta \psi_\Sigma &= 0 & \boldsymbol{r} &\in \Sigma \\
\left[\varepsilon_0 \partial_n \varphi_{\mathcal{B}_a^0} - \partial_n \psi_\Sigma \right] &= 0 & \boldsymbol{r} &\in \mathcal{S}_a^2 \\
\left[\varphi_{\mathcal{B}_a^0} - \varphi_\Sigma \right] &= 0 & \boldsymbol{r} &\in \mathcal{S}_a^2 \\
\varepsilon_0 \varepsilon_\infty \mathcal{L}_\Lambda \varphi_\Sigma &= -\frac{1}{\lambda^2} \psi_\Sigma & \boldsymbol{r} &\in \Sigma
\end{aligned}
\right\}
\tag{4.55}
$$

The first equation is exactly the same as in the local case, and therefore, with the same arguments as in Section 3.5.1, we can conclude that with $r := \|\boldsymbol{r}\|$ it is solved by

$$
\varphi_{\mathcal{B}_a^0}(r) = \frac{q}{4\pi\varepsilon_0} \frac{1}{r} + \mathcal{C}
\tag{4.56}
$$

Continuity of the potential φ thus immediately tells us that on the boundary $\Gamma \equiv \mathcal{S}_a^2$, we have

$$
\varphi_{\mathcal{B}_a^0}(r = a) = \frac{q}{4\pi\varepsilon_0} \frac{1}{a} + \mathcal{C} = \varphi_\Sigma(r = a)
\tag{4.57}
$$

and the second boundary condition yields

$$
\begin{aligned}
\partial_n \varphi_{\mathcal{B}_a^0}(r = a) &= -\frac{q}{4\pi\varepsilon_0} \frac{1}{a^2} \\
&= \partial_n \psi_\Sigma(r = a) \\
\Rightarrow \qquad \psi_\Sigma(r) &= \frac{q}{4\pi r} + \mathcal{C}'
\end{aligned}
\tag{4.58}
$$

Since we still have the freedom of gauging our potentials with an additive constant, we can set $\mathcal{C}' = 0$ (remember that the relations between φ_Σ and ψ_Σ only hold up to arbitrary additive constants, and thus the material equation in this case reads

$$
\varepsilon_0 \varepsilon_\infty \mathcal{L}_\Lambda \varphi_\Sigma = -\frac{1}{\lambda^2} \frac{q}{4\pi r}
$$

Using the definition of the Yukawa differential operator

$$
\mathcal{L}_\Lambda = \Delta - \frac{1}{\Lambda^2}
$$

and making use of the spherical symmetry of the problem, this becomes

$$
\varepsilon_0 \varepsilon_\infty \left(\Delta - \frac{1}{\Lambda^2} \right) \varphi_\Sigma = -\frac{1}{\lambda^2} \frac{q}{4\pi r}
\tag{4.59}
$$

$$
\Leftrightarrow \left[\frac{1}{r^2} \left(\frac{\partial}{\partial r} \left(r^2 \frac{\partial}{\partial r} \right) \right) - \frac{1}{\Lambda^2} \right] \varphi_\Sigma(r) = -\frac{1}{\varepsilon_0 \varepsilon_\infty \lambda^2} \frac{q}{4\pi r}
\tag{4.60}
$$

It is easy to check that (4.60) is indeed solved by

$$
\varphi_\Sigma(r) = \frac{q}{4\pi\varepsilon_0\varepsilon_\Sigma} \frac{1}{r} \left\{ 1 + \frac{\varepsilon_\Sigma - \varepsilon_\infty}{\varepsilon_\infty} \frac{\sinh \nu}{\nu} e^{-\nu \frac{r}{a}} \right\}
\tag{4.61}
$$

and with the boundary condition (4.57) we have

$$
\frac{q}{4\pi\varepsilon_0\varepsilon_\Sigma} \frac{1}{a} \left\{ 1 + \frac{\varepsilon_\Sigma - \varepsilon_\infty}{\varepsilon_\infty} \frac{\sinh \nu}{\nu} e^{-\nu} \right\} = \frac{q}{4\pi\varepsilon_0} \frac{1}{a} + \mathcal{C}
\tag{4.62}
$$

$$
\Rightarrow \frac{q}{4\pi\varepsilon_0} \frac{1}{a} \left(\frac{1}{\varepsilon_\Sigma} - 1 \right) + \frac{q}{4\pi\varepsilon_0\varepsilon_\Sigma} \frac{1}{a} \left\{ \frac{\varepsilon_\Sigma - \varepsilon_\infty}{\varepsilon_\infty} \frac{\sinh \nu}{\nu} e^{-\nu} \right\} = \mathcal{C}
\tag{4.63}
$$

And thus with equation (4.56) we obtain for the electrostatic potential inside the ion

$$\varphi_\Omega(r) = \frac{q}{4\pi\varepsilon_0}\frac{1}{r} + \mathcal{C} \tag{4.64}$$

$$= \frac{q}{4\pi\varepsilon_0}\left[\frac{1}{r} + \frac{1}{a}\left(\frac{1}{\varepsilon_\Sigma} - 1\right) + \frac{1}{\varepsilon_\Sigma}\frac{1}{a}\left\{\frac{\varepsilon_\Sigma - \varepsilon_\infty}{\varepsilon_\infty}\frac{\sinh\nu}{\nu}e^{-\nu}\right\}\right] \tag{4.65}$$

$$= \frac{q}{4\pi\varepsilon_0}\left[\frac{1}{r} + \frac{1}{\varepsilon_\Sigma a}\left\{1 - \varepsilon_\Sigma + \frac{\varepsilon_\Sigma - \varepsilon_\infty}{\varepsilon_\infty}\frac{\sinh\nu}{\nu}e^{-\nu}\right\}\right] \tag{4.66}$$

Comparing these results for φ_Σ (equation (4.61)) and for φ_Ω (equation (4.66)) with those obtained via the spherical shell model (equations (3.58) and (3.57)) shows that both computations consistently lead to the same result. We have thus been able rederive in a much more straightforward way the analytical result for the electrostatic potential for monoatomic ions in the Lorentzian model using our novel formulation.

4.2.4. The planar case

Even though the spherically symmetric Born model is of enormous importance for the computation of electrostatic quantities for monoatomic systems, where it impressively illustrates the advantages of a nonlocal description, it is not the only system that is analytically tractable in our novel formulation. In this section, we will discuss some semi–analytical results for a planar system which is of special interest to us since it will serve as a starting point for the investigation of membrane electrostatics in the near future. In particular, there is reason to believe that experimental results of atomic–force microscopy measurements on force–deflection curves at charged mica substrates in water and solutions of monovalent ions [TCdS01] can be explained in the nonlocal framework, if counterion effects are included. Initial estimation suggests that for a shifted correlation length – i.e. the combination of the water–water correlation length λ and the screening length[4] κ – on the order of 100 Å the prediction agrees very well with the experiment. The presentation in this section closely follows the derivation by Ralf Blossey, which can be found in [HBR$^+$04].

The model geometry we want to study is that of a point charge q embedded on the z–axis in the semi–infinite domain $\Omega := \left\{\boldsymbol{r} \in \mathbb{R}^3 \,\middle|\, \boldsymbol{r}\cdot\hat{\boldsymbol{e}}_z > 0\right\}$ depicted in Fig. 4.1. As in the spherically symmetric case, we will first concern ourselves with the classical local computation, which will yield important insight into the solution of the nonlocal formulation. Since the computation in the local setting is a classical textbook example (see e.g. [Jac98]), we will only briefly cover it here. With the definition of Ω, we immediately obtain $\Sigma = \left\{\boldsymbol{r} \in \mathbb{R}^3 \,\middle|\, \boldsymbol{r}\cdot\hat{\boldsymbol{e}}_z < 0\right\}$ and $\Gamma = \left\{\boldsymbol{r} \in \mathbb{R}^3 \,\middle|\, \boldsymbol{r}\cdot\hat{\boldsymbol{e}}_z = 0\right\}$, which is the x–y plane at $z = 0$. This type of problem is conveniently solved by the method of *image charges:* we assume that the reaction of the medium can be described by a virtual charge distribution, the so–called image charges, in the medium. In our case it turns out that a single image point charge suffices to compute the electrostatic potential, and thus we assume that a virtual image charge of strength q' is situated inside Σ. The symmetry of the problem motivates a symmetrical arrangement of real and virtual charge, i.e. if the distance between q and Γ is d, then we place the image charge q' opposite to q, at a distance of d behind Γ. This problem possesses axial symmetry, and thus, expressing all quantities in cylindrical coordinates (ϱ, ϕ, z) is appropriate. The potential at any point $P = (\varrho, \phi, z) \in \Omega \setminus \{(0,0,d)\}$ is then given by the sum of the fields of the point charges, both the *real* charge q and the *virtual* charge q':

$$\varphi_\Omega(\varrho, \phi, z) = \frac{1}{4\pi\varepsilon_\Omega}\left(\frac{q}{\sqrt{\varrho^2 + (d-z)^2}} + \frac{q'}{\sqrt{\varrho^2 + (d+z)^2}}\right) \tag{4.67}$$

---

4 c.f. the treatment of the theory of ionic screening in Section 4.2.2
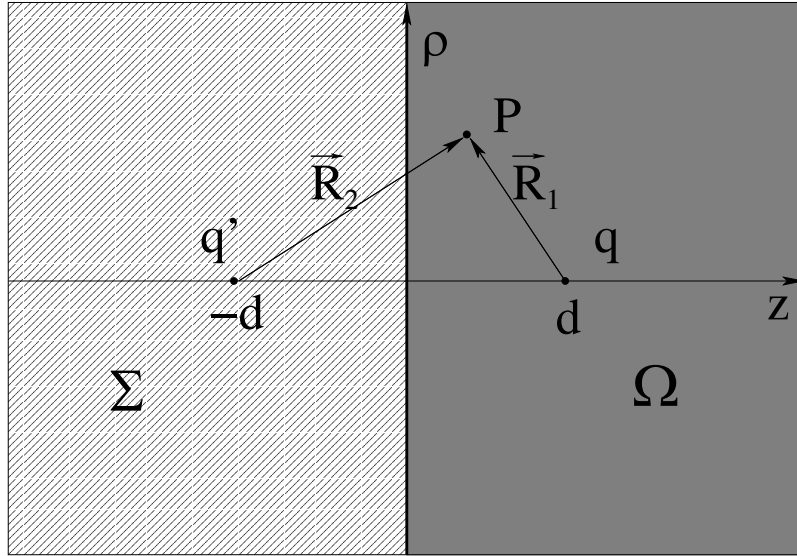
Figure 4.1.: Geometry of the problem of a charge q placed at a distance d from a dielectric boundary.

In order to fix the value of the unknown q' which we have introduced as a virtual charge, we now need to compute the potential inside Σ and then couple both fields. Since there are no **real** charges in Σ, the potential φ_Σ must solve the Laplace equation and cannot possess singularities inside Σ. φ_Σ is thus determined by the *real* charge q alone, and we may thus assume that it can be written in the form

$$\varphi_\Sigma(\varrho, \phi, z) = \frac{1}{4\pi\varepsilon_\Sigma} \frac{q''}{\sqrt{\varrho^2 + (d-z)^2}} \tag{4.68}$$

i.e. φ_Σ is the potential of a virtual charge of strength q'' at the position of the real charge q.

In order to couple the fields φ_Σ and φ_Ω, we will need to fulfill the local boundary conditions of system (2.45)

$$\left.\begin{array}{r} [\partial_n(\varepsilon_\Omega\varphi_\Omega) - \partial_n(\varepsilon_\Sigma(\boldsymbol{r})\varphi_\Sigma)] = 0 \\ [\varphi_\Omega(\boldsymbol{r}) - \varphi_\Sigma(\boldsymbol{r})] = 0 \end{array}\right\} \quad \boldsymbol{r} \in \Gamma \tag{4.69}$$

Since in our case Γ is simply the plane $z = 0$, the second boundary condition trivially leads to

$$\frac{1}{\varepsilon_\Omega}\left(\frac{q}{\sqrt{\varrho^2 + d^2}} + \frac{q'}{\sqrt{\varrho^2 + d^2}}\right) = \frac{1}{\varepsilon_\Sigma}\frac{q''}{\sqrt{\varrho^2 + d^2}}$$

$$\Leftrightarrow \qquad \frac{1}{\varepsilon_\Omega}\left(q + q'\right) = \frac{1}{\varepsilon_\Sigma}q'' \tag{4.70}$$

For the first boundary condition, we now need to compute the normal derivatives of the potentials. The normal to Γ is given by the normal vector in z direction $\hat{\boldsymbol{e}}_z$ everywhere on Γ, and thus we need to compute the terms

$$\frac{\partial}{\partial z}\left(\frac{1}{\sqrt{\varrho^2 + (d-z)^2}}\right)\Bigg|_{z=0} = -\frac{\partial}{\partial z}\left(\frac{1}{\sqrt{\varrho^2 + (d+z)^2}}\right)\Bigg|_{z=0} = \frac{d}{(\varrho^2 + d^2)^{\frac{3}{2}}} \tag{4.71}$$

which we can insert into (4.69) to yield

$$\frac{\partial}{\partial z}\left(\frac{q}{\sqrt{\varrho^2+(d-z)^2}}+\frac{q'}{\sqrt{\varrho^2+(d+z)^2}}\right)\Bigg|_{z=0}=\frac{\partial}{\partial z}\frac{q''}{\sqrt{\varrho^2+(d-z)^2}}\Bigg|_{z=0} \tag{4.72}$$

$$\Leftrightarrow \qquad \left(\frac{qd}{\left(\varrho^2+d^2\right)^{\frac{3}{2}}}-\frac{q'd}{\left(\varrho^2+d^2\right)^{\frac{3}{2}}}\right)=\frac{q''d}{\left(\varrho^2+d^2\right)^{\frac{3}{2}}} \tag{4.73}$$

so that we can conclude for our second boundary equation

$$q-q'=q'' \tag{4.74}$$

Together, both boundary conditions form a system of equations

$$\begin{pmatrix} 1 & 1 \\ -1 & \frac{\varepsilon_\Omega}{\varepsilon_\Sigma} \end{pmatrix}\begin{pmatrix} q' \\ q'' \end{pmatrix}=\begin{pmatrix} q \\ q \end{pmatrix} \tag{4.75}$$

which can be solved to yield the values for the image charges q' and q'':

$$q'=\frac{\varepsilon_\Omega-\varepsilon_\Sigma}{\varepsilon_\Omega+\varepsilon_\Sigma}q \tag{4.76}$$

$$q''=\frac{2\varepsilon_\Sigma}{\varepsilon_\Omega+\varepsilon_\Sigma}q \tag{4.77}$$

and thus the potentials in the local setting are given by

$$\varphi_\Omega(\varrho,\phi,z)=\frac{1}{4\pi\varepsilon_\Omega}\left\{\frac{q}{\sqrt{\varrho^2+(d-z)^2}}+\left(\frac{\varepsilon_\Omega-\varepsilon_\Sigma}{\varepsilon_\Omega+\varepsilon_\Sigma}\right)\frac{q}{\sqrt{\varrho^2+(d+z)^2}}\right\} \tag{4.78}$$

$$\varphi_\Sigma(\varrho,\phi,z)=\frac{1}{2\pi\left(\varepsilon_\Omega+\varepsilon_\Sigma\right)}\frac{q}{\sqrt{\varrho^2+(d-z)^2}} \tag{4.79}$$

In the nonlocal case it is easy to see that the equations for ψ_Σ have the same form as those for φ_Σ in the local case, and thus we assume the solutions to be similar. The normal boundary condition then remains unchanged, while the tangential boundary condition leads to

$$\partial_\varrho\varphi_\Sigma=\frac{1}{4\pi\varepsilon_0\varepsilon_\Omega}\frac{(q+q')}{\left[\varrho^2+d^2\right]^{\frac{3}{2}}}\varrho \tag{4.80}$$

at $z=0$. Through numerical integration of this equation, the nonlocal electrostatic potential at the boundary can now be determined. On the other hand we now that for $\varrho,z\to\infty$, φ_Σ must necessarily vanish for the energy of the system to be finite, which yields us a second boundary condition, this time at infinity. With the help of these two conditions we can then compute the electrostatic potential φ_Σ in all of Σ from equation (4.47) using numerical techniques. This requires considerable effort without providing much additional insight into the nonlocal effect, and we will thus only present the lowest order effect here, which can be assessed analytically. For $\varrho\ll\sqrt{2}d$, the electrostatic potential inside Ω has the same form as in the local theory if we assume a "renormalized" dielectric constant $\varepsilon_\Sigma=\varepsilon_{\Sigma,\text{loc}}-2\varepsilon_\infty(\frac{\lambda^2}{d^2})$. We thus find that transverse variations of the permittivity in the nonlocal medium induce a change of the effective local permittivity proportional to λ^2d^{-2} in the vicinity of the dielectric boundary, which means that – just as expected – the effect vanishes for $\lambda\to0$ and for deeply buried charges with $d\to\infty$.

4. A novel formulation of nonlocal electrostatics

5. The Boundary Element Method

In the previous chapters, we have shown how to derive a novel formulation of the theory of nonlocal electrostatics for a certain class of models for the dielectric function of water – a formulation that is purely differential in nature and thus much more amenable to numerical and analytical computations. We have also shown how to apply this technique to geometrically simple model systems, which allowed comparison to experimental data. Since these comparisons showed very good agreement with the experimental values, it seems highly desirable to apply the theory of nonlocal electrostatics to more involved geometries, in particular to arbitrarily shaped biomolecules. In the general case, we can of course not hope for analytical results – even the analytical parametrization of the molecular surface Γ is typically infeasible, and therefore, the need for a hand–tailored numerical technique, both efficient and highly accurate, arises.

For the solution of systems of partial differential equations like (4.54), several different numerical schemes exist, each with its own advantages and shortcomings. The most important techniques are

1. *Finite difference methods:* Σ, Ω and Γ are mapped onto a *regular lattice or grid*. Differential operators then become *finite difference operators* of the discretized functions. This reduces partial differential equations to algebraic difference equations, and several different techniques – depending on the system at hand. Finite difference methods are very popular in electrostatics computations due to their unsurpassable ease of use [DM91, PPL96, BNDS97], but typically at the cost of accuracy – an exact implementation of the boundary conditions is e.g. problematic at least, if not even impossible, and the results sensitively depend on parameters like the step size. In addition, finite difference methods require the handling of a fully three–dimensional discretization of the domains of interest, and thus the manipulation of often prohibitively large system matrices. Detailed treatments of the shortcomings of the finite difference method and a comparison to the boundary element method can be found in [Ras93, ZM88, Ras90, JBvK$^+$91, VGS92, BWS$^+$95].

2. *Finite element methods:* the domains of interest, Σ and Ω, are replaced by a so–called *simplicial approximation*, , i.e. they are approximated by a *simplicial complex*[Mun93]. A simplicial complex $\mathcal{K}$ in $\mathbb{R}^n$ is a collection of *simplices* in $\mathbb{R}^n$, such that

   a) Every face of a simplex of $\mathcal{K}$ is in $\mathcal{K}$ and

   b) The intersection of any two simplices of $\mathcal{K}$ is a face of each of them

   For the purposes of finite element methods, the simplices are typically chosen to be tetrahedrae or boxes, and the simplicial complex property demands that any two of those simplices are either disjoint or have exactly one face in common. The differential equation is then converted into an integral equation on Σ and Ω, and the integrals are subdivided into sums of integrals over each simplex. To evaluate these integrals, the restriction of each function of interest onto a given simplex is then approximated as a weighted sum of *test functions* on the simplex, e.g. low–rank polynomials. This reduces the partial differential equations – via the integral–equation route – to algebraic equations, which can be efficiently solved. Some examples for typical finite element applications to molecular electrostatics can be found in [CF97a, CF97b, HBW00, BHW00, BSHM01]

3. *Boundary element methods:* contrary to the finite difference and the finite element approaches, all computations in a boundary element method are carried out only on Γ. This is achieved by converting the original equation into a *boundary integral equation* that has to be solved on the interface Γ between the domains Σ and Ω only, thus dispensing with the need for a fully three–dimensional discretization. The boundary is then approximated by a simplicial complex, with either triangles or quadrilateral elements as simplices, and all functions are approximated as weighted sums over a set of test–functions over each simplex, reducing the differential equations to algebraic ones. The obvious peculiarity of the boundary element method is the reduction to a two–dimensional computation only on the boundary of the domain, but this comes at a certain cost: the boundary element method is not as generally applicable as the other two methods. Roughly speaking the main requirement is the existence of a fundamental solution to the original differential equation. It also requires considerably more mathematical effort in the preparation of the equations before a solver can be implemented. On the other hand, it has been demonstrated that for classical electrostatics problems, the boundary element method provides a highly accurate and nonetheless very efficient numerical technique [VS96, VGS92, SP99, TA01, CC03].

Since for typical applications in bioinformatics the accuracy of the computed electrostatic quantities is crucial, and since we wanted to allow for a fair comparison between local and nonlocal electrostatics, not clouded by numerical artifacts, we ruled out the possibility of a finite difference approach immediately, even though it would have been nearly trivial to implement. The choice between the remaining two schemes, finite element and boundary element methods, though, is a more difficult one. Following [Hun04], we will briefly give a comparison of the main advantages and disadvantages of the finite element method (FEM) and the boundary element method (BEM).

FEM	BEM
Entire domain mesh required	Only boundary mesh required
Entire domain solution computed at once	Solution computed at boundary first, then only at points of interest
Fluxes, $\boldsymbol{E}(\boldsymbol{r})$, $\boldsymbol{D}(\boldsymbol{r})$ less accurate than potentials	All fields computed with the same accuracy
Approximation of the *differential equation* and the *boundary conditions*	Approximation *only on the boundary conditions*, **not** on the *differential equation*
Integrals for each simplex easy to evaluate	Integrals more difficult to evaluate due to possibly singular integrands
Widely applicable, even to nonlinear problems	Naive application only possible for a certain class of linear problems
Sparse system matrices $\Rightarrow$ efficient implementation easily possible. But: dimensionality of matrices is large due to the domain meshing	System matrices in naive implementation fully populated and nonsymmetric! But: efficient approximation or compression schemes for the matrices possible, and dimensionality smaller because of boundary meshing
Easy to implement; straightforward route from differential equation to implementation	Much more difficult to implement; extensive mathematical manipulation of original equation required

As can bee seen from this comparison, the main advantages of the finite element method when compared to the boundary element method are related to its ease of use – if the boundary element method *can* be applied to the problem, most of its drawbacks can be overcome by investing more efforts into the derivation of the final algorithms. We therefore opted for developing a boundary element approach, which seems to allow for the most accurate and still highly efficient implementation.

5.1. The Boundary Element Method

The Boundary Element Method (BEM) is a powerful tool for the numerical solution of a wide class of partial differential equations, where the main requirement for the applicability is the existence of a fundamental solution[1] which has to be known analytically. Even though boundary element methods become increasingly popular in mathematics, physics and engineering, good monographs on this technique are a scarce commodity. Currently, [Ste03] (in German) and [Ste02] probably provide the most detailed treatment of the mathematical backgrounds and the numerical peculiarities of the method. A less rigorous presentation that is more aimed at engineers can be found e.g. in [Ame01] and [GKW03], and a good general overview is contained in [Hun04].

Historically, the works of Somigliana [Som85], Fredholm [Fre03] and Kupradze [Kup65] can be seen as the most important starting points for the boundary element method. Fredholm, for example, conducted a rigorous study of a wide class of integral equations, strongly influencing potential theory and related fields, like elasticity, but relying on purely analytical manipulations and solutions greatly reduced the possible application to the method to more or less trivial problems, until Jaswon [Jas63] and Symm [Sym63] used numerical techniques to solve a set of integral equations arising in two–dimensional potential theory. In these works, they discretized the boundary of their system into a simplicial complex made up of straight line elements, over which the potentials where approximated as constant functions. Building on these results, Rizzo[Riz67] was able to extend this approach to solve two–dimensional elastostatic problems, again approximating the potentials as constants. This was in turn generalized by Cruse[Cru69] to three–dimensional elastostatic problems, where he discretized the boundary into a set of flat triangular elements with potentials constant in each simplex. In a later work [Cru74], he also employed so–called *linear elements*, i.e. he approximated the potentials as piecewise linear functions over each triangle. Since then, a lot of research has been devoted to the boundary element method, leading to applications in a variety of sciences, including local molecular electrostatics [VS96, VGS92, SP99, TA01, CC03].

5.1.1. The weighted residual

The starting point for both, finite element and boundary element methods, is the concept of the *weighted residual*. Consider a differential equation

$$\mathcal{L}u = 0 \tag{5.1}$$

in a domain Ω, where $\mathcal{L}$ is an arbitrary differential operator. Using numerical techniques on a computer, we will in general not be able to recover the *exact* solution u, but will rather obtain an *approximate numerical* solution $\tilde{u}$, which will **not** exactly fulfill equation (5.1). Thus, under the action of the differential operator, the function $\tilde{u}$ will not vanish everywhere, as the exact solution u would, but will rather lead to a certain function ϵ, carrying the spatially resolved error of our solution:

$$\mathcal{L}\tilde{u} = \epsilon \tag{5.2}$$

The function ϵ, describing the error of the approximate solution, is called the *residual* of $\tilde{u}$ under $\mathcal{L}$. A good approximation is characterized by a small error, which means that the function ϵ has to be controlled or minimized in a certain way to obtain a good numerical approximation to the solution of equation (5.1). Minimizing this function now can be given a variety of different meanings, by e.g. choosing the norm in which the minimization is to be carried out. In finite– and boundary element

---

1 If no fundamental solution to the *full* differential operator exists, but for some of the terms it contains, the boundary element method can sometimes still be fruitfully applied by coupling it to more general techniques.

approaches the so–called *weighted residual* approach is taken: taking a (still arbitrary) *test function* w, we hope to find an approximate solution $\tilde{u}$ such that

$$\langle \epsilon, w \rangle = \int\limits_{\Omega} \epsilon(\boldsymbol{r}) w(\boldsymbol{r}) \, d\boldsymbol{r} = 0 \tag{5.3}$$

that is, we look for solutions $\tilde{u}$, such that the resulting approximation error function ϵ is *orthogonal* to the test function w in the $\mathcal{L}^2(\Omega)$ norm. With the help of equation (5.2), equation (5.3) can be rewritten to yield

$$\langle \mathcal{L}\tilde{u}, w \rangle = \int\limits_{\Omega} [\mathcal{L}\tilde{u}(\boldsymbol{r})] \, w(\boldsymbol{r}) \, d\boldsymbol{r} = 0 \tag{5.4}$$

5.1.2. The Galerkin approach

While the finite element method and the boundary element method differ in their choice of the test function w, they are both so–called *Galerkin–methods* , i.e. the solution $\tilde{u}$ is projected in a certain space of Ansatz– or basis functions. Let

$$\mathcal{A} := \operatorname{span}\left\{ (\chi)_{k=1}^m \right\}$$

denote such an Ansatz space with m basis functions χ_k. In a Galerkin approach, we now set

$$\tilde{u}(\boldsymbol{r}) := \sum_{k=1}^m u_k \chi_k(\boldsymbol{r}) \in \mathcal{A}$$

that is, we approximate the solution u to the differential equation as a weighted sum of basis functions, with expansion coefficients u_k. We have thus reduced the original problem of finding a solution to the original differential equation in an infinite–dimensional function space to the approximately equivalent, but much less complex problem of determining the coefficients $u_1 \ldots u_m$ such that the scalar product of the resulting function $\tilde{u}$ with the test function w vanishes:

$$\sum_{k=1}^m u_k \langle \chi_k, w \rangle = 0$$

The finite element method now proceeds by choosing the test function from *the same Ansatz space* $\mathcal{A}$ as the approximation $\tilde{u}$:

$$w = \sum_{k=1}^m w_k \chi_k(\boldsymbol{r}) \in \mathcal{A}$$

This approach is commonly termed a *Galerkin–Bubnov method,* and has the intuitive interpretation, that the error or residual function is made orthogonal to the approximation. In the boundary element method, on the other hand, we take a different route. The test function is not taken from the same function space $\mathcal{A}$ as the approximation $\tilde{u}$, but from a different space $\mathcal{B}$, which is the characteristic feature of so–called *Galerkin–Petrov methods.* Let us assume that the differential operator $\mathcal{L}$ possesses a fundamental solution $\mathcal{G}$, and that the analytical expression for $\mathcal{G}$ is known. The boundary element method is then characterized by the choice $w = \mathcal{G}$, i.e. the fundamental solution is used as the test function. If we are then able to shift the differential operator from the *unknown* function $\tilde{u}$ to the *known*, analytically given function $\mathcal{G}$, we can make use of the fundamental function property: under the action of $\mathcal{L}$, $\mathcal{G}$ will turn into a Dirac δ–distribution, which will in turn replace the domain integral with a simple function evaluation at a single point. We will soon see that in the process of shifting the differential operator to the fundamental solution, boundary integral terms arise as side effects from

necessary partial integrations. In this way, we are able to reduce a partial differential equation via an integro–differential equation to a purely *boundary integral equation*.

In order to see how this hand–wavingly introduced technique works in a practice, and how we further process the resulting boundary integral equations to obtain a solution to our original problem, we will now show how to derive a boundary element method for the case of the local Laplace equation inside a certain domain Ω, without coupling to an exterior domain Σ. We will then extend this simple and illustrative example to a boundary element solver for the local cavity model, which we will again extend to the much more involved case of the nonlocal cavity model (4.54). For notational convenience, we will in the following suppose that we are implicitly aware that the function $\tilde{u}$ is only a numerical approximation to the exact solution u, and will thus drop the tilde and use the same symbol for the approximate and the exact solution.

5.2. A Boundary Element Method for the interior Laplace–equation

In this section, we will try to derive a boundary element technique for the Laplace–equation inside a domain Ω with Lipshitz boundary Γ,

$$\Delta\varphi = 0 \text{ in } \Omega \tag{5.5}$$

In order to allow general boundary conditions, we assume that Γ is partitioned into pairwise disjoint partial boundaries

$$\Gamma = \bar{\Gamma}_D \cup \bar{\Gamma}_N \cup \bar{\Gamma}_R$$

and prescribe to equation (5.5) the following boundary conditions

- On Γ_D, we prescribe conditions on the field φ itself, so–called *Dirichlet conditions:*

$$\gamma_0^{\text{int}}\varphi(\boldsymbol{r}) = g_D(\boldsymbol{r}), \ \boldsymbol{r} \in \Gamma_D$$

  where γ_0^{int} is the internal Dirichlet trace operator as defined in Section 2.2.1.

- On Γ_N, we instead prescribe conditions on the *normal derivative of the field* φ, so–called *Neumann conditions*:

$$\gamma_1^{\text{int}}\varphi(\boldsymbol{r}) = g_N(\boldsymbol{r}), \ \boldsymbol{r} \in \Gamma_N$$

  where γ_1^{int} is the internal Neumann trace operator or conormal derivative of the Laplacian

$$\gamma_1^{\text{int}}\varphi(\boldsymbol{r}) := \partial_{\hat{\boldsymbol{n}}}\varphi(\boldsymbol{r}) := \boldsymbol{\nabla}\varphi(\boldsymbol{r})\cdot\hat{\boldsymbol{n}}(\boldsymbol{r}), \ \boldsymbol{r} \in \Gamma \tag{5.6}$$

- On Γ_R, we prescribe conditions on a weighted combination of the field and its normal derivative, so–called *Robin conditions:*

$$\gamma_1^{\text{int}}\varphi(\boldsymbol{r}) + \kappa(\boldsymbol{r})\gamma_0^{\text{int}}\varphi(\boldsymbol{r}) = g_R(\boldsymbol{r}), \ \boldsymbol{r} \in \Gamma_R$$

  where $\kappa(\boldsymbol{r})$ is given real function on the boundary.

In the weighted residual approach, we now have to consider the functional

$$\int_{\Omega} [\Delta\varphi(\boldsymbol{r})]\, w(\boldsymbol{r})\, d\boldsymbol{r} = 0 \tag{5.7}$$

Equation (5.7) is of a very special form: it is an integral over the Laplacian of a function times a second function, a form that suggests to apply the famous integral theorems of Green:

Theorem 5.2.1 (Green's integral theorems). *Let $\Omega \subset \mathbb{R}^3$ be a domain in three–dimensional space with positively oriented, piecewise smooth, simple closed boundary Γ, and let φ and ψ be continuous scalar functions with continuous partial derivatives up to second order on Ω. Let $\hat{n}$ denote the outward unit normal vector, and let $d\Gamma$ denote the infinitesimal surface element on Γ. Then, the following identities hold:*

$$\int_{\Omega} (\varphi \Delta \psi + \boldsymbol{\nabla}\varphi \cdot \boldsymbol{\nabla}\psi) \, d\boldsymbol{r} = \oint_{\Gamma} (\gamma_0^{int}\varphi)(\gamma_1^{int}\psi) d\Gamma \tag{5.8}$$

$$\int_{\Omega} (\varphi \Delta \psi - \psi \Delta \varphi) \, d\boldsymbol{r} = \oint_{\Gamma} \left[(\gamma_0^{int}\varphi)(\gamma_1^{int}\psi) - (\gamma_0^{int}\psi)(\gamma_1^{int}\varphi) \right] d\Gamma \tag{5.9}$$

where we have used the internal Dirichlet trace

$$\gamma_0^{int} f(\boldsymbol{r}) := \lim_{\Omega \ni \tilde{\boldsymbol{r}} \to \boldsymbol{r} \in \Gamma} f(\tilde{\boldsymbol{r}}), \quad \boldsymbol{r} \in \Gamma$$

and the internal Neumann trace or inner conormal derivative of the Laplacian

$$\gamma_1^{int}\varphi(\boldsymbol{r}) := \partial_{\hat{\boldsymbol{n}}}\varphi(\boldsymbol{r}) := \boldsymbol{\nabla}\varphi(\boldsymbol{r}) \cdot \hat{\boldsymbol{n}}(\boldsymbol{r}), \ \boldsymbol{r} \in \Gamma$$

Proof. To show the first identity, we perform an integration by parts, making use of the Gauss divergence law (2.8):

$$
\begin{aligned}
\int_{\Omega} \varphi \Delta \psi \, d\boldsymbol{r} &= \int_{\Omega} \varphi \sum_{i=1}^{3} \partial_{x_i} \partial_{x_i} \psi \, d\boldsymbol{r} \\
&= \int_{\Omega} \sum_{i=1}^{3} \partial_{x_i} (\varphi \partial_{x_i} \psi) \, d\boldsymbol{r} - \int_{\Omega} \sum_{i=1}^{3} (\partial_{x_i}\varphi)(\partial_{x_i}\psi) \, d\boldsymbol{r} \\
&= \int_{\Omega} \boldsymbol{\nabla} \cdot (\varphi \boldsymbol{\nabla}\psi) \, d\boldsymbol{r} - \int_{\Omega} (\boldsymbol{\nabla}\varphi) \cdot (\boldsymbol{\nabla}\psi) \, d\boldsymbol{r} \\
&\overset{(2.8)}{=} \oint_{\Gamma} (\gamma_0^{int}\varphi)(\gamma_1^{int}\psi) d\Gamma - \int_{\Omega} (\boldsymbol{\nabla}\varphi) \cdot (\boldsymbol{\nabla}\psi) \, d\boldsymbol{r} \qquad \square
\end{aligned}
$$

To prove the second identity, we note that by interchanging the role of φ and ψ in equation (5.8), we obtain

$$\int_{\Omega} (\psi \Delta \varphi + \boldsymbol{\nabla}\varphi \cdot \boldsymbol{\nabla}\psi) \, d\boldsymbol{r} = \oint_{\Gamma} (\gamma_0^{int}\psi)(\gamma_1^{int}\varphi) d\Gamma$$

Subtracting this result from equation (5.8), we obtain

$$\int_{\Omega} (\varphi \Delta \psi - \psi \Delta \varphi) \, d\boldsymbol{r} = \oint_{\Gamma} \left[(\gamma_0^{int}\varphi)(\gamma_1^{int}\psi) - (\gamma_0^{int}\psi)(\gamma_1^{int}\varphi) \right] d\Gamma \quad \square$$

With Green's second identity, equation (5.9), we can now rewrite the weighted residual equation for the Laplace operator (5.7) to yield:

$$0 = \int_{\Omega} [\Delta \varphi] w \, d\boldsymbol{r} = \int_{\Omega} \varphi [\Delta w] \, d\boldsymbol{r} + \oint_{\Gamma} (\gamma_0^{int}w)(\gamma_1^{int}\varphi) d\Gamma - \oint_{\Gamma} (\gamma_0^{int}\varphi)(\gamma_1^{int}w) d\Gamma \tag{5.10}$$

which is equivalent to

$$\int_\Omega \varphi \left[\Delta w\right] dr = \oint_\Gamma \left(\gamma_0^{\text{int}}\varphi\right)\left(\gamma_1^{\text{int}}w\right)d\Gamma - \oint_\Gamma \left(\gamma_0^{\text{int}}w\right)\left(\gamma_1^{\text{int}}\varphi\right)d\Gamma \tag{5.11}$$

which is called the *weak formulation* of the Laplace equation. Equation (5.11) contains a volume integral on the left hand side, and two boundary integrals on the right hand side, which are of course much easier to evaluate, since their dimensionality is lower by one. This motivates a choice for the still arbitrary test function w which eliminates the domain integration on the left hand side, and this of course means that Δw must become proportional to a Dirac δ–distribution, and thus, the test function w must be proportional to the fundamental solution of the Laplace operator! It turns out that a convenient normalization is possible, if – with the definition of the Laplacian's fundamental solution $\mathcal{F}$ – we choose

$$w(\boldsymbol{r}) := -\mathcal{F}(\boldsymbol{r}, \boldsymbol{\xi})$$

where the second argument $\boldsymbol{\xi}$ is considered constant. This leads to

$$\int_\Omega \varphi(\boldsymbol{r}) \left[\Delta w\right](\boldsymbol{r}) \, dr = -\int_\Omega \varphi \left[\Delta \mathcal{F}(\boldsymbol{r}, \boldsymbol{\xi})\right] \, dr \tag{5.12}$$

$$= -\int_\Omega \varphi(\boldsymbol{r})\delta(\boldsymbol{r} - \xi) \, dr \tag{5.13}$$

$$= \begin{cases} -\varphi(\boldsymbol{\xi}) & \boldsymbol{\xi} \in \Omega \\ 0 & \boldsymbol{\xi} \in \Sigma \\ \text{undefined} & \boldsymbol{\xi} \in \Gamma \end{cases} \tag{5.14}$$

Inserting equation (5.14) for $\boldsymbol{\xi} \in \Omega$ into equation (5.11) and using $w = -\mathcal{F}$ now finally yields the important *representation formula* for the solution φ of the Laplace equation (5.7) **inside** Ω,

$$\boxed{\varphi(\boldsymbol{\xi}) = \oint_\Gamma \left[\left(\gamma_0^{\text{int}}\varphi(\boldsymbol{r})\right)\left(\gamma_1^{\text{int}}\mathcal{F}(\boldsymbol{r}, \boldsymbol{\xi})\right) - \left(\gamma_0^{\text{int}}\mathcal{F}(\boldsymbol{r}, \boldsymbol{\xi})\right)\left(\gamma_1^{\text{int}}\varphi(\boldsymbol{r})\right)\right]d\Gamma} \tag{5.15}$$

At first glance it might seem as if not much was gained in deriving equation (5.15): we have started with a partial differential equation, converted it into an integro–differential equation, which after some tedious manipulation was cast into yet another equation containing integrals and differentials, the representation formula (5.15). But two important features clearly distinguish the representation formula from the formulations we started with, yielding enormous simplifications for the solution procedures we will later implement. The first of these features can be easily seen: equation (5.15) is really a representation of φ everywhere in Ω in terms of *boundary integrals* only, without the necessity of performing expensive domain or volume integrations. In this sense, we could hand–wavingly argue that the dimensionality of our problem has been reduced by one. Even more important, but more difficult to see, is the second feature: if we were given the *full* boundary conditions, the functions $\gamma_0^{\text{int}}\varphi$ and $\gamma_1^{\text{int}}\varphi$, everywhere on Γ – these are known as *Cauchy data* – the representation formula (5.15) would no longer be an *integral– or integro–differential equation* in the true sense of the meaning, since all integrations and differentiations would be applied to *known* functions. Thus, all integrands were fully known, and thus, the sought potential φ, the solution to the Laplace equation (5.7), could be trivially computed by a numerical approximation of the boundary integrals, which can be performed very accurately and highly efficient.

Unfortunately, in our general formulation of the problem, we are not initially given the full Cauchy data on Γ, but instead, we are provided with values for $\gamma_0^{\text{int}}\varphi$ on Γ_D, $\gamma_1^{\text{int}}\varphi$ on Γ_N, and $\gamma_1^{\text{int}}\varphi + \kappa\gamma_0^{\text{int}}\varphi$ on Γ_R. In fact, it can be shown using a maximum principle approach that it is in general not possible to prescribe arbitrary values for the full Cauchy data for the Laplace equation – the system would be overspecified, and in general, no solution will exist for an arbitrary set of Cauchy data [Jos02]. This is due to the fact, that given one component of the Cauchy data on a certain subset of Γ, i.e. either $\gamma_0^{\text{int}}\varphi$ on Γ_D, or $\gamma_1^{\text{int}}\varphi$ on Γ_N, the other component is uniquely determined if the function fulfills a Laplace equation inside Ω. In fact, looking at the representation formula (5.15) this seems like a triviality, since we might be tempted to think that taking $\boldsymbol{\xi}$ to lie *on the boundary*, the term on the left hand side would become $\gamma_0^{\text{int}}\varphi$ and we would arrive at an equation coupling the fields $\gamma_0^{\text{int}}\varphi$ and $\gamma_1^{\text{int}}\varphi$.

Unfortunately, the derivation of an equation for the missing component of the Cauchy data is not quite that simple, since the hand–wavingly introduced idea of taking $\boldsymbol{\xi}$ to lie on the boundary Γ cannot be justified: the representation formula (5.15) is *only* valid strictly *inside* the domain Ω, and it is not trivial to extend it onto its boundary, since the Dirac δ–distribution occurring in the derivation of equation (5.15) is *undefined* if $\boldsymbol{\xi} \in \Gamma$, as can be seen from equation (5.14). The general idea, though, turns out to lead to the desired result: in order to relate the Dirichlet data to the Neumann data and thus to generate the full set of Cauchy data everywhere on Γ, we will examine how we can put the point $\boldsymbol{\xi}$ under consideration onto the boundary, without arriving at meaningless undefined quantities. This can be achieved by virtually extending the boundary around this "load point", and considering a limiting process that shrinks this virtual extension to zero. For this process, we chose a load point $\boldsymbol{\xi}$
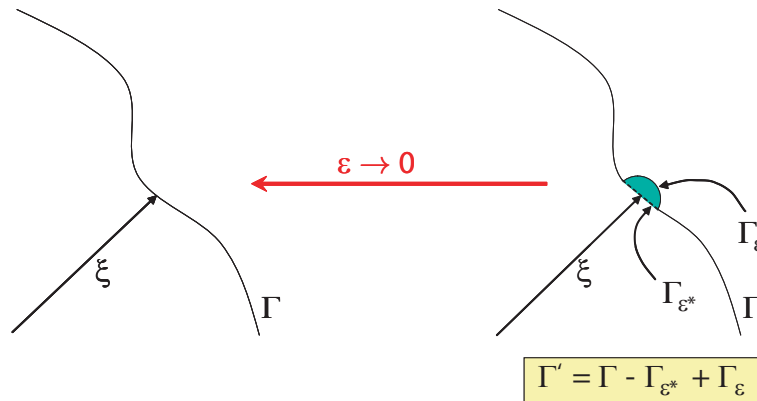
Figure 5.1.: The boundary extension used for the derivation of the boundary integral equation.

on Γ, and extend the boundary around it by replacing a small surrounding Γ_ϵ^* of $\boldsymbol{\xi}$ by a semi-sphere Γ_ϵ of radius ϵ. This replaces the old boundary Γ with a new, extended boundary Γ', such that

$$\Gamma = \lim_{\epsilon \to 0} \Gamma'$$

with the decomposition (c.f. Fig. 5.1)

$$\Gamma' = (\Gamma - \Gamma_\epsilon^* + \Gamma_\epsilon) \tag{5.16}$$

Since for arbitrary small but finite ϵ, $\boldsymbol{\xi}$ is embedded in the new boundary Γ' and thus lies inside the corresponding domain Ω', the representation formula for the solution of the Laplace equation inside a

domain (5.15) is again valid, and we can thus consider the equation

$$\varphi(\boldsymbol{\xi}) = \lim_{\epsilon \to 0} \oint_{\Gamma'} \left[\left(\gamma_0^{\text{int}} \varphi(\boldsymbol{r}) \right) \left(\gamma_1^{\text{int}} \mathcal{F}(\boldsymbol{r}, \boldsymbol{\xi}) \right) - \left(\gamma_0^{\text{int}} \mathcal{F}(\boldsymbol{r}, \boldsymbol{\xi}) \right) \left(\gamma_1^{\text{int}} \varphi(\boldsymbol{r}) \right) \right] d\Gamma_r \tag{5.17}$$

$$= \lim_{\epsilon \to 0} \int_{\Gamma - \Gamma_\epsilon^*} \left(\gamma_0^{\text{int}} \varphi(\boldsymbol{r}) \right) \left(\gamma_1^{\text{int}} \mathcal{F}(\boldsymbol{r}, \boldsymbol{\xi}) \right) d\Gamma_r - \lim_{\epsilon \to 0} \int_{\Gamma - \Gamma_\epsilon^*} \left(\gamma_0^{\text{int}} \mathcal{F}(\boldsymbol{r}, \boldsymbol{\xi}) \right) \left(\gamma_1^{\text{int}} \varphi(\boldsymbol{r}) \right) d\Gamma_r$$

$$+ \lim_{\epsilon \to 0} \int_{\Gamma_\epsilon} \left(\gamma_0^{\text{int}} \varphi(\boldsymbol{r}) \right) \left(\gamma_1^{\text{int}} \mathcal{F}(\boldsymbol{r}, \boldsymbol{\xi}) \right) d\Gamma_r - \lim_{\epsilon \to 0} \int_{\Gamma_\epsilon} \left(\gamma_0^{\text{int}} \mathcal{F}(\boldsymbol{r}, \boldsymbol{\xi}) \right) \left(\gamma_1^{\text{int}} \varphi(\boldsymbol{r}) \right) d\Gamma_r \tag{5.18}$$

for all $\boldsymbol{\xi} \in \Omega$. As promised, this limiting process now allows us to apply the representation formula to points lying on the boundary Γ themselves, i.e. to compute the *internal Dirichlet trace* of $\gamma_0^{\text{int}} \varphi(\boldsymbol{\xi})$. To this end, we will now introduce a number of *boundary integral operators*, which are of tremendous importance for the boundary element method.

5.2.1. Boundary integral operators

In the derivation of boundary integral equations, some particular integral operators occur frequently, and thus warrant a detailed investigation of their properties. In this section, we will only cover those operators which will become important in our further computations.

The single layer potential

The first important boundary integral operator is given by the so–called *single layer potential operator*, which is characterized by an integration over the Dirichlet trace of the fundamental solution:

$$\tilde{V} \colon H^{-\frac{1}{2}}(\Gamma) \to H^1(\Omega) \tag{5.19}$$

$$\left[\tilde{V} f \right](\boldsymbol{\xi}) := - \oint_{\Gamma} \left(\gamma_0^{\text{int}} \mathcal{F}(\boldsymbol{r}, \boldsymbol{\xi}) \right) f(\boldsymbol{r}) \, d\Gamma_r \quad \boldsymbol{\xi} \in \Omega \cup \Sigma \equiv \mathbb{R}^3 \setminus \Gamma \tag{5.20}$$

Theorem 5.2.2 (Harmonicity of the single layer potential). *For $f \in H^{-\frac{1}{2}}(\Gamma)$, the function*

$$\varphi(\boldsymbol{\xi}) := \left[\tilde{V} f \right](\boldsymbol{\xi}), \quad \boldsymbol{\xi} \in \Omega \cup \Sigma$$

is harmonic in $\Omega \cup \Sigma$:

$$\Delta \varphi(\boldsymbol{\xi}) = 0, \quad \boldsymbol{\xi} \in \Omega \cup \Sigma$$

and its $H^1(\Omega)$ norm is bounded by the norm of the density f:

$$\|\varphi\|_{H^1(\Omega)} = \|\tilde{V} f\|_{H^1(\Omega)} \leq c \|f\|_{H^{-\frac{1}{2}}(\Gamma)} \tag{5.21}$$

Proof. Since the proof of the norm inequality (5.21) is of no further importance for us, we will only prove here the harmonicity of the single layer potential. For a proof of (5.21), the interested reader is referred to [Ste03].

To show that

$$\Delta \varphi(\boldsymbol{\xi}) = 0$$

in $\Omega \cup \Sigma$, we make use of the fact that for $r \in \Gamma$ and $\xi \in \Omega \cup \Sigma$, $\mathcal{F}(r, \xi)$ is $\mathcal{C}^\infty$, and thus we can commute differentiation and integration to yield

$$
\begin{aligned}
\Delta \varphi(\xi) &= \Delta \left[\tilde{V} f \right] (\xi) \\
&= -\Delta \oint_\Gamma \left(\gamma_0^{\text{int}} \mathcal{F}(r, \xi) \right) f(r) \, d\Gamma_r \\
&= -\oint_\Gamma \left(\gamma_0^{\text{int}} \underbrace{\Delta_\xi \mathcal{F}(r, \xi)}_{=0, \, r \neq \xi} \right) f(r) \, d\Gamma_r \\
&= 0 \qquad\qquad\qquad\qquad\qquad\qquad \square
\end{aligned}
$$

Remark 5.2.1. The norm inequality (5.21) is of enormous theoretical importance, since it guarantees a certain sense of continuity in the solution of the Dirichlet problem for the Laplace equation with the help of the single layer potential: assume that the *real* Dirichlet data f is perturbed, e.g. through numerical approximation, to a function $\tilde{f}$. Then, from equation (5.21) we can conclude

$$
\| \varphi - \tilde{\varphi} \|_{H^1(\Omega)} \leq c \| f - \tilde{f} \|_{H^{-\frac{1}{2}}(\Gamma)}
$$

and thus slight changes in the boundary data yield only slight changes in the solution, which ensures a sense of stability.

Let us now again consider the process of extending the representation formula (5.15) to the boundary. In this process, we will have to compute the traces – the Dirichlet trace as well as the Neumann trace – of the single layer potential operator. From the decomposition (5.16) and the resulting equation (5.18), we conclude

$$
\oint_\Gamma \left(\gamma_0^{\text{int}} \mathcal{F}(r, \xi) \right) f(r) \, d\Gamma_r = \lim_{\epsilon \to 0} \int_{\Gamma - \Gamma_\epsilon^*} \left(\gamma_0^{\text{int}} \mathcal{F}(r, \xi) \right) f(r) \, d\Gamma_r + \lim_{\epsilon \to 0} \int_{\Gamma_\epsilon} \left(\gamma_0^{\text{int}} \mathcal{F}(r, \xi) \right) f(r) \, d\Gamma_r
$$

For the Laplace equation, the fundamental solution $\mathcal{F}(r, \xi)$ is given by (c.f. theorem C.1.3 in Appendix C.1.2)

$$
\mathcal{G}^L(r - \xi) = -\frac{1}{4\pi} \frac{1}{|r - \xi|} \tag{5.22}
$$

and thus the integrand appearing in the definition of the single layer potential is well–defined and continuous everywhere inside the domain $\Omega \cup \Sigma$ of $\tilde{V}$, since here, the vectors ξ and r are taken from the obviously disjoint sets $\mathbb{R}^3 \setminus \Gamma$ and Γ, respectively. In the computation of the Dirichlet trace, though, ξ and r are members of the same set Γ, and in thus in the evaluation of the single layer potential operator we have to integrate over the singularity at $r = \xi$. In the case of the single layer potential, this is unproblematic, since the integrand is merely *weakly singular* , i.e. while the integrand might possesses a singularity at $r := |r - \xi| = 0$, the integral itself exists, and is continuous at $r = 0$. This can be seen by considering the indefinite integral

$$
\begin{aligned}
\int \frac{1}{r} \, dr &= 4\pi \int r^2 \frac{1}{r} \, dr \\
&= 4\pi \int r \, dr \\
&= 2\pi r^2 + \mathcal{C}
\end{aligned}
$$

which is clearly continuous for $r = 0$. Having thus shown that the integral appearing in the definition of $\tilde{V}$ is continuous even if $\boldsymbol{\xi}$ is taken from Γ, we can now compute[2]

$$\gamma_{0,\xi}^{\mathrm{int}} \oint_{\Gamma} \left(\gamma_0^{\mathrm{int}} \mathcal{G}^L(\boldsymbol{r}, \boldsymbol{\xi})\right) f(\boldsymbol{r}) \, d\Gamma_r = \gamma_{0,\xi}^{\mathrm{int}} \lim_{\epsilon \to 0} \int_{\Gamma'} \left(\gamma_{0,r}^{\mathrm{int}} \mathcal{G}^L(\boldsymbol{r}, \boldsymbol{\xi})\right) f(\boldsymbol{r}) \, d\Gamma_r$$

$$= \lim_{\epsilon \to 0} \int_{\Gamma'} \left(\gamma_{0,\xi}^{\mathrm{int}} \gamma_{0,r}^{\mathrm{int}} \mathcal{G}^L(\boldsymbol{r}, \boldsymbol{\xi})\right) f(\boldsymbol{r}) \, d\Gamma_r$$

where the trace operation could be shifted into the integral since we are integrating over the *extended* boundary Γ'. With the arguments of this paragraph, the integral over

$$\mathcal{A}_\xi(\boldsymbol{r}) := \left(\gamma_{0,\xi}^{\mathrm{int}} \gamma_{0,r}^{\mathrm{int}} \mathcal{G}^L(\boldsymbol{r}, \boldsymbol{\xi})\right) f(\boldsymbol{r})$$

appearing in this equation is continuous, and we are thus able to separate the integrals over the boundary extensions into integrals over the terms of this decomposition

$$\lim_{\epsilon \to 0} \int_{\Gamma'} \mathcal{A}_\xi(\boldsymbol{r}) \, d\Gamma_r = \oint_{\Gamma} \mathcal{A}_\xi(\boldsymbol{r}) \, d\Gamma_r - \lim_{\epsilon \to 0} \int_{\Gamma_\epsilon^*} \mathcal{A}_\xi(\boldsymbol{r}) \, d\Gamma_r + \lim_{\epsilon \to 0} \int_{\Gamma_\epsilon} \mathcal{A}_\xi(\boldsymbol{r}) \, d\Gamma_r$$

Again using continuity of the integrals, and the the fact that for the last two integrals, the area of integration vanishes with $\epsilon \to 0$, we can conclude that the last two terms themselves must vanish in the limit $\epsilon \to 0$, and finally arrive at

$$\boxed{\left[\left(\gamma_{0,\xi}^{\mathrm{int}} \tilde{V}\right) f\right](\boldsymbol{\xi}) = - \oint_{\Gamma} \left(\gamma_{0,\xi}^{\mathrm{int}} \gamma_{0,r}^{\mathrm{int}} \mathcal{G}^L(\boldsymbol{r}, \boldsymbol{\xi})\right) f(\boldsymbol{r}) \, d\Gamma_r} \tag{5.23}$$

This Dirichlet trace of the single layer potential $\gamma_0^{\mathrm{int}} \tilde{V}$ is often abbreviated by

$$V := \gamma_0^{\mathrm{int}} \tilde{V}$$

and since we have $\tilde{V} \colon H^{-\frac{1}{2}}(\Gamma) \to H^1(\Omega)$ and $\gamma_0^{\mathrm{int}} \colon H^s(\Omega) \to H^{s-\frac{1}{2}}(\Gamma)$, we can conclude that their composition is a mapping from the Sobolev space $H^{-\frac{1}{2}}(\Gamma)$ to the Sobolev space $H^{1-\frac{1}{2}}(\Gamma)$, and thus

$$V \colon H^{-\frac{1}{2}}(\Gamma) \to H^{\frac{1}{2}}(\Gamma)$$

which means that by application of the boundary integral operator V, we gain one Sobolev index in smoothness.

Remark 5.2.2. Building the Dirichlet traces of the continuous function $\mathcal{G}^L$ with respect to its arguments $\boldsymbol{r}$ and $\boldsymbol{\xi}$ is trivial, and thus the trace operators $\gamma_{0,r}^{\mathrm{int}}$ and $\gamma_{0,\xi}^{\mathrm{int}}$ are often suppressed from the notation, leading to

$$\boxed{[Vf](\boldsymbol{\xi}) = - \oint_{\Gamma} \mathcal{G}^L(\boldsymbol{r}, \boldsymbol{\xi}) f(\boldsymbol{r}) \, d\Gamma_r} \tag{5.24}$$

In the derivation of (5.24), we never made explicit use of the fact that we took $\boldsymbol{\xi}$ from the *interior*, $\boldsymbol{\xi} \in \Omega$ instead of the *exterior* Σ, and thus, the same result holds for the *external Dirichlet trace*

$$\gamma_0^{\mathrm{ext}} \tilde{V}(\boldsymbol{r}) := \lim_{\Sigma \ni \tilde{\boldsymbol{r}} \to \boldsymbol{r} \in \Gamma} \tilde{V}(\tilde{\boldsymbol{r}})$$

of the single layer potential. Putting those results together leads to the following important theorem

---

2 As usual, $\gamma_{0,r}^{\mathrm{int}}$ denotes that the trace is taken with respect to the argument $\boldsymbol{r}$, and similarly for $\gamma_{0,\xi}^{\mathrm{int}}$.

Theorem 5.2.3 (Dirichlet traces and jump conditions of the Laplacian's single layer potential).
Let $\tilde{V}$ denote the boundary integral operator for the single layer potential of the Laplace operator,

$$\tilde{V}: \ H^{-\frac{1}{2}}(\Gamma) \to H^1(\Omega)$$

$$\left[\tilde{V}f\right](\boldsymbol{\xi}) := -\oint_{\Gamma} \left(\gamma_0^{int}\mathcal{F}(\boldsymbol{r},\boldsymbol{\xi})\right)f(\boldsymbol{r})\,d\Gamma_r \quad \textit{for } \boldsymbol{\xi} \in \Omega \cup \Sigma \equiv \mathbb{R}^3 \setminus \Gamma$$

Then, the following equations hold for the Dirichlet traces of $\tilde{V}$:

$$\left[\left(\gamma_0^{int}\tilde{V}\right)f\right](\boldsymbol{\xi}) = -\oint_{\Gamma} \mathcal{G}^L(\boldsymbol{r},\boldsymbol{\xi})\,f(\boldsymbol{r})\,d\Gamma_r \tag{5.25}$$

$$\left[\left(\gamma_0^{ext}\tilde{V}\right)f\right](\boldsymbol{\xi}) = -\oint_{\Gamma} \mathcal{G}^L(\boldsymbol{r},\boldsymbol{\xi})\,f(\boldsymbol{r})\,d\Gamma_r \tag{5.26}$$

and thus, the jump condition for the single layer potential is given by

$$\left[\left(\gamma_0^{ext}\tilde{V}\right)f - \left(\gamma_0^{int}\tilde{V}\right)f\right](\boldsymbol{\xi}) = 0, \quad \boldsymbol{\xi} \in \Gamma \tag{5.27}$$

The double layer potential

The next boundary integral operator we will consider is – unsurprisingly – called the *double layer potential*, and is characterized by an integration over the Neumann trace of the fundamental solution:

$$W: \ H^{\frac{1}{2}}(\Gamma) \to H^1(\Omega) \tag{5.28}$$

$$[Wf](\boldsymbol{\xi}) := -\oint_{\Gamma} \left(\gamma_{1,r}^{int}\mathcal{F}(\boldsymbol{r},\boldsymbol{\xi})\right)f(\boldsymbol{r})\,d\Gamma_r \quad \boldsymbol{\xi} \in \Omega \cup \Sigma \equiv \mathbb{R}^3 \setminus \Gamma \tag{5.29}$$

Theorem 5.2.4 (Harmonicity of the double layer potential). *For $f \in H^{\frac{1}{2}}(\Gamma)$, the function*

$$\varphi(\boldsymbol{\xi}) := [Wf](\boldsymbol{\xi}), \quad \boldsymbol{\xi} \in \Omega \cup \Sigma$$

is harmonic in $\Omega \cup \Sigma$:

$$\Delta\varphi(\boldsymbol{\xi}) = 0, \quad \boldsymbol{\xi} \in \Omega \cup \Sigma$$

and its $H^1(\Omega)$ norm is bounded[3] by the norm of the density f:

$$\|\varphi\|_{H^1(\Omega)} = \|Wf\|_{H^1(\Omega)} \leq c\|f\|_{H^{\frac{1}{2}}(\Gamma)} \tag{5.30}$$

Proof. The proof of the harmonicity is completely analogous to that of the harmonicity of the single layer potential, and for the proof of the norm inequality (5.30), the reader is again referred to [Ste03]. $\square$

Unfortunately, the evaluation of the trace operators for the double layer potential is significantly more involved than for the single layer potential, since the integrand appearing in equation (5.29) is *strongly singular*, i.e. the integral itself is singular at the point of singularity of the integrand as well. Fortunately, the decomposition of the boundary Γ (5.16) still allows an evaluation of the Dirichlet trace of the double layer potential, as we will see in the following.

---

3 For a discussion of the interpretation and the importance of this norm inequality, see remark 5.2.1

For our derivations, we will need the Neumann trace or conormal derivative of the fundamental solution of the Laplace operator

$$
\begin{aligned}
\gamma_{1,r}^{\text{int}}\mathcal{G}^L(\boldsymbol{r}-\boldsymbol{\xi}) &= -\gamma_{1,r}^{\text{int}}\frac{1}{4\pi}\frac{1}{|\boldsymbol{r}-\boldsymbol{\xi}|} \\
&= -\frac{1}{4\pi}\left(\boldsymbol{\nabla}_{\boldsymbol{r}}\frac{1}{|\boldsymbol{r}-\boldsymbol{\xi}|}\right)\cdot\hat{\boldsymbol{n}}_r \\
&= \frac{1}{4\pi}\frac{(\boldsymbol{r}-\boldsymbol{\xi})\cdot\hat{\boldsymbol{n}}_r}{|\boldsymbol{r}-\boldsymbol{\xi}|^3}
\end{aligned}
\tag{5.31}
$$

which is strongly singular at $\boldsymbol{r}=\boldsymbol{\xi}$. Inserting this expression into the definition of the double layer potential, and applying the decomposition (5.16), we arrive at

$$
\begin{aligned}
\left[(\gamma_{0,\xi}^{\text{int}}W)f\right](\boldsymbol{\xi}) &= -\lim_{\epsilon\to 0}\gamma_{0,\xi}^{\text{int}}\int\limits_{\Gamma-\Gamma_\epsilon^*}\left(\frac{1}{4\pi}\frac{(\boldsymbol{r}-\boldsymbol{\xi})\cdot\hat{\boldsymbol{n}}_r}{|\boldsymbol{r}-\boldsymbol{\xi}|^3}\right)f(\boldsymbol{r})\,d\Gamma_r \\
&\quad -\lim_{\epsilon\to 0}\gamma_{0,\xi}^{\text{int}}\int\limits_{\Gamma_\epsilon}\left(\frac{1}{4\pi}\frac{(\boldsymbol{r}-\boldsymbol{\xi})\cdot\hat{\boldsymbol{n}}_r}{|\boldsymbol{r}-\boldsymbol{\xi}|^3}\right)f(\boldsymbol{r})\,d\Gamma_r
\end{aligned}
$$

Since these integrals are carried out over the boundary extension instead of the original boundary, the trace operators and the integrals commute just as in the derivation of the Dirichlet trace of the single layer potential. We can thus move the trace operation under the integrals to obtain

$$
\begin{aligned}
\left[(\gamma_{0,\xi}^{\text{int}}W)f\right](\boldsymbol{\xi}) &= -\lim_{\epsilon\to 0}\int\limits_{\Gamma-\Gamma_\epsilon^*}\left(\gamma_{0,\xi}^{\text{int}}\frac{1}{4\pi}\frac{(\boldsymbol{r}-\boldsymbol{\xi})\cdot\hat{\boldsymbol{n}}_r}{|\boldsymbol{r}-\boldsymbol{\xi}|^3}\right)f(\boldsymbol{r})\,d\Gamma_r \\
&\quad -\lim_{\epsilon\to 0}\int\limits_{\Gamma_\epsilon}\left(\gamma_{0,\xi}^{\text{int}}\frac{1}{4\pi}\frac{(\boldsymbol{r}-\boldsymbol{\xi})\cdot\hat{\boldsymbol{n}}_r}{|\boldsymbol{r}-\boldsymbol{\xi}|^3}\right)f(\boldsymbol{r})\,d\Gamma_r
\end{aligned}
\tag{5.32}
$$

but while it was possible to further decompose the first term on the right hand side in the case of the single layer potential into integrals over Γ and Γ_ϵ^*, respectively, since the integral was continuous, this is not possible for the strongly singular kernel of the double layer potential. In fact, the integrals over Γ and over Γ_ϵ^* do not even exist at $\boldsymbol{r}=\boldsymbol{\xi}$. It turns out, though, that the fact that the integrals over Γ and Γ_ϵ^* both possess the same singularity at $\boldsymbol{r}=\boldsymbol{\xi}$, the limit $\epsilon\to 0$ of the integral over the difference $\Gamma-\Gamma_\epsilon^*$ is finite and well–defined nonetheless. Since

$$
\Gamma-\Gamma_\epsilon^* = \{\boldsymbol{r}\in\Gamma\colon|\boldsymbol{r}-\boldsymbol{\xi}|\geq\epsilon\}
$$

the first term on the right hand side of equation (5.32) becomes

$$
\lim_{\epsilon\to 0}\int\limits_{\Gamma-\Gamma_\epsilon^*}\left(\gamma_{0,\xi}^{\text{int}}\frac{1}{4\pi}\frac{(\boldsymbol{r}-\boldsymbol{\xi})\cdot\hat{\boldsymbol{n}}_r}{|\boldsymbol{r}-\boldsymbol{\xi}|^3}\right)f(\boldsymbol{r})\,d\Gamma_r = \lim_{\epsilon\to 0}\int\limits_{\boldsymbol{r}\in\Gamma\colon|\boldsymbol{r}-\boldsymbol{\xi}|\geq\epsilon}\left(\gamma_{0,\xi}^{\text{int}}\frac{1}{4\pi}\frac{(\boldsymbol{r}-\boldsymbol{\xi})\cdot\hat{\boldsymbol{n}}_r}{|\boldsymbol{r}-\boldsymbol{\xi}|^3}\right)f(\boldsymbol{r})\,d\Gamma_r
$$

Definition 5.2.1 (Cauchy principal value). Let $\mathcal{A}(\boldsymbol{r})$ denote a – possibly strongly singular – real or complex valued function, that possesses at most one singularity, and let $\boldsymbol{\xi}$ denote the position of that singularity if it exists, or an arbitrary point in the domain of $\mathcal{A}$ otherwise. Then, the *Cauchy principle value* of the integral of $\mathcal{A}$ over the domain Ω with differential volume or surface[4] element $d\Omega$ about the point $\boldsymbol{\xi}$, is defined as (c.f. [Cau74, MF53]):

$$
\boxed{\oint\limits_{\Omega}\mathcal{A}d\Omega := \lim_{\epsilon\to 0}\int\limits_{\boldsymbol{r}\in\Omega\colon|\boldsymbol{r}-\boldsymbol{\xi}|\geq\epsilon}\mathcal{A}(\boldsymbol{r})d\Omega}
\tag{5.33}
$$

---

4 We thus explicitly include two–dimensional domains in the definition.

5. The Boundary Element Method

With the definition of the Cauchy principle value and with the above manipulations, we thus have

$$
\left[(\gamma_{0,\xi}^{\text{int}} W) f \right] (\boldsymbol{\xi}) = - \oint_{\Gamma} \left(\gamma_{0,\xi}^{\text{int}} \frac{1}{4\pi} \frac{(\boldsymbol{r} - \boldsymbol{\xi}) \cdot \hat{\boldsymbol{n}}_r}{|\boldsymbol{r} - \boldsymbol{\xi}|^3} \right) f(\boldsymbol{r}) \, d\Gamma_r
$$

$$
- \lim_{\epsilon \to 0} \int_{\Gamma_\epsilon} \left(\gamma_{0,\xi}^{\text{int}} \frac{1}{4\pi} \frac{(\boldsymbol{r} - \boldsymbol{\xi}) \cdot \hat{\boldsymbol{n}}_r}{|\boldsymbol{r} - \boldsymbol{\xi}|^3} \right) f(\boldsymbol{r}) \, d\Gamma_r \tag{5.34}
$$

This equation still leaves the second term on the right hand side for consideration. A first simplification can be achieved by writing

$$
f(\boldsymbol{r}) = (f(\boldsymbol{r}) - f(\tilde{\boldsymbol{r}})) + f(\tilde{\boldsymbol{r}})
$$

for some $\tilde{\boldsymbol{r}} \in \Gamma_\epsilon$. With this decomposition, the term under consideration becomes

$$
\lim_{\epsilon \to 0} \int_{\Gamma_\epsilon} \left(\gamma_{0,\xi}^{\text{int}} \frac{1}{4\pi} \frac{(\boldsymbol{r} - \boldsymbol{\xi}) \cdot \hat{\boldsymbol{n}}_r}{|\boldsymbol{r} - \boldsymbol{\xi}|^3} \right) f(\boldsymbol{r}) \, d\Gamma_r = \lim_{\epsilon \to 0} \int_{\Gamma_\epsilon} \left(\gamma_{0,\xi}^{\text{int}} \frac{1}{4\pi} \frac{(\boldsymbol{r} - \boldsymbol{\xi}) \cdot \hat{\boldsymbol{n}}_r}{|\boldsymbol{r} - \boldsymbol{\xi}|^3} \right) [f(\boldsymbol{r}) - f(\tilde{\boldsymbol{r}})] \, d\Gamma_r
$$

$$
+ \lim_{\epsilon \to 0} f(\tilde{\boldsymbol{r}}) \int_{\Gamma_\epsilon} \left(\gamma_{0,\xi}^{\text{int}} \frac{1}{4\pi} \frac{(\boldsymbol{r} - \boldsymbol{\xi}) \cdot \hat{\boldsymbol{n}}_r}{|\boldsymbol{r} - \boldsymbol{\xi}|^3} \right) d\Gamma_r
$$

To show that the first integral on the right hand side vanishes, we make use of the inequality

$$
\left| \int_{\Gamma_\epsilon} (\gamma_{0,\xi}^{\text{int}} \gamma_{1,r}^{\text{int}} \mathcal{G}^L(\boldsymbol{r}, \boldsymbol{\xi})) [f(\boldsymbol{r}) - f(\tilde{\boldsymbol{r}})] \, d\Gamma_r \right| \leq \sup_{\tilde{\boldsymbol{r}} \in \Gamma_\epsilon} |f(\boldsymbol{r}) - f(\tilde{\boldsymbol{r}})| \int_{\Gamma_\epsilon} \left| (\gamma_{0,\xi}^{\text{int}} \gamma_{1,r}^{\text{int}} \mathcal{G}^L(\boldsymbol{r}, \boldsymbol{\xi})) \right| d\Gamma_r
$$

$$
= \sup_{\tilde{\boldsymbol{r}} \in \Gamma_\epsilon} |f(\boldsymbol{r}) - f(\tilde{\boldsymbol{r}})| \frac{1}{4\pi} \int_{\Gamma_\epsilon} \frac{1}{|\boldsymbol{r} - \boldsymbol{\xi}|^2} d\Gamma_r
$$

$$
= \sup_{\tilde{\boldsymbol{r}} \in \Gamma_\epsilon} |f(\boldsymbol{r}) - f(\tilde{\boldsymbol{r}})| \xrightarrow[\epsilon \to 0]{} 0
$$

This means that in the limit of vanishing ϵ, the first integral on the right hand side must vanish as well, and thus, the integral that is left to consider is given by

$$
\lim_{\epsilon \to 0} \int_{\Gamma_\epsilon} \left(\gamma_{0,\xi}^{\text{int}} \frac{1}{4\pi} \frac{(\boldsymbol{r} - \boldsymbol{\xi}) \cdot \hat{\boldsymbol{n}}_r}{|\boldsymbol{r} - \boldsymbol{\xi}|^3} \right) f(\boldsymbol{r}) \, d\Gamma_r = \lim_{\epsilon \to 0} f(\tilde{\boldsymbol{r}}) \int_{\Gamma_\epsilon} \left(\gamma_{0,\xi}^{\text{int}} \frac{1}{4\pi} \frac{(\boldsymbol{r} - \boldsymbol{\xi}) \cdot \hat{\boldsymbol{n}}_r}{|\boldsymbol{r} - \boldsymbol{\xi}|^3} \right) d\Gamma_r \tag{5.35}
$$

Remembering that the boundary extension Γ_ϵ was defined as a spherical cap around the load point $\boldsymbol{\xi}$, we can decompose it into the sphere $\mathcal{S}_\epsilon^2(\boldsymbol{\xi}) := \partial \mathcal{B}_\epsilon^0(\boldsymbol{\xi})$ of radius ϵ centered at $\boldsymbol{\xi}$ minus that part of $\mathcal{S}_\epsilon^2(\boldsymbol{\xi})$ that is contained inside Ω:

$$
\Gamma_\epsilon = \mathcal{S}_\epsilon^2(\boldsymbol{\xi}) \setminus \{\boldsymbol{r} \in \Omega : |\boldsymbol{r} - \boldsymbol{\xi}| = \epsilon\} \tag{5.36}
$$

and thus the integral from (5.34) can be decomposed with the help of equation (5.35) and equation (5.36) to yield

$$
\lim_{\epsilon \to 0} f(\tilde{\boldsymbol{r}}) \int_{\Gamma_\epsilon} \left(\gamma_{0,\xi}^{\text{int}} \frac{1}{4\pi} \frac{(\boldsymbol{r} - \boldsymbol{\xi}) \cdot \hat{\boldsymbol{n}}_r}{|\boldsymbol{r} - \boldsymbol{\xi}|^3} \right) d\Gamma_r = \lim_{\epsilon \to 0} f(\tilde{\boldsymbol{r}}) \oint_{\mathcal{S}_\epsilon^2(\boldsymbol{\xi})} \left(\gamma_{0,\xi}^{\text{int}} \frac{1}{4\pi} \frac{(\boldsymbol{r} - \boldsymbol{\xi}) \cdot \hat{\boldsymbol{n}}_r}{|\boldsymbol{r} - \boldsymbol{\xi}|^3} \right) d\Gamma_r
$$

$$
- \lim_{\epsilon \to 0} f(\tilde{\boldsymbol{r}}) \int_{\boldsymbol{r} \in \Omega : |\boldsymbol{r} - \boldsymbol{\xi}| = \epsilon} \left(\gamma_{0,\xi}^{\text{int}} \frac{1}{4\pi} \frac{(\boldsymbol{r} - \boldsymbol{\xi}) \cdot \hat{\boldsymbol{n}}_r}{|\boldsymbol{r} - \boldsymbol{\xi}|^3} \right) d\Gamma_r
$$

The integral over the sphere $\mathcal{S}_\epsilon^2(\boldsymbol{\xi})$ can easily be evaluated with the help of a little trick. To this end, let us consider the representation formula (5.15) for $\Omega = \mathcal{B}_\epsilon^0(\boldsymbol{\xi})$:

$$\varphi(\boldsymbol{\xi}) = \oint_{\mathcal{S}_\epsilon^2(\boldsymbol{\xi})} \left[\left(\gamma_0^{\mathrm{int}} \varphi(\boldsymbol{r}) \right) \left(\gamma_1^{\mathrm{int}} \mathcal{G}^L(\boldsymbol{r}, \boldsymbol{\xi}) \right) - \left(\gamma_0^{\mathrm{int}} \mathcal{G}^L(\boldsymbol{r}, \boldsymbol{\xi}) \right) \left(\gamma_1^{\mathrm{int}} \varphi(\boldsymbol{r}) \right) \right] d\Gamma$$

For $\varphi(\boldsymbol{\xi}) \equiv 0$ in Ω, the Neumann trace $\gamma_1^{\mathrm{int}} \varphi(\boldsymbol{r})$ vanishes and the Dirichlet trace equals unity, $\gamma_0^{\mathrm{int}} \varphi(\boldsymbol{r}) \equiv 1$, and thus

$$1 = \oint_{\mathcal{S}_\epsilon^2(\boldsymbol{\xi})} \left(\gamma_{1,r}^{\mathrm{int}} \mathcal{G}^L(\boldsymbol{r}, \boldsymbol{\xi}) \right) d\Gamma = \oint_{\mathcal{S}_\epsilon^2(\boldsymbol{\xi})} \left(\gamma_{0,\xi}^{\mathrm{int}} \gamma_{1,r}^{\mathrm{int}} \mathcal{G}^L(\boldsymbol{r}, \boldsymbol{\xi}) \right) d\Gamma$$

for all finite ϵ which yields

$$\lim_{\epsilon \to 0} f(\tilde{\boldsymbol{r}}) \oint_{\mathcal{S}_\epsilon^2(\boldsymbol{\xi})} \left(\gamma_{0,\xi}^{\mathrm{int}} \frac{1}{4\pi} \frac{(\boldsymbol{r} - \boldsymbol{\xi}) \cdot \hat{\boldsymbol{n}}_r}{|\boldsymbol{r} - \boldsymbol{\xi}|^3} \right) d\Gamma_r = \lim_{\epsilon \to 0} f(\tilde{\boldsymbol{r}}) \tag{5.37}$$

and since with $\epsilon \to 0$, $\Gamma_\epsilon \to \boldsymbol{\xi}$, it follows that $\Gamma_\epsilon \ni \tilde{\boldsymbol{r}} \to \boldsymbol{\xi}$. We thus have

$$\lim_{\epsilon \to 0} f(\tilde{\boldsymbol{r}}) \oint_{\mathcal{S}_\epsilon^2(\boldsymbol{\xi})} \left(\gamma_{0,\xi}^{\mathrm{int}} \frac{1}{4\pi} \frac{(\boldsymbol{r} - \boldsymbol{\xi}) \cdot \hat{\boldsymbol{n}}_r}{|\boldsymbol{r} - \boldsymbol{\xi}|^3} \right) d\Gamma_r = f(\boldsymbol{\xi}) \tag{5.38}$$

The final term which we have to compute to yield the Dirichlet trace of the double layer potential is the second term of the decomposition (5.36), the integral

$$- \lim_{\epsilon \to 0} f(\tilde{\boldsymbol{r}}) \int_{\boldsymbol{r} \in \Omega: |\boldsymbol{r} - \boldsymbol{\xi}| = \epsilon} \left(\gamma_{0,\xi}^{\mathrm{int}} \frac{1}{4\pi} \frac{(\boldsymbol{r} - \boldsymbol{\xi}) \cdot \hat{\boldsymbol{n}}_r}{|\boldsymbol{r} - \boldsymbol{\xi}|^3} \right) d\Gamma_r \tag{5.39}$$

Noting that on $\{\boldsymbol{r} \in \Omega : |\boldsymbol{r} - \boldsymbol{\xi}| = \epsilon\}$, the normal vector $\hat{\boldsymbol{n}}_r$ is given by[5]

$$\hat{\boldsymbol{n}}_r := \frac{1}{\epsilon} (\boldsymbol{r} - \boldsymbol{\xi})$$

we can directly compute integral (5.39):

$$\lim_{\epsilon \to 0} f(\tilde{\boldsymbol{r}}) \int_{\boldsymbol{r} \in \Omega: |\boldsymbol{r} - \boldsymbol{\xi}| = \epsilon} \left(\gamma_{0,\xi}^{\mathrm{int}} \frac{1}{4\pi} \frac{(\boldsymbol{r} - \boldsymbol{\xi}) \cdot \hat{\boldsymbol{n}}_r}{|\boldsymbol{r} - \boldsymbol{\xi}|^3} \right) d\Gamma_r = \lim_{\epsilon \to 0} f(\tilde{\boldsymbol{r}}) \int_{\boldsymbol{r} \in \Omega: |\boldsymbol{r} - \boldsymbol{\xi}| = \epsilon} \left(\gamma_{0,\xi}^{\mathrm{int}} \frac{1}{4\pi} \frac{|\boldsymbol{r} - \boldsymbol{\xi}|^2}{\epsilon |\boldsymbol{r} - \boldsymbol{\xi}|^3} \right) d\Gamma_r \tag{5.40}$$

$$= f(\boldsymbol{\xi}) \frac{1}{4\pi} \lim_{\epsilon \to 0} \frac{1}{\epsilon^2} \int_{\boldsymbol{r} \in \Omega: |\boldsymbol{r} - \boldsymbol{\xi}| = \epsilon} d\Gamma_r \tag{5.41}$$

$$=: f(\boldsymbol{\xi}) \sigma(\boldsymbol{r}) \tag{5.42}$$

with the definition of the geometrical quantity

$$\sigma(\boldsymbol{\xi}) := \lim_{\epsilon \to 0} \frac{1}{4\pi} \frac{1}{\epsilon^2} \int_{\boldsymbol{r} \in \Omega: |\boldsymbol{r} - \boldsymbol{\xi}| = \epsilon} d\Gamma_r \tag{5.43}$$

---

5 Remember that this set is the part of an open ball with radius ϵ centered at $\boldsymbol{\xi}$ that is cut out by Ω.

Remark 5.2.3. If the boundary Γ is smooth – i.e. at least differentiable – in a surrounding of the point $\boldsymbol{\xi} \in \Gamma$, then from the definition of $\sigma(\boldsymbol{r})$ immediately follows (c.f. [Ste03])

$$\sigma(\boldsymbol{\xi}) = \frac{1}{2} \quad \text{for almost all } \boldsymbol{\xi} \in \Gamma \tag{5.44}$$

Putting all of this together, we obtain for the internal Dirichlet trace of the double layer potential

$$\left[(\gamma_{0,\xi}^{\text{int}} W)f\right](\boldsymbol{\xi}) = -\oint_\Gamma \left(\gamma_{0,\xi}^{\text{int}} \frac{1}{4\pi} \frac{(\boldsymbol{r} - \boldsymbol{\xi}) \cdot \hat{\boldsymbol{n}}_r}{|\boldsymbol{r} - \boldsymbol{\xi}|^3}\right) f(\boldsymbol{\xi}) \, d\Gamma_r + [-1 + \sigma(\boldsymbol{\xi})] f(\boldsymbol{r}) \tag{5.45}$$

With the definition of a further boundary integral operator K:

$$[Kf](\boldsymbol{\xi}) = -\oint_\Gamma \left(\gamma_{0,\xi}^{\text{int}} \gamma_{1,r}^{\text{int}} \mathcal{F}(\boldsymbol{r}, \boldsymbol{\xi})\right) f(\boldsymbol{r}) \, d\Gamma_r \tag{5.46}$$

this reduces to

$$\left[(\gamma_{0,\xi}^{\text{int}} W)f\right](\boldsymbol{\xi}) = [-1 + \sigma(\boldsymbol{\xi})] f(\boldsymbol{\xi}) + [Kf](\boldsymbol{\xi}) \tag{5.47}$$

for $\xi \in \Gamma$ and $f \in H^{\frac{1}{2}}(\Gamma)$.

The computation of the *external* Dirichlet trace of the double layer potential is mostly analogous, with the only exception of the integral

$$\oint_{\mathcal{S}_\epsilon^2(\boldsymbol{\xi})} \left(\gamma_{0,\xi}^{\text{ext}} \gamma_{1,r}^{\text{ext}} \mathcal{G}^L(\boldsymbol{r}, \boldsymbol{\xi})\right) d\Gamma$$

which can no longer be equal to unity, since it is a solution to the exterior problem, for which constant solutions cannot occur since they are defined in an unbounded domain and thus, a constant solution to the exterior problem would contain an infinite amount of energy. Instead, it is easy to see that in this case, the integral vanishes, and thus we obtain for the external Dirichlet trace of the double layer potential

$$\left[(\gamma_{0,\xi}^{\text{ext}} W)f\right](\boldsymbol{\xi}) = \sigma(\boldsymbol{\xi}) f(\boldsymbol{\xi}) + [Kf](\boldsymbol{\xi}) \tag{5.48}$$

Remembering that $W : H^{\frac{1}{2}}(\Gamma) \to H^1(\Omega)$, and that $\gamma_0^{\text{int}} : H^s(\Omega) \to H^{s-\frac{1}{2}}(\Gamma)$, these results can be put together in the following theorem

Theorem 5.2.5 (Dirichlet traces and jump conditions of the Laplacian's double layer potential).
Let W denote the boundary integral operator for the double layer potential of the Laplace operator

$$W : H^{\frac{1}{2}}(\Gamma) \to H^1(\Omega)$$

$$[Wf](\boldsymbol{\xi}) := -\oint_\Gamma \left(\gamma_1^{\text{int}} \mathcal{F}(\boldsymbol{r}, \boldsymbol{\xi})\right) f(\boldsymbol{r}) \, d\Gamma_r \quad \boldsymbol{\xi} \in \Omega \cup \Sigma \equiv \mathbb{R}^3 \setminus \Gamma$$

Let K be defined by

$$[Kf](\boldsymbol{\xi}) = -\oint_\Gamma \left(\gamma_{0,\xi}^{\text{int}} \gamma_{1,r}^{\text{int}} \mathcal{F}(\boldsymbol{r}, \boldsymbol{\xi})\right) f(\boldsymbol{r}) \, d\Gamma_r$$

and $\sigma(\boldsymbol{\xi})$ by

$$\sigma(\boldsymbol{\xi}) := \lim_{\epsilon \to 0} \frac{1}{4\pi} \frac{1}{\epsilon^2} \int_{\boldsymbol{r} \in \Omega : |\boldsymbol{r} - \boldsymbol{\xi}| = \epsilon} d\Gamma_r$$

Then, the following equations hold for the Dirichlet traces[6]

$$\gamma_0^{int} W : H^{\frac{1}{2}}(\Gamma) \to H^{\frac{1}{2}}(\Gamma)$$

$$\gamma_0^{ext} W : H^{\frac{1}{2}}(\Gamma) \to H^{\frac{1}{2}}(\Gamma)$$

of W:

$$\left[(\gamma_{0,\xi}^{int} W) f\right](\boldsymbol{\xi}) = \left[-1 + \sigma(\boldsymbol{\xi})\right] f(\boldsymbol{\xi}) + \left[Kf\right](\boldsymbol{\xi}) \tag{5.49}$$

$$\left[(\gamma_{0,\xi}^{ext} W) f\right](\boldsymbol{\xi}) = \sigma(\boldsymbol{\xi}) f(\boldsymbol{\xi}) + \left[Kf\right](\boldsymbol{\xi}) \tag{5.50}$$

and thus, the jump condition for the double layer potential is given by

$$\left[(\gamma_0^{ext} W) f - (\gamma_0^{int} W) f\right](\boldsymbol{\xi}) = f(\boldsymbol{\xi}), \quad \boldsymbol{\xi} \in \Gamma \tag{5.51}$$

The adjoint double layer potential

The next integral operator we have to consider arises when applying the Neumann trace to the single layer potential:

$$\gamma_1^{int} \tilde{V} : H^{-\frac{1}{2}}(\Gamma) \to H^{-\frac{1}{2}}(\Gamma)$$

$$
\begin{aligned}
\left[\left(\gamma_{1,\xi}^{int} \tilde{V}\right) f\right](\boldsymbol{\xi}) &= - \gamma_{1,\xi}^{int} \oint_\Gamma \left(\gamma_{0,r}^{int} \mathcal{F}(\boldsymbol{r}, \boldsymbol{\xi})\right) f(\boldsymbol{r}) \, d\Gamma_r \\
&= - \lim_{\epsilon \to 0} \gamma_{1,\xi}^{int} \int_{\Gamma - \Gamma_\epsilon^*} \left(\gamma_{0,r}^{int} \mathcal{G}^L(\boldsymbol{r}, \boldsymbol{\xi})\right) f(\boldsymbol{r}) \, d\Gamma_r \\
&\quad - \lim_{\epsilon \to 0} \gamma_{1,\xi}^{int} \int_{\Gamma_\epsilon} \left(\gamma_{0,r}^{int} \mathcal{G}^L(\boldsymbol{r}, \boldsymbol{\xi})\right) f(\boldsymbol{r}) \, d\Gamma_r \\
&= - \lim_{\epsilon \to 0} \int_{\boldsymbol{r} \in \Gamma : |\boldsymbol{r} - \boldsymbol{\xi}| \geq \epsilon} \left(\gamma_{1,\xi}^{int} \gamma_{0,r}^{int} \mathcal{G}^L(\boldsymbol{r}, \boldsymbol{\xi})\right) f(\boldsymbol{r}) \, d\Gamma_r \\
&\quad - \lim_{\epsilon \to 0} \gamma_{1,\xi}^{int} \left\{ \int_{\mathcal{S}_\epsilon^2(\boldsymbol{\xi})} \left(\gamma_{0,r}^{int} \mathcal{G}^L(\boldsymbol{r}, \boldsymbol{\xi})\right) f(\boldsymbol{r}) \, d\Gamma_r \right. \\
&\qquad \left. - \int_{\boldsymbol{r} \in \Omega : |\boldsymbol{r} - \boldsymbol{\xi}| = \epsilon} \left(\gamma_{0,r}^{int} \mathcal{G}^L(\boldsymbol{r}, \boldsymbol{\xi})\right) f(\boldsymbol{r}) \, d\Gamma_r \right\}
\end{aligned}
\tag{5.52}
$$

where we were able to move the Neumann trace operators into the integrand since the integrand is continuous and smooth when integrating over the extended boundary. In addition, we made use of the decompositions of the different domains which we have already employed in the computations of the Dirichlet traces of single and double layer potential. We note that the first integral on the right hand side of equation (5.52) is a Cauchy principal value integral

$$- \lim_{\epsilon \to 0} \int_{\boldsymbol{r} \in \Gamma : |\boldsymbol{r} - \boldsymbol{\xi}| \geq \epsilon} \left(\gamma_{1,\xi}^{int} \gamma_{0,r}^{int} \mathcal{G}^L(\boldsymbol{r}, \boldsymbol{\xi})\right) f(\boldsymbol{r}) \, d\Gamma_r = - \oint_\Gamma \left(\gamma_{1,\xi}^{int} \gamma_{0,r}^{int} \mathcal{G}^L(\boldsymbol{r}, \boldsymbol{\xi})\right) f(\boldsymbol{r}) \, d\Gamma_r =: \left[K'f\right](\boldsymbol{\xi})$$

---

6 For the external trace, the internal trace operators in the definitions of the boundary integral operators have to be replaced by external traces.

where we have introduced a new boundary integral operator, the so–called *adjoint double layer potential* K', defined by

$$\left[K'f\right](\boldsymbol{\xi}) := -\oint_{\Gamma} \left(\gamma_{1,\xi}^{\text{int}}\gamma_{0,r}^{\text{int}}\mathcal{G}^L(\boldsymbol{r},\boldsymbol{\xi})\right)f(\boldsymbol{r})\,d\Gamma_r \tag{5.53}$$

To compute the remaining two integrals on the right hand side of equation (5.52) we first avoid the inconvenient $f(\boldsymbol{r})$ terms by again using the decomposition

$$f(\boldsymbol{r}) = (f(\boldsymbol{r}) - f(\tilde{\boldsymbol{r}})) - f(\tilde{\boldsymbol{r}})$$

and the fact that in the limit of $\epsilon \to 0$, the difference $f(\boldsymbol{r}) - f(\tilde{\boldsymbol{r}})$ vanishes (c.f. the derivation of the Neumann trace of the double layer potential). For the first integral in braces, we thus obtain

$$\lim_{\epsilon\to 0}\gamma_{1,\xi}^{\text{int}}\int_{\mathcal{S}_\epsilon^2(\boldsymbol{\xi})}\left(\gamma_{0,r}^{\text{int}}\mathcal{G}^L(\boldsymbol{r},\boldsymbol{\xi})\right)f(\boldsymbol{r})\,d\Gamma_r = \lim_{\epsilon\to 0}f(\tilde{\boldsymbol{r}})\gamma_{1,\xi}^{\text{int}}\int_{\mathcal{S}_\epsilon^2(\boldsymbol{\xi})}\gamma_{0,r}^{\text{int}}\mathcal{G}^L(\boldsymbol{r},\boldsymbol{\xi})\,d\Gamma_r$$

$$= \lim_{\epsilon\to 0}\frac{-f(\tilde{\boldsymbol{r}})}{4\pi}\gamma_{1,\xi}^{\text{int}}\int_{\mathcal{S}_\epsilon^2(\boldsymbol{\xi})}\frac{1}{|\boldsymbol{r}-\boldsymbol{\xi}|}\,d\Gamma_r$$

$$= \lim_{\epsilon\to 0}\frac{-f(\tilde{\boldsymbol{r}})}{4\pi}\gamma_{1,\xi}^{\text{int}}\int_{\mathcal{S}_\epsilon^2(0)}\frac{1}{|\boldsymbol{r}|}\,d\Gamma_r$$

$$= \lim_{\epsilon\to 0}\frac{-f(\tilde{\boldsymbol{r}})}{4\pi}\gamma_{1,\xi}^{\text{int}}\left(4\pi\epsilon\right) \tag{5.54}$$

$$= \lim_{\epsilon\to 0}\frac{-f(\tilde{\boldsymbol{r}})}{4\pi}\hat{\boldsymbol{n}}(\boldsymbol{\xi})\cdot\boldsymbol{\nabla}\underbrace{\left(4\pi\epsilon\right)}_{=\text{const}}$$

$$= 0 \tag{5.55}$$

This leaves only one more integral for consideration, namely the term

$$\lim_{\epsilon\to 0}f(\tilde{\boldsymbol{r}})\,\gamma_{1,\xi}^{\text{int}}\int_{\boldsymbol{r}\in\Omega:|\boldsymbol{r}-\boldsymbol{\xi}|=\epsilon}\gamma_{0,r}^{\text{int}}\mathcal{G}^L(\boldsymbol{r},\boldsymbol{\xi})\,d\Gamma_r = \lim_{\epsilon\to 0}f(\tilde{\boldsymbol{r}})\int_{\boldsymbol{r}\in\Omega:|\boldsymbol{r}-\boldsymbol{\xi}|=\epsilon}\gamma_{1,\xi}^{\text{int}}\gamma_{0,r}^{\text{int}}\mathcal{G}^L(\boldsymbol{r},\boldsymbol{\xi})\,d\Gamma_r$$

$$= \lim_{\epsilon\to 0}\frac{f(\tilde{\boldsymbol{r}})}{4\pi}\int_{\boldsymbol{r}\in\Omega:|\boldsymbol{r}-\boldsymbol{\xi}|=\epsilon}\frac{(\boldsymbol{\xi}-\boldsymbol{r})\cdot\hat{\boldsymbol{n}}(\boldsymbol{\xi})}{|\boldsymbol{r}-\boldsymbol{\xi}|^3}\,d\Gamma_r$$

To compute this expression, we first note that as $\epsilon \to 0$, $\tilde{\boldsymbol{r}} \to \boldsymbol{r}$, and since we are only considering $\boldsymbol{r} \in \Omega$ with $|\boldsymbol{r}-\boldsymbol{\xi}| = \epsilon$, $\boldsymbol{r} \to \boldsymbol{\xi}$ as well. We can thus conclude that in the limit $\epsilon \to 0$, $f(\tilde{\boldsymbol{r}}) \to f(\boldsymbol{\xi})$. The remaining integral can now be computed by remembering that the normal vector at position $\boldsymbol{\xi}$ on this part of a sphere is given by

$$\hat{\boldsymbol{n}}(\boldsymbol{\xi}) = \frac{1}{\epsilon}\left(\boldsymbol{\xi}-\boldsymbol{r}\right)$$

and we obtain

$$\lim_{\epsilon\to 0}\frac{f(\tilde{\boldsymbol{r}})}{4\pi}\int_{\boldsymbol{r}\in\Omega:|\boldsymbol{r}-\boldsymbol{\xi}|=\epsilon}\frac{(\boldsymbol{\xi}-\boldsymbol{r})\cdot\hat{\boldsymbol{n}}(\boldsymbol{\xi})}{|\boldsymbol{r}-\boldsymbol{\xi}|^3}\,d\Gamma_r = f(\boldsymbol{\xi})\lim_{\epsilon\to 0}\frac{1}{4\pi}\frac{1}{\epsilon}\int_{\boldsymbol{r}\in\Omega:|\boldsymbol{r}-\boldsymbol{\xi}|=\epsilon}\frac{|\boldsymbol{r}-\boldsymbol{\xi}|^2}{|\boldsymbol{r}-\boldsymbol{\xi}|^3}\,d\Gamma_r$$

$$= f(\boldsymbol{\xi})\lim_{\epsilon\to 0}\frac{1}{4\pi}\frac{1}{\epsilon^2}\int_{\boldsymbol{r}\in\Omega:|\boldsymbol{r}-\boldsymbol{\xi}|=\epsilon}d\Gamma_r$$

But the limit appearing in this expression is just the geometrical quantity $\sigma(\boldsymbol{\xi})$, which was defined in (5.43), and we thus obtain for this term

$$\lim_{\epsilon \to 0} \frac{f(\tilde{\boldsymbol{r}})}{4\pi} \int\limits_{\boldsymbol{r} \in \Omega : |\boldsymbol{r} - \boldsymbol{\xi}| = \epsilon} \frac{(\boldsymbol{\xi} - \boldsymbol{r}) \cdot \hat{\boldsymbol{n}}(\boldsymbol{\xi})}{|\boldsymbol{r} - \boldsymbol{\xi}|^3} d\Gamma_r = \sigma(\boldsymbol{\xi}) f(\boldsymbol{\xi}) \tag{5.56}$$

Inserting all those results into equation (5.52), we finally obtain the internal Neumann trace for the single layer potential:

$$\boxed{\left[\left(\gamma_{1,\xi}^{\text{int}} \tilde{V} \right) f \right](\boldsymbol{\xi}) = \sigma(\boldsymbol{\xi}) f(\boldsymbol{\xi}) + \left[K' f \right](\boldsymbol{\xi})} \tag{5.57}$$

An equivalent computation for the *external* Neumann trace of the single layer potential leads to

$$\left[\left(\gamma_{1,\xi}^{\text{ext}} \tilde{V} \right) f \right](\boldsymbol{\xi}) = [\sigma(\boldsymbol{\xi}) - 1] f(\boldsymbol{\xi}) + \left[K' f \right](\boldsymbol{\xi}) \tag{5.58}$$

These results can be put together in the following theorem:

Theorem 5.2.6 (Neumann traces and jump conditions of the Laplacian's single layer potential).
Let $\tilde{V}$ denote the boundary integral operator for the single layer potential of the Laplace operator

$$\tilde{V} : H^{-\frac{1}{2}}(\Gamma) \to H^1(\Omega)$$

$$\left[\tilde{V} f \right](\boldsymbol{\xi}) := -\oint\limits_{\Gamma} \left(\gamma_{0,\xi}^{int} \mathcal{F}(\boldsymbol{r}, \boldsymbol{\xi}) \right) f(\boldsymbol{r}) \, d\Gamma_r \quad \boldsymbol{\xi} \in \Omega \cup \Sigma \equiv \mathbb{R}^3 \setminus \Gamma$$

Let the adjoint double layer potential K' be defined by

$$\left[K' f \right](\boldsymbol{\xi}) = -\oint\limits_{\Gamma} \left(\gamma_{1,\xi}^{int} \gamma_{0,r}^{int} \mathcal{F}(\boldsymbol{r}, \boldsymbol{\xi}) \right) f(\boldsymbol{r}) \, d\Gamma_r$$

and $\sigma(\boldsymbol{\xi})$ by

$$\sigma(\boldsymbol{\xi}) := \lim_{\epsilon \to 0} \frac{1}{4\pi} \frac{1}{\epsilon^2} \int\limits_{\boldsymbol{r} \in \Omega : |\boldsymbol{r} - \boldsymbol{\xi}| = \epsilon} d\Gamma_r$$

Then, the following equations hold for the Neumann traces[7]

$$\gamma_1^{int} \tilde{V} : H^{-\frac{1}{2}}(\Gamma) \to H^{-\frac{1}{2}}(\Gamma)$$
$$\gamma_1^{ext} \tilde{V} : H^{-\frac{1}{2}}(\Gamma) \to H^{-\frac{1}{2}}(\Gamma)$$

of $\tilde{V}$:

$$\left[\left(\gamma_{1,\xi}^{int} \tilde{V} \right) f \right](\boldsymbol{\xi}) = \sigma(\boldsymbol{\xi}) f(\boldsymbol{\xi}) + \left[K' f \right](\boldsymbol{\xi}) \tag{5.59}$$

$$\left[\left(\gamma_{1,\xi}^{ext} \tilde{V} \right) f \right](\boldsymbol{\xi}) = [\sigma(\boldsymbol{\xi}) - 1] f(\boldsymbol{\xi}) + \left[K' f \right](\boldsymbol{\xi}) \tag{5.60}$$

and thus, the Neumann jump condition for the single layer potential is given by

$$\left[\left(\gamma_1^{ext} \tilde{V} \right) f - \left(\gamma_1^{int} \tilde{V} \right) f \right](\boldsymbol{\xi}) = -f(\boldsymbol{\xi}), \quad \boldsymbol{\xi} \in \Gamma \tag{5.61}$$

---

7 For the external trace, the internal trace operators in the definitions of the boundary integral operators have to be replaced by external traces.

The hypersingular boundary integral operator

Having computed the Neumann trace of the single layer potential, it seems natural to now apply this conormal derivative operator to the double layer potential as well. This leads to another boundary integral operator

$$\gamma_1^{\text{int}} W \colon H^{\frac{1}{2}}(\Gamma) \to H^{-\frac{1}{2}}(\Gamma)$$

$$[Df](\boldsymbol{\xi}) := - \left[(\gamma_1^{\text{int}} W) f \right](\boldsymbol{\xi}) = - \lim_{\Omega \ni \boldsymbol{\zeta} \to \boldsymbol{\xi} \in \Gamma} \hat{\boldsymbol{n}}(\boldsymbol{\xi}) \cdot \boldsymbol{\nabla}_{\boldsymbol{\zeta}} \left[Wf \right](\boldsymbol{\zeta}) \quad \text{for } \boldsymbol{\xi} \in \Gamma \qquad (5.62)$$

The double layer potential W already includes a Neumann trace operation on the fundamental solution $\mathcal{G}^L$, and thus *its* Neumann trace will contain second order derivatives of this function. The first Neumann trace operation changed a weakly singular integrand into a strongly singular one, which can only be represented by the help of Cauchy principal value integrals, and so it can be suspected that the application of an additional differential operator makes matters worse. In fact, it turns out that the resulting integrand is even stronger singular than the integrand of the double layer potential – the integrals do **not** even exist in the sense of Cauchy principal value integrals. For this reason, the boundary integral operator D is called the *hypersingular boundary integral operator*, and explicit representations can only be found using suitable regularization schemes [Ste03]. It can be shown that for continuous f, such a representation is given by

$$\boxed{[Df](\boldsymbol{\xi}) = \oint_{\Gamma} \gamma_{1,\boldsymbol{\xi}}^{\text{int}} \gamma_{1,\boldsymbol{r}}^{\text{int}} \mathcal{F}(\boldsymbol{r}, \boldsymbol{\xi}) \left[f(\boldsymbol{r}) - f(\boldsymbol{\xi}) \right] d\Gamma_{\boldsymbol{r}} \quad \text{for } \boldsymbol{\xi} \in \Gamma} \qquad (5.63)$$

The Newton potential

The last integral operator we finally have to consider is the so–called *Newton potential*. While this does not occur for homogeneous equations like the Laplace equation, it plays an important role for inhomogeneous equations like the inhomogeneous Yukawa equation (4.47) of our novel formulation of nonlocal electrostatics. Let us consider a differential equation of the type

$$\mathcal{L}\varphi(\boldsymbol{r}) = f(\boldsymbol{r}) \quad \text{for } \boldsymbol{r} \in \Omega$$

The equivalent of the representation formula (5.15) for this operator will then not only contain boundary integrals, but will rather include a domain integral arising from the inhomogeneity $f(\boldsymbol{r})$. This domain integral is called the Newton potential

$$\tilde{N}_0 \colon \tilde{H}^{-1}(\Omega) \to H^1(\Omega)$$

$$\left[\tilde{N}_0 f \right](\boldsymbol{\xi}) := \int_{\Omega} \mathcal{F}(\boldsymbol{r}, \boldsymbol{\xi}) f(\boldsymbol{r}) d\boldsymbol{r} \quad \text{for } \boldsymbol{r} \in \Omega \qquad (5.64)$$

The computation of the traces γ_0^{int} and γ_1^{int} of the Newton potential is straightforward and fortunately, we will not need an explicit representation of these operators in the following. Here, we will thus only define the operators

$$N_0 := \gamma_0^{\text{int}} \tilde{N}_0 \colon \tilde{H}^{-1}(\Omega) \to H^{\frac{1}{2}}(\Gamma) \qquad (5.65)$$

$$N_1 := \gamma_1^{\text{int}} \tilde{N}_0 \colon \tilde{H}^{-1}(\Omega) \to H^{-\frac{1}{2}}(\Gamma) \qquad (5.66)$$

In general, the appearance of the Newton potential is problematic for the boundary element method, since it requires the evaluation of a three–dimensional domain integral, which seems to be in contradiction of the paradigm of this method: the reduction of differential equations to *boundary* integral

equations. Different techniques exist for coping with these terms, and the interested reader is again referred to [Ste03, GKW03, Ame01] for details. Fortunately, we have been able to avoid the computation of the Newton potential at all in all our applications, and we will later show how this can be achieved.

5.2.2. Boundary integral equations for the interior Laplace equation

In the beginning of this section, we had derived the *representation formula* (5.15)

$$\varphi(\boldsymbol{\xi}) = \oint_{\Gamma} \left[\left(\gamma_0^{\text{int}} \varphi(\boldsymbol{r})\right) \left(\gamma_1^{\text{int}} \mathcal{F}(\boldsymbol{r}, \boldsymbol{\xi})\right) - \left(\gamma_0^{\text{int}} \mathcal{F}(\boldsymbol{r}, \boldsymbol{\xi})\right) \left(\gamma_1^{\text{int}} \varphi(\boldsymbol{r})\right) \right] d\Gamma$$

for the solution of the interior Laplace equation

$$\Delta \varphi = 0 \quad \text{in } \Omega$$

subject to Dirichlet boundary conditions on Γ_D, Neumann boundary conditions on Γ_N and Robin boundary conditions on Γ_R, with

$$\partial \Omega =: \Gamma = \bar{\Gamma}_D + \bar{\Gamma}_N + \bar{\Gamma}_R$$

We have also seen that if we were given the full Cauchy data $\left[\gamma_0^{\text{int}} \varphi, \gamma_1^{\text{int}} \varphi\right]$, i.e. the potential as well as its normal derivative – the flux – everywhere on Γ, we could compute the solution $\varphi(\boldsymbol{r})$ to Laplace's equation everywhere in Ω with the help of equation (5.15). But our set of boundary conditions only provides us with the Dirichlet data $\gamma_0^{\text{int}} \varphi$ on Γ_D, the Neumann data on $\gamma_1^{\text{int}} \varphi$ in Γ_N, and a mixture of both on Γ_R, and therefore, we need a way to compute Neumann data from given Dirichlet data and vice versa. Such a function, relating the trace operators γ_0^{int} and γ_1^{int} is called a *Dirichlet–to–Neumann* or *Neumann–to–Dirichlet* map, and we will show in this section that our considerations from Section 5.2.1 provide us with everything we need for their derivation.

The first step in the derivation of a Dirichlet–to–Neumann map for the interior Laplace problem under consideration lies in recognizing that the representation formula (5.15) can be rewritten in terms of the boundary integral operators defined in Section 5.2.1 as follows

$$\varphi(\boldsymbol{\xi}) = \oint_{\Gamma} \left[\left(\gamma_0^{\text{int}} \varphi(\boldsymbol{r})\right) \left(\gamma_1^{\text{int}} \mathcal{F}(\boldsymbol{r}, \boldsymbol{\xi})\right) - \left(\gamma_0^{\text{int}} \mathcal{F}(\boldsymbol{r}, \boldsymbol{\xi})\right) \left(\gamma_1^{\text{int}} \varphi(\boldsymbol{r})\right) \right] d\Gamma$$

$$= \left[\tilde{V} \left(\gamma_1^{\text{int}} \varphi\right) \right] (\boldsymbol{\xi}) - \left[W \left(\gamma_0^{\text{int}} \varphi\right) \right] (\boldsymbol{\xi}) \tag{5.67}$$

From equation (5.67), it is now easy to compute the Dirichlet data $\gamma_0^{\text{int}} \varphi$ with the help of the theorems 5.2.3 and 5.2.5

$$\left(\gamma_0^{\text{int}} \varphi\right)(\boldsymbol{\xi}) = \left[V \left(\gamma_1^{\text{int}} \varphi\right) \right] (\boldsymbol{\xi}) + \left[\{1 - \sigma(\boldsymbol{\xi})\} \left(\gamma_0^{\text{int}} \varphi\right) \right] (\boldsymbol{\xi}) - \left[K \left(\gamma_0^{\text{int}} \varphi\right) \right] (\boldsymbol{\xi}) \tag{5.68}$$

The Neumann data $\gamma_1^{\text{int}} \varphi$ follows equivalently by applying theorem 5.2.6 and definition (5.62)

$$\left(\gamma_1^{\text{int}} \varphi\right)(\boldsymbol{\xi}) = \sigma(\boldsymbol{\xi}) \left(\gamma_1^{\text{int}} \varphi\right)(\boldsymbol{\xi}) + \left[K' \left(\gamma_1^{\text{int}} \varphi\right) \right] (\boldsymbol{\xi}) + \left[D \left(\gamma_0^{\text{int}} \varphi\right) \right] (\boldsymbol{\xi}) \tag{5.69}$$

This leads to the following theorem

Theorem 5.2.7 (Boundary integral equations for the interior Laplace equation). *Let $\varphi(\boldsymbol{r})$ denote the solution of the interior Laplace equation*

$$\Delta \varphi = 0 \quad \text{in } \Omega$$

5. The Boundary Element Method

let $\sigma(\boldsymbol{\xi})$ denote the geometrical quantity

$$\sigma(\boldsymbol{\xi}) := \lim_{\epsilon \to 0} \frac{1}{4\pi} \frac{1}{\epsilon^2} \int\limits_{\boldsymbol{r} \in \Omega : |\boldsymbol{r} - \boldsymbol{\xi}| = \epsilon} d\Gamma_r$$

let I denote the identity operator, and let for $\boldsymbol{\xi} \in \Gamma$ V, K, K' and D denote the boundary integral operators defined by

$$[Vf](\boldsymbol{\xi}) := -\oint_\Gamma \left(\gamma_{0,\xi}^{int} \gamma_{0,r}^{int} \mathcal{G}^L(\boldsymbol{r}, \boldsymbol{\xi}) \right) f(\boldsymbol{r}) \, d\Gamma_r \tag{5.70}$$

$$[Kf](\boldsymbol{\xi}) := -\oint_\Gamma \left(\gamma_{0,\xi}^{int} \gamma_{1,r}^{int} \mathcal{G}^L(\boldsymbol{r}, \boldsymbol{\xi}) \right) f(\boldsymbol{r}) \, d\Gamma_r \tag{5.71}$$

$$\left[K'f\right](\boldsymbol{\xi}) := -\oint_\Gamma \left(\gamma_{1,\xi}^{int} \gamma_{0,r}^{int} \mathcal{G}^L(\boldsymbol{r}, \boldsymbol{\xi}) \right) f(\boldsymbol{r}) \, d\Gamma_r \tag{5.72}$$

$$[Df](\boldsymbol{\xi}) := \oint_\Gamma \left(\gamma_{1,\xi}^{int} \gamma_{1,r}^{int} \mathcal{G}^L(\boldsymbol{r}, \boldsymbol{\xi}) \right) [f(\boldsymbol{r}) - f(\boldsymbol{\xi})] \, d\Gamma_{\boldsymbol{r}} \tag{5.73}$$

with the Laplacian's fundamental solution

$$\mathcal{G}^L(\boldsymbol{r} - \boldsymbol{\xi}) = -\frac{1}{4\pi} \frac{1}{|\boldsymbol{r} - \boldsymbol{\xi}|}$$

Then, the following system of boundary integral equations holds

$$\boxed{\begin{pmatrix} \gamma_0^{int} \varphi \\ \gamma_1^{int} \varphi \end{pmatrix} = \begin{pmatrix} (1 - \sigma)I - K & V \\ D & \sigma I + K' \end{pmatrix} \begin{pmatrix} \gamma_0^{int} \varphi \\ \gamma_1^{int} \varphi \end{pmatrix}} \tag{5.74}$$

where the matrix

$$\mathcal{C} := \begin{pmatrix} (1 - \sigma)I - K & V \\ D & \sigma I + K' \end{pmatrix} \tag{5.75}$$

of boundary integral operators is known as the Calderón–projector .

It is an easy exercise to show that the Dirichlet trace of the single layer potential, the operator V, is bounded and $H^{-\frac{1}{2}}(\Gamma)$–elliptic, i.e.

$$\exists \, c_1^A > 0 : \langle Vf, f \rangle \geq c_1^A \|f\|_{H^{-\frac{1}{2}}(\Gamma)}^2 \quad \forall f \in H^{-\frac{1}{2}}(\Gamma)$$

which allows us to apply the important lemma of Lax and Milgram [DM90, Zei95]:

Theorem 5.2.8 (Lemma of Lax–Milgram). *Let $A \colon X \to X'$ be a bounded and X–elliptic operator. Then, for all $f \in X'$, the operator equation*

$$Au = f \tag{5.76}$$

has a unique solution $u \in X$, which is bounded by

$$\|u\|_X \leq \frac{1}{c_1^A} \|f\|_{X'} \tag{5.77}$$

In particular, the lemma of Lax and Milgram tells us that for bounded and X–elliptic A, the inverse operator $A^{-1} \colon X' \to X$ exists (we can always solve for $u = A^{-1} f$), and is itself bounded and X'–elliptic. We can thus conclude, that the Dirichlet trace of the single layer potential – being bounded and $H^{-\frac{1}{2}}(\Gamma)$–elliptic – is invertible, with bounded and $H^{\frac{1}{2}}(\Gamma)$–elliptic inverse

$$V^{-1} \colon H^{\frac{1}{2}}(\Gamma) \to H^{-\frac{1}{2}}(\Gamma)$$

which we can use to finally derive the desired mapping between Dirichlet and Neumann data on the boundary:

Theorem 5.2.9 (Dirichlet–to–Neumann map for the interior Laplace equation). *Let* $\varphi(\boldsymbol{r})$, $\sigma(\boldsymbol{r})$, I, V, K, K' *and* D *be defined as in theorem 5.2.7. Then, for given Dirichlet data* $\gamma_0^{int}\varphi$, *the Neumann data* $\gamma_1^{int}\varphi$ *is given by*

$$\boxed{\gamma_1^{int}\varphi(\boldsymbol{\xi}) = V^{-1}(\sigma I + K)\,\gamma_0^{int}\varphi(\boldsymbol{\xi}) \quad \boldsymbol{\xi} \in \Gamma} \tag{5.78}$$

Proof. From the first row of the Calderón projector (5.75), we have

$$\left(\gamma_0^{\text{int}}\varphi\right)(\boldsymbol{\xi}) = \left[V\left(\gamma_1^{\text{int}}\varphi\right)\right](\boldsymbol{\xi}) + \left[\{1 - \sigma(\boldsymbol{\xi})\}\left(\gamma_0^{\text{int}}\varphi\right)\right](\boldsymbol{\xi}) - \left[K\left(\gamma_0^{\text{int}}\varphi\right)\right](\boldsymbol{\xi})$$

$$\Leftrightarrow \left[V\left(\gamma_1^{\text{int}}\varphi\right)\right](\boldsymbol{\xi}) = \left[\{\sigma(\boldsymbol{\xi}) + K\}\left(\gamma_0^{\text{int}}\varphi\right)\right](\boldsymbol{\xi})$$

which is a *Fredholm integral equation of the first kind*. Boundedness and $H^{-\frac{1}{2}}(\Gamma)$–ellipticity of the Dirichlet trace of the single layer potential V guarantee the existence of the inverse operator V^{-1} by virtue of the lemma of Lax–Milgram, and left–multiplication with V^{-1} yields the proposed equation. $\qquad\square$

Definition 5.2.2 (The Steklov–Poincaré operator). The operator

$$S \colon H^{\frac{1}{2}}(\Gamma) \to H^{-\frac{1}{2}}(\Gamma)$$

$$S := V^{-1}(\sigma I + K) \tag{5.79}$$

is called the *Steklov–Poincaré operator* of the Laplacian.

With the help of the Steklov–Poincaré operator, we can finally convert given Dirichlet data to Neumann data, yielding the full Cauchy data on Γ_D, and thus enabling us to completely solve fully Dirichlet problems. In a similar way we can derive a Neumann–to–Dirichlet map also from the first row of the Calderón projector, leading to

$$\boxed{\gamma_0^{\text{int}}\varphi(\boldsymbol{\xi}) = (\sigma I + K)^{-1}\left[V\left(\gamma_1^{\text{int}}\varphi(\boldsymbol{\xi})\right)\right] \quad \boldsymbol{\xi} \in \Gamma} \tag{5.80}$$

which can e.g. be obtained by solving the boundary integral equation

$$(\sigma I + K)\,\gamma_0^{\text{int}}\varphi(\boldsymbol{\xi}) = \left[V\left(\gamma_1^{\text{int}}\varphi\right)\right](\boldsymbol{\xi}) \tag{5.81}$$

This is a *Fredholm integral equation of the second kind*, and can thus be solved with the help of a *Neumann series* [Arf85]

$$\gamma_0^{\text{int}}\varphi(\boldsymbol{\xi}) = \sum_{l=0}^{\infty} \left([1 - \sigma]\,I - K\right)^l \left[V\left(\gamma_1^{\text{int}}\varphi\right)\right](\boldsymbol{\xi}) \quad \boldsymbol{\xi} \in \Gamma \tag{5.82}$$

We can thus convert Dirichlet data to Neumann data on Γ_D, and Neumann data to Dirichlet data on Γ_N, and similar results can easily be found for the Robin data on Γ_R. Also, additional Dirichlet to Neumann maps and vice versa with different numerical properties can be found by using the second row of the Calderón projector. For details on those, and on how to combine the different equations for the general mixed boundary value problem, the reader is again referred to [Ste03].

5.2.3. The indirect Boundary Element Method

A boundary element technique like the one we have just derived, i.e., an approach that generates the full Cauchy data on Γ from the Calderón projector before using the representation formula (5.15) is called a **direct** boundary element method. But from Section 5.2.1, and in particular from the theorems 5.2.2 and 5.2.4, we suspect that the *full* representation formula is not even necessary to find a solution to the Laplace equation since the single layer potential or the double layer potential itself is already harmonic in Ω.

This leads to the question whether it is possible to neglect the full representation formula and work with either the single layer potential $\tilde{V}$ or the double layer potential W instead. Comparison with the representation formula

$$\varphi(\boldsymbol{\xi}) = \left[\tilde{V}\left(\gamma_1^{\text{int}}\varphi\right)\right](\boldsymbol{\xi}) - \left[W\left(\gamma_0^{\text{int}}\varphi\right)\right](\boldsymbol{\xi})$$

immediately tells us that for the two particular cases of the purely Dirichlet problem with

$$\gamma_0^{\text{int}}\varphi \equiv 0 \quad \text{on } \Gamma \tag{5.83}$$

and for the purely Neumann problem with

$$\gamma_1^{\text{int}}\varphi \equiv 0 \quad \text{on } \Gamma \tag{5.84}$$

this is indeed the case: in the first case, the double layer potential W in the representation formula vanishes, leaving only the single layer potential term $\tilde{V}$, and for the second case vice versa.

This motivates the following idea: instead of using the Dirichlet and Neumann data of the sought solution φ in the full representation formula, we could use either a *single layer potential Ansatz*

$$\varphi(\boldsymbol{\xi}) = \left[\tilde{V}w\right](\boldsymbol{\xi}) = -\oint_\Gamma \mathcal{F}(\boldsymbol{r},\boldsymbol{\xi})w(\boldsymbol{r})d\Gamma_r \quad \text{for } \boldsymbol{\xi} \in \Omega \tag{5.85}$$

or a *double layer potential Ansatz*

$$\varphi(\boldsymbol{\xi}) = -[Wv](\boldsymbol{\xi}) = \oint_\Gamma \gamma_{1,r}^{\text{int}}\mathcal{F}(\boldsymbol{r},\boldsymbol{\xi})v(\boldsymbol{r})d\Gamma_r \quad \text{for } \boldsymbol{\xi} \in \Omega \tag{5.86}$$

where the functions w and v in general **unphysical** density functions, which are yet to determine. Of course, for such an Ansatz to be of any use, the resulting function φ has to be the same as the one obtained from the full representation formula. This means for the single layer potential Ansatz, for example, that the density w corresponds to the Neumann trace of an interior Laplacian problem with vanishing Dirichlet data on Γ, that is equivalent to the original problem in the sense that both have the same solution φ. But then the determination of w is easily possible: since both problems have the same solution φ, the Dirichlet traces of both must be the same as well.

Let us now assume that we want to use a single layer potential Ansatz for a purely Dirichlet problem, i.e. $\Gamma_D \equiv \Gamma$:

$$\Delta\varphi = 0 \qquad \text{in } \Omega \tag{5.87}$$

$$\gamma_0^{\text{int}}\varphi(\boldsymbol{\xi}) = g(\boldsymbol{\xi}) \qquad \boldsymbol{\xi} \in \Gamma \tag{5.88}$$

$$\varphi(\boldsymbol{\xi}) = \left[\tilde{V}w\right](\boldsymbol{\xi}) \quad \boldsymbol{\xi} \in \Gamma \tag{5.89}$$

Applying the Dirichlet trace operator γ_0^{int} to equation (5.89), and using theorem 5.2.3 then yields for the unknown density w:

$$[Vw](\boldsymbol{\xi}) = g(\boldsymbol{\xi}), \quad \boldsymbol{\xi} \in \Gamma \tag{5.90}$$

and existence of the inverse of the operator V by virtue of the Lax–Milgram lemma guarantees a unique solution

$$w(\boldsymbol{\xi}) = \left[V^{-1}g\right](\boldsymbol{\xi}), \quad \boldsymbol{\xi} \in \Gamma \tag{5.91}$$

Similarly, a double layer potential Ansatz for the same problem leads to the boundary integral equation

$$[(1 - \sigma(\boldsymbol{\xi}))\, v](\boldsymbol{\xi}) - [Kv](\boldsymbol{\xi}) = g(\boldsymbol{\xi}), \quad \boldsymbol{\xi} \in \Gamma \tag{5.92}$$

which can be solved with the help of the Neumann series

$$v(\boldsymbol{\xi}) = \sum_{l=0}^{\infty} \left(\sigma I + K\right)^l g(\boldsymbol{\xi}), \quad \boldsymbol{\xi} \in \Gamma \tag{5.93}$$

For a purely Neumann problem

$$\Delta \varphi = 0 \qquad \text{in } \Omega \tag{5.94}$$

$$\gamma_1^{\mathrm{int}} \varphi(\boldsymbol{\xi}) = g(\boldsymbol{\xi}) \qquad \boldsymbol{\xi} \in \Gamma \tag{5.95}$$

an analogous computation reveals for a single layer potential Ansatz the boundary integral equation

$$\left(\sigma I + K'\right) w(\boldsymbol{\xi}) = g(\boldsymbol{\xi}), \quad \boldsymbol{\xi} \in \Gamma \tag{5.96}$$

with the Neumann series solution

$$w(\boldsymbol{\xi}) = \sum_{l=0}^{\infty} \left(\{1 - \sigma\} I - K'\right)^l g(\boldsymbol{\xi}), \quad \boldsymbol{\xi} \in \Gamma \tag{5.97}$$

and for a double layer potential Ansatz the hypersingular equation

$$[Dv](\boldsymbol{\xi}) = g(\boldsymbol{\xi}), \quad \boldsymbol{\xi} \in \Gamma \tag{5.98}$$

It can be shown[Ste03] that the hypersingular operator D is bounded and $H_*^{\frac{1}{2}}(\Gamma)$–elliptic, and thus, by virtue of the Lax–Milgram lemma, a unique solution $v \in H_*^{\frac{1}{2}}(\Gamma)$ exists with

$$v(\boldsymbol{\xi}) = \left[D^{-1}g\right](\boldsymbol{\xi}), \quad \boldsymbol{\xi} \in \Gamma \tag{5.99}$$

Similar equation for Robin conditions can be similarly derived[Ste03], and for a fully general mixed boundary value problem, all different combinations of boundary integral equations for the Dirichlet problem inside Γ_D, the Neumann problem inside Γ_N, and the Robin problem inside Γ_R can be employed, leading to a large variety of possible formulations.

Boundary element methods based on such a single or double layer potential Ansatz with unphysical density function w or v are known as **indirect** boundary element methods, in contrast to the direct ones, based on the full representation formula. The variety of different combinations of boundary integral equations, both direct and indirect formulations, presents the user with a large freedom of choice, where each combination of representations might have numerical or theoretical advantages or disadvantages for the problem at hand, and should thus be chosen after a careful examination of the original problem. For us, it is sufficient here to note that we have finally succeeded in deriving a variety of possible boundary element methods for the interior Laplace equation, just as we promised at the beginning of this chapter, and can now proceed to the first application to biomolecular systems.

5.3. A Boundary Element Method for the local Cavity Model

While the derivation of a boundary element method for the interior Laplace problem (5.5) turned out to be a somewhat complicated process, extending these results to the full system of local cavity electrostatics (2.45) for a spatially independent dielectric constant ε_Σ in the solvent is relatively simple, since most of the required techniques and tools have already been derived in Section 5.2.

The first necessary step that has to be taken is the generalization from the interior Laplace– to the interior local Poisson–equation, i.e. to

$$\Delta\varphi(\boldsymbol{r}) = -\frac{1}{\varepsilon_0\varepsilon_\Omega}\rho(\boldsymbol{r}) \quad \boldsymbol{r} \in \Omega$$

From a theoretical point of view, this does not complicate matters at all, since with the definition

$$f(\boldsymbol{r}) := -\frac{1}{\varepsilon_0\varepsilon_\Omega}\rho(\boldsymbol{r})$$

we only need to add a Newton potential term $\tilde{N}_0 f$ to the representation formula (5.15), and the boundary integral equations have to be complemented by its Dirichlet and Neumann traces N_0 and N_1. But for a real–world implementation, this seemingly harmless additional terms lead to enormous complications: the appearance of *domain* integrals would require completely different integration techniques, including a three–dimensional discretization of the whole domain, something that we wanted to avoid for the boundary element method in the first place.

In an important special case this problem does not really arise: if the charge distribution – in our case representing the charges of a given biomolecular system – is a sum of Dirac δ–distributions, then the domain integral of the Newton potential is replaced by a finite sum, since each δ sieves out a single point of the integration domain:

$$\rho(\boldsymbol{r}) = \sum_{i=0}^{N} q_i \delta(\boldsymbol{r} - \boldsymbol{r}_i) \tag{5.100}$$

$$\rightsquigarrow -\frac{1}{\varepsilon_0\varepsilon_\Omega}\tilde{N}_0\rho(\boldsymbol{r}) = \frac{1}{\varepsilon_0\varepsilon_\Omega}\frac{1}{4\pi}\sum_{i=0}^{N}\int_\Omega \frac{q_i}{|\boldsymbol{r} - \boldsymbol{r}_i|}\delta(\boldsymbol{r} - \boldsymbol{r}_i)d\boldsymbol{r}$$

$$= \frac{1}{4\pi\varepsilon_0\varepsilon_\Omega}\sum_{i=0}^{N}\frac{q_i}{|\boldsymbol{r} - \boldsymbol{r}_i|} \tag{5.101}$$

Remarkably, the Newton potential of this special charge distribution $\rho(\boldsymbol{r})$ is just the potential of the same charge distribution in an infinite medium of dielectric constant ε_Ω, and this is just what we called the *molecular potential* in Section 2.4 Since the Newton potential is an additive term to the solution $\varphi(\boldsymbol{r})$ of the Poisson equation

$$\varphi(\boldsymbol{\xi}) = \left[\tilde{V}\left(\gamma_1^{\text{int}}\varphi\right)\right](\boldsymbol{\xi}) - \left[W\left(\gamma_0^{\text{int}}\varphi\right)\right](\boldsymbol{\xi}) - \frac{1}{\varepsilon_0\varepsilon_0}\left[\tilde{N}_0\rho\right](\boldsymbol{\xi})$$

it seems that φ can be decomposed into the molecular potential φ_{mol} and the *reaction field potential* φ^*, where

$$\varphi^*(\boldsymbol{\xi}) = \left[\tilde{V}\left(\gamma_1^{\text{int}}\varphi^*\right)\right](\boldsymbol{\xi}) - \left[W\left(\gamma_0^{\text{int}}\varphi^*\right)\right](\boldsymbol{\xi})$$

describes the response of the medium to the charge distribution, just as described in Section 2.4.

This property – a decomposition of the electrostatic potential into the molecular potential and the reaction field – turns out to be a general feature of the boundary element approach. This can be seen as follows: by definition, the Newton potential is an integral over the inhomogeneity – the charge distribution times the necessary normalization constants – times the fundamental solution $\mathcal{F}(\boldsymbol{r}, \boldsymbol{\xi})$. Remembering that the fundamental solution is the free space Green's function of the differential operator, we find that the Newton potential yields the potential of the charge distribution embedded in free space, filled with a homogeneous medium of dielectric constant ε_Ω, which is just the definition of the molecular potential.

From the linearity of the differential equations encountered in the cavity models – both local and nonlocal – we can now conclude that we can explicitly compute the potentials φ^* and φ_{mol} more or less independently from each other using the boundary element method. This is a huge advantage over conventional methods like finite difference based algorithms, where the reaction field potential has to be computed in a possibly time–consuming and tendentially numerically instable process from the *sum* of φ^* and φ_{mol}. Additionally, the infinities appearing in the molecular potential, which lead to infinite self energies and thus to numerical problems are not only handled exactly in the boundary element method: they do not even enter the computation of the reaction field potential, which is in a way the natural and finite output of a boundary element approach to molecular electrostatics.

This feature can be integrated into our approach, if we replace the original system of local cavity electrostatics, equations (2.45), by a system for the two fields φ^* and φ_{mol}, where the first fulfills a Laplace equation inside Ω and the second a Poisson–equation everywhere:[8]

$$\left.\begin{aligned} \Delta\varphi_{\text{mol}}(\boldsymbol{r}) &= \frac{-\rho(\boldsymbol{r})}{\varepsilon_0\varepsilon_\Omega} & \boldsymbol{r} &\in \mathbb{R}^3 \\ \Delta\varphi^*(\boldsymbol{r}) &= 0 & \boldsymbol{r} &\in \Omega \\ \Delta\varphi_\Sigma(\boldsymbol{r}) &= 0 & \boldsymbol{r} &\in \Sigma \\ [\varepsilon_\Omega\partial_n(\varphi_{\text{mol}} + \varphi^*) - \varepsilon_\Sigma\partial_n\varphi_\Sigma] &= 0 & \boldsymbol{r} &\in \Gamma \\ [(\varphi_{\text{mol}}(\boldsymbol{r}) + \varphi^*(\boldsymbol{r})) - \varphi_\Sigma(\boldsymbol{r})] &= 0 & \boldsymbol{r} &\in \Gamma \end{aligned}\right\} \tag{5.102}$$

Remark 5.3.1. In the remainder of this work, we will always assume that the molecular potential φ_{mol} can be evaluated analytically. This is no restriction on the generality of the method – we would be able to include numerical solutions for φ_{mol} e.g. via the Newton potential – it will significantly simplify the notation, and – if the assumption holds – will lead to a remarkable speed–up and increased numerical stability of the method. In addition, most of the approximate charge distributions used for the description of biomolecular systems in fact lead to analytically given molecular potentials, most notably the de–facto standard of a sum of atom centered partial point charges, where each atom is assigned a partial charge value and contributes to the charge distribution via a Dirac δ–distribution located at its center. In that case, the molecular potential is just given by

$$\varphi_{\text{mol}}(\boldsymbol{r}) = \frac{1}{4\pi\varepsilon_0\varepsilon_\Omega} \sum_{i=0}^{N} \frac{q_i}{|\boldsymbol{r} - \boldsymbol{r}_i|} \tag{5.103}$$

If nothing else is stated explicitly, we will assume that equation (5.103) holds. In our implementations, we have as well used a Lorentzian charge model for each individual atom, but the effects on the

---

8 Please note that – as we said in the beginning of this section – we will only deal with the case of spatially independent dielectric constants ε_Σ in Σ here. The boundary element method can be generalized to several models for a local but spatially dependent dielectric function $\varepsilon_\Sigma(\boldsymbol{r})$, but those are of no interest to us at this point, since we will focus on deriving a method for the nonlocal model, and while a local dielectric function might be able to improve the local results in some cases, no such function will be able to capture the fully nonlocal response for any geometry.

resulting reaction fields were only minor.

Assuming that φ_{mol} is known analytically, we can of course drop the first equation from system (5.102), yielding

$$\left.\begin{aligned} \Delta\varphi^*(\boldsymbol{r}) &= 0 & \boldsymbol{r} \in \Omega \\ \Delta\varphi_\Sigma(\boldsymbol{r}) &= 0 & \boldsymbol{r} \in \Sigma \\ [\varepsilon_\Omega\partial_n(\varphi_{\mathsf{mol}}+\varphi^*) - \varepsilon_\Sigma\partial_n\varphi_\Sigma] &= 0 & \boldsymbol{r} \in \Gamma \\ [(\varphi_{\mathsf{mol}}(\boldsymbol{r})+\varphi^*(\boldsymbol{r})) - \varphi_\Sigma(\boldsymbol{r})] &= 0 & \boldsymbol{r} \in \Gamma \end{aligned}\right\} \tag{5.104}$$

Remark 5.3.2 *(Notation of the trace operators).* At this point, we have arrived at a hardly avoidable, but fortunately mild, clash of notation: while for the derivation of the physical theory of local and nonlocal electrostatics, the explicit mentioning of internal and external trace operators often lead to confusion and complicate comparison with contemporary physics literature, a strict development of the boundary integral equations derived in the last chapter often relies on being aware of the difference of a field and its – say – Dirichlet trace. When we now want to derive a boundary element method for the system of equations (5.104), we somehow have to reconcile these two notational standards. In our opinion, it is easiest to work with the typical physics convention of not mentioning trace operators explicitly during the derivations to come, but we will also state the result in the more strict notation afterwards. We especially want to remind the reader at this point that the role of the Neumann trace operator γ_1^{int} is now played by the normal derivative operator ∂_n on the boundary.

The direct boundary element approach to local cavity electrostatics

In this section, we will derive all necessary equations for a boundary element method for solving the local cavity model of biomolecular electrostatics, system (5.104). This will allow us to compute the reaction field potential as well as the full electrostatic potential of a given biomolecular system both efficiently and numerically stable. For simplicity, we will chose a *direct* approach, i.e. we will make use of the full representation formula with the physical densities instead of the unphysical single– or double layer potential representations of an indirect approach.

In the system of equations which we now want to solve,

$$\left.\begin{aligned} \Delta\varphi^*(\boldsymbol{r}) &= 0 & \boldsymbol{r} \in \Omega \\ \Delta\varphi_\Sigma(\boldsymbol{r}) &= 0 & \boldsymbol{r} \in \Sigma \\ [\varepsilon_\Omega\partial_n(\varphi_{\mathsf{mol}}+\varphi^*) - \varepsilon_\Sigma\partial_n\varphi_\Sigma] &= 0 & \boldsymbol{r} \in \Gamma \\ [(\varphi_{\mathsf{mol}}(\boldsymbol{r})+\varphi^*(\boldsymbol{r})) - \varphi_\Sigma(\boldsymbol{r})] &= 0 & \boldsymbol{r} \in \Gamma \end{aligned}\right\} \tag{5.105}$$

both, φ_Σ and φ^* are harmonic, and thus our results for the representation of the solutions of Laplace's equation from Section 5.2.2 apply. The reaction field potential φ^* in this case belongs to an *interior* problem, and thus the direct boundary integral equation (5.68) – here given in the notation without trace operators –

$$\varphi^*(\boldsymbol{\xi}) = [V(\partial_n\varphi^*)](\boldsymbol{\xi}) + [\{1 - \sigma(\boldsymbol{\xi})\}\,\varphi^*](\boldsymbol{\xi}) - [K\varphi^*](\boldsymbol{\xi}), \quad \boldsymbol{\xi} \in \Gamma \tag{5.106}$$

holds, while for the field φ_Σ, solving an *exterior* problem, we analogously obtain with the help of the theorems on the external traces of the boundary integral operators from Section 5.2.1

$$\varphi_\Sigma(\boldsymbol{\xi}) = -[V(\partial_n\varphi_\Sigma)](\boldsymbol{\xi}) + [\{1 - \sigma(\boldsymbol{\xi})\}\,\varphi_\Sigma](\boldsymbol{\xi}) + [K\varphi_\Sigma](\boldsymbol{\xi}), \quad \boldsymbol{\xi} \in \Gamma \tag{5.107}$$

This yields the system of boundary integral equations

$$\left.\begin{aligned} \sigma(\boldsymbol{\xi})\varphi^*(\boldsymbol{\xi}) - [V(\partial_n\varphi^*)](\boldsymbol{\xi}) + [K\varphi^*](\boldsymbol{\xi}) &= 0 \\ \sigma(\boldsymbol{\xi})\varphi_\Sigma(\boldsymbol{\xi}) + [V(\partial_n\varphi_\Sigma)](\boldsymbol{\xi}) - [K\varphi_\Sigma](\boldsymbol{\xi}) &= 0 \end{aligned}\right\} \quad \boldsymbol{\xi} \in \Gamma \tag{5.108}$$

Adding the second equation to the first and suppressing the argument $\boldsymbol{\xi}$, we arrive at

$$\sigma\left[\varphi^* + \varphi_\Sigma\right] + \left[V\partial_n(\varphi_\Sigma - \varphi^*)\right] + \left[K\left(\varphi^* - \varphi_\Sigma\right)\right] = 0 \tag{5.109}$$

From the fourth equation in system (5.105), we know that on the boundary

$$\varphi_\Sigma = \varphi^* + \varphi_{\mathsf{mol}}$$

which we can use in equation (5.109) to yield:[9]

$$\sigma\left[2\varphi^* + \varphi_{\mathsf{mol}}\right] + \left[V\partial_n(\varphi_\Sigma - \varphi^*)\right] + \left[K\left(\varphi^* - \varphi^* - \varphi_{\mathsf{mol}}\right)\right] = 0 \tag{5.110}$$

Using the second boundary condition from system (5.105)

$$\left[\varepsilon_\Omega\partial_n(\varphi_{\mathsf{mol}} + \varphi^*) - \varepsilon_\Sigma\partial_n\varphi_\Sigma\right] = 0$$
$$\Leftrightarrow \qquad \frac{\varepsilon_\Omega}{\varepsilon_\Sigma}\partial_n(\varphi_{\mathsf{mol}} + \varphi^*) = \partial_n\varphi_\Sigma$$

we can completely eliminate the exterior potential φ_Σ from equation (5.110) to yield

$$\sigma\left[2\varphi^* + \varphi_{\mathsf{mol}}\right] + \left[V\left(\frac{\varepsilon_\Omega}{\varepsilon_\Sigma}\partial_n\varphi_{\mathsf{mol}} + \frac{\varepsilon_\Omega}{\varepsilon_\Sigma}\partial_n\varphi^* - \partial_n\varphi^*\right)\right] - \left[K\varphi_{\mathsf{mol}}\right] = 0 \tag{5.111}$$

Separating the known functions φ_{mol} and $\partial_n\varphi_{\mathsf{mol}}$ from the unknown reaction field φ^* and its normal derivative $\partial_n\varphi^*$ leads to

$$\sigma\left[2\varphi^*\right] + \left(\frac{\varepsilon_\Omega}{\varepsilon_\Sigma} - 1\right)\left[V\left(\partial_n\varphi^*\right)\right] = \left[K\varphi_{\mathsf{mol}}\right] - \sigma\left[\varphi_{\mathsf{mol}}\right] - \frac{\varepsilon_\Omega}{\varepsilon_\Sigma}\left[V(\partial_n\varphi_{\mathsf{mol}})\right] \tag{5.112}$$

With equation (5.112), we have one boundary integral equation for the computation of the two unknown functions φ^* and $\partial_n\varphi^*$. But the normal derivative $\partial_n\varphi^*$ can be completely eliminated, if we make use of the Neumann–to–Dirichlet map (5.80), which can be brought into the form

$$\left[V(\partial_n\varphi^*)\right] = \sigma\varphi^* + \left[K\varphi^*\right]$$

Insertion into (5.112) yields

$$\sigma\left[2\varphi^*\right] + \left(\frac{\varepsilon_\Omega}{\varepsilon_\Sigma} - 1\right)\left(\sigma\varphi^* + \left[K\varphi^*\right]\right) = \left[K\varphi_{\mathsf{mol}}\right] - \sigma\left[\varphi_{\mathsf{mol}}\right] - \frac{\varepsilon_\Omega}{\varepsilon_\Sigma}\left[V(\partial_n\varphi_{\mathsf{mol}})\right] \tag{5.113}$$

which is equivalent to

$$\boxed{\left(1 + \frac{\varepsilon_\Omega}{\varepsilon_\Sigma}\right)\sigma\left[\varphi^*\right] + \left(\frac{\varepsilon_\Omega}{\varepsilon_\Sigma} - 1\right)\left[K\varphi^*\right] = \left[(K - \sigma)\,\varphi_{\mathsf{mol}}\right] - \frac{\varepsilon_\Omega}{\varepsilon_\Sigma}\left[V(\partial_n\varphi_{\mathsf{mol}})\right]} \tag{5.114}$$

In combination with a Dirichlet–to–Neumann map, this equation provides us with all we need for our boundary element method for the local cavity model. Such a map is for example given by the Steklov–Poincaré operator (5.79)

$$S\colon H^{\frac{1}{2}}(\Gamma) \to H^{-\frac{1}{2}}(\Gamma)$$

$$S := V^{-1}(\sigma I + K) \tag{5.115}$$

for which we have the identity (5.78)

$$\partial_n\varphi^*(\boldsymbol{\xi}) = S[\varphi^*(\boldsymbol{\xi})] \quad \boldsymbol{\xi} \in \Gamma$$

These results can be combined in the following theorem:

---

9 Please note that this equation can not be used to simplify the single layer potential V–term in equation (5.109) since the quantities appearing there are not the potentials themselves but rather their normal derivatives. This becomes more clear when inserting explicitly the trace operators γ_0^{int} and γ_1^{int}.

Theorem 5.3.1 (Boundary Element Method for local Cavity Electrostatics). *The system of local cavity electrostatics*

$$\left.\begin{array}{rl} \Delta\varphi^*(\boldsymbol{r}) = 0 & \boldsymbol{r} \in \Omega \\ \Delta\varphi_\Sigma(\boldsymbol{r}) = 0 & \boldsymbol{r} \in \Sigma \\ [\varepsilon_\Omega \partial_n(\varphi_{mol} + \varphi^*) - \varepsilon_\Sigma \partial_n \varphi_\Sigma] = 0 & \boldsymbol{r} \in \Gamma \\ [(\varphi_{mol}(\boldsymbol{r}) + \varphi^*(\boldsymbol{r})) - \varphi_\Sigma(\boldsymbol{r})] = 0 & \boldsymbol{r} \in \Gamma \end{array}\right\} \tag{5.116}$$

for known molecular potential φ_{mol} leads to the following system of boundary integral equations:

$$\left(1 + \frac{\varepsilon_\Omega}{\varepsilon_\Sigma}\right) \sigma\left[\varphi^*\right] + \left(\frac{\varepsilon_\Omega}{\varepsilon_\Sigma} - 1\right)[K\varphi^*] = [(K - \sigma)\,\varphi_{mol}] - \frac{\varepsilon_\Omega}{\varepsilon_\Sigma}[V(\partial_n\varphi_{mol})] \tag{5.117}$$

$$\partial_n\varphi^*(\boldsymbol{\xi}) = V^{-1}(\sigma I + K)[\varphi^*(\boldsymbol{\xi})] \tag{5.118}$$

for $\boldsymbol{\xi} \in \Gamma$. From the solution $[\varphi^*, \partial_n\varphi^*]$ on Γ – the full Cauchy data – the electrostatic potentials inside Ω and Σ can then be determined from the representation formulae:

$$\varphi_\Omega(\boldsymbol{\xi}) = \left[\tilde{V}\left(\partial_n\varphi^*\right)\right](\boldsymbol{\xi}) - [W\left(\varphi^*\right)](\boldsymbol{\xi}) + \varphi_{mol}(\boldsymbol{\xi}), \qquad \boldsymbol{\xi} \in \Omega \tag{5.119}$$

$$\varphi_\Sigma(\boldsymbol{\xi}) = [W\left(\varphi^* + \varphi_{mol}\right)](\boldsymbol{\xi}) - \frac{\varepsilon_\Omega}{\varepsilon_\Sigma}\left[\tilde{V}\left(\partial_n\left(\varphi^* + \varphi_{mol}\right)\right)\right](\boldsymbol{\xi}), \quad \boldsymbol{\xi} \in \Sigma \tag{5.120}$$

The electrostatic energy of the system can be determined from the reaction field $\varphi^* = \varphi_\Omega - \varphi_{mol}$ via

$$W^{rf} = \int_\Omega \varphi^* \rho \, d\Omega \tag{5.121}$$

which for the important special case of a partial point charge model

$$\rho(\boldsymbol{r}) = \sum_{i=0}^{N} q_i \delta(\boldsymbol{r} - \boldsymbol{r}_i)$$

reduces to

$$W^{rf}_{ppc} = \sum_{i=0}^{N} q_i \varphi^*(\boldsymbol{r}_i) \tag{5.122}$$

Proof. The system of boundary integral equations has already been derived in the last paragraph, and the first representation formula is just a consequence of the representation formula of the reaction field

$$\varphi^*(\boldsymbol{\xi}) = \left[\tilde{V}\left(\partial_n\varphi^*\right)\right](\boldsymbol{\xi}) - [W\left(\varphi^*\right)](\boldsymbol{\xi}), \quad \boldsymbol{\xi} \in \Omega$$

combined with the decomposition

$$\varphi_\Omega = \varphi^* + \varphi_{mol}$$

The second representation formula follows just as easily from the representation

$$\varphi_\Sigma(\boldsymbol{\xi}) = -\left[\tilde{V}\left(\partial_n\varphi_\Sigma\right)\right](\boldsymbol{\xi}) + [W\left(\varphi_\Sigma\right)](\boldsymbol{\xi}), \quad \boldsymbol{\xi} \in \Sigma$$

and the boundary conditions

$$\varphi_\Sigma = \varphi_\Omega = \varphi^* + \varphi_{mol} \text{ on } \Gamma$$

and

$$\partial_n\varphi_\Sigma = \frac{\varepsilon_\Omega}{\varepsilon_\Sigma}\partial_n\varphi_\Omega \text{ on } \Gamma \qquad\qquad \square$$

Remark 5.3.3. With explicit trace operators, the equations in theorem 5.3.1, assume the form:

$$\left(1 + \frac{\varepsilon_\Omega}{\varepsilon_\Sigma}\right) \sigma \left[\gamma_0^{\text{int}} \varphi^*\right] + \left(\frac{\varepsilon_\Omega}{\varepsilon_\Sigma} - 1\right) \left[K\gamma_0^{\text{int}} \varphi^*\right] = \left[(K - \sigma)\gamma_0^{\text{int}} \varphi_{\text{mol}}\right] - \frac{\varepsilon_\Omega}{\varepsilon_\Sigma} \left[V\left(\gamma_1^{\text{int}} \varphi_{\text{mol}}\right)\right]$$

$$\gamma_1^{\text{int}} \varphi^*(\boldsymbol{\xi}) = V^{-1}(\sigma I + K)\left[\gamma_0^{\text{int}} \varphi^*(\boldsymbol{\xi})\right]$$

and

$$\varphi_\Omega(\boldsymbol{\xi}) = \left[\tilde{V}\left(\gamma_1^{\text{int}} \varphi^*\right)\right](\boldsymbol{\xi}) - \left[W\left(\gamma_0^{\text{int}} \varphi^*\right)\right](\boldsymbol{\xi}) + \varphi_{\text{mol}}(\boldsymbol{\xi})$$

$$\varphi_\Sigma(\boldsymbol{\xi}) = \left[W\gamma_0^{\text{int}}\left(\varphi^* + \varphi_{\text{mol}}\right)\right](\boldsymbol{\xi}) - \frac{\varepsilon_\Omega}{\varepsilon_\Sigma}\left[\tilde{V}\left(\gamma_1^{\text{int}}\left(\varphi^* + \varphi_{\text{mol}}\right)\right)\right](\boldsymbol{\xi})$$

Theorem 5.3.1 contains everything that is needed for our boundary element approach, and we will show soon how to solve the appearing integral equations numerically. But before we introduce these techniques, we will proceed by extending our derivations to the nonlocal case.

5.4. A Boundary Element Method for the nonlocal Cavity Model

In this section, we will finally derive the central result of this chapter: a boundary integral representation of nonlocal cavity electrostatics for the Lorentzian model (3.23), which will allow for a fast and reliable boundary element solver. To this end, we will employ the decomposition of the interior electrostatic potential into a singular molecular potential and the regular reaction field, introduced in Section 5.3:

$$\varphi_\Omega = \varphi^* + \varphi_{\text{mol}} \tag{5.123}$$

with the same assumptions on the analytical knowledge of the molecular potential as discussed in remark 5.3.1. This allows us to reduce the nonlocal cavity model for the Lorentzian nonlocal dielectric function

$$\left. \begin{aligned} \varepsilon_0 \varepsilon_\Omega \Delta \varphi_\Omega &= -\rho & \boldsymbol{r} &\in \Omega \\ \Delta \psi_\Sigma &= 0 & \boldsymbol{r} &\in \Sigma \\ \left[\varepsilon_0 \varepsilon_\Omega \partial_n \varphi_\Omega - \partial_n \psi_\Sigma\right] &= 0 & \boldsymbol{r} &\in \Gamma \\ \left[\varphi_\Omega - \varphi_\Sigma\right] &= 0 & \boldsymbol{r} &\in \Gamma \\ \varepsilon_0 \varepsilon_\infty \mathcal{L}_\Lambda \varphi_\Sigma &= -\frac{1}{\lambda^2} \psi_\Sigma & \boldsymbol{r} &\in \Sigma \end{aligned} \right\} \tag{5.124}$$

to the simpler system

$$\left. \begin{aligned} \Delta \varphi^* &= 0 & \boldsymbol{r} &\in \Omega \\ \Delta \psi_\Sigma &= 0 & \boldsymbol{r} &\in \Sigma \\ \left[\varepsilon_0 \varepsilon_\Omega \partial_n \left(\varphi^* + \varphi_{\text{mol}}\right) - \partial_n \psi_\Sigma\right] &= 0 & \boldsymbol{r} &\in \Gamma \\ \left[\left(\varphi^* + \varphi_{\text{mol}}\right) - \varphi_\Sigma\right] &= 0 & \boldsymbol{r} &\in \Gamma \\ \varepsilon_0 \varepsilon_\infty \mathcal{L}_\Lambda \varphi_\Sigma &= -\frac{1}{\lambda^2} \psi_\Sigma & \boldsymbol{r} &\in \Sigma \end{aligned} \right\} \tag{5.125}$$

In this system, the potentials φ^* and ψ_Σ are harmonic, and thus the results of the last section can be applied:

$$\sigma(\boldsymbol{\xi})\gamma_0^{\text{int}} \varphi^*(\boldsymbol{\xi}) = \left[V\left(\gamma_1^{\text{int}} \varphi^*\right)\right] - \left[K\left(\gamma_0^{\text{int}} \varphi^*\right)\right] \tag{5.126}$$

$$(1 - \sigma(\boldsymbol{\xi}))\gamma_0^{\text{int}} \psi_\Sigma(\boldsymbol{\xi}) = -\left[V\left(\gamma_1^{\text{ext}} \psi_\Sigma\right)\right] + \left[K\left(\gamma_0^{\text{ext}} \psi_\Sigma\right)\right] \tag{5.127}$$

5. The Boundary Element Method

In the following derivations and the numerical implementation, though, it turns out to be favorable not to work with the field ψ_Σ directly, but rather to employ the linear combination

$$\Psi := \frac{1}{\varepsilon_\infty} \left\{ \frac{1}{\varepsilon_0} \psi_\Sigma - \varepsilon_\Omega \varphi_{\text{mol}} \right\} \tag{5.128}$$

Since $\rho \equiv 0$ in Σ, $\Delta\varphi_{\text{mol}} = 0$ in Σ, and thus, the field Ψ is also harmonic in Σ, leading to the representation formula

$$(1 - \sigma(\boldsymbol{\xi})) \gamma_0^{\text{int}} \Psi(\boldsymbol{\xi}) = - \left[V \left(\gamma_1^{\text{ext}} \Psi \right) \right] + \left[K \left(\gamma_0^{\text{ext}} \Psi \right) \right] \tag{5.129}$$

From the definition of Ψ, equation (5.128), we have

$$\psi_\Sigma := \varepsilon_0 \left\{ \varepsilon_\infty \Psi + \varepsilon_\Omega \varphi_{\text{mol}} \right\} \tag{5.130}$$

and thus the last equation in system (5.125) becomes

$$\varepsilon_0 \varepsilon_\infty \mathcal{L}_\Lambda \varphi_\Sigma = -\frac{1}{\lambda^2} \varepsilon_0 \left\{ \varepsilon_\infty \Psi + \varepsilon_\Omega \varphi_{\text{mol}} \right\} \tag{5.131}$$

$$\Leftrightarrow \mathcal{L}_\Lambda \varphi_\Sigma = -\frac{1}{\lambda^2} \left\{ \Psi + \frac{\varepsilon_\Omega}{\varepsilon_\infty} \varphi_{\text{mol}} \right\} \tag{5.132}$$

which is again an inhomogeneous Yukawa–equation with source term

$$\varrho \equiv -\frac{1}{\lambda^2} \left\{ \Psi + \frac{\varepsilon_\Omega}{\varepsilon_\infty} \varphi_{\text{mol}} \right\}$$

In the same spirit that lead to the development of a boundary integral representation for the Laplace equation, we can now consider the weighted residual formulation, using the fundamental solution of the Yukawa–operator $-\mathcal{G}^Y$, (4.10), which is defined by

$$\mathcal{G}^Y(\boldsymbol{r} - \boldsymbol{\xi}) := \frac{1}{4\pi} \frac{e^{-\frac{|\boldsymbol{r}-\boldsymbol{\xi}|}{\lambda}}}{|\boldsymbol{r} - \boldsymbol{\xi}|}$$

as weighting function:

$$\int_\Sigma \mathcal{G}^Y(\boldsymbol{r} - \boldsymbol{\xi}) \left[\mathcal{L}'_\Lambda \varphi_\Sigma \right] (\boldsymbol{r}) d\boldsymbol{r} = \underbrace{\int_\Sigma \mathcal{G}^Y(\boldsymbol{r} - \boldsymbol{\xi}) \varrho(\boldsymbol{r}) d\boldsymbol{r}}_{=:-\left[\tilde{N}_0^Y \varrho \right]} \tag{5.133}$$

where we have introduced the *Newton potential* of the Yukawa–operator $\left[\tilde{N}_0^Y \varrho \right]$. In the following, we will try to derive a representation formula equivalent to that of the Laplace operator, equation (5.15), for the inhomogeneous Yukawa equation. To this end, we will expand the left hand side of equation

(5.133) by inserting the definition (4.11) of the operator $\mathcal{L}_\Lambda = \left(\Delta - \frac{1}{\Lambda^2} \right)$, which leads to

$$\int\limits_\Sigma \mathcal{G}^Y(\boldsymbol{r} - \boldsymbol{\xi}) \left[\mathcal{L}_\Lambda \varphi_\Sigma \right](\boldsymbol{r}) d\boldsymbol{r} = \int\limits_\Sigma \mathcal{G}^Y(\boldsymbol{r} - \boldsymbol{\xi}) \left(\Delta - \frac{1}{\Lambda^2} \right) \varphi_\Sigma(\boldsymbol{r}) d\boldsymbol{r} \tag{5.134}$$

$$= \int\limits_\Sigma \mathcal{G}^Y(\boldsymbol{r} - \boldsymbol{\xi}) \Delta \varphi_\Sigma(\boldsymbol{r}) d\boldsymbol{r}$$

$$- \int\limits_\Sigma \mathcal{G}^Y(\boldsymbol{r} - \boldsymbol{\xi}) \frac{1}{\Lambda^2} \varphi_\Sigma(\boldsymbol{r}) d\boldsymbol{r} \tag{5.135}$$

$$= \int\limits_\Sigma \mathcal{G}^Y(\boldsymbol{r} - \boldsymbol{\xi}) \Delta \varphi_\Sigma(\boldsymbol{r}) d\boldsymbol{r}$$

$$- \int\limits_\Sigma \frac{1}{\Lambda^2} \mathcal{G}^Y(\boldsymbol{r} - \boldsymbol{\xi}) \varphi_\Sigma(\boldsymbol{r}) d\boldsymbol{r} \tag{5.136}$$

As in the derivation for the representation formula of the Laplace operator in Section 5.2, we will now try to shift the Yukawa–operator from the unknown potential to the known fundamental solution $\mathcal{G}^Y(\boldsymbol{r}-\boldsymbol{\xi})$, since this will introduce a Dirac δ–distribution, which in turn reduces the volume integration to the evaluation at a single point. In the case of the Laplace equation, the key for this was the use of Green's second integral theorem, which allows to shift the Laplace operator via partial integration, and since the striking similarity of the Yukawa– and the Laplace–operator, a similar approach can be expected to turn out useful. And in fact, the decomposition (5.136) of the weighted residual shows that we only need to shift the Laplacian to shift the whole Yukawa operator. But before we can apply Green's second theorem, equation (5.9), we need to be aware of a certain pitfall: in equation (5.136), we are considering an *exterior problem*, i.e. a problem defined in the semi–infinite domain Σ with boundary Γ. But our notation is more adapted to the *interior problem* inside Ω, and in particular, what we denote by $\hat{\boldsymbol{n}}(\boldsymbol{\xi})$ are the *outward–pointing* normals on Γ *as seen from Ω*. Since application of Green's second theorem for the domain Σ requires the usage of normal vectors pointing "from Σ to Ω", i.e. *inwards* in our previous definitions, the boundary integrals will have to be multiplied by -1. Thus, in our notation, Green's second theorem yields

$$\int\limits_\Omega (\varphi \Delta \psi - \psi \Delta \varphi) \, d\boldsymbol{r} = \oint\limits_\Gamma \left[\left(\gamma_0^{\text{int}} \varphi \right) \left(\gamma_1^{\text{int}} \psi \right) - \left(\gamma_0^{\text{int}} \psi \right) \left(\gamma_1^{\text{int}} \varphi \right) \right] d\Gamma \tag{5.137}$$

$$\int\limits_\Sigma (\varphi \Delta \psi - \psi \Delta \varphi) \, d\boldsymbol{r} = - \oint\limits_\Gamma \left[\left(\gamma_0^{\text{ext}} \varphi \right) \left(\gamma_1^{\text{ext}} \psi \right) + \left(\gamma_0^{\text{ext}} \psi \right) \left(\gamma_1^{\text{ext}} \varphi \right) \right] d\Gamma \tag{5.138}$$

if we use the same definition of the normal $\hat{\boldsymbol{n}}(\boldsymbol{\xi})$ for both interior and exterior Neumann traces $\gamma_1^{\text{int}}, \gamma_1^{\text{ext}}$. We can thus simplify the first integral in equation (5.136)

$$\int\limits_\Sigma \underbrace{\mathcal{G}^Y(\boldsymbol{r} - \boldsymbol{\xi})}_{\sim \varphi} \underbrace{\Delta \varphi_\Sigma(\boldsymbol{r})}_{\sim \Delta \psi} \, d\boldsymbol{r}$$

– where we have indicated by $\sim$ the role of the corresponding term in Green's integral theorem – by applying equation (5.138), to yield

$$
\begin{aligned}
\int_{\Sigma} \mathcal{G}^Y(\boldsymbol{r} - \boldsymbol{\xi}) \Delta \varphi_{\Sigma}(\boldsymbol{r}) d\boldsymbol{r} = \ & \int_{\Sigma} \left\{ \Delta \mathcal{G}^Y(\boldsymbol{r} - \boldsymbol{\xi}) \right\} \varphi_{\Sigma}(\boldsymbol{r}) d\boldsymbol{r} \\
& - \oint_{\Gamma} \left(\gamma_{0,r}^{\text{ext}} \mathcal{G}^Y \right) \left(\gamma_{1,r}^{\text{ext}} \varphi_{\Sigma} \right) d\Gamma_r \\
& + \oint_{\Gamma} \left(\gamma_{0,r}^{\text{ext}} \varphi_{\Sigma} \right) \left(\gamma_{1,r}^{\text{ext}} \mathcal{G}^Y \right) d\Gamma_r
\end{aligned}
\tag{5.139}
$$

If we now generalize the definitions of the boundary integral operators from Section 5.2.1 to the Yukawa–operator[10]

$$
\left[\tilde{V}^Y \left(\gamma_1^{\text{ext}} \varphi_{\Sigma} \right) \right] := \oint_{\Gamma} \left(\gamma_{0,r}^{\text{ext}} \mathcal{G}^Y \right) \left(\gamma_{1,r}^{\text{ext}} \varphi_{\Sigma} \right) d\Gamma_r
\tag{5.140}
$$

$$
\left[\tilde{W}^Y \left(\gamma_0^{\text{ext}} \varphi_{\Sigma} \right) \right] := \oint_{\Gamma} \left(\gamma_{0,r}^{\text{ext}} \varphi_{\Sigma} \right) \left(\gamma_{1,r}^{\text{ext}} \mathcal{G}^Y \right) d\Gamma_r
\tag{5.141}
$$

equation (5.136) can be rewritten with the help of equation (5.139) as

$$
\begin{aligned}
\int_{\Sigma} \mathcal{G}^Y(\boldsymbol{r} - \boldsymbol{\xi}) \left[\mathcal{L}_{\Lambda} \varphi_{\Sigma} \right](\boldsymbol{r}) d\boldsymbol{r} = \ & \int_{\Sigma} \mathcal{G}^Y(\boldsymbol{r} - \boldsymbol{\xi}) \Delta \varphi_{\Sigma}(\boldsymbol{r}) d\boldsymbol{r} - \int_{\Sigma} \frac{1}{\Lambda^2} \mathcal{G}^Y(\boldsymbol{r} - \boldsymbol{\xi}) \varphi_{\Sigma}(\boldsymbol{r}) d\boldsymbol{r} \\
= \ & \int_{\Sigma} \left\{ \left(\Delta - \frac{1}{\Lambda^2} \right) \mathcal{G}^Y(\boldsymbol{r} - \boldsymbol{\xi}) \right\} \varphi_{\Sigma}(\boldsymbol{r}) d\boldsymbol{r} \\
& - \left[\tilde{V}^Y \left(\gamma_1^{\text{ext}} \varphi_{\Sigma} \right) \right] + \left[\tilde{W}^Y \left(\gamma_0^{\text{ext}} \varphi_{\Sigma} \right) \right]
\end{aligned}
\tag{5.142}
$$

The differential operator in the first integral on the right hand side of this equation is again the Yukawa–operator $\mathcal{L}_{\Lambda}$, and since $\mathcal{G}^Y(\boldsymbol{r} - \boldsymbol{\xi})$ is the negative of its fundamental solution, we obtain

$$
\int_{\Sigma} \varphi_{\Sigma}(\boldsymbol{r}) \underbrace{\underbrace{\left(\Delta - \frac{1}{\Lambda^2} \right)}_{\mathcal{L}_{\Lambda}} \mathcal{G}^Y(\boldsymbol{r} - \boldsymbol{\xi})}_{-\delta(\boldsymbol{r} - \boldsymbol{\xi})} d\boldsymbol{r} = -\varphi_{\Sigma}(\boldsymbol{\xi})
\tag{5.143}
$$

and we can combine equations (5.133), (5.142) and (5.143) to yield the desired representation formula for the solution of the inhomogeneous Yukawa–equation

$$
\boxed{ \varphi_{\Sigma}(\boldsymbol{\xi}) = - \left[\tilde{V}^Y \left(\gamma_1^{\text{ext}} \varphi_{\Sigma} \right) \right] + \left[\tilde{W}^Y \left(\gamma_0^{\text{ext}} \varphi_{\Sigma} \right) \right] + \left[\tilde{N}_0^Y \varrho \right] }
\tag{5.144}
$$

5.4.1. A dual reciprocity method for the Newton potential of the inhomogeneous Yukawa equation

There is an important difference between this representation formula for the Yukawa–equation and the earlier one for the Laplace equation, namely the appearance of a Newton–potential term. This

---

[10] The apparently differing choice of sign stems from the fact that $\mathcal{G}^Y(\boldsymbol{r} - \boldsymbol{\xi})$ is not the fundamental solution itself, but rather the fundamental solution multiplied by -1.

seems to imply that a computation of the nonlocal electrostatic potential at some point in space would require the evaluation of a volume integral, contrary in spirit to the boundary integral approach we wanted to take. Fortunately, the evaluation of this domain integral can be again avoided by using a so–called *dual reciprocity approach*. In our case, this comes down to interpreting the fundamental solution $\mathcal{G}^Y$ as the Laplacian of another function $\tilde{\mathcal{G}}$:

$$\mathcal{G}^Y = \Delta\tilde{\mathcal{G}} \tag{5.145}$$

Equation (5.145) provides us with a Poisson equation for the determination of the unknown function $\tilde{\mathcal{G}}$. But instead of solving this equation directly, we can easily find the solution by applying the Yukawa differential operator:

$$\mathcal{L}_\Lambda \Delta\tilde{\mathcal{G}} = -\delta \tag{5.146}$$

$$\Leftrightarrow \left(\Delta - \frac{1}{\Lambda^2}\right)\Delta\tilde{\mathcal{G}} = -\delta \tag{5.147}$$

$$\Leftrightarrow \left(\Delta^2 - \frac{1}{\Lambda^2}\Delta\right)\tilde{\mathcal{G}} = -\delta \tag{5.148}$$

$$\Leftrightarrow \Delta\left(\Delta - \frac{1}{\Lambda^2}\right)\tilde{\mathcal{G}} = -\delta \tag{5.149}$$

Equation (5.149) tells us that the quantity in parentheses is the negative of the fundamental solution of the Laplacian, and thus we can conclude

$$\rightsquigarrow \left(\Delta - \frac{1}{\Lambda^2}\right)\tilde{\mathcal{G}} = \frac{1}{4\pi}\frac{1}{|\boldsymbol{r} - \boldsymbol{r}'|} \tag{5.150}$$

$$\Leftrightarrow \quad \Delta\tilde{\mathcal{G}} - \frac{1}{\Lambda^2}\tilde{\mathcal{G}} = \frac{1}{4\pi}\frac{1}{|\boldsymbol{r} - \boldsymbol{r}'|} \tag{5.151}$$

$$\Leftrightarrow \quad \mathcal{G}^Y - \frac{1}{\Lambda^2}\tilde{\mathcal{G}} = \frac{1}{4\pi}\frac{1}{|\boldsymbol{r} - \boldsymbol{r}'|} \tag{5.152}$$

$$\Rightarrow \quad \tilde{\mathcal{G}} = \Lambda^2\left(\mathcal{G}^Y - \frac{1}{4\pi}\frac{1}{|\boldsymbol{r} - \boldsymbol{r}'|}\right) \tag{5.153}$$

$$= \frac{\Lambda^2}{4\pi}\left(\frac{e^{-\frac{|\boldsymbol{r} - \boldsymbol{r}'|}{\lambda}} - 1}{|\boldsymbol{r} - \boldsymbol{r}'|}\right) \tag{5.154}$$

which leads us to the following representation of $\mathcal{G}^Y$:

$$\boxed{\mathcal{G}^Y = \Delta\tilde{\mathcal{G}} = \Lambda^2\Delta\left(\mathcal{G}^Y - \mathcal{G}^L\right)} \tag{5.155}$$

where $-\mathcal{G}^Y$ is the fundamental solution of the Yukawa operator and $-\mathcal{G}^L$ is the fundamental solution of the Laplacian. With this decomposition we have succeeded in writing the Yukawa fundamental solution as the Laplacian of another function, and thus we can use our previous results on the reduction of domain integrals over Laplace operators to boundary integrals to replace the Newton potential of the Yukawa operator by a boundary representation:

$$\left[N_0^Y \varrho\right] = -\int_\Sigma \mathcal{G}^Y \varrho\, d\boldsymbol{r} = -\Lambda^2\int_\Sigma \Delta\left(\mathcal{G}^Y - \mathcal{G}^L\right)\varrho\, d\boldsymbol{r} \tag{5.156}$$

At this point, we can again apply the external version of Green's second integral theorem, equation (5.138), to yield

$$
-\Lambda^2 \int_\Sigma \Delta\big(\mathcal{G}^Y - \mathcal{G}^L\big)\, \varrho\, d\boldsymbol{r} = -\Lambda^2 \Bigg(\int_\Sigma (\Delta\varrho)\big(\mathcal{G}^Y - \mathcal{G}^L\big)\, d\boldsymbol{r}
$$

$$
- \oint_\Gamma \big(\gamma_0^{\text{ext}}\varrho\big)\big(\gamma_1^{\text{ext}}\big(\mathcal{G}^Y - \mathcal{G}^L\big)\big)\, d\Gamma
$$

$$
+ \oint_\Gamma \big(\gamma_0^{\text{ext}}\big(\mathcal{G}^Y - \mathcal{G}^L\big)\big)\big(\gamma_1^{\text{ext}}\varrho\big)\, d\Gamma \Bigg) \tag{5.157}
$$

$$
= -\Lambda^2 \Bigg(-\frac{1}{\lambda^2}\int_\Sigma \underbrace{\Delta\left(\Psi + \frac{\varepsilon_\Omega}{\varepsilon_\infty}\varphi_{\text{mol}}\right)}_{=0 \text{ in } \Sigma}\big(\mathcal{G}^Y - \mathcal{G}^L\big)\, d\boldsymbol{r}
$$

$$
+ \frac{1}{\lambda^2}\oint_\Gamma \gamma_0^{\text{ext}}\left(\Psi + \frac{\varepsilon_\Omega}{\varepsilon_\infty}\varphi_{\text{mol}}\right)\gamma_1^{\text{ext}}\big(\mathcal{G}^Y - \mathcal{G}^L\big)\, d\Gamma
$$

$$
- \frac{1}{\lambda^2}\oint_\Gamma \gamma_0^{\text{ext}}\big(\mathcal{G}^Y - \mathcal{G}^L\big)\gamma_1^{\text{ext}}\left(\Psi + \frac{\varepsilon_\Omega}{\varepsilon_\infty}\varphi_{\text{mol}}\right)\, d\Gamma \Bigg) \tag{5.158}
$$

$$
= -\frac{\Lambda^2}{\lambda^2}\left[\big(W^Y - W\big)\left[\gamma_0^{\text{ext}}\left(\Psi + \frac{\varepsilon_\Omega}{\varepsilon_\infty}\varphi_{\text{mol}}\right)\right]\right]
$$

$$
+ \frac{\Lambda^2}{\lambda^2}\left[\big(\tilde{V}^Y - \tilde{V}\big)\left[\gamma_1^{\text{ext}}\left(\Psi + \frac{\varepsilon_\Omega}{\varepsilon_\infty}\varphi_{\text{mol}}\right)\right]\right] \tag{5.159}
$$

Inserting this representation of the Newton potential of the Yukawa operator into equation (5.144), we finally arrive at a *purely boundary integral representation formula* for the inhomogeneous Yukawa equation and thus for the nonlocal cavity model of electrostatics :

$$
\varphi_\Sigma(\boldsymbol{\xi}) = -\tilde{V}^Y\big[\gamma_1^{\text{ext}}\varphi_\Sigma\big] + W^Y\big[\gamma_0^{\text{ext}}\varphi_\Sigma\big]
$$

$$
+ \frac{\varepsilon_\infty}{\varepsilon_\Sigma}\Bigg\{ \big(\tilde{V}^Y - \tilde{V}\big)\left[\gamma_1^{\text{ext}}\left(\Psi + \frac{\varepsilon_\Omega}{\varepsilon_\infty}\varphi_{\text{mol}}\right)\right]
$$

$$
- \big(W^Y - W\big)\left[\gamma_0^{\text{ext}}\left(\Psi + \frac{\varepsilon_\Omega}{\varepsilon_\infty}\varphi_{\text{mol}}\right)\right]\Bigg\} \tag{5.160}
$$

Just as in our derivation of a boundary element method for the *local* cavity model, we will now have to compute the Dirichlet trace γ_0^{ext} of φ_Σ in order to derive a boundary integral equation for this quantity, which we will then couple to the remaining quantities of interest. This again requires an investigation of the properties of the traces of the boundary integral operators appearing in equation (5.160), like we did for their Laplacian counterparts in Section 5.2.1. Fortunately it turns out that the results obtained there readily generalize to the case of the Yukawa operator: the only difference in the definition of the single and double layer potential operators appearing in (5.160) and those of the Laplace operator is the replacement of the fundamental solution of the Laplacian operator by that of the Yukawa operator. Comparing the two functions

$$
\mathcal{G}^L(\boldsymbol{r} - \boldsymbol{\xi}) = -\frac{1}{4\pi}\frac{1}{|\boldsymbol{r} - \boldsymbol{\xi}|} \tag{5.161}
$$

$$
\mathcal{G}^Y(\boldsymbol{r} - \boldsymbol{\xi}) = \frac{1}{4\pi}\frac{e^{-\frac{|\boldsymbol{r} - \boldsymbol{\xi}|}{\lambda}}}{|\boldsymbol{r} - \boldsymbol{\xi}|} \tag{5.162}
$$

we find that they are not only remarkably similar, but more importantly have identical singularities for $r \to \xi$. And since our considerations in Section 5.2.1 were concerned with the singularities of the different operators, we can directly apply the results found there. We can thus conclude from theorem 5.2.3, that

$$[V^Y f](\xi) := \left[\left(\gamma_{0,\xi}^{\text{ext}} \tilde{V}^Y\right)f\right](\xi) = -\oint_\Gamma \mathcal{G}^Y(r - \xi) f(r) \, d\Gamma_r \tag{5.163}$$

and from theorem 5.2.5 we have

$$\left[\left(\gamma_{0,\xi}^{\text{ext}} W^Y\right)f\right](\xi) = \sigma(\xi) f(\xi) + \left[K^Y f\right](\xi) \tag{5.164}$$

with the geometrical quantity $\sigma(\xi)$ which we already encountered in Section 5.2.1

$$\sigma(\xi) := \lim_{\epsilon \to 0} \frac{1}{4\pi} \frac{1}{\epsilon^2} \int_{r \in \Omega : |r - \xi| = \epsilon} d\Gamma_r \tag{5.165}$$

and with the boundary integral operator K^Y defined by

$$\left[K^Y f\right](\xi) = -\oint_\Gamma \left(\gamma_{0,\xi}^{\text{ext}} \gamma_{1,r}^{\text{int}} \mathcal{G}^Y(r - \xi)\right) f(r) \, d\Gamma_r \tag{5.166}$$

This enables us to apply the Dirichlet trace γ_0^{ext} to the representation formula (5.160):

$$
\begin{aligned}
\gamma_0^{\text{ext}} \varphi_\Sigma(\xi) = -\,\gamma_0^{\text{ext}} \Bigg(& \tilde{V}^Y \left[\gamma_1^{\text{ext}} \varphi_\Sigma\right] + W^Y \left[\gamma_0^{\text{ext}} \varphi_\Sigma\right] \\
& + \frac{\varepsilon_\infty}{\varepsilon_\Sigma} \bigg\{ \left(\tilde{V}^Y - \tilde{V}\right) \left[\gamma_1^{\text{ext}} \left(\Psi + \frac{\varepsilon_\Omega}{\varepsilon_\infty} \varphi_{\text{mol}}\right)\right] \\
& \qquad - \left(W^Y - W\right) \left[\gamma_0^{\text{ext}} \left(\Psi + \frac{\varepsilon_\Omega}{\varepsilon_\infty} \varphi_{\text{mol}}\right)\right] \bigg\} \Bigg)
\end{aligned}
\tag{5.167}
$$

$$
\begin{aligned}
= & -V^Y \left[\gamma_1^{\text{ext}} \varphi_\Sigma\right](\xi) + \sigma(\xi) \left(\gamma_0^{\text{ext}} \varphi_\Sigma\right)(\xi) \\
& + K^Y \left[\left(\gamma_0^{\text{ext}} \varphi_\Sigma\right)\right](\xi) + \frac{\varepsilon_\infty}{\varepsilon_\Sigma} \bigg\{ \left(V^Y - V\right) \left[\gamma_1^{\text{ext}} \left(\Psi + \frac{\varepsilon_\Omega}{\varepsilon_\infty} \varphi_{\text{mol}}\right)\right] \\
& - \underbrace{\left(\sigma(\xi) - \sigma(\xi)\right)}_{=0} \left[\gamma_0^{\text{ext}} \left(\Psi + \frac{\varepsilon_\Omega}{\varepsilon_\infty} \varphi_{\text{mol}}\right)\right] \\
& - \left(K^Y - K\right) \left[\gamma_0^{\text{ext}} \left(\Psi + \frac{\varepsilon_\Omega}{\varepsilon_\infty} \varphi_{\text{mol}}\right)\right] \bigg\} \Bigg)
\end{aligned}
\tag{5.168}
$$

$$
\begin{aligned}
\Leftrightarrow [1 - \sigma(\xi)] \left(\gamma_0^{\text{ext}} \varphi_\Sigma\right)(\xi) = & -V^Y \left[\gamma_1^{\text{ext}} \varphi_\Sigma\right](\xi) \\
& + K^Y \left[\gamma_0^{\text{ext}} \varphi_\Sigma\right](\xi) \\
& + \left(V^Y - V\right) \left[\gamma_1^{\text{ext}} \left(\frac{\varepsilon_\infty}{\varepsilon_\Sigma} \Psi + \frac{\varepsilon_\Omega}{\varepsilon_\Sigma} \varphi_{\text{mol}}\right)\right] \\
& - \left(K^Y - K\right) \left[\gamma_0^{\text{ext}} \left(\frac{\varepsilon_\infty}{\varepsilon_\Sigma} \Psi + \frac{\varepsilon_\Omega}{\varepsilon_\Sigma} \varphi_{\text{mol}}\right)\right]
\end{aligned}
\tag{5.169}
$$

Equation (5.169) is the boundary integral equation we need to set up a boundary element solver for the nonlocal cavity model of electrostatics. But to this end, we need to couple it to the remaining quantities of interest. These are the fields φ^* inside Ω and Ψ and ψ_Σ inside Σ. As we have seen at the

beginning of this section, those quantities are harmonic, and thus are subject to the boundary integral equations

$$\sigma(\boldsymbol{\xi})\left(\gamma_0^{\mathsf{int}}\varphi^*\right)(\boldsymbol{\xi}) = V\left[\gamma_1^{\mathsf{int}}\varphi^*\right](\boldsymbol{\xi}) - K\left[\gamma_0^{\mathsf{int}}\varphi^*\right](\boldsymbol{\xi}) \tag{5.170}$$

$$(1-\sigma(\boldsymbol{\xi}))\left(\gamma_0^{\mathsf{ext}}\Psi\right)(\boldsymbol{\xi}) = -V\left[\gamma_1^{\mathsf{ext}}\Psi\right](\boldsymbol{\xi}) + K\left[\gamma_0^{\mathsf{ext}}\Psi\right](\boldsymbol{\xi}) \tag{5.171}$$

$$(1-\sigma(\boldsymbol{\xi}))\left(\gamma_0^{\mathsf{ext}}\psi_\Sigma\right)(\boldsymbol{\xi}) = -V\left[\gamma_1^{\mathsf{ext}}\psi_\Sigma\right](\boldsymbol{\xi}) + K\left[\gamma_0^{\mathsf{ext}}\psi_\Sigma\right](\boldsymbol{\xi}) \tag{5.172}$$

To set up a system of boundary integral equations, i.e. to prescribe a coupling between the aforementioned fields, we will now need to take a closer look at the boundary conditions. From the original system (5.125), we have

$$\left.\begin{aligned} \varphi^* + \varphi_{\mathsf{mol}} &= \varphi_\Sigma \\ \varepsilon_0\varepsilon_\Omega\partial_n\left(\varphi^* + \varphi_{\mathsf{mol}}\right) &= \partial_n\psi_\Sigma \\ \Leftrightarrow \varepsilon_0\varepsilon_\Omega\partial_n\left(\varphi^* + \varphi_{\mathsf{mol}}\right) &= \partial_n\left(\varepsilon_0\left(\varepsilon_\Omega\varphi_{\mathsf{mol}} + \varepsilon_\infty\Psi\right)\right) \\ \Rightarrow \varepsilon_\Omega\partial_n\varphi^* &= \partial_n\varepsilon_\infty\Psi \end{aligned}\right\} \text{ on } \Gamma \tag{5.173}$$

Or, in the trace operator notation

$$\gamma_0^{\mathsf{int}}\left(\varphi^* + \varphi_{\mathsf{mol}}\right) = \gamma_0^{\mathsf{ext}}\varphi_\Sigma \tag{5.174}$$

$$\varepsilon_0\varepsilon_\Omega\gamma_1^{\mathsf{int}}\left(\varphi^* + \varphi_{\mathsf{mol}}\right) = \gamma_1^{\mathsf{ext}}\psi_\Sigma \tag{5.175}$$

$$\varepsilon_\Omega\gamma_1^{\mathsf{int}}\varphi^* = \varepsilon_\infty\gamma_1^{\mathsf{int}}\Psi \tag{5.176}$$

In order to close our system of boundary integral equations in the former formulation, we need an equation coupling the fields ψ_Σ or Ψ to the field φ_Σ, and such an equation is not yet contained in the conditions above. Several possibilities to remedy this problem can be imagined, approximate and exact ones, from which we chose a particularly promising *approximate* one. This approximate closure will lead to a slightly different model, which will no longer feature the infinitely sharp protein/water interface assumed earlier, but rather assume a continuous onset of the dielectric effect. The difference in the predicted potentials of both models should be relatively minor[11], but in fact it might be argued that the approximate representation is an additional feature, and not a shortcoming: as we will discuss in Section 6.1, the very concept of a sharp molecular interface is in a way an unphysical idealization.

The idea of the aforementioned approximation is as follows: if we consider the behavior of the electrostatic potential at the molecular boundary, the cavity model predicts a discontinuous jump in the dielectric response. The (nonlocal) dielectric effect of the water is considered to "start" completely as soon as the boundary is crossed. To us, this seems unrealistic, since in reality, not a single water molecule is located directly at the boundary. From a physical point of view, it seems to be more sensible to assume that the nonlocal response is smoothly "switched on" in a small but finite slab around the surface of the original molecule. But this means that the discontinuous onset contained in the "exact" boundary conditions might be overestimating the effect slightly. We thus propose to assume that the electrostatic potential in the water, φ_Σ, "starts" like a vacuum potential, which means that there is no coupling of the normal derivative of the nonlocal effect to the inside of the molecule – an assumption that makes sense in itself, since we do not expect correlations between water molecules and the internals of the protein to play an important role for the dielectric behavior of the system as a whole.[12] This can be achieved by remembering that in the boundary condition

$$\varepsilon_0\varepsilon_\Omega\gamma_1^{\mathsf{int}}\left(\varphi^* + \varphi_{\mathsf{mol}}\right) = \gamma_1^{\mathsf{ext}}\psi_\Sigma \tag{5.177}$$

---

11 This can e.g. be shown for the spherically symmetric systems. A detailed investigation of the implications of the described approximation will be made in the future by implementing a (costly) *exact* representation of the original model as a reference system.

12 Please note that this does **not** imply that there are no hydrogen bonds between water molecules and the protein – these bonds are in fact very common. But with this water molecules at the molecular boundary, the correlation "stops" – it does not penetrate deeper into the protein.

we can replace the Neumann trace $\gamma_1^{\text{ext}}\psi_\Sigma$ by the normal component of the nonlocal displacement field[13] $\boldsymbol{D}(\boldsymbol{r})$, since

$$\boldsymbol{D}_\Sigma(\boldsymbol{r}) = -\boldsymbol{\nabla}\psi_\Sigma(\boldsymbol{r}) + \boldsymbol{\nabla}\times\xi(\boldsymbol{r}) \tag{5.178}$$

where $\boldsymbol{\nabla}\times\xi(\boldsymbol{r})$ is obviously divergence free and thus has smooth normal component along the boundary, which has to vanish since $\xi(\boldsymbol{r})$ vanishes inside Ω (c.f. Section 4.1). Inserting the definition of $\boldsymbol{D}_\Sigma(\boldsymbol{r})$

$$\boldsymbol{D}_\Sigma(\boldsymbol{r}) = -\varepsilon_0\varepsilon_\infty\boldsymbol{\nabla}\varphi_\Sigma(\boldsymbol{r}) + \varepsilon_0\tilde{\varepsilon}\int\limits_\Sigma d\boldsymbol{r}'\,\mathcal{G}(\boldsymbol{r}-\boldsymbol{r}')\boldsymbol{\nabla}_{\boldsymbol{r}'}\varphi_\Sigma(\boldsymbol{r}') \tag{5.179}$$

and taking the normal component yields

$$\boldsymbol{D}_\Sigma(\boldsymbol{r})\cdot\hat{\boldsymbol{n}} = -\varepsilon_0\varepsilon_\infty\gamma_{1,r}^{\text{ext}}\varphi_\Sigma(\boldsymbol{r}) + \varepsilon_0\tilde{\varepsilon}\int\limits_\Sigma d\boldsymbol{r}'\,\mathcal{G}(\boldsymbol{r}-\boldsymbol{r}')\gamma_{1,r'}^{\text{ext}}\varphi_\Sigma(\boldsymbol{r}') \tag{5.180}$$

The approximate boundary condition we motivated above can now be achieved by neglecting the nonlocal integral operator in equation (5.180), and thus setting

$$\boldsymbol{D}_\Sigma(\boldsymbol{r})\cdot\hat{\boldsymbol{n}} = -\varepsilon_0\varepsilon_\infty\gamma_{1,r}^{\text{ext}}\varphi_\Sigma(\boldsymbol{r}) \tag{5.181}$$

Therefore, in our approximate implementation of the boundary conditions, we will replace all occurrences of $\gamma_1^{\text{ext}}\psi_\Sigma$ or the equivalent quantity $\varepsilon_\Omega\gamma_1^{\text{ext}}\varphi_{\text{mol}}+\varepsilon_\infty\gamma_1^{\text{ext}}\Psi$ by the "vacuum field" $\varepsilon_0\varepsilon_\infty\gamma_1^{\text{ext}}\varphi_\Sigma$.

At this point, we want to stress that even though we think that our approximate choice of the boundary conditions is physically sound and motivated, and in addition should only lead to a slight approximation of the analytical results, it is absolutely possible to choose a different approach. Other approximations, or even exact implementations, are possible and will be investigated in our future research. In order to set up the system of boundary equations, we will now apply the boundary conditions mentioned above to the boundary integral equations (5.169) − (5.172)

$$\left(1 - \sigma - K^Y\right)\left(\gamma_0^{\text{ext}}\varphi_\Sigma\right) = -V^Y\left[\gamma_1^{\text{ext}}\varphi_\Sigma\right]$$
$$+ \left(V^Y - V\right)\left[\frac{1}{\varepsilon_0\varepsilon_\Sigma}\gamma_1^{\text{ext}}\psi_\Sigma\right]$$
$$- \left(K^Y - K\right)\left[\frac{1}{\varepsilon_0\varepsilon_\Sigma}\gamma_0^{\text{ext}}\psi_\Sigma\right] \tag{5.182}$$
$$\sigma\left(\gamma_0^{\text{int}}\varphi^*\right) = \quad V\left[\gamma_1^{\text{int}}\varphi^*\right] - K\left[\gamma_0^{\text{int}}\varphi^*\right] \tag{5.183}$$
$$\left(1 - \sigma\right)\left(\gamma_0^{\text{ext}}\psi_\Sigma\right) = -V\left[\gamma_1^{\text{ext}}\psi_\Sigma\right] + K\left[\gamma_0^{\text{ext}}\psi_\Sigma\right] \tag{5.184}$$
$$\left(1 - \sigma\right)\left(\gamma_0^{\text{ext}}\Psi\right) = -V\left[\gamma_1^{\text{ext}}\Psi\right] + K\left[\gamma_0^{\text{ext}}\Psi\right] \tag{5.185}$$

Since the last two equations in this system are more or less equivalent − the quantities Ψ and ψ_Σ only differ by a prefactor and the assumedly known quantity φ_{mol} − we will only need one of them in the final system. For reasons of simplicity, we start by setting up the system containing the quantity ψ_Σ, which we will later switch to a system including Ψ. If we replace the function $\gamma_1^{\text{ext}}\varphi_\Sigma$ in accordance with the first boundary condition in (5.174) by the sum $\gamma_0^{\text{int}}\left(\varphi^* + \varphi_{\text{mol}}\right)$, and the function $\frac{1}{\varepsilon_0\varepsilon_\Sigma}\gamma_1^{\text{ext}}\psi_\Sigma$

---

13 In fact, in our derivation of the boundary conditions, we started working with the displacement field and only later replaced it by the Neumann trace of the rotation free part of its potential.

according to the second boundary condition (5.175) by the quantity $\frac{\varepsilon_\Omega}{\varepsilon_\Sigma}\gamma_1^{\text{int}}(\varphi^* + \varphi_{\text{mol}})$, we arrive at

$$
\begin{aligned}
\left(1 - \sigma - K^Y\right)\left(\gamma_0^{\text{int}}\varphi^*\right) & \\
+ V^Y\left[\gamma_1^{\text{ext}}\varphi_\Sigma\right] & \\
- \frac{\varepsilon_\Omega}{\varepsilon_\Sigma}\left(V^Y - V\right)\left[\gamma_1^{\text{int}}\varphi^*\right] & \\
+ \frac{1}{\varepsilon_0\varepsilon_\Sigma}\left(K^Y - K\right)\left[\gamma_0^{\text{ext}}\psi_\Sigma\right] = & -\left(1 - \sigma - K^Y\right)\left[\gamma_0^{\text{int}}\varphi_{\text{mol}}\right] \\
& + \frac{\varepsilon_\Omega}{\varepsilon_\Sigma}\left(V^Y - V\right)\left[\gamma_1^{\text{int}}\varphi_{\text{mol}}\right]
\end{aligned}
\tag{5.186}
$$

$$
\sigma\left(\gamma_0^{\text{int}}\varphi^*\right) - V\left[\gamma_1^{\text{int}}\varphi^*\right] + K\left[\gamma_0^{\text{int}}\varphi^*\right] = 0
\tag{5.187}
$$

$$
\left(1 - \sigma\right)\left(\gamma_0^{\text{ext}}\psi_\Sigma\right) + \varepsilon_0\varepsilon_\Omega V\left[\gamma_1^{\text{int}}\varphi^*\right] - K\left[\gamma_0^{\text{ext}}\psi_\Sigma\right] = -\varepsilon_0\varepsilon_\Omega V\left[\gamma_1^{\text{int}}\varphi_{\text{mol}}\right]
\tag{5.188}
$$

This system can be written in a more condensed form by introducing the matrix

$$
\underline{\underline{\mathbf{M}}}_0 := \begin{pmatrix} 1 - \sigma - K^Y & -\frac{\varepsilon_\Omega}{\varepsilon_\Sigma}\left(V^Y - V\right) & V^Y & \frac{1}{\varepsilon_0\varepsilon_\Sigma}\left(K^Y - K\right) \\ \sigma + K & -V & 0 & 0 \\ 0 & \varepsilon_0\varepsilon_\Omega V & 0 & 1 - \sigma - K \end{pmatrix}
\tag{5.189}
$$

such that system (5.186) can be written as

$$
\underline{\underline{\mathbf{M}}}_0 \begin{pmatrix} \gamma_0^{\text{int}}\varphi^* \\ \gamma_1^{\text{int}}\varphi^* \\ \gamma_1^{\text{ext}}\varphi_\Sigma \\ \gamma_0^{\text{ext}}\psi_\Sigma \end{pmatrix} = \begin{pmatrix} -\left(1 - \sigma - K^Y\right)\left[\gamma_0^{\text{int}}\varphi_{\text{mol}}\right] + \frac{\varepsilon_\Omega}{\varepsilon_\Sigma}\left(V^Y - V\right)\left[\gamma_1^{\text{int}}\varphi_{\text{mol}}\right] \\ 0 \\ -\varepsilon_0\varepsilon_\Omega V\left[\gamma_1^{\text{int}}\varphi_{\text{mol}}\right] \end{pmatrix}
\tag{5.190}
$$

In order to remove the quantity $\gamma_1^{\text{ext}}\varphi_\Sigma$ from system (5.190), we can now make use of our approximate boundary condition

$$
\varepsilon_0\varepsilon_\Omega\gamma_1^{\text{int}}\left(\varphi^* + \varphi_{\text{mol}}\right) = \varepsilon_0\varepsilon_\infty\gamma_1^{\text{ext}}\varphi_\Sigma \Leftrightarrow \gamma_1^{\text{ext}}\varphi_\Sigma = \frac{\varepsilon_\Omega}{\varepsilon_\infty}\gamma_1^{\text{int}}\left(\varphi^* + \varphi_{\text{mol}}\right)
$$

The Neumann trace $\gamma_1^{\text{int}}\varphi_{\text{mol}}$ can again be brought to the inhomogeneity on the right hand side of the equation, and the remaining trace $\gamma_1^{\text{int}}\varphi^*$ is already contained in our solution vector, which means that we can eliminate the third column from the matrix $\underline{\underline{\mathbf{M}}}_0$ to yield

$$
\underline{\underline{\mathbf{M}}}_1 := \begin{pmatrix} 1 - \sigma - K^Y & \frac{\varepsilon_\Omega}{\varepsilon_\infty}V^Y - \frac{\varepsilon_\Omega}{\varepsilon_\Sigma}\left(V^Y - V\right) & \frac{1}{\varepsilon_0\varepsilon_\Sigma}\left(K^Y - K\right) \\ \sigma + K & -V & 0 \\ 0 & \varepsilon_0\varepsilon_\Omega V & 1 - \sigma - K \end{pmatrix}
\tag{5.191}
$$

and the resulting system

$$
\underline{\underline{\mathbf{M}}}_1 \begin{pmatrix} \gamma_0^{\text{int}}\varphi^* \\ \gamma_1^{\text{int}}\varphi^* \\ \gamma_0^{\text{ext}}\psi_\Sigma \end{pmatrix} = \begin{pmatrix} -\left(1 - \sigma - K^Y\right)\left[\gamma_0^{\text{int}}\varphi_{\text{mol}}\right] - \left(\frac{\varepsilon_\Omega}{\varepsilon_\infty}V^Y - \frac{\varepsilon_\Omega}{\varepsilon_\Sigma}\left(V^Y - V\right)\right)\left[\gamma_1^{\text{int}}\varphi_{\text{mol}}\right] \\ 0 \\ -\varepsilon_0\varepsilon_\Omega V\left[\gamma_1^{\text{int}}\varphi_{\text{mol}}\right] \end{pmatrix}
$$

We will now – as promised – exchange the quantity ψ_Σ occurring in this system by the quantity Ψ which is easier to handle in the numerical implementation. To this end, we first notice that due to the definition of Ψ

$$
\Psi := \frac{1}{\varepsilon_\infty}\left(\frac{1}{\varepsilon_0}\psi_\Sigma - \varepsilon_\Omega\varphi_{\text{mol}}\right)
$$

we can exchange $\gamma_0^{\text{ext}}\psi_\Sigma$ by using

$$
\gamma_0^{\text{ext}}\psi_\Sigma = \varepsilon_\infty\varepsilon_0\Psi + \varepsilon_\infty\varepsilon_\Omega\varphi_{\text{mol}}
$$

changing the $(1,3)$ component of $\underline{\underline{\mathbf{M}}}_1$ into

$$\frac{1}{\varepsilon_0 \varepsilon_\Sigma} \left(K^Y - K \right) \gamma_0^{\text{ext}} \psi_\Sigma \rightsquigarrow \frac{\varepsilon_\infty}{\varepsilon_\Sigma} \left(K^Y - K \right) \gamma_0^{\text{ext}} \Psi + \frac{\varepsilon_\Omega}{\varepsilon_\Sigma} \left(K^Y - K \right) \gamma_0^{\text{int}} \varphi_{\text{mol}}$$

Remembering that Ψ – being harmonic in Σ – fulfills the boundary integral equation (5.171)

$$(1 - \sigma(\boldsymbol{\xi})) \left(\gamma_0^{\text{ext}} \Psi \right)(\boldsymbol{\xi}) = -V \left[\gamma_1^{\text{ext}} \Psi \right](\boldsymbol{\xi}) + K \left[\gamma_0^{\text{ext}} \Psi \right](\boldsymbol{\xi})$$

we can apply the boundary condition (5.176):

$$\varepsilon_\Omega \gamma_1^{\text{int}} \varphi^* = \varepsilon_\infty \gamma_1^{\text{ext}} \Psi \Leftrightarrow \gamma_1^{\text{ext}} \Psi = \frac{\varepsilon_\Omega}{\varepsilon_\infty} \gamma_1^{\text{int}} \varphi^*$$

This yields the equation

$$(1 - \sigma(\boldsymbol{\xi})) \left(\gamma_0^{\text{ext}} \Psi \right)(\boldsymbol{\xi}) + \frac{\varepsilon_\Omega}{\varepsilon_\infty} V \left[\gamma_1^{\text{ext}} \varphi^* \right](\boldsymbol{\xi}) - K \left[\gamma_0^{\text{ext}} \Psi \right](\boldsymbol{\xi}) = 0$$

which provides us with the desired replacement for the third row of the matrix $\underline{\underline{\mathbf{M}}}_1$. Putting all of this together, we can finally set up the sought system of boundary integral equations, which with the definition of

$$\beta := - \left(1 - \sigma - K^Y - \frac{\varepsilon_\Omega}{\varepsilon_\Sigma} \left(K^Y - K \right) \right) \left[\gamma_0^{\text{int}} \varphi_{\text{mol}} \right] - \left(\frac{\varepsilon_\Omega}{\varepsilon_\infty} V^Y - \frac{\varepsilon_\Omega}{\varepsilon_\Sigma} \left(V^Y - V \right) \right) \left[\gamma_1^{\text{int}} \varphi_{\text{mol}} \right]$$

is given by

$$\begin{pmatrix} 1 - \sigma - K^Y & \frac{\varepsilon_\Omega}{\varepsilon_\infty} V^Y - \frac{\varepsilon_\Omega}{\varepsilon_\Sigma} \left(V^Y - V \right) & \frac{\varepsilon_\infty}{\varepsilon_\Sigma} \left(K^Y - K \right) \\ \sigma + K & -V & 0 \\ 0 & \frac{\varepsilon_\Omega}{\varepsilon_\infty} V & 1 - \sigma - K \end{pmatrix} \begin{pmatrix} \gamma_0^{\text{int}} \varphi^* \\ \gamma_1^{\text{int}} \varphi^* \\ \gamma_0^{\text{ext}} \Psi \end{pmatrix} = \begin{pmatrix} \beta \\ 0 \\ 0 \end{pmatrix} \quad (5.192)$$

Those derivations can be combined into the following theorem, the main result of this chapter:

Theorem 5.4.1 (Boundary element method for the nonlocal cavity model). *The cavity model of nonlocal electrostatics, using the Lorentzian dielectric function (3.23)*

$$\begin{rcases} \Delta \varphi^* = 0 & \boldsymbol{r} \in \Omega \\ \Delta \psi_\Sigma = 0 & \boldsymbol{r} \in \Sigma \\ [\varepsilon_0 \varepsilon_\Omega \partial_n \left(\varphi^* + \varphi_{mol} \right) - \partial_n \psi_\Sigma] = 0 & \boldsymbol{r} \in \Gamma \\ [\left(\varphi^* + \varphi_{mol} \right) - \varphi_\Sigma] = 0 & \boldsymbol{r} \in \Gamma \\ \varepsilon_0 \varepsilon_\infty \mathcal{L}_\Lambda \varphi_\Sigma = -\frac{1}{\lambda^2} \psi_\Sigma & \boldsymbol{r} \in \Sigma \end{rcases} \quad (5.193)$$

with the approximation (5.181), i.e. under the assumption of a continuous onset of the dielectric effect inside Σ and the prohibition of a coupling of the water–water correlations to the interior of the protein, can be solved as follows: let

$$\mathcal{G}^L(\boldsymbol{r} - \boldsymbol{\xi}) := -\frac{1}{4\pi} \frac{1}{|\boldsymbol{r} - \boldsymbol{\xi}|} \quad (5.194)$$

$$-\mathcal{G}^Y(\boldsymbol{r} - \boldsymbol{\xi}) := -\frac{1}{4\pi} \frac{e^{-\frac{|\boldsymbol{r} - \boldsymbol{\xi}|}{\lambda}}}{|\boldsymbol{r} - \boldsymbol{\xi}|} \quad (5.195)$$

denote the fundamental solutions of the Laplacian and of the Yukawa operator, let

$$\sigma(\boldsymbol{\xi}) := \lim_{\epsilon \to 0} \frac{1}{4\pi} \frac{1}{\epsilon^2} \int_{\boldsymbol{r} \in \Omega:|\boldsymbol{r}-\boldsymbol{\xi}|=\epsilon} d\Gamma_r \tag{5.196}$$

$$[Vf](\boldsymbol{\xi}) := -\oint_{\Gamma} \mathcal{G}^L(\boldsymbol{r}, \boldsymbol{\xi})\, f(\boldsymbol{r})\, d\Gamma_r \tag{5.197}$$

$$[Kf](\boldsymbol{\xi}) := -\oint_{\Gamma} \left(\gamma_{0,\xi}^{int}\gamma_{1,r}^{int}\mathcal{G}^L(\boldsymbol{r}, \boldsymbol{\xi})\right) f(\boldsymbol{r})\, d\Gamma_r \tag{5.198}$$

$$[V^Y f](\boldsymbol{\xi}) := -\oint_{\Gamma} \mathcal{G}^Y(\boldsymbol{r} - \boldsymbol{\xi})\, f(\boldsymbol{r})\, d\Gamma_{\boldsymbol{r}} \tag{5.199}$$

$$[K^Y f](\boldsymbol{\xi}) := -\oint_{\Gamma} \left(\gamma_{0,\xi}^{ext}\gamma_{1,r}^{int}\mathcal{G}^Y(\boldsymbol{r} - \boldsymbol{\xi})\right) f(\boldsymbol{r})\, d\Gamma_r \tag{5.200}$$

and let

$$\beta := -\left(1 - \sigma - K^Y - \frac{\varepsilon_\Omega}{\varepsilon_\Sigma}\left(K^Y - K\right)\right)\left[\gamma_0^{int}\varphi_{mol}\right] - \left(\frac{\varepsilon_\Omega}{\varepsilon_\infty}V^Y - \frac{\varepsilon_\Omega}{\varepsilon_\Sigma}\left(V^Y - V\right)\right)\left[\gamma_1^{int}\varphi_{mol}\right]$$

Then, the quantities φ^*, φ_Ω, ψ_Σ, Ψ, and φ_Σ can be determined in their respective domains, by first solving the system of boundary integral equations

$$\begin{pmatrix} 1 - \sigma - K^Y & \frac{\varepsilon_\Omega}{\varepsilon_\infty}V^Y - \frac{\varepsilon_\Omega}{\varepsilon_\Sigma}\left(V^Y - V\right) & \frac{\varepsilon_\infty}{\varepsilon_\Sigma}\left(K^Y - K\right) \\ \sigma + K & -V & 0 \\ 0 & \frac{\varepsilon_\Omega}{\varepsilon_\infty}V & 1 - \sigma - K \end{pmatrix} \begin{pmatrix} \gamma_0^{int}\varphi^* \\ \gamma_1^{int}\varphi^* \\ \gamma_0^{ext}\Psi \end{pmatrix} = \begin{pmatrix} \beta \\ 0 \\ 0 \end{pmatrix}$$

and then inserting the results into the representation formulae

$$\sigma(\boldsymbol{\xi})\gamma_0^{int}\varphi^*(\boldsymbol{\xi}) = \left[V\left(\gamma_1^{int}\varphi^*\right)\right] - \left[K\left(\gamma_0^{int}\varphi^*\right)\right] \tag{5.201}$$

$$\varphi_\Omega(\boldsymbol{\xi}) = \varphi^*(\boldsymbol{\xi}) + \varphi_{mol}(\boldsymbol{\xi}) \tag{5.202}$$

$$(1 - \sigma(\boldsymbol{\xi}))\,\gamma_0^{int}\psi_\Sigma(\boldsymbol{\xi}) = -\left[V\left(\gamma_1^{ext}\psi_\Sigma\right)\right] + \left[K\left(\gamma_0^{ext}\psi_\Sigma\right)\right] \tag{5.203}$$

$$(1 - \sigma(\boldsymbol{\xi}))\,\gamma_0^{int}\Psi(\boldsymbol{\xi}) = -\left[V\left(\gamma_1^{ext}\Psi\right)\right] + \left[K\left(\gamma_0^{ext}\Psi\right)\right] \tag{5.204}$$

$$\begin{aligned} \varphi_\Sigma(\boldsymbol{\xi}) = &-V^Y\left[\gamma_1^{ext}\varphi_\Sigma\right](\boldsymbol{\xi}) \\ &+ K^Y\left[\gamma_0^{ext}\varphi_\Sigma\right](\boldsymbol{\xi}) \\ &+ \left(V^Y - V\right)\left[\gamma_1^{ext}\left(\frac{\varepsilon_\infty}{\varepsilon_\Sigma}\Psi + \frac{\varepsilon_\Omega}{\varepsilon_\Sigma}\varphi_{mol}\right)\right] \\ &- \left(K^Y - K\right)\left[\gamma_0^{ext}\left(\frac{\varepsilon_\infty}{\varepsilon_\Sigma}\Psi + \frac{\varepsilon_\Omega}{\varepsilon_\Sigma}\varphi_{mol}\right)\right] \end{aligned} \tag{5.205}$$

In particular, we can make use of theorem 5.4.1 to compute the electrostatic contribution to the free energy of solvation in the nonlocal cavity model using the Lorentzian dielectric function as follows:

Theorem 5.4.2 (Computation of the electrostatic contribution to the free energy of solvation). *The electrostatic contribution to the free energy of solvation in the nonlocal cavity model using the Lorentzian model for the nonlocal dielectric function can be computed – assuming the same approximation as in theorem 5.4.1 – as follows: first, compute the quantity φ^*_{water} in the nonlocal model as described in theorem 5.4.1. Then, compute the nonlocal reaction field energy via (c.f. Section 2.4)*

$$W^*_{water} = \frac{1}{2}\int \rho(\boldsymbol{r})\varphi^*_{water}(\boldsymbol{r})\, d\boldsymbol{r} \tag{5.206}$$

Finally, compute the reaction field φ^*_{vacuum} by using the boundary element method for the local cavity model described in Section 5.3, and from this determine the vacuum reaction field energy via

$$W^*_{vacuum} = \frac{1}{2} \int \rho(\boldsymbol{r}) \varphi^*_{vacuum}(\boldsymbol{r}) \, d\boldsymbol{r} \tag{5.207}$$

Then, the electrostatic contribution to the free energy of solvation, ΔG^{polar} is given by (c.f. Section 2.5)

$$\boxed{\Delta G = \mathcal{N}_a \left(W^*_{water} - W^*_{vacuum} \right)} \tag{5.208}$$

Remark 5.4.1. Typically, we have $\rho(\boldsymbol{r}) = \sum_{i=1}^{n} q_i \delta(\boldsymbol{r} - \boldsymbol{r}_i)$. In this case, the integrals in the above computations reduce to simple summations, and we arrive at the simple expression

$$\boxed{\Delta G = \mathcal{N}_a \left(\frac{1}{2} \sum_{i=1}^{n} q_i \varphi^*_{\text{water}}(\boldsymbol{r}_i) - \frac{1}{2} \sum_{i=1}^{n} q_i \varphi^*_{\text{vacuum}}(\boldsymbol{r}_i) \right)} \tag{5.209}$$

At this point, the only problem left to address is to actually *solve* the systems of boundary integral equations and representation formulae we have derived so far. Fortunately, standard techniques for this kind of operators exist and will be described in the next section.

5.5. Solving the boundary integral equations

In this section we will describe the techniques for the solution of the boundary integral equations we chose in our implementation. We have already mentioned at the beginning of this chapter (c.f. Section 5.1.2) that the boundary element method uses a Galerkin–Petrov approach, where the solutions of the boundary integral equations are approximated as low–rank polynomials over a discretization of the boundary. This hand–waving explanations will now be made precise.

5.5.1. Boundary element discretization

Let $\Omega \subset \mathbb{R}^3$ be a Lipshitz–domain, i.e. a domain with piecewise smooth Lipshitz–boundary $\Gamma := \partial\Omega$. Since we cannot expect to represent an arbitrary boundary curve analytically on a computer, we will have to deal with some kind of approximate representation. In the beginning of this chapter, we have already mentioned that in the boundary element method, the original boundary is replaced by a *simplicial complex approximation* [Mun93], which is defined as follows:

Definition 5.5.1 (Simplicial complex). A simplicial complex $\mathcal{K}$ in $\mathbb{R}^n$ is a collection of *simplices* in $\mathbb{R}^n$, such that

 (i) Every face of a simplex of $\mathcal{K}$ is in $\mathcal{K}$ and

 (ii) The intersection of any two simplices of $\mathcal{K}$ is a face of each of them

Informally, we can think of the simplices as certain kinds of polygons, and of the faces as there edges. For the boundary element method, the simplices are typically either chosen as quadrilateral or triangular elements, and for this work we will exclusively make use of the latter choice. Our implementation will thus work on a *triangulation* of the molecular surface, which will serve as an approximate representation of the original boundary Γ. For reasons of notational simplicity, we will not denote this approximate boundary with the letter Γ in our following derivations, not the original exact boundary.

Such a decomposition of the boundary into triangles leads to the representation of Γ as

$$\bar{\Gamma} = \bigcup_{i=1}^{n} \bar{\tau}_i \tag{5.210}$$

where the τ_i are the individual triangles. To represent those triangles on the computer, we first define the *reference triangle* τ as

$$\tau := \left\{ (\xi_1, \xi_2) \in \mathbb{R}^2 \,\middle|\, 0 \leq \xi_1 \leq 1 \wedge 0 \leq \xi_2 \leq 1 - \xi_1 \right\} \tag{5.211}$$

Each triangle τ_i can now be represented by specifying the linear transformation mapping the reference triangle to τ_i: assume that the vertices of τ_i are denoted by $\boldsymbol{x}_i^1, \boldsymbol{x}_i^2, \boldsymbol{x}_i^3$. Then, there is a unique linear transformation $\mathcal{T}_i$ mapping the vertices of the reference triangle τ,

$$\boldsymbol{x}^1 := (0,0)$$
$$\boldsymbol{x}^2 := (0,1)$$
$$\boldsymbol{x}^3 := (1,0)$$

to the vertices of τ_i, such that

$$\mathcal{T}_i(\boldsymbol{x}^j) = \boldsymbol{x}_i^j, \qquad j = 1, 2, 3$$

With the help of $\mathcal{T}_i$, we have obtained a parametrization of τ_i with respect to the reference element τ, i.e. the points in τ_i can be written as a function of the points $\boldsymbol{\xi}$ in the reference triangle, since

$$\boldsymbol{r}(\boldsymbol{\xi}) = \mathcal{T}_i(\boldsymbol{\xi}), \quad \boldsymbol{\xi} \in \tau \tag{5.212}$$

It is easy to show that the linear transformation $\mathcal{T}_i$ can be written as

$$\mathcal{T}_i(\boldsymbol{\xi}) := \boldsymbol{x}_1^i + \underline{\underline{\mathbf{J}}}_i \boldsymbol{\xi} \tag{5.213}$$

where

$$\underline{\underline{\mathbf{J}}}_i := \begin{pmatrix} (x_{2,1}^i - x_{1,1}^i) & (x_{3,1}^i - x_{1,1}^i) \\ (x_{2,2}^i - x_{1,2}^i) & (x_{3,2}^i - x_{1,2}^i) \\ (x_{2,3}^i - x_{1,3}^i) & (x_{3,3}^i - x_{1,3}^i) \end{pmatrix}$$

leading to

$$\boldsymbol{r}(\boldsymbol{\xi}) = \boldsymbol{x}_1^i + \xi_1 \left(\boldsymbol{x}_2^i - \boldsymbol{x}_1^i \right) + \xi_2 \left(\boldsymbol{x}_3^i - \boldsymbol{x}_1^i \right) \tag{5.214}$$

Among other things, this parametrization allows us to rewrite any function f on a given triangle τ_i in our discretization as a function on the *reference triangle* via

$$f(\boldsymbol{r}) = f(\boldsymbol{x}_1^i + \underline{\underline{\mathbf{J}}}_i \boldsymbol{\xi}) =: \tilde{f}_i(\boldsymbol{\xi}), \quad \boldsymbol{\xi} \in \tau \tag{5.215}$$

which will soon allow us to replace integrations over arbitrary three–dimensional triangles in the boundary representation with the much simpler integration over a two–dimensional reference triangle.

Obviously, one given boundary allows for an infinite number of approximate triangulations. But not all of those are equally well suited for our numerical computations. A trivial first restriction on the discretization is that it should be "as similar as possible" to the original boundary Γ, and in particular, we strictly forbid that the triangulation procedure introduces holes, i.e. missing triangles, into the approximate boundary. Such a disruption of the surface would have drastic consequences, since the whole boundary elements approach is built on the usage of Greens's and Gauss' theorems, which only
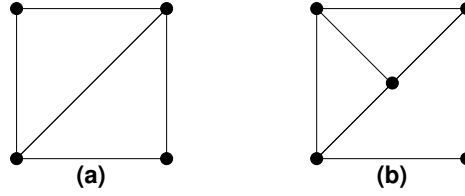
Figure 5.2.: A conforming (a) and a non-conforming (b) complex.

hold for **closed** boundaries.

In addition, we have already demanded the simplicial complex property from our approximation, which ensures that two neighboring triangles have either one vertex or one edge in common, but no "partial" edges (c.f. Fig. 5.2). Another useful property we will demand is the *Delaunay– or empty circle property*: for each edge in the triangulation, we can find a circle touching the edges endpoints, but **not** containing any other vertices of the boundary [Del34]. The Delaunay property leads to many desirable features of the triangulation, one of the most important of which is the max–min angle criterion [Mus97, Law77, Sib78]. This can be paraphrased as the property that a Delaunay triangulation maximizes the minimum angle in any triangle, and thus is a first countermeasure against the feared *degenerate* triangles, i.e. simplices for which one edge has a significantly different length (i.e. it is either much larger or much smaller) than the other two. These triangles pose serious difficulties to any numerical implementation: to give an example, for degenerate triangles, neither area nor normal vectors can be computed in a numerically robust fashion[BK04], the mapping to the reference triangle and vice–versa becomes unstable, and so on.

It can be shown that the Delaunay–property itself is not sufficient to prevent those numerical difficulties. Therefore, some additional quality measures are commonly used to ensure that a given triangulation conforms with the numerical requirements of a boundary element method. To this end, we introduce with the help of the *area*

$$\Delta_i := \int_{\tau_i} d\Gamma \tag{5.216}$$

of the triangle τ_i the *local mesh width*

$$h_i := \sqrt{\Delta_i} \tag{5.217}$$

the *global mesh width*

$$h := \max_{i=1,\ldots,n} h_i \tag{5.218}$$

and the *minimum mesh width*

$$h_{\mathsf{min}} := \min_{i=1,\ldots,n} h_i \tag{5.219}$$

of the triangulation. Then, a measure for the *global uniformity* of the discretization is given by

$$c_g := \frac{h}{h_{\mathsf{min}}} \tag{5.220}$$

while

$$c_j := \frac{h_i}{h_j}, \quad i = 1, \ldots, n \tag{5.221}$$

for all triangles τ_j adjacent to τ_i measures the *local uniformity*. Finally, a measure for the *shape regularity* can be defined if we use the *diameter* d_i of the element τ_i

$$d_i := \sup_{x,y \in \tau_i} |\boldsymbol{x} - \boldsymbol{y}| \tag{5.222}$$

A triangle can be considered to have *regular shape*, if its edges are "not too different". In that case, the triangle is close to equilateral with edge lengths

$$e_i^j \approx d_i, \quad j = 1, 2, 3$$

and area

$$h_i^2 = \Delta_i \approx \frac{1}{4}\sqrt{3}\,d_i^2$$

and thus,

$$c_s^i := \frac{d_i}{h_i} \tag{5.223}$$

serves as a measure of the shape regularity of triangle i, and

$$c_s := \max_{i=1,\ldots,n} c_s^i \tag{5.224}$$

as a measure of the global shape regularity of the discretization. Implementing a discretization procedure that conforms with all those constraints is a highly nontrivial problem, and we therefore decided to use existing reference implementations instead of building our own, in order to minimize the probability of introducing additional sources of error through a non–optimal triangulation process. The details about the procedures we chose, and of the up–to–now avoided question of the definition of the molecular surface itself, will be discussed in the next chapter. At this point, we will just assume that a discretization conforming with our quality measures has been obtained in some fashion and can be used for our further considerations.

5.6. Ansatz–spaces on the boundary element discretization

In the beginning of this chapter, we mentioned that the boundary element method is a so–called *Galerkin–Petrov* method, where the solution to the boundary integral equations is sought in a certain *Ansatz–space*

$$\mathcal{A} := \mathrm{span}\left\{(\chi)_{k=1}^m\right\}$$

on the boundary[14] Γ. Obvious choices for such Ansatz–spaces are spaces of locally polynomial functions, which are especially attractive for their simplicity and numerical well–behavedness. Choosing a space of piecewise polynomial functions of a fixed degree often allows to develop specifically adapted numerical techniques, and in addition, these spaces can be shown to fulfill certain approximation criteria. The two most simple and in practice most important polynomial Ansatz–spaces $\mathcal{S}_h^0(\Gamma)$ and $\mathcal{S}_h^1(\Gamma)$ are the spaces of piecewise *constant* and piecewise *linear* polynomials, which can be defined as follows[Ste03]:

Definition 5.6.1 (The piecewise constant Ansatz space $\mathcal{S}_h^0(\Gamma)$). For $i \in \{1, \ldots, n\}$, we define the *piecewise constant basis functions* $\varphi_i^0(\boldsymbol{r})$ as

$$\varphi_i^0(\boldsymbol{r}) := \begin{cases} 1 & \boldsymbol{r} \in \tau_i \\ 0 & \text{else} \end{cases} \tag{5.225}$$

Then, the space of piecewise constant polynomials on Γ is defined as the convex hull of the piecewise constant basis functions:

$$\mathcal{S}_h^0(\Gamma) := \mathrm{span}\{\varphi_i^0\}_{k=1}^n \tag{5.226}$$

---

[14] We would like to remind the reader that in this chapter, Γ denotes the already approximated boundary, i.e. the triangulation, not the analytical or exact surface of the molecule

Definition 5.6.2 (The piecewise linear Ansatz space $\mathcal{S}_h^1(\Gamma)$). Let v be the number of vertices in the discretization of Γ. Then we define for $i \in \{1, \ldots, v\}$ the *piecewise linear and globally continuous basis functions* $\varphi_i^1(\boldsymbol{r})$ as

$$\varphi_i^1(\boldsymbol{r}) := \begin{cases} 1 & \boldsymbol{r} = \boldsymbol{r}_i \\ 0 & \boldsymbol{r} = \boldsymbol{r}_j \neq \boldsymbol{r}_i \\ \text{linear} & \text{else} \end{cases} \tag{5.227}$$

Then, the space of piecewise linear and globally continuous polynomials on Γ is defined as the convex hull of the piecewise linear basis functions:

$$\mathcal{S}_h^1(\Gamma) := \text{span}\{\varphi_i^1\}_{k=1}^V \tag{5.228}$$

In order to uniquely define a piecewise polynomial function of degree p on Γ, we need to specify its coefficients in the corresponding space of basis functions, and thus, if we denote by n the number of triangles and by v the number of nodes in the discretization, any *piecewise constant* function on Γ is determined by n values, and any *piecewise linear and globally continuous* function by v values. This in turn means that if we have to solve for a certain function on the boundary, we have to solve for n unknowns in the case of constant elements, and for v unknowns in the case of linear ones.

The quality of an $\mathcal{S}_h^0(\Gamma)$ or a $\mathcal{S}_h^1(\Gamma)$ approximation can be assessed with the help of the following approximation theorems:

Theorem 5.6.1 (Approximation properties of the constant Ansatz space $\mathcal{S}_h^0(\Gamma)$). *Let Q_h denote the $\mathcal{L}^2(\Gamma)$–projection operator into the space of piecewise constant functions $\mathcal{S}_h^0(\Gamma)$ on Γ, i.e. for $u \in \mathcal{L}^2(\Gamma)$, $Q_h u \in \mathcal{S}_h^0(\Gamma)$, such that*

$$\langle Q_h u, v_h \rangle_{\mathcal{L}^2(\Gamma)} = \langle u, v_h \rangle_{\mathcal{L}^2(\Gamma)} \quad \forall v_h \in \mathcal{S}_h^0(\Gamma)$$

and let $\varphi \in H^s(\Gamma)$ for $s \in [0, 1]$. Then, the approximation error for the $\mathcal{L}^2(\Gamma)$ projection $Q_h \varphi \in \mathcal{S}_h^0(\Gamma)$ can be bounded with respect to the local mesh width h_i of the triangulation by

$$\|\varphi - Q_h \varphi\|_{\mathcal{L}^2(\Gamma)}^2 \leq c \sum_{i=1}^n h_i^{2s} |\varphi|_{H^2(\tau_i)}^2 \tag{5.229}$$

and with respect to the global mesh width h by

$$\|\varphi - Q_h \varphi\|_{\mathcal{L}^2(\Gamma)}^2 \leq ch^s |\varphi|_{H^2(\Gamma)} \tag{5.230}$$

In addition, we have for $\sigma \in [-1, 0]$, $s \in [\sigma, 1]$ and $u \in H^s(\Gamma)$ the approximation property of $\mathcal{S}_h^0(\Gamma)$:

$$\inf_{u_h \in \mathcal{S}_h^0(\Gamma)} \|u - u_h\|_{H^\sigma(\Gamma)} \leq ch^{s-\sigma} |u|_{H^s(\Gamma)} \tag{5.231}$$

Theorem 5.6.2 (Approximation properties of the linear Ansatz space $\mathcal{S}_h^1(\Gamma)$). *Let Γ be a sufficiently smooth boundary discretization conforming with the simplicial complex property and let I_h denote the linear interpolation operator for the space of piecewise constant and globally continuous functions $\mathcal{S}_h^1(\Gamma)$ on Γ with $I_h u(\boldsymbol{r}_i) = u(\boldsymbol{r}_i)$ for $u \in H^2(\Gamma)$ and all nodes $\boldsymbol{r}_i$ of the discretization. Then, the approximation error for the linear interpolation $I_h \varphi$ of a function $\varphi \in H^2(\Gamma)$ can be bounded with respect to the local mesh width h_i of the triangulation by*

$$\|\varphi - I_h \varphi\|_{\mathcal{L}^2(\Gamma)} \leq c \sum_{i=1}^n h_i^4 |\varphi|_{H^2(\tau_i)}^2 \tag{5.232}$$

and with respect to the global mesh width h by

$$\|\varphi - I_h\varphi\|_{\mathcal{L}^2(\Gamma)} \leq ch^4|\varphi|^2_{H^2(\Gamma)} \tag{5.233}$$

In addition, we have for $\sigma \in [0,1]$, $s \in [\sigma, 2]$, and $u \in H^2(\Gamma)$ the approximation property of $\mathcal{S}_h^1(\Gamma)$:

$$\inf_{u_h \in \mathcal{S}_h^1(\Gamma)} \|u - u_h\|_{H^\sigma(\Gamma)} \leq ch^{s-\sigma}|u|_{H^2(\Gamma)} \tag{5.234}$$

Proof. The proof of the approximation theorems 5.6.1 and 5.6.2 is rather technical and out of the scope of this work. The interested reader is therefore again referred to [Ste03]. □

Remark 5.6.1. From the approximation theorems 5.6.1 and 5.6.2 we can infer that it makes sense to approximate any function of interest u on Γ either through its projection into the space of piecewise constant functions $\mathcal{S}_h^0(\Gamma)$ on Γ:

$$H^s(\Gamma) \ni u(\boldsymbol{r}) \approx \widetilde{u}(\boldsymbol{r}) = \sum_{i=1}^{n} \hat{u}_i^0 \varphi_i^0(\boldsymbol{r}) \in \mathcal{S}_h^0(\Gamma) \tag{5.235}$$

or through its projection into the space of piecewise linear and globally continuous functions on Γ, $\mathcal{S}_h^1(\Gamma)$:

$$H^s(\Gamma) \ni u(\boldsymbol{r}) \approx \widetilde{u}(\boldsymbol{r}) = \sum_{i=1}^{v} \hat{u}_i^1 \varphi_i^1(\boldsymbol{r}) \in \mathcal{S}_h^1(\Gamma) \tag{5.236}$$

where n denotes the number of triangles and v the number of vertices in the discretization.

5.7. Approximation of the boundary integral operators

In this section we will use the results of section 5.6 to derive polynomial approximations to the boundary integral operators described in the earlier sections of this chapter. These will then lead to an algebraic representation of the systems of boundary integral equations which can be solved using standard techniques from numerical linear algebra.

5.7.1. The collocation method

The reduction of the boundary integral equations to linear algebraic ones is not canonical, i.e. there are a number of different mathematical techniques to achieve this goal, each with their own advantages and disadvantages. But one particular technique, the so–called *point collocation method*, is clearly the most popular, mostly due to its numerical efficiency. In this work, we will exclusively describe and make use of the collocation method, and refer the reader to [Ste03, Ste02] or [SMNM92] for alternative approaches. To demonstrate this reduction process, we will consider the simple boundary element equation for the Laplacian operator

$$(\sigma(\boldsymbol{\xi}) + K)\left[\gamma_0^{\mathsf{int}}\varphi^*\right](\boldsymbol{\xi}) - V\left[\gamma_1^{\mathsf{int}}\varphi^*\right](\boldsymbol{\xi}) = 0$$

as a model example. Inserting the appropriate approximations

$$\gamma_0^{\mathsf{int}}\varphi^*(\boldsymbol{\xi}) \approx \sum_{i=1}^{m} \hat{u}_i^m \varphi_i^m(\boldsymbol{\xi}) \tag{5.237}$$

$$\gamma_1^{\mathsf{int}}\varphi^*(\boldsymbol{\xi}) \approx \sum_{i=1}^{m} \hat{q}_i^m \varphi_i^m(\boldsymbol{\xi}) \tag{5.238}$$

yields for the boundary integral equation

$$\sum_{i=1}^{m} \left\{ \hat{u}_i^m \left(\sigma(\boldsymbol{\xi}) + K \right) [\varphi_i^m] (\boldsymbol{\xi}) - \hat{q}_i^m V [\varphi_i^m] (\boldsymbol{\xi}) \right\} = 0 \tag{5.239}$$

At this point, we should remember that for a polynomial approximation of degree m, we need to specify the values of p_m expansion coefficients, or equivalently the values of the function at p_m points on the boundary. In the case of constant elements, we thus have to specify the value at one point per triangle (this point is usually taken to be its center of gravity), and for linear elements we need the values at three points per triangle (typically its vertices)[15]. Let $P_m(\Gamma)$ denote the set of those discretization points, i.e. for $m = 0$ the set of triangle centers and for $m = 1$ the set of vertices. Then, the point collocation method sequentially uses the points in $P_m(\Gamma)$ as the load point $\boldsymbol{\xi}$ of the boundary integral equations, i.e. it evaluates the boundary integral equation at the $p_m = |P_m(\Gamma)|$ nodes of the approximation.

In our model example (5.239), this means that we evaluate the p_m equations

$$\sum_{i=1}^{p_m} \left\{ \hat{u}_i^m \left(\sigma(\boldsymbol{\xi}_j) + K \right) [\varphi_i^m] (\boldsymbol{\xi}_j) - \hat{q}_i^{p_m} V [\varphi_i^m] (\boldsymbol{\xi}_j) \right\} = 0, \quad j \in P_m(\Gamma) \tag{5.240}$$

For a given value of j, we know that $\varphi_i^m(\boldsymbol{\xi}_j) = \delta_{ij}$, since each basis function equals one on exactly one node of the approximation and zero on all others. This reduces the first term in (5.240) to

$$\sum_{i=1}^{p_m} \hat{u}_i^m \sigma(\boldsymbol{\xi}_j) \varphi_i^{p_m} (\boldsymbol{\xi}_j) = \sigma(\boldsymbol{\xi}_j) \hat{u}_j^m \tag{5.241}$$

Simplifying the integral operators appearing in equation (5.240) requires a bit more care. To this end, we will take a closer look at the second term in this equation: by definition of the operator K, we can write

$$\sum_{i=1}^{p_m} \hat{u}_i^m K [\varphi_i^m] (\boldsymbol{\xi}_j) = - \sum_{i=1}^{p_m} \hat{u}_i^m \oint_{\Gamma} \left(\gamma_{0,\xi}^{\text{int}} \gamma_{1,r}^{\text{int}} \mathcal{G}^L (\boldsymbol{r}, \boldsymbol{\xi}_j) \right) \varphi_i^m (\boldsymbol{r}) \, d\Gamma_r \tag{5.242}$$

and this integral can be broken into a sum of integrals over the individual triangles τ_i to yield

$$\sum_{i=1}^{p_m} \hat{u}_i^m K [\varphi_i^m] (\boldsymbol{\xi}_j) = - \sum_{i=1}^{p_m} \sum_{k=1}^{n} \hat{u}_i^m \oint_{\tau_k} \left(\gamma_{0,\xi}^{\text{int}} \gamma_{1,r}^{\text{int}} \mathcal{G}^L (\boldsymbol{r}, \boldsymbol{\xi}_j) \right) \varphi_i^m (\boldsymbol{r}) \, d\Gamma_r \tag{5.243}$$

This double sum can again be simplified by noting that $\varphi_i^m(\boldsymbol{r})$ vanishes for $i \neq k$, i.e. of the second sum, only those terms with $i = k$ survive to yield

$$\sum_{i=1}^{p_m} \hat{u}_i^m K [\varphi_i^m] (\boldsymbol{\xi}_j) = - \sum_{i=1}^{p_m} \hat{u}_i^m \underbrace{\oint_{\tau_i} \left(\gamma_{0,\xi}^{\text{int}} \gamma_{1,r}^{\text{int}} \mathcal{G}^L (\boldsymbol{r}, \boldsymbol{\xi}_j) \right) \varphi_i^m (\boldsymbol{r}) \, d\Gamma_r}_{=: -K_{ji}} \tag{5.244}$$

A similar definition of the coefficients V_{ji} for the single layer potential operator V can be straightforwardly inferred from this last equation, and we can thus simplify equation (5.240) to

$$\sigma(\boldsymbol{\xi}_j) \hat{u}_j^m + \sum_{i=1}^{p_m} \hat{u}_i^m K_{ji} - \sum_{i=1}^{p_m} \hat{q}_i^m V_{ji} = 0, \quad j \in P_m(\Gamma) \tag{5.245}$$

---

15 Note that in the case of linear elements we have to ensure that the values at the incident vertices of adjacent triangles coincide to guarantee global continuity, and thus, we cannot really prescribe three *independent* values for each triangle. Rather, we have to prescribe exactly one value per vertex in the discretization

5. The Boundary Element Method

Each of those p_m equations can now be interpreted as one row of a linear system of p_m equations for p_m unknowns. With the definitions of the $p_m \times p_m$ *system matrices* $\underline{\underline{\mathbf{K}}}$ and $\underline{\underline{\mathbf{V}}}$ which are made up of the coefficients K_{ij} and V_{ij} as defined above, the diagonal matrix

$$\underline{\underline{\sigma}} := \mathrm{diag}(\sigma(\boldsymbol{\xi}_1), \ldots, \sigma(\boldsymbol{\xi}_{p_m}))$$

and with the definitions of the vectors

$$\hat{\boldsymbol{u}} := (\hat{u}_1, \ldots, \hat{u}_{p_m})^t$$

and

$$\hat{\boldsymbol{q}} := (\hat{q}_1, \ldots, \hat{q}_{p_m})^t$$

we thus obtain the *discretized form of the boundary integral equation* (5.239):

$$\left(\underline{\underline{\sigma}} + \underline{\underline{\mathbf{K}}} \right) \hat{\boldsymbol{u}} - \underline{\underline{\mathbf{V}}} \hat{\boldsymbol{q}} = \mathbf{0} \tag{5.246}$$

Similarly, we can assign system matrices to all the boundary integral operators appearing in the systems of boundary integral equations (5.117), (5.118), and (5.192). We can thus conclude

Theorem 5.7.1 (Discrete boundary element system for the cavity model of local electrostatics). *To approximately solve the system of boundary integral equations for the cavity model of local electrostatics, (5.117) and (5.118), we solve the linear algebraic system*

$$\left\{ \left(1 + \frac{\varepsilon_\Omega}{\varepsilon_\Sigma} \right) \underline{\underline{\sigma}} + \left(\frac{\varepsilon_\Omega}{\varepsilon_\Sigma} - 1 \right) \underline{\underline{\mathbf{K}}} \right\} \hat{\boldsymbol{u}} = \left(\underline{\underline{\mathbf{K}}} - \underline{\underline{\sigma}} \right) \hat{\boldsymbol{u}}_{mol} - \frac{\varepsilon_\Omega}{\varepsilon_\Sigma} \underline{\underline{\mathbf{V}}} \hat{\boldsymbol{q}}_{mol} \tag{5.247}$$

where the matrices K_{ij}, V_{ij}, and σ_{ij} for the boundary integral operators are defined as above as the response of the corresponding boundary integral operator to the basis function φ_j when evaluated at $\boldsymbol{\xi}_i$, where the vector

$$\hat{\boldsymbol{u}} := (\hat{u}_1, \ldots, \hat{u}_{p_m})^t$$

contains the approximation coefficients of the Dirichlet– and Neumann traces $\gamma_0^{int}\varphi^*$, respectively, and where the vectors $\hat{\boldsymbol{u}}_{mol}$ and $\hat{\boldsymbol{q}}_{mol}$ contain the expansion coefficients of the Dirichlet and Neumann traces of the analytically given molecular potential φ_{mol}. The vector of the approximation coefficients for the Neumann trace $\gamma_1^{int}\varphi^*$,

$$\hat{\boldsymbol{q}} := (\hat{q}_1, \ldots, \hat{q}_{p_m})^t$$

can then be computed from the linear equation

$$\hat{\boldsymbol{q}} = \underline{\underline{\mathbf{V}}}^{-1} \left(\underline{\underline{\sigma}} + \underline{\underline{\mathbf{K}}} \right) \hat{\boldsymbol{u}} \tag{5.248}$$

Theorem 5.7.2 (Discrete boundary element system for the cavity model of nonlocal electrostatics). *To approximately solve the system of boundary integral equations for the cavity model of nonlocal electrostatics, (5.192), we solve the linear algebraic system*

$$\begin{pmatrix} \underline{\underline{\mathbf{I}}} - \underline{\underline{\sigma}} - \underline{\underline{\mathbf{K}}}^Y & \frac{\varepsilon_\Omega}{\varepsilon_\infty} \underline{\underline{\mathbf{V}}}^Y - \frac{\varepsilon_\Omega}{\varepsilon_\Sigma} \left(\underline{\underline{\mathbf{V}}}^Y - \underline{\underline{\mathbf{V}}} \right) & \frac{\varepsilon_\infty}{\varepsilon_\Sigma} \left(\underline{\underline{\mathbf{K}}}^Y - \underline{\underline{\mathbf{K}}} \right) \\ \underline{\underline{\sigma}} + \underline{\underline{\mathbf{K}}} & -\underline{\underline{\mathbf{V}}} & 0 \\ 0 & \frac{\varepsilon_\Omega}{\varepsilon_\infty} \underline{\underline{\mathbf{V}}} & 1 - \underline{\underline{\sigma}} - \underline{\underline{\mathbf{K}}} \end{pmatrix} \begin{pmatrix} \hat{\boldsymbol{u}} \\ \hat{\boldsymbol{q}} \\ \hat{\boldsymbol{w}} \end{pmatrix} = \begin{pmatrix} \beta \\ 0 \\ 0 \end{pmatrix} \tag{5.249}$$

where we have used the notation of theorem 5.7.1, the variable

$$\beta := - \left(\underline{\underline{\mathbf{I}}} - \underline{\underline{\sigma}} - \underline{\underline{\mathbf{K}}}^Y - \frac{\varepsilon_\Omega}{\varepsilon_\Sigma} \left(\underline{\underline{\mathbf{K}}}^Y - \underline{\underline{\mathbf{K}}} \right) \right) \hat{\boldsymbol{u}}_{mol} - \left(\frac{\varepsilon_\Omega}{\varepsilon_\infty} \underline{\underline{\mathbf{V}}}^Y - \frac{\varepsilon_\Omega}{\varepsilon_\Sigma} \left(\underline{\underline{\mathbf{V}}}^Y - \underline{\underline{\mathbf{V}}} \right) \right) \hat{\boldsymbol{q}}_{mol}$$

and the vector $\hat{\boldsymbol{w}}$ of the expansion coefficients of the external potential Ψ.

Theorem 5.7.3 (Complexity of the nonlocal cavity model). *Using a point collocation method and the approximation of the boundary condition described in section 5.4, the nonlocal cavity model has the same asymptotic complexity as the local cavity model.*

Proof. The only qualitative difference between the discrete systems (5.247) and (5.249) is the fact that while the first is a system of size $p_m \times p_m$, the latter has size $(3p_m \times 3p_m) = 9(p_m \times p_m)$. Thus, both systems can be solved with the same asymptotic complexity. □

Remark 5.7.1. The values of the interesting potentials in the local and in the nonlocal case, and thus also the electrostatic potential and solvation energies can be computed as soon as the discrete systems have been solved by simply replacing the boundary integral operators with their respective matrix discretization, and the Dirichlet and Neumann traces on Γ with their respective vectors of approximation coefficients.

5.8. Numerical evaluation of the boundary integral operators

The major remaining problem now that we have developed a boundary element scheme for the solution of both the local and nonlocal system of cavity electrostatics lies in the numerical evaluation of the boundary integral operators. This numerical integration is typically carried out over the reference triangle τ instead of the actual triangle τ_i at hand, which can be achieved by transforming the integrand onto τ via equation (5.215). Carrying out the integration is not straightforward, though, since the integrands appearing might possess singularities in the domain of integration.

The discretization of the boundary integral operators is composed of integrals of the form

$$\mathcal{I} = \int_{\tau_i} \mathcal{F}(\boldsymbol{r}, \boldsymbol{\xi}) \, \varphi(\boldsymbol{r}), d\Gamma_r$$

where $\mathcal{F}$ denotes a fundamental solution or its Neumann trace, and thus, depending on the relative locations of $\boldsymbol{r}$ and $\boldsymbol{\xi}$, we can distinguish three possible integral types [GKW03]:

Point locations	Integral type
The load point $\boldsymbol{\xi}$ is far away from τ_i, i.e. for the transformed load point $\tilde{\boldsymbol{\xi}}$: $\|\tilde{\boldsymbol{\xi}}\| \ll 1$.	**Regular integral:** the evaluation of the integrand is carried out far from its singularity. Thus, the integral is regular and can be numerically solved using standard quadrature techniques.
The load point $\boldsymbol{\xi}$ is *close* to τ_i, but not *on* τ_i, i.e. for the transformed load point $\tilde{\boldsymbol{\xi}}$: $\tilde{\boldsymbol{\xi}} = 1 + \epsilon$.	**Quasi–singular integrals:** the integrand is not evaluated at its singularity and thus, the integral is still regular, and thus a numerical quadrature is possible. But in the neighbourhood of the point of singularity, the integrand is sharply peaked, leading to efficiency and accuracy problems due to the necessary high polynomial degree of the approximating function in the quadrature. Thus, special transforms are often derived for this particular situation [GKW03, Tel87, ND99].

The load point ξ lies in the boundary element ξ.	**Weakly or strongly singular integral:** in this case, the integrand will necessarily be evaluated at the location of its singularity. Depending on the type of integrand, a distinction between weakly and strongly singularities is necessary, since both will require different solution techniques. In both cases, it is clear, though, that a standard numerical quadrature will inevitably fail due to the exposed singularity at $r = \xi$.

5.8.1. Regular and quasi–singular integration

The regular integrals pose no special problems, so that we can just take a standard quadrature approach: the integrand is approximated by a polynomial of a certain degree, which can be exactly integrated over the reference triangle. For the three–dimensional integrals we have to compute, this is conveniently achieved by taking the product of three one–dimensional polynomial quadratures of degrees n_1, n_2, n_3, respectively. In order to determine this polynomial approximation for a function $f(\xi)$ over the reference triangle τ the values $f(\xi_i)$ at $n_1 \times n_2 \times n_3$ are needed – these points are typically referred to as *Gauss points* or *Quadrature points*. This reduces the integration of $f(\xi)$ over the reference triangle τ to a weighted sum over the function evaluation at the Gauss points $\xi^{ijk}, i = 1, \ldots, n_1, j = 1, \ldots, n_2, k = 1, \ldots, n_3$:

$$\int_\tau f(\xi)d\xi \approx \sum_{i=1}^{n_1} \sum_{j=1}^{n_2} \sum_{k=1}^{n_3} f(\xi^{ijk})w_i w_j w_k \tag{5.250}$$

In the *Gaussian quadrature method*, the set of required Gauss points, and the required *weighting coefficients* w_i, w_j, w_k are determined from the requirement that the quadrature formula of degree n for a one–dimensional problem *exactly integrates* all polynomials of degree up to $2n - 1$. Determination of the unknowns is then possible by applying the quadrature rules to a basis of the space of polynomials under consideration, which yields the required of $2n$ equations for the corresponding Gauss points ξ^i and the weights w_i. For any given degree, the values can be precomputed and are typically found tabulated in reference works.

With the help of numerical techniques like the Gaussian quadrature method, the regular and – in principle – the quasi–singular integrals can now be computed, but as we have already stated, the sharply peaked form of a quasi–singular integrand often suggests the usage of certain regularizing transformations. Since the concept of regularization will be covered in the sections on weakly and strongly singular integration, we will not discuss these techniques in this work, and again refer the interested reader to the treatment in [Tel87] or [ND99].

5.8.2. Weakly singular integration

As we have already stated in our discussion about the single layer potential, an integral is called *weakly singular* if the integrand possesses a singularity at a point r_s in the domain of integration, but the integral exists and is continuous at r_s. An analytical treatment is thus in principle possible, but a standard quadrature approach will break down.

Regularising transformations

The main numerical approach for handling weakly singular integrals consists in treating the integrand with a special transformation with vanishing Jacobian at the point of singularity. These transfor-

mations are called *regularising transformations* due to their rectifying properties. For the important special case of a $\|\boldsymbol{r} - \boldsymbol{\xi}\|^{-1}$ dependence of the integrand – or for all kinds of weaker singularities at $\boldsymbol{r} = \boldsymbol{\xi}$, this can be easily achieved by translating the coordinate system such that $\boldsymbol{\xi} \rightsquigarrow \boldsymbol{0}$ and consequently expressing the integral over the reference triangle in polar coordinates. Since the Jacobian of the transformation to polar coordinates introduces a factor r into the integrand, and since we assumed that the singularity at $\boldsymbol{r} = 0$ was at most of the r^{-1} kind, the resulting integrand will contain no further singularities and thus the integral can be solved using standard quadrature techniques.

A similar approach to the regularization of boundary integrals is based on the *Lachat–Watson transformation* [LW76]

$$x = u + 1 \tag{5.251}$$

$$y = \frac{1}{2}(u + 1)(v + 1) \tag{5.252}$$

with Jacobian

$$J = (\partial_u x)(\partial_v y) - (\partial_v x)(\partial_u y) = \frac{1}{2}(u + 1) \tag{5.253}$$

which vanishes for $u = -1$. Thus, the Lachat–Watson transformation can be used in the same way as the transformation to polar coordinates for the rectification of certain types of weakly singular integrands.

5.8.3. Strongly singular integration

For strongly singular integrands, the integral itself is singular at the point of singularity of the integrand (c.f. the discussion of the double layer potential in section 5.2.1). But fortunately, as we have seen in the treatment of the boundary integral operators, strongly singular integrals can often still be given a well–defined meaning in the sense of Cauchy principal value integrals[16] where a limiting process is employed to approach the singularity from "both sides". This Cauchy principal value integration process induces a decomposition into two so–called *finite part integrals,* one for the approach "from the left" and one "from the right". These finite part integrals are renormalized versions of the strongly singular integral in the sense that their singular part is subtracted from the integrand. To give a simple one–dimensional example, let us consider the integral over[17] x^{-1}, where we have for the Cauchy principle value integral:

$$\fint_{-a}^{b} \frac{1}{x}\,dx := \lim_{\varepsilon \to 0}\left(\int_{-a}^{-\epsilon} \frac{1}{x}\,dx + \int_{\varepsilon}^{b} \frac{1}{x}\,dx\right) \tag{5.254}$$

$$= \lim_{\varepsilon \to 0}\left\{\ln(|-\varepsilon|) - \ln(|-a|) + \ln(b) - \ln(\varepsilon))\right\} \tag{5.255}$$

$$= \ln\left(\frac{b}{a}\right) \tag{5.256}$$

As we can see, the antisymmetry of the integrand

$$\lim_{\varepsilon \to 0} f(x_s + \varepsilon) = -\lim_{\varepsilon \to 0} f(x_s - \varepsilon) \tag{5.257}$$

in combination with the symmetrical approach of the singularity that is typical for the Cauchy principal value effectively removes the infinite parts of the respective integrals. Thus, if we can decompose the

---

16 For a pathological case where this is not possible see the discussion of the hypersingular potential in section 5.2.1.

17 Please keep in mind that while a r^{-1} dependence in three dimensions is only weakly singular, a x^{-1} dependence leads to a strong singularity when integrated over only one dimension.

integrand $f(x)$ into a *finite part* $g(x)$ and a *infinite part* $s(x)$, and if the infinite part is anti symmetrical in the above sense, the Cauchy principal value will exist and have a finite value. This motivates the definition of the important *finite part integrals,* which in the case of a one–dimensional strongly singular integrand with x^{-1}–type singularity

$$f(x) = \frac{g(x)}{x}$$

assume the form

$$\int\limits_{-a}^{0} g(x)\frac{1}{x}\,dx := \lim_{\varepsilon\to 0}\left\{\int\limits_{-a}^{-\varepsilon} g(x)\frac{1}{x}\,dx - g(0)\ln(\varepsilon)\right\} \tag{5.258}$$

and

$$\int\limits_{0}^{b} g(x)\frac{1}{x}\,dx := \lim_{\varepsilon\to 0}\left\{\int\limits_{\varepsilon}^{b} g(x)\frac{1}{x}\,dx + g(0)\ln(\varepsilon)\right\} \tag{5.259}$$

and with the help of the finite part integrals, the Cauchy principal value integral can be computed as

$$\oint\limits_{-a}^{b} \frac{g(x)}{x}\,dx = \int\limits_{-a}^{0} \frac{g(x)}{x}\,dx + \int\limits_{0}^{b} \frac{g(x)}{x}\,dx \tag{5.260}$$

Taking special care about approaching the singularity equally from left and right, the finite part integrals can in principle be evaluated with the help of standard quadrature formulae. In the three–dimensional case, similar approaches, i.e. the regularization or renormalization by subtracting the singularity from the integrand, can be developed. For a short introduction into the matter, the reader is referred to [GKW03], or to one of the original articles in that field, e.g. to [LHM85, GG90, WJD91, DS92, Dum94].

6. Implementation of a BEM solver for nonlocal biomolecular electrostatics

Over the course of the last chapters, we have developed the theory of nonlocal cavity electrostatics, and derived a formulation that is amenable to numerical techniques. Most importantly, we have succeeded in devising a boundary element formulation for this problem, which for the first time gives reason to hope for applicability to non–trivial real–world problems in the field of biomolecular interactions, like for example the protein docking problem. In the current chapter, we will describe the implementation of a solver for the system of both local and nonlocal cavity electrostatics, following the route laid out in theorem 5.4.2, which will allow us to compute all relevant potentials and fields both in the local and nonlocal framework as well as the corresponding free energy of solvation.

6.1. Choice and computation of the molecular boundary Γ

A remaining question that has to be addressed before we can start with our implementation is the choice of a suitable molecular surface. In principle, this choice is arbitrary to a certain degree, since the notion of a molecular surface itself is ill–defined: quantum mechanics tells us that the location of each individual electron in the molecule is subject to a non–compactly supported probability distribution, and thus, each atom is in a way spread out infinitely into space. For most if not all practical reasons, though, this effect can be neglected due to the fast decay of the probability density, and thus, by for example introducing a cut–off at a certain probability threshold, atoms can be considered as approximately spherical systems of a certain *radius*, which of course depends on the chosen threshold.

But even if we assume that a suitable set of atom radii has been defined, and that the molecule can be considered as a union of such atomic spheres, there is still some freedom in the choice of the molecular *boundary* Γ. A seemingly obvious definition would be the surface of the set of interlocked atomic spheres composing the molecule, the *Van–der–Waals surface* of the molecule. While the Van–der–Waals surface might at first seem as the natural or canonical definition of the molecule's boundary, a more careful consideration of the problem will soon lead to a number of issues that have to be addressed. First of all, the boundary we have in mind in the cavity model of electrostatics in water is the interface of the biomolecule with the surrounding water. But if we take into account that the water molecules themselves have a finite volume, it is clear that not all regions of the Van–der–Waals surface of the biomolecule are available to the water, in the sense that they can not be reached. Furthermore, the surface of a set of interlocked spheres is far from being well–behaved or continuous, posing severe problems for the triangulation procedure as well as for the numerical boundary integration routines. The first of this two considerations led Lee and Richards to the definition of the *solvent–accessible surface (SAS)* [LR71]: if we assume that the water molecules can be describes as spherical entities themselves – which for the case of molecular surface computations can be considered a very good approximation – we can virtually roll one of those water molecules as a *probe sphere* over the Van–der–Waals surface of the biomolecule. The solvent–accessible surface of the biomolecule is then defined as the surface on which the center of the probe sphere is situated during this rolling over. Thus, the solvent–accessible surface is very similar to the Van–der–Waals surface, but extended about the radius of the probe sphere to reflect the finite size of the water molecules. This process also leads to another, slightly more complicated definition that also dates back to Richards [Ric77] and

was made popular by the implementations of Connolly [Con81b, Con81a, Con83]: instead of taking the surface that is traced out by the *center* of the water probe sphere, the *molecular surface*, which is often also known under the name *solvent–excluded surface (SES)* or *Connolly surface* is defined as the interface between the probe sphere and the Van–der–Waals surface during the process of rolling the probe over the biomolecule (c.f. Fig. 6.1). Thus, the solvent–excluded surface is the contact surface of the electron hulls of water and of the biomolecule, which fits very well into our definition of the water–protein interface Γ in the cavity model of electrostatics. As an important side–effect, the solvent–excluded surface is considerably more amenable to the numerical integration routines, and efficient triangulation routines exist [Con85, WMFR89, ZM90, WM90, WFF90, ZYY95, Zau95].
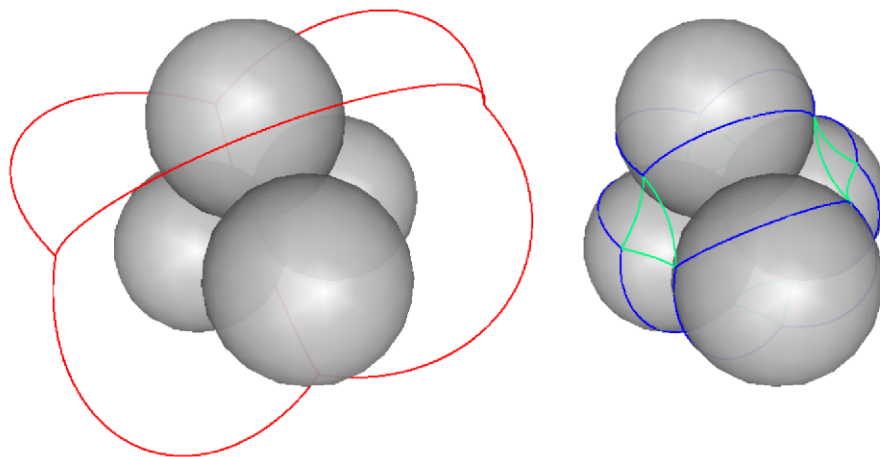
Figure 6.1.: Sketch of the behaviour of the SAS (to the left) and the SES (to the right) around an agglomeration of atoms.

More information about the different definitions of molecular surfaces, and about the historical process of their definition and implementation can be found in an online review by Michael Connolly[1] [Con].

Having deciding upon using the solvent–excluded surface for our boundary element solver, we tested several of the different existing triangulation procedures. Soon it turned out problematic that most of the conventional implementations are aimed at a molecular *graphics* setting instead of the numerical integration we have in mind, and thus tend to produce triangles not conforming with the quality measures derived in Section 5.5.1. For example, degenerate or quasi–degenerate triangles, and a very large local variation in the areas and radii of the triangles in the mesh are common since they typically present no problems for visualizational purposes. In addition, the number of triangles that are usually generated is extremely high to ensure smooth appearance of the surface in the molecular viewers, and thus, such overly fine meshes are inapplicable to boundary element purposes, where the size of the system matrices is quadratic in the number of elements in the triangulation.

Our tests led us to use two different algorithms for the triangulation, the solvent–excluded surface triangulation implemented in the **BALL**–library [Koh, Str03], and the **SMART**–algorithm by Randy Zauhar [Zau95] for each molecule we want to process. Then, the resulting two meshes are examined for their concordance with the quality measures defined in Section 5.5.1, and the more successful triangulation is kept for further processing. This is performed by using mesh optimization and repair

---

1 As an anecdotal sidenote, Connolly groups the history of molecular graphics into two different periods: "B.C." which is his abbreviation for *before Connolly*, and "A.D.", *after Dots*, where *Dots* is his original program for the computation of solvent–excluded surfaces.
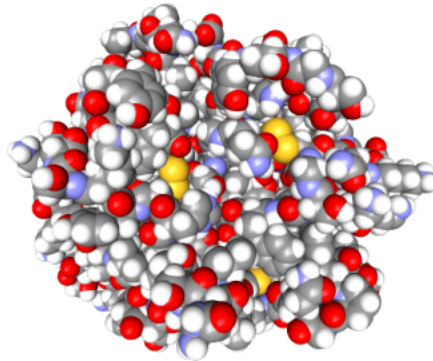
(a) Van–der–Waals
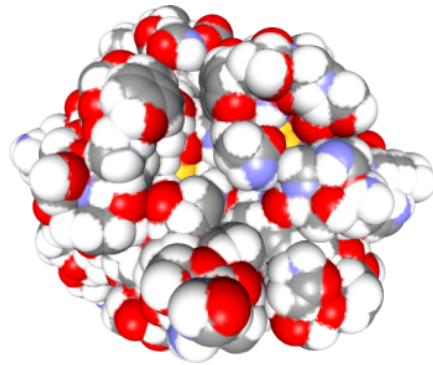
(b) Solvent Accessible Surface (SAS)
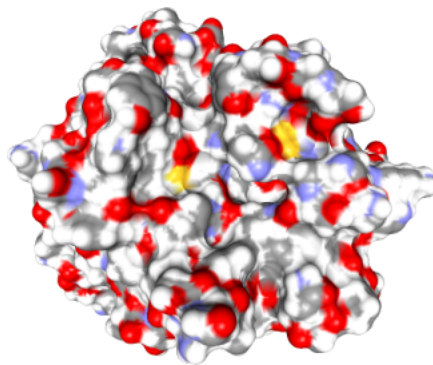
(c) Solvent Excluded Surface (SES)

Figure 6.2.: Different surface types for trypsin.

techniques from the *gts–* library [Pea] and the **NETGEN** program [SGG], leading to a triangulation that is more suited to numerical processing. This improved triangulation simplifies and stabilizes the numerical integration by conforming with our quality measures and is simultaneously sparse enough – its small size allows for a representation of the full system matrices in memory (in our current implementation, this is possible for up to about $12.000 - 15.000$ triangles).

This somewhat awkward process will be significantly simplified in the near future, mainly by two different approaches: first of all, we will adapt the triangulation routines implemented in the **BALL**–library to the numerical requirements we have in mind, and second by implementing a space–efficient approximation technique for the system of boundary element equations, reducing the amount of space that is required[2] from $\mathcal{O}(n^2)$ to at most $\mathcal{O}(n\log(n))$ or even $\mathcal{O}(n)$.

6.2. Constructing the system matrices and solving the equations

The next step in the solution of the boundary element systems we have proposed consists in the construction of the system matrices. In close collaboration with Professor Sergej Rjasanow and Dr. Sergej Goreinov, we have implemented a plain–C integrated solver containing the complete construction step. To this end, we first read the triangulated surface, the positions of all atoms and the amounts of all partial charges, and perform the necessary preprocessing operations like the computation of the centers of gravity, area and surface normals for each triangle. Choosing constant elements as our representation, the discretized system matrices can now be set up. For the computation of the boundary integral operators containing the fundamental solution of the Laplacian, we use a specifically adapted integration technique developed by Sergej Rjasanow [Rja90], while the evaluation of those boundary integral operators related to the fundamental solution of the Yukawa–operator is performed using a Radon 7–point cubature [Rad48, Kri67].

Having constructed the system matrices and the inhomogeneity vector, the resulting linear system of equations is then solved numerically. Since we are using a *direct* boundary element approach, this directly yields the values of the internal traces of the reaction field potential $\gamma_0^{\text{int}}\varphi^*, \gamma_1^{\text{int}}\varphi^*$ and, in the nonlocal case, the external Dirichlet trace of the Ψ–potential $\gamma_0^{\text{ext}}\Psi$ on the molecular surface Γ. This full set of *Cauchy data* can then be stored for further post processing.

To ensure the highest possible performance while maintaining numerical stability, all low–level operations on the system matrices and the solution and inhomogeneity vectors are performed using a C–interface to the **BLAS**–library [LHKK79, DDCHH88b, DDCHH88a, DDCDH90b, DDCDH90a], while all high–level operations, i.e. the solution of the linear system of equations, is performed using a C–interface to the **LAPACK**–library [ABB+99]. All **BLAS** and **LAPACK** routines where taken from the self–optimizing **ATLAS** project [WPD01, WD99, WD98, WD97, Wea], which is currently the probably most efficient freely available general purpose implementation.

Setting up the system of boundary integral equations can be performed straightforwardly in quadratic time in the number of triangles, since the evaluation of each cell in the system matrices consists of the evaluation of a constant number of boundary integral operators, which in turn require a constant amount of steps using for example the quadrature techniques explained above. Solving the resulting system is in principle possible in $\mathcal{O}(n^{\log_2(7)}) \approx \mathcal{O}(n^3)$ time, where n denotes the number of triangles in the mesh, using Strassen's matrix multiplication algorithm [Str69] and a subsequent reduction [AHU83, CLRS01], but in practice the involved constants hidden in the asymptotic notation often let a naive $\mathcal{O}(n^3)$ algorithm outperform the more sophisticated implementation. Thus, it is safe to

---

2 This will be discussed briefly in the *Outlook* of this thesis.

assume that building up and solving the resulting system of equations in our current implementation, using the full set of system matrices[3] takes $\mathcal{O}(n^3)$ time.

6.3. Postprocessing: generation of fields and potentials everywhere in space

Having computed the full Cauchy data on the boundary Γ, we are now able to compute all quantities of interest, i.e. all relevant potentials and fields, at any point in space. To this end, we just have to evaluate the respective representation formulae derived in Chapter 5. Since these representation formulae are based on evaluating the same set of boundary integral operators that was used for the construction of the system matrices, no additional numerical techniques have to be employed.

A remarkable difference between the set–up of the system matrices and the evaluation of the representation formulae, though, lies in the fact that the latter does **not** introduce any additional unknowns into the system. Instead of solving a system of (discretized) boundary integral equations, we merely have to evaluate a set of (discretized) boundary integrals over completely known (discretized) quantities – the Cauchy data of the current system. Since with the help of the already explained quadrature rules, these break down into simple *sums* over the Gauss points in the triangles in the mesh of the molecular surface mapped to the reference triangle, this evaluation can be performed very efficiently: in the currently chosen approach[4] employing the *full* system matrices, evaluation of the representation formulae is linear in the number of triangles in the discretization.

In particular, given the full set of Cauchy data, we can now easily compute the reaction field energy of a given biomolecule in the local and in the nonlocal framework, by evaluating the reaction field potential at the locations of the partial charges of the individual atoms in $\mathcal{O}(nm)$ time, where n denotes the number of triangles in the discretization and m the number of atoms in the molecule. Remembering that in the current implementation, the setup and solution of the boundary integral equations takes $\mathcal{O}(n^3)$ time, we can thus conclude:

Theorem 6.3.1 (Asymptotic complexity of the local and nonlocal cavity model of biomolecular electrostatics). *Given a triangulation of the solvent–excluded surface Γ of a molecule, containing n triangles, and given the positions and amount all partial charges located in the molecule, all relevant fields and potentials of both the local and the nonlocal cavity model of biomolecular electrostatics at a set of p arbitrary points in space can be computed using the full representation of the system matrices in $\mathcal{O}(n^2 + p)$ space and $\mathcal{O}(n^3 + np)$ time.*

Corollary 6.3.1 (Complexity of the computation of the free energy of solvation in the local and nonlocal cavity model of biomolecular electrostatics). *For a molecule composed of m partial charges, the reaction field energies of both the local and the nonlocal cavity model, and thus the electrostatic contribution to the free energy of solvation, can be computed in $\mathcal{O}(n^2 + m)$ space and $\mathcal{O}(n^3 + nm)$ time.*

Remark 6.3.1. According to theorem 5.7.3, runtime and space consumption of the nonlocal cavity model is about 9 times higher than that of the local cavity model.

---

3 As opposed to the more efficient approximate approaches, replacing the full system matrices by sparse ones employing the fast decay of the integral kernels – these approaches will be briefly explained in the *Outlook* of this thesis.
4 c.f. footnote 6.2

6.4. Testing the implementation

Having implemented a boundary element solver for the cavity model of nonlocal electrostatics for the first time allowed us to apply this theory to the nontrivial geometrical settings arising in biomolecular computations. But of course, before we could employ the implementation for the computation of analytically inaccessible quantities, a number of tests against theoretically known results had to be performed to assess the correctness and accuracy of the solver.

6.4.1. Expansion in spherical harmonics

The first test we performed was devised by Sergej Goreinov and is based on an expansion of the analytical solution in spherical harmonics, using the *addition theorems* [Arf85, San91]

$$\frac{1}{4\pi r} = \sum_{n\geq 0} \sum_{|m|\leq n} \frac{a^n}{\rho^{n+1}} \frac{1}{2n+1} Y_{nm}(\vartheta_1, \phi_1) Y_{nm}^*(\vartheta_2, \phi_2) \tag{6.1}$$

$$\frac{e^{-\kappa r}}{4\pi r} = \sum_{n\geq 0} \sum_{|m|\leq n} \frac{2\kappa}{\pi} i_n(\kappa a) k_n(\kappa\rho) Y_{nm}(\vartheta_1, \phi_1) Y_{nm}^*(\vartheta_2, \phi_2) \tag{6.2}$$

where $a < \rho$ (for $a > \rho$, a and ρ have to be interchanged in the above formulae), and where we have used the definitions

$$r := |\boldsymbol{x} - \boldsymbol{y}| \tag{6.3}$$

$$\boldsymbol{x} := (a, \vartheta_1, \phi_1) \tag{6.4}$$

$$\boldsymbol{y} := (\rho, \vartheta_2, \phi_2) \tag{6.5}$$

and where i_n is related to the *modified Bessel function of the first kind*

$$I_n(z) = \frac{1}{2\pi\imath} \oint e^{\left(\frac{z}{2}\right)\left(t+\frac{1}{t}\right)} t^{-n-1}\, dt, \quad z \in \mathbb{C} \tag{6.6}$$

via

$$i_n(z) := \sqrt{\frac{\pi}{2z}} I_{n+\frac{1}{2}}(z) \tag{6.7}$$

and where k_n is related to the *modified Bessel function of the second kind*

$$K_n(z) = \frac{\pi}{2} \frac{I_{-n}(z) - I_n(z)}{\sin(n\pi)}, \quad z \in \mathbb{C} \tag{6.8}$$

via

$$k_n(z) := \sqrt{\frac{\pi}{2z}} K_{n+\frac{1}{2}}(z) \tag{6.9}$$

such that for the first few values of n, we obtain

$$
\begin{aligned}
i_0(z) &= \frac{\sinh(z)}{z} & k_0(z) &= \frac{\pi}{2z} e^{-z} \\
i_1(z) &= -\frac{\sinh(z)}{z^2} + \frac{\cosh(z)}{z} & k_1(z) &= \frac{\pi}{2z} e^{-z}\left(1 + z^{-1}\right) \\
i_2(z) &= \left(\frac{3}{z^3} + \frac{1}{z}\right)\sinh(z) - \frac{3}{z^2}\cosh(z) & k_2(z) &= \frac{\pi}{2z} e^{-z}\left(1 + 3z^{-1} + 3z^{-2}\right)
\end{aligned}
\tag{6.10}
$$

Since the spherical harmonics Y_{nm} are eigenfunctions of the Laplace operator on the unit sphere, we can set up a system of eigenvector − eigenvalue equations for the boundary integral operators V and K for the Laplacian:

$$VY_{nm} = \lambda_n^V Y_{nm} \tag{6.11}$$

$$KY_{nm} = \lambda_n^K Y_{nm} \tag{6.12}$$

A similar system can be obtained for the boundary integral operators V^Y and K^Y of the Yukawa differential operator, which is just the Laplacian plus a constant, and thus preserving the eigenfunctions due to

$$\Delta Y_{nm} = \lambda Y_{nm} \tag{6.13}$$

$$\Rightarrow \left(\Delta - \frac{1}{\Lambda^2}\right) Y_{nm} = \left(\lambda - \frac{1}{\Lambda^2}\right) Y_{nm} \tag{6.14}$$

Thus, the spherical harmonics provide a system of eigenfunctions for the Yukawa–operator as well, which carries through to its boundary integral operators, such that we arrive at the second set of eigenvector − eigenvalue equations

$$V^Y Y_{nm} = \lambda_n^{V^Y} Y_{nm} \tag{6.15}$$

$$K^Y Y_{nm} = \lambda_n^{K^Y} Y_{nm} \tag{6.16}$$

Inserting the addition theorems (6.1) and (6.2), and using the orthogonality conditions of the spherical harmonics, we arrive at

$$\lambda_n^V = \frac{a}{2n+1} \tag{6.17}$$

$$\lambda_n^K = -\frac{1}{2(2n+1)} \tag{6.18}$$

$$\lambda_n^{V^Y} = a^2 \frac{2\kappa}{\pi} i_n(\kappa a) k_n(\kappa a) \tag{6.19}$$

$$\lambda_n^{K^Y} = -\frac{2(\kappa a)^2}{\pi} i_n(\kappa a) k_{n+1}(\kappa a) + \frac{2\kappa a n}{\pi} i_n(\kappa a) k_n(\kappa a) + \frac{1}{2} \tag{6.20}$$

For several setups, these values can be checked against the numerical results, and these tests showed very good convergence properties. Taking for example a single charge inside a sphere, the operator matrices reduce to a scalar equation. The convergence of the first component of that system for a certain random choice of the constants ϵ_Σ and λ to the analytical value 2.89 is shown in the following table.

Points	Faces	Value
482	960	2.98
642	1280	2.96
2560	5120	2.91

6.4.2. Numerical recomputation of the free energy of solvation of monoatomic ions

The next test we performed to evaluate the accuracy of our numerical solver was the recomputation of the analytical results for the free energy of solvation of monoatomic ions, which we have discussed in detail in Section 3.5.4. The triangulations of the atomic sphere we employed to this end typically consisted of several hundred to about 3.000 elements, and for meshes of this size, a full computation of the free energy of solvation in the nonlocal cavity model, i.e. a nonlocal reaction field computation

in water followed by a local reaction field computation in vacuum as described in theorem 5.4.2, takes several seconds up to about 2–3 minutes on a typical Pentium IV − class processor.

The results of this recomputation are extremely accurate, as can be seen in Fig. 6.3. with a correlation coefficient between the numerically computed values and the theoretical results from Section 3.5.4 of $r \approx 0.99992$, which can be considered an almost perfect correlation.
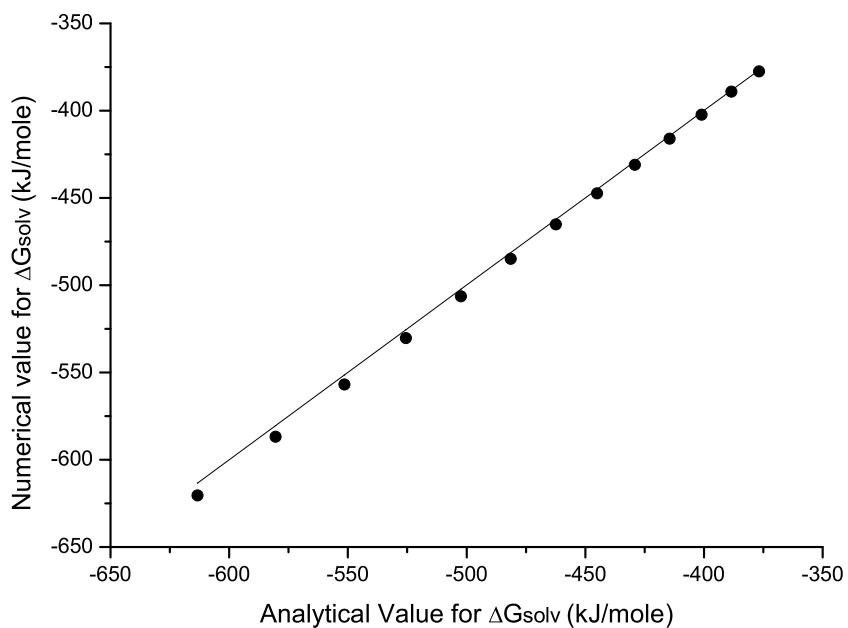
Figure 6.3.: Numerical values for the free energy of solvation as derived in Section 3.5.4 plotted against the numerical results of the boundary element implementation.

7. Results

The results of the numerical tests described in Section 6.4 clearly show that the boundary element solver we have implemented is able to reproduce the analytical results of the theory of nonlocal electrostatics with astonishing accuracy. This convinced us that we were now in a position to apply the techniques developed in this thesis to real–world situations, i.e. to geometries that are far more complex than the trivial spherical monoatomic ions considered so far. To our knowledge, the results described in this section are the very first application of the theory of nonlocal electrostatics to polyatomic systems.

7.1. The free energy of solvation for polyatomic ions and neutral amino acid side–chain analogs

While from a scientific point of view the investigation of polyatomic systems might be of much more interest than that of spherical systems, it is also more problematic in a variety of senses. We have already in detail discussed the analytical and numerical problems that are related to the complicated geometries of molecular surfaces, and have shown in the last chapters how to deal with them in the context of a boundary element approach. But another deeply rooted problem cannot be so easily avoided: comparison to experimental values in the case of polyatomic molecules becomes considerably harder. The main reason for this is that the potentials and fields themselves can currently not be measured with the required accuracy to decide upon the quality of the theoretical results.[1] What typically *can* be measured, though, is the free energy of solvation of the molecule, the quantity we already employed for our investigation of the monoatomic ions. In contrast to the small and spherically symmetric monoatomic systems, though, where we were able to neglect all *nonpolar contributions* to the free energy of solvation like entropic or cavity terms as a very good approximation, these effects begin to play a major role for more complicated geometries. In fact, the nonpolar contributions can sometimes equal or even dominate the polar ones. In addition, the free energy of solvation can not be measured with arbitrary accuracy, posing another problem for a sound comparison of experimental and theoretical values. We therefore have to carefully chose a set of test molecules for which we have both reliable experimental data and well–established theoretical results for the nonpolar contributions at hand.

Of course, several more or less successful models for the nonpolar contributions exist [Uhl37, AM97, HC72, CT99] and can in principle be employed. But when replacing the conventional local theory of electrostatics with the more sophisticated nonlocal one, there is another subtle pitfall involved: the current models for the nonpolar contribution have been designed and their parameters fitted so as to reproduce the *total* free energy of solvation in conjunction with the *conventional local* electrostatics. This means that the parameters of the nonpolar models have been adapted in such a way that they will already compensate at least some of the error of the local polar estimator. This is particularly important when working with molecules from the training sets of the conventional free energy models.

An additional complication arises in the definition of the atom radii. In our discussion in Section 3.5.2 we have argued that the whole concept of an "atom radius" is troublesome at least and that a

---

1 For a possible approach to this problem that might allow the indirect measurement of electric fields close to a planar membrane, see the subsection *"The planar case"* in section 4.2.2.

determination of this somewhat virtual quantity leads to a whole range of problems of its own. For the monoatomic ions we were able to find a physically motivated set of radii in the ones proposed by Åqvist [Å90], but unfortunately that approach does not seem to scale well to polyatomic systems: there is no reason to believe that the effective radii of an atom in a molecule, i.e. in the presence of a chemically nontrivial environment and under the influence of the chemical bonds it participates in, should be describable with the same radius as its monoatomic ion put in water. Thus, in order to determine the effective radii in an Åqvist–like approach, it seems necessary to perform a full free energy perturbation and subsequent radius fitting process as described in [Å90] for each atom in each molecule under investigation. The required amount of work for such a process could probably be significantly reduced by introducing a set of atom types, depending on their chemical environment, and deriving radii only for the atoms in this set, similar in spirit to the **PARSE**–radii set [SSH94], or the **AMBER**–parameter set [PCC+95], but unfortunately it turns out that the interpretation of the radial density functions lying at the heart of the Åqvist–approach (c.f. Section 3.5.2) becomes extremely difficult for polyatomic systems.

We have therefore decided to start with a conceptually much simpler approach: we assume that the atom *classification* in the **AMBER** parameter set [PCC+95] is chemically sound, and thus we assume the same atom types for our computations. But since the values of the radii in the **AMBER** parameter set work well in the context of a *local* electrostatic setting we have to assume that they are in effect **too large:** local electrostatics typically underestimates the potential in water and thus overestimates the energy difference between water and vacuum, which is in effect the electrostatic contribution to the free energy of solvation. This effect is typically countered by increasing the size of the atoms, reducing the values of the potential in vacuum more than in water, and thus decreasing the free energy of solvation. We thus perform our own fit for the radii of the **AMBER** atom types, decreasing the radii from the assumedly overestimated **AMBER** values to the lower bound of the pure *element radii*. As an additional constraint, we demand that the radii for different types of the same element do not vary too much (a value of 0.7 Å is employed in the current implementation).

Similarly, the partial charges of each atom in the molecule still have to be assigned. This is typically also performed using fixed parameter sets, and such an approach is of course possible for nonlocal electrostatics as well. But in order to avoid this parametrization as an additional source of error, we chose to compute the partial charges using the quantum mechanics program **GAMESS** [SBB+93].

Having thus decided upon the general process, we chose a set of neutral amino acid side–chain analogs as training data for the radii. This choice was mainly motivated by two considerations: the obvious importance of amino acids for biomolecular applications and the particular difficulties posed by *neutral* molecules which require much higher precision than ionic molecules of comparable size since the total charge or monopole moment of those molecules vanishes. Therefore, the electrostatic contribution to their free energy of solvation is only due to the higher multipole moments and thus considerably smaller than in the cases of the monoatomic ions we considered so far. But owing to their small size, the nonpolar contribution is not completely dominating the results, so that changes in the electrostatic setting are really reflected in the values of the free energy of solvation.

The final set of neutral training molecules consisted of the amino acid side–chain analogs of `Ser`, `Thr`, `Phe`, `Asn`, `Gln`, and `His` where the backbone has been replaced by a single hydrogen atom (c.f. Fig. 7.2). Those molecules were constructed in `Hyperchem`, then optimized using **GAMESS** at the 6–31 G*–level, which was also used to compute the values of the partial charges of each atom. The atom type radii for these structures were then varied under the constraints described above, and for each choice of radii a triangulation of the molecular surface was performed. The generated triangulations had to be carefully investigated for conforming with the fundamental surface quality measures described

in Section 5.5.1. The quality of the surfaces turned out to be somewhat problematic during the fitting, since for some radii combinations the triangulation procedures we employed (the SES–algorithm from **BALL** and the `SMART` program) ran into numerical instabilities. These cases were identified with the help of the described surface measures and could be resolved using very minor perturbation of the density of probe positions on the surface, the radius of the probe sphere, or the radii of the atom types. In all those cases, we performed additional tests to ensure that the perturbations were really insignificant for the intended results, and only important for the quality of the generated surfaces. In this way it turned out that, as expected, the numerical results seem to be continuous in the employed radii, as long as the resulting molecular surface triangulation has acceptable quality.
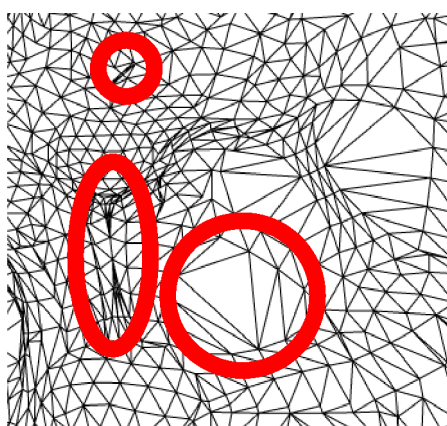
Figure 7.1.: Close–up of a problematic part of the triangulation of trypsin. Encircled in red are some degenerate triangles and an area with large local variation of the element size.

The results of this process can be found in the following table, where all values are given in^2 $\mathrm{kcal}\,/\mathrm{mol}$. The nonpolar values in this table have been computed using the **BALL** implementation of the *Uhlig* model [Uhl37], where care was taken that the same radii were employed for the computation of the polar and the nonpolar part. The experimental data was taken from [WACS81].

The average absolute error of the results is $e_{\mathsf{abs}} \approx 1.17\,\mathrm{kcal}\,/\mathrm{mol}$, the root mean square error $e_{\mathsf{rms}} \approx 1.49\,\mathrm{kcal}\,/\mathrm{mol}$, and the correlation coefficient $r \approx 0.955$. According to [SPSP03], these results can be considered as an *"extremely precise"* prediction of the free energy of solvation, and we are very confident that using a model for the nonpolar contribution that is specifically adapted to the nonlocal theory of electrostatics will allow us to even improve the prediction considerably.

---

2 In this chapter we chose to use the non–SI unit kcal to simplify comparison with the cited reference works for the experimental data and with predictions from conventional local methods which are typically given in $\mathrm{kcal}\,/\mathrm{mol}$.

(a) Serine   (b) Serine analog
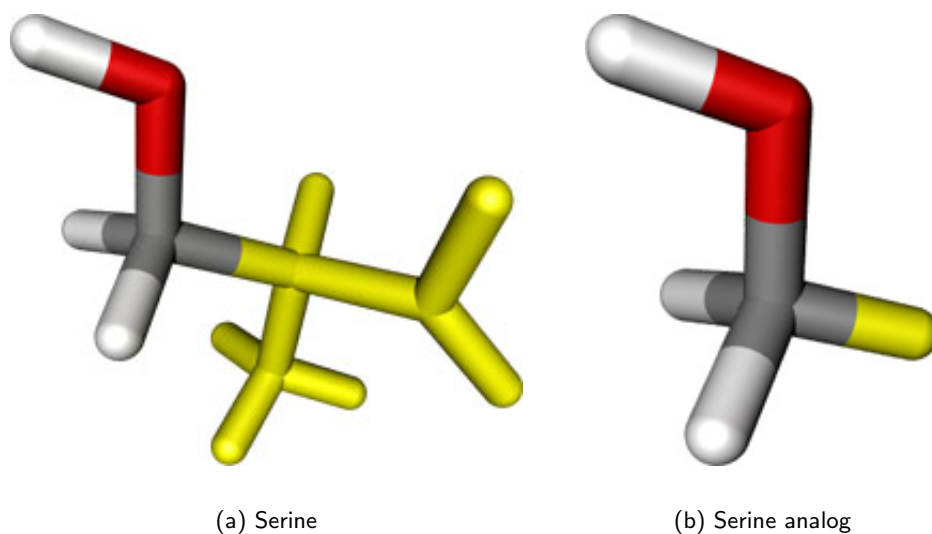
Figure 7.2.: The amino acid analog is generated by replacing the backbone (shown in yellow in Fig. (a)) by a single hydrogen atom.

Amino acid analog	ΔG polar	ΔG nonpolar	ΔG_{total}	ΔG experimental
Ser	-6.87	1.50	-5.36	-5.06
Thr	-7.09	1.65	-5.44	-4.88
Phe	-2.36	2.08	-0.27	-0.76
Asn	-12.93	1.83	-11.09	-9.68
Gln	-13.64	2.02	-11.62	-9.38
His	-11.83	2.01	-9.82	-10.27
Tyr	-11.04	2.16	-8.88	-6.11

While the nice agreement of these optimized values with the experimental data seems to support the theory of nonlocal electrostatics, we still have to exclude the possibility that this is an artifact of the fit. In order to show that the high quality of the results can be reproduced using the radii determined in the fitting process, we applied the technique to a second set of data: a number of polyatomic ions. This set of test data does not possess any additional degrees of freedom or fit parameters, yielding in fact a useful test for the nonlocal theory.

Since we chose a set of ionic molecules with nonvanishing monopole moment as the test set, the corresponding values for the electrostatic contribution to the free energy of solvation will be about one order of magnitude larger than that for the neutrals described above. Thus, the polar term should in these cases clearly dominate the nonpolar contribution, so that a possibly erroneous parametrization of the nonpolar part should not affect our results for the polyatomic ions significantly. On the other hand, the quality of the experimental data is much worse than in the case of the neutrals: a typical estimate of the error of measurement is in the order of 5 to $6\,\mathrm{kcal}\,/\mathrm{mol}$. This can for example be illustrated by comparing the tabulated experimental data found in [CHCT96], [HCT97], and [HCT98]. These papers where written by the same authors and appeared in three consecutive years, but the given data varies significantly to reflect the most current experimental results at the time.

As for the neutral amino acid side–chain analogs, the structures for the ions were generated using Hyperchem and subsequently optimized with the quantum chemistry code from **GAMESS**, which was also employed for the electronic structure computations yielding the values for the partial charges.

Using the radii determined from the amino acid side–chain analogs, we arrived at the results gathered in the following table, where again all data is given in $\mathrm{kcal\,/mol}$, and where the experimental data was taken from [HCT97] and [HCT98].

Ionic molecule	$\Delta G^{\text{total}}_{\text{calc}}$	ΔG experimental
$CH_3NH_3^+$	-73.2	-73
$C_5H_5NH^+$	-63.5	-59
NH_4^+	-86.1	-81
CH_3O^-	-92.2	-95
CH_3S^-	-75.3	-76
$C_6H_5O^-$	-70.2	-72
$C_6H_5S^-$	-70.7	-67

Obviously, in *all* cases the computed values fall well within the reported experimental uncertainty of $\approx 5 - 6\ \mathrm{kcal\,/mol}$. The average absolute error amounts to $e_{\text{abs}} \approx 2.68\ \mathrm{kcal\,/mol}$, the root mean square error to $e_{\text{rms}} \approx 3.19\ \mathrm{kcal\,/mol}$, and the correlation coefficient equals $r \approx 0.963$. These results can be considered as being in excellent agreement with experiment.

We thus were not only able to show the principal or technical applicability of the theory of nonlocal cavity electrostatics to polyatomic systems – an application that seemed completely infeasible in the conventional integro–differential formulation of nonlocal electrostatics, but have also shown that the results that can be obtained with the help of this physically appealing theory are of excellent quality.

7.2. The nonlocal electrostatics of Trypsin

While the results described in the last section are important in their own respect – the computation of solvation quantities for small molecules is a subject receiving much attention in the literature [SPSP03] – our motivation for investigating the theory of nonlocal electrostatics was always a possible future application to *large* biomolecular systems like proteins. While this seemed impossible in the former integro–differential formulation, our purely differential approach in combination with the successfully tested boundary element solver promises to allow for these biologically relevant applications. But in trying to work with systems of the enormous complexity of proteins or other large biomolecules, a number of severe obstacles arises.

The main problem again consists of the properties of a suitable triangulation of the molecules solvent–excluded surface. Not only do the errors or glitches in the meshing procedure become more and more pronounced with growing surface complexity (we often encountered cases of missing triangles, i.e. holes, or even "triangles" with five neighbouring elements). It also becomes painfully apparent that the common triangulation algorithms seem to be more adapted to visualizational purposes: the number of triangles generated tends to become extremely large, with considerable local size and area variability, including degenerate or quasi–degenerate triangles.

While the numerical instabilities due to these non–optimal triangulations might be circumvented by using e.g. mesh–optimization postprocessing routines from the *gts*–library [Pea], or from the **NET-GEN** program [SGG], the sheer size of the mesh in terms of the number of triangles seems to render a numerical solution infeasible: in the currently implemented boundary element method, the main memory requirement stems from the full representation of the system matrices. In the case of the nonlocal model (c.f. theorem 6.3.1 and the following corollary and remark), the system matrix is composed of $9n^2$ floating point values, where n is the number of elements in the triangulation. A typical molecular

surface triangulation adapted to visualizational purposes has on the order of magnitude of 100.000 elements, and using double precision with 8 bytes per value for the system matrices, we would need approximately $8 \times 9 \times 100.000^2$ bytes, equaling approximately 670 GB of RAM[3]. Fortunately, though, it turns out that for boundary element purposes such a fine triangulation is not at all required [JV98].

We thus decided to choose a model example and carefully handcraft the triangulation by using mesh refinement and coarsening techniques from the *gts*–library and the **NETGEN** program, which were also used to repair possible errors in the triangulation or quasi–degenerate triangles. As exemplary molecule, we chose the digestion enzyme *trypsin* taken from the complex structure with its inhibitor *BPTI* which can be found in the PDB database [BWF$^+$00] (PDB-ID 2PTC). The choice of trypsin was mainly due to its importance as a standard example for protein–protein docking techniques [JS95, Lea94, CMJW02], and due to its manageable size of 3223 atoms. The initial triangulation, generated with the **SMART** program, adapted for the use of flat triangles, contained 54.394 nodes and 108.744 triangles. Using the techniques described above, we were able to generate a high quality, but significantly coarsened, mesh from this initial triangulation, containing only 6356 nodes and 12.668 triangles. The results can be seen in Fig. 7.3.

Quantitative assessment of the results in the case of trypsin is unfortunately not as trivial as it is for small molecules. Even if precise values for the free energy of solvation were available, for a system of the size of trypsin the nonpolar contribution will be significant. Thus, any errors in the nonpolar contribution will lead to noticeable errors in the total free energy of solvation, so that we can not decide whether the source of deviations from experimental values would lie in the polar or the nonpolar part. In the future we hope to provide a different test for the application to proteins through the computation of pK$_a$ values – a measure for the free enthalpy of deprotonation – which are directly related to the magnitude of the electrostatic field at the location of the basic and of the acidic side chains. But even before we have such a testing procedure available, we can check whether the results are physically, chemically, and biologically sound in a qualitative sense.

The most obvious feature we would expect from a successful prediction of the nonlocal electrostatic potential – for both, biological and physical reasons – concerns the protein's visibility. Since conventional local computations tend to overestimate the dielectric shielding significantly, the potentials and fields resulting from such an approach will typically be much lower and decay more rapidly with distance than in reality. In fact, a constant shielding of about 78 will often render the potential insignificant at even small distances from the molecule. It is thus to be expected that in a more realistic theoretical framework that includes solvent structure based effects, the potentials and fields will extend much further into space, greatly enhancing the protein's range of visibility. This is consistent with biological considerations: it is well–known that many enzymes work too efficient – in the sense of a large kinetic constant – to assume a purely diffusional approach of their substrate. Therefore, a certain attraction of enzyme and substrate has to be postulated over a certain distance range, and this attraction can only be electrostatic in nature. But using a conventional local approach, the resulting fields would be too weak to explain the observed effect satisfactorily.

Another expected feature of a nonlocal result for a complicated geometry like that of trypsin is more complicated in nature and not as easily interpreted as the overall reduction in shielding described in the last paragraph. This effect is concerned with a nontrivial dependence of the effective local dielectric shielding on the protein's geometry: a water molecule in the bulk, i.e. far away from the perturbing cavity Ω which represents the protein is completely surrounded by other water molecules, all of which

---

3 In a more space efficient implementation using a compressed approximate representation of the system matrices, we can achieve a space requirement of only $\mathcal{O}(n \log(n))$ with approximately the same prefactors. For the same triangulation with about 100.000 triangles, we would thus only require about 0.077 GB or 79 MB.
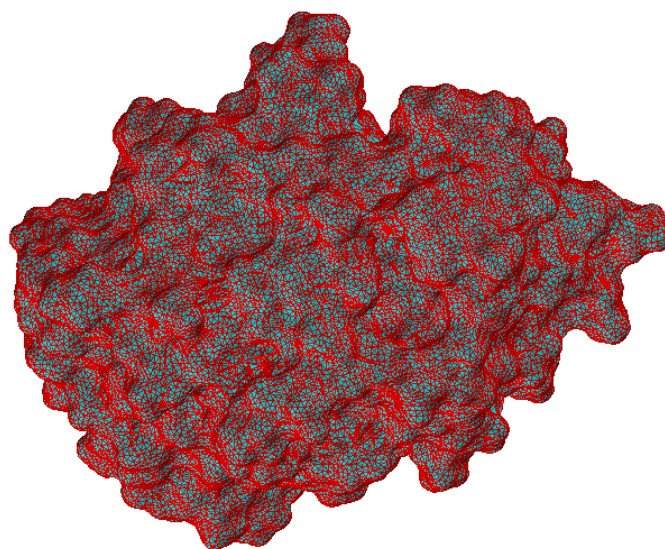
(a) Initial triangulation
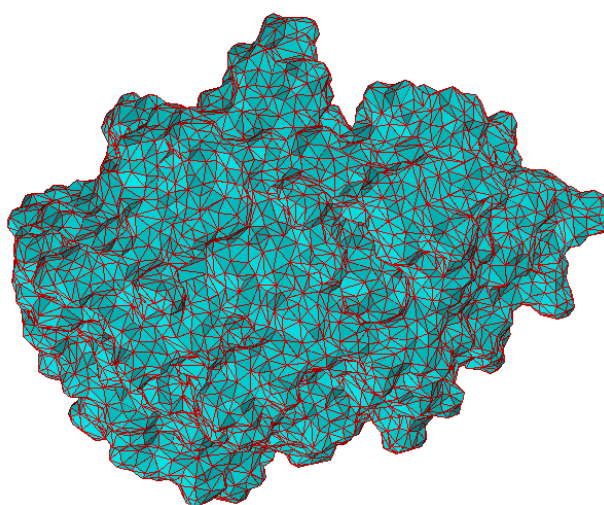
(b) Refined triangulation

Figure 7.3.: Initial and refined triangulation of trypsin. The initial triangulation, shown in (a) contained 54.394 nodes, and 108.744 triangles, several of which were degenerate. In addition, the orientation of 2256 triangles was incorrect. The refined triangulation, with only 6356 nodes and 12.668 triangles, does not suffer from these instabilities.

try to force it into a different direction. Remembering that the reason for the existence of the nonlocal effect lies in the complicated correlations between the water molecules, we thus see that for a water molecule in the bulk, at least part of the nonlocal effect is averaged out over all directions. Therefore, far away from the protein, the local limit is restored. But due to the presence of a cavity in the system, water molecules *close* to the boundary Γ experience a direction–dependent *loss* of correlation since there are no water molecules inside the protein. Being no longer completely surrounded by other water molecules, the nonlocal effect for such a molecule will not average out, and will thus be much more pronounced close to the protein's surface. A strong nonlocal effect causes a weak dielectric shielding, and thus the effective ϵ is expected to be *lower* in the vicinity of the molecular surface. Thus, the *shape* or geometry of the molecular surface will have a nontrivial influence on the behaviour of the dielectric shielding, leading to an enriched electrostatic structure in regions with interesting geometric properties, like for example a protein's binding pocket.

Following this line of thought led us to expect what we call the *parabolic reflector effect* of nonlocal electrostatics: close to surface regions of large inward curvature, the nonlocal effect should allow a certain outward projection of the electrostatic potential, since the shape of the surface acts on the effective dielectric shielding similar to a parabolic reflector. If this hypothetical effect could be confirmed, it might help to explain an important feature of many known docking sites that can not be fully understood in the framework of local electrostatics: the burial of charges deep in the binding pocket. In the conventional local approach, such charges are typically not visible outside the pocket due to the overestimated shielding, and thus could only play a part in the recognition process if the putative binding partner is already entering the active site. Through the – still hypothetical – parabolic reflector effect, nonlocal electrostatics might circumvent this problem since the geometry of the binding pocket might allow for an outward projection of the potential of a buried charge in the active site.

7.2.1. Numerical results for trypsin

Fig. 7.4 gives a first view of the numerical results of the nonlocal cavity model for trypsin. Fig. 7.4(a) shows the solvent–excluded surface around the binding pocket, colored by distance to enhance recognition of the three–dimensional structure. Fig. 7.4(b) shows the contour surfaces of the local electrostatic potential, computed with the Poisson–Boltzmann implementation from the **BALL** framework, for the values $\varphi = 0.1$ V (blue) and $\varphi = -0.1$ V (red), and Fig. 7.4(c) does the same for the nonlocal potential, computed with our boundary element solver. From this plot it is obvious at first glance that the electrostatic visibility of the considered protein – trypsin – in the nonlocal framework is in fact greatly enhanced, just as we had expected: the contour surfaces in the local approximation stick very closely to the molecular surface, while the nonlocal potential extends far into space. Fig. 7.5 shows these contour surfaces from a slightly different perspective.

Fig. 7.4 also shows that the nonlocal electrostatic potential features an interesting structure in the vicinity of the binding pocket: while in the local case, the potential around the active site seems very simple, the nonlocal potential shows an interesting bridge–like structure, where two negative "arms" sticking out of the "wall" of positive potential clearly mark the position of the binding site. This seems to suggest possible anchoring points for a suitably charged binding partner, and as we will soon see, the known inhibitor BPTI indeed has positively charged side chains at the positions of the negative potential contour surfaces in the nonlocal model.

Looking at the contour surfaces of the nonlocal electrostatic potential from different perspectives, we find a remarkable number of potential clouds "floating" above cleft– or dish–like areas of the molecular surface. For a value of $\varphi = -0.1$V, we have gathered several occurrences of this intriguing effect in Fig. 7.6. These findings might be seen as confirmation of the parabolic reflector effect mentioned in
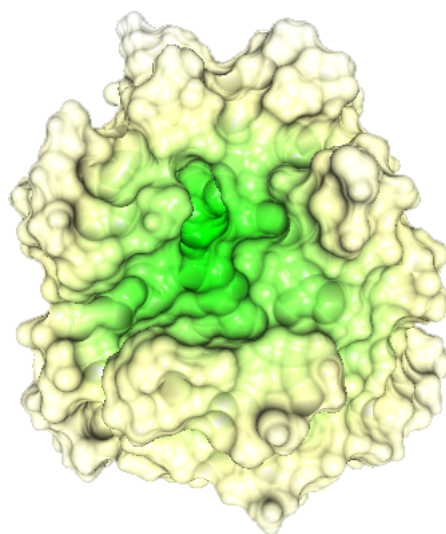
(a) Solvent–excluded surface around the binding pocket of trypsin
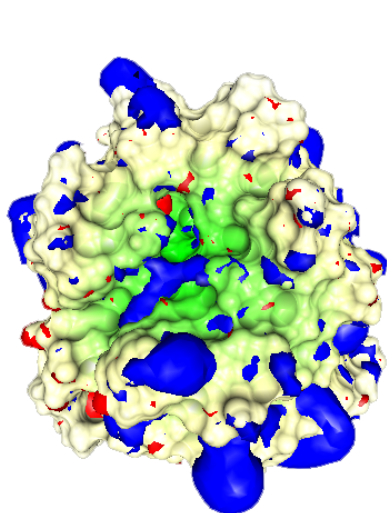
(b) Local potential of trypsin, computed with the **BALL** Poisson–Boltzmann implementation
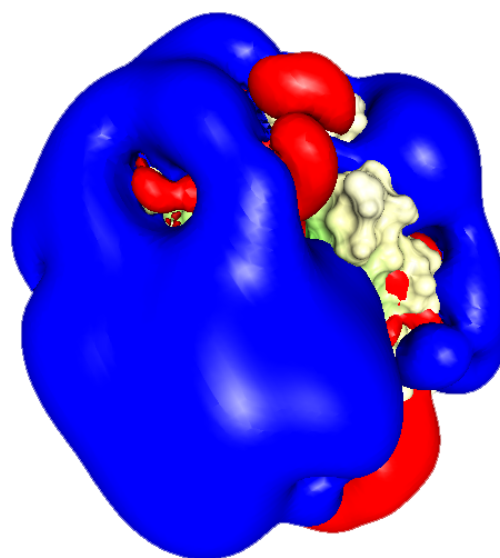
(c) Nonlocal potential of trypsin, computed with the boundary element solver described in this work

Figure 7.4.: Comparison of local and nonlocal potential for trypsin in the region of the binding pocket. Shown in blue is the contour surface of the electrostatic potential φ for a threshold of $\varphi = 0.1\mathrm{V}$, while the red surface corresponds to $\varphi = -0.1\mathrm{V}$. In this representation, the remarkably enhanced visibility of the protein in the nonlocal framework can be clearly demonstrated.
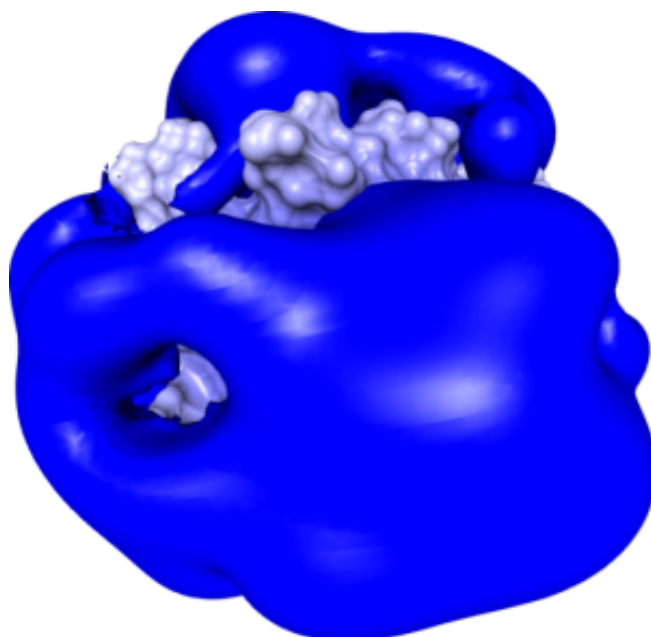
(a) Contour surface of the nonlocal potential of trypsin for the threshold $\varphi = 0.1\text{V}$
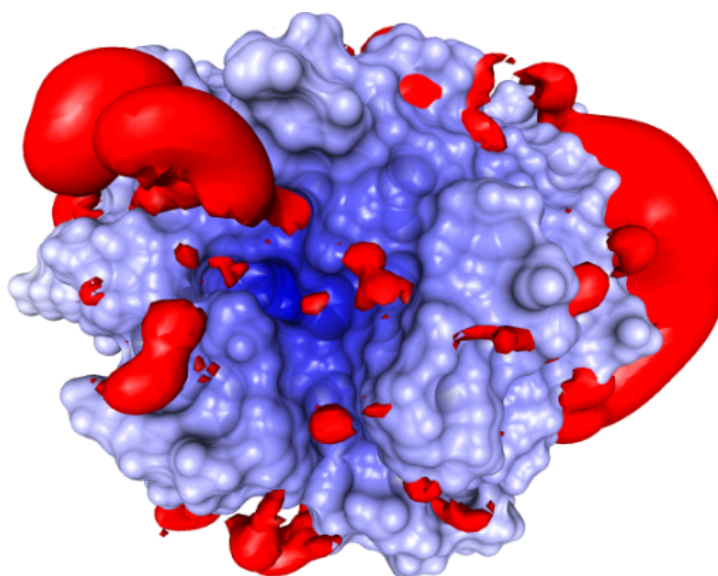
(b) Contour surface of the nonlocal potential of trypsin for the threshold $\varphi = -0.1\text{V}$

Figure 7.5.: Positive and negative contours of the nonlocal potential of trypsin.

(a)
(b)

(c)
(d)
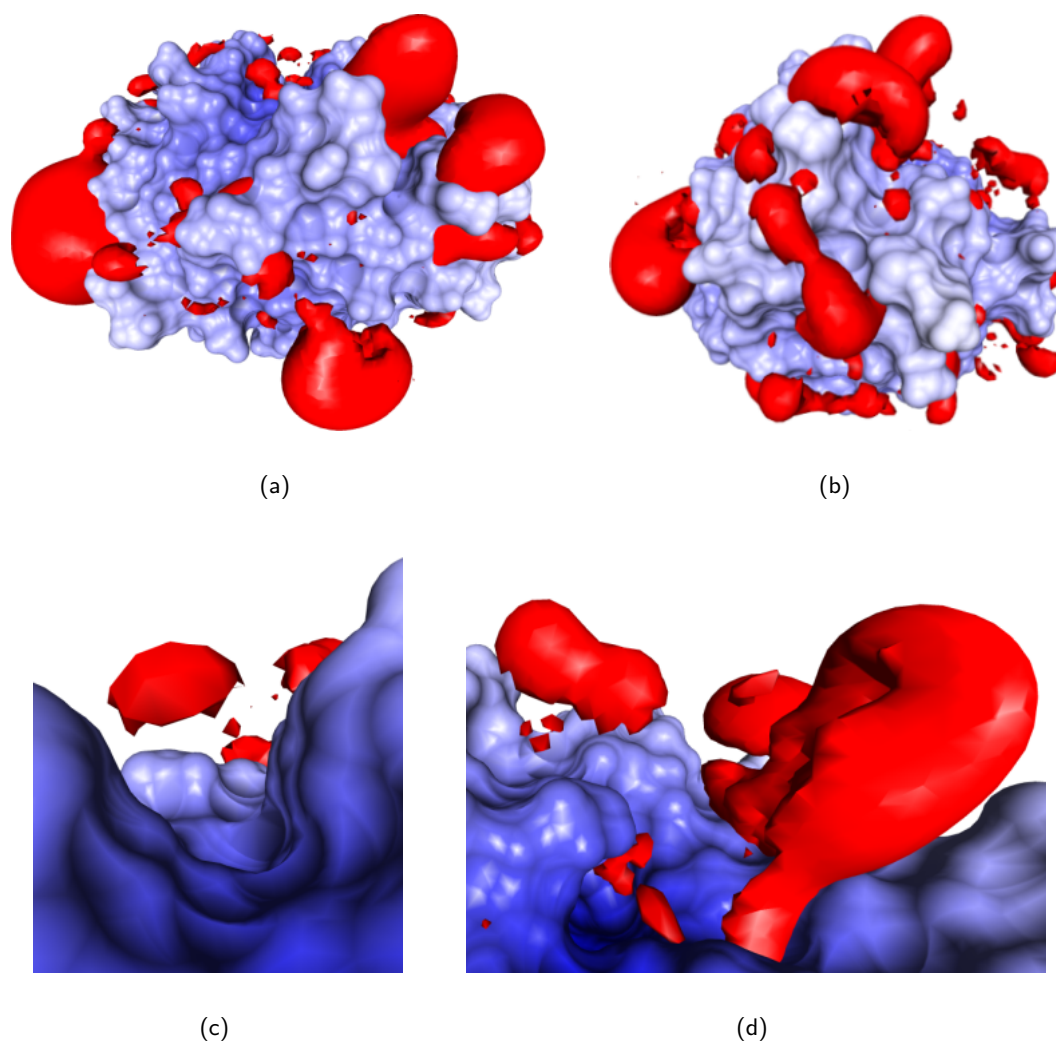
Figure 7.6.: Different perspectives of the parabolic reflector effect in the contour surface of the nonlocal electrostatic potential of trypsin for a threshold of $\varphi = -0.1\mathrm{V}$. Figs. (c) and (d) show close–ups of interesting areas of Figs. (a) and (b). The parabolic reflector effect is clearly recognizable in the floating potential clouds above areas of high inward surface curvature.

the last section – the outward projection of the potential of charges close to boundary regions with large inward curvature. The magnitude of this effect seems remarkable: in many cases, clearly distinct structures in the potential are projected a noticeable distance away from the molecular boundary.

Interestingly, we observed a very good agreement of the nonlocal potential with the electronic structure of the known inhibitor BPTI. Fig. 7.7(a) shows the position of the inhibitor in the contour of the nonlocal electrostatic potential, where the inhibitor has been colored according to its partial charges. Three positively charged side chains dominate the electrostatics of BPTI in the vicinity of trypsin's binding pocket, the arginines 17 and 39 and lysine 15. These three residues are shown in their respective positions in the final complex in plot 7.7(b). Figs. 7.8 and 7.9 finally show the remarkable correspondence of the negative potential clouds with the positions of the positive inhibitor side chains, fitting nicely into the "negative holes" of the positive potential wall of trypsin. Particularly remarkable is the influence of the parabolic reflector effect: some of the negative potential clouds are projected into the positively charged side chains with astonishing precision. But while this agreement of the

153

nonlocal potential with the electrostatics of BPTI is indeed remarkable, the interpretation of this result is not as straightforward as it might seem at first glance. In particular it might be tempting to assume that the compatibility of the nonlocal electrostatic potential of trypsin with BPTI would guarantee a favorable value for the predicted free energy of binding as must be the case in reality since we know that complex formation takes place. But upon binding, the geometry of the system under consideration changes: with the inhibitor approaching the binding pocket, we would have to include an additional cavity Ω_{BPTI}, influencing the solvent–solvent correlation in a nontrivial way. Even more importantly, in its final position in the active site, BPTI will have pushed out most if not all of the water molecules. Information about the electrostatic properties of the final complex can thus not be simply inferred from the nonlocal electrostatic potential of unbound trypsin we have discussed in this section and would rather require a similar computation of the potential of the complex as a whole. What the information about the potential around the binding pocket in the unbound state *can* possibly provide, though, is insight into the arrangement inhibitor's orientation in an early stage of the binding process: with the strong outward projection of the electrostatic structure of the binding pocket, approaching molecules might feel a significant torque rotating it into an orientation suitable for later binding. In the near future, additional studies will be performed to investigate whether this hypothesis can be confirmed.
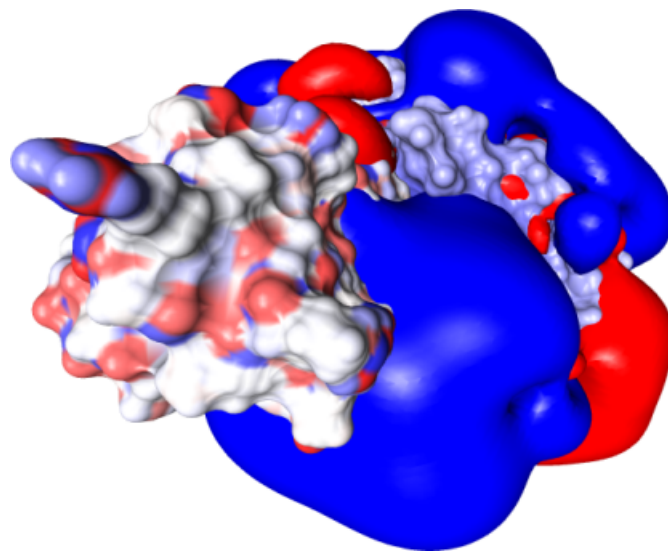
(a)
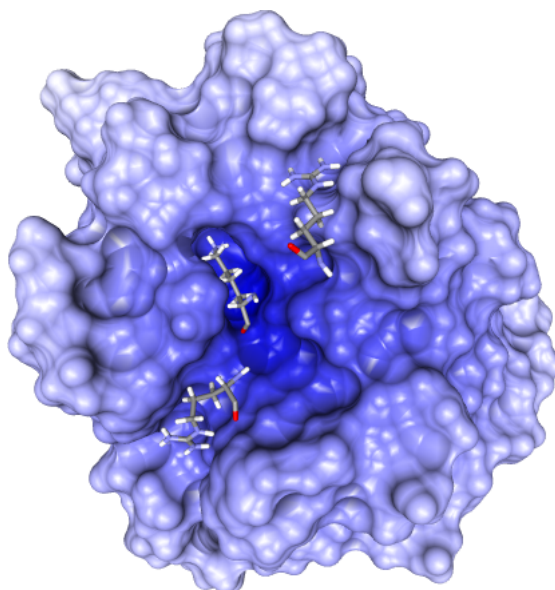
(b)

Figure 7.7.: Complex between trypsin and BPTI. For clarity, only the positively charged residues of the inhibitor close to the binding pocket are shown in (b).
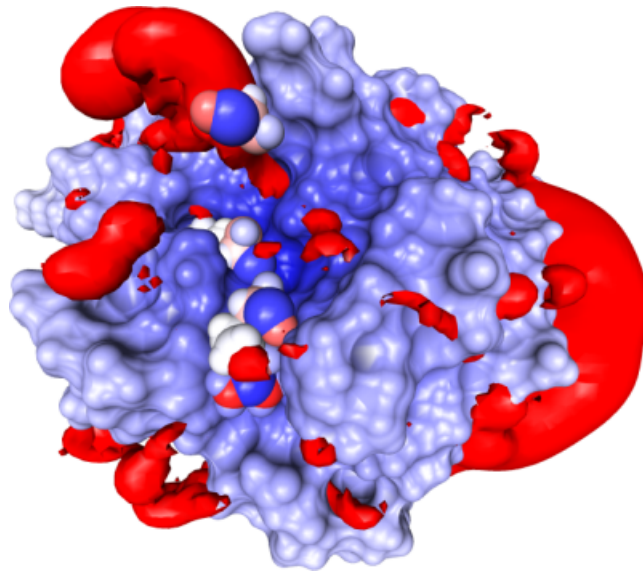
(a) Positions of arginine 17, arginine 39, and lysine 15 in the contour surface of the nonlocal electrostatic potential of trypsin with $\varphi = -0.1$ V.
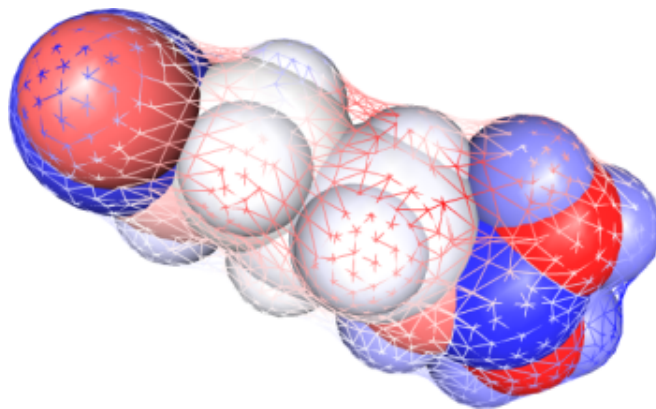
(b) Correlation of the partial charges of arginine 39 with the nonlocal electrostatic potential of trypsin. The Van–der–Waals spheres of this residue are colored by atom charge, while the wireframe SES (the triangles) are colored by the value of the nonlocal potential. Thus, areas with red triangles and a blue sphere or vice versa correspond to favorable interactions.

Figure 7.8.: The positively charged side chains arginine 17, arginine 39, and lysine 15 of BPTI in the vicinity of trypsin's binding pocket fit nicely into the predicted electrostatic potential.
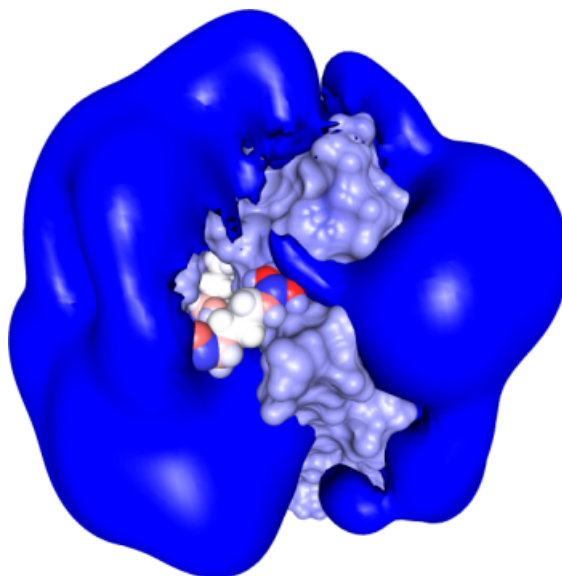
(a) Binding pocket of trypsin.
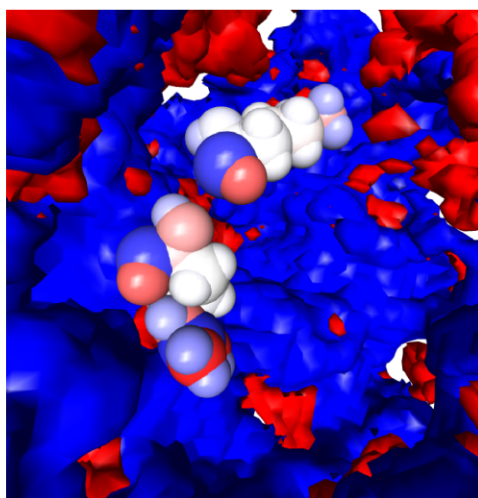
(b) View from the inside of trypsin (not shown) on the nonlocal potential contour surfaces. The two "inner" side chains Lys 15 and Arg 17 keep "below" the onset of the positive potential above the molecular surface.

Figure 7.9.: Positioning of the positively charged side chains Arginine 17, Arginine 39, and Lysine 15 of BPTI in the vicinity of the binding pocket of trypsin. The contour surfaces correspond to values of the nonlocal electrostatic potential of $\varphi = 0.1$ V (blue) and $\varphi = -0.1$ V (red). Apparently, the positively charged side chains fit very well into the "holes" of the large "wall" of positive potential around the active site.

8. Conclusion and Outlook

This thesis was concerned with the application of nonlocal electrostatics to biomolecular systems. As we have seen in the last chapters, nonlocal electrostatics provides a very promising theoretical framework for the inclusion of solvent–solvent correlation effects into the computation of electrostatic fields and potentials in ponderable media – a feature that is essential for computations in a biomolecular setting, where almost every reaction takes place in the presence of water, and where the length scales of the potentials are on the same order of magnitude as the water–water correlations which are mediated through the hydrogen bond network.

Nonlocal electrostatics in its conventional formulation arises as a straight–forward generalization (c.f. Chapter 3) of the classical local theory of electrostatics (c.f. Chapter 2). If a suitable model for the functional form of the water–water correlation (c.f. Section 3.4) is supplied, analytical solutions for the values of the potentials and fields in this setting can in principle be sought. Prior to the work presented in this thesis, though, analytical or numerical solutions were only possible for the most trivial kind of geometries like spheres or cylindrical systems. Using the analytical solution for the spherically symmetric case and a special model for the water–water correlation (c.f. Section 3.5.1) we were able to clearly demonstrate the advantages of a nonlocal approach for the prediction of solvation quantities: at least for monoatomic ions the quality of computed free energies of solvation could be improved by several orders of magnitude compared to a straight–forward local approach. Thus, the lack of efficient solution procedures for more involved geometries was seen as a major obstacle for a detailed understanding of the electrostatic properties of biomolecular systems in solution.

We have therefore reinvestigated the derivation of nonlocal electrostatics as a whole, and were able to reformulate the underlying equations for a wide class of models for the water–water correlation in a fashion much more amenable to analytical and numerical means – a system of coupled linear partial differential equations of second order (c.f. Chapter 4). The equations appearing in this system are commonplace in related areas of mathematical or theoretical physics – the Poisson and Laplace equation are already present in the local theory while the Yukawa equation has been used to describe shielding phenomena e.g. in plasma physics [LR96]. This reduction in itself seems like a beneficial achievement for the further investigation of electrostatics in its nonlocal description: not only does the simplified presentation allow for the application of standard solution techniques from the mathematical theory of partial differential equations, but also leads to a considerable number of additional advantages. These include the applicability of the complete apparatus for studying the properties of partial differential equations and of conclusions that can be drawn from the appearance of the equations in different theoretical contexts, like in plasma physics. An example of such a conclusion is the interpretation of the Yukawa equation – the nonlocal differential material equation coupling the displacement field to the electric field in the water – as an inhomogeneous Debye–Hückel equation (c.f. Section 4.2.2) which allows us to interpret the effect of the water on the electrostatic potential as that of a virtual cloud of counterions in a linearized Poisson–Boltzmann setting, where the nonlocal displacement field acts as a virtual charge distribution. This astonishing relationship is an important example for interesting insight into the mechanisms of electrostatics in solution qualitatively different from those that could be inferred from the more approximate local theory. In addition, the novel formulation derived in this work hints at several possible generalizations, the most important one of which is the inclusion of counterion effects into the considerations. We have shown (c.f. 4.2.2) that

the nonlocal material equation can accommodate a Poisson–Boltzmann term, and that a linearized Debye–Hückel description should only manifest itself in a shifted correlation length of the nonlocal response. Thus, a careful investigation of this property might allow for the inclusion of counterion effects in the linearized Debye–Hückel framework into nonlocal electrostatics using *exactly the same* solution techniques derived in this work, including the boundary element solver.

But while the derivation of a simpler formulation of nonlocal electrostatics is thus in itself a valuable aim of its own, a real contribution to our understanding of biomolecular processes would require the availability of efficient and accurate numerical techniques for the computation of electrostatic properties in the nonlocal framework. We have thus investigated several approaches from the numerical theory of partial differential equations, leading us to the choice of a boundary element method. As described in detail in Chapter 5, developing a boundary element solver requires considerably more analytical preparations of the equations than other standard techniques, like for example finite difference methods, but the achievable accuracy, the existence of highly efficient approximation techniques for this class of solvers, and the fact that all required computations are only performed on the molecular *boundary*, clearly justify these efforts. In Chapter 5, we have thus derived the necessary representation formulae for nonlocal electrostatics using the Lorentzian model of the water–water correlation, and cast the system into the required system of boundary integral equations. These equations can then be discretized and converted into a linear system of equations (c.f. 5.7.1), which can in turn be solved using standard techniques from numerical linear algebra. We have implemented the set–up and solution of these equations, yielding the nonlocal potentials on the molecular boundary, and the representation formulae to compute the potentials anywhere in space from the potential on the surface, for both local and nonlocal electrostatics (c.f. Chapter 6), and all subsequent tests against numerical results showed excellent agreement.

Being thus convinced that the numerical implementation indeed yields results with a very high accuracy, we were now for the first time in a position to apply the theory of nonlocal electrostatics to polyatomic systems – an application that seemed unfeasible in the conventional formulation due to the complexity of the geometry. But for this process, a number of additional problems had to be addressed, like assessing and improving the quality of the molecular surface triangulations or the choice of a suitable set of radii (c.f. 6). Using the radii as fit parameters in a reasonable range, we were able to reproduce the experimental values of the free energy of solvation for some neutral amino acid side–chain analogs with extremely high precision. The radii obtained in this fit were tested with a set of small polyatomic ions, and in all cases, the computed results were well within the experimental error margin (c.f. Chapter 7).

We concluded that the application of nonlocal electrostatics to geometrically nontrivial situations yields astonishingly accurate results. An application to large biomolecular systems like proteins thus seemed highly desirable, but is problematic due to the size of the triangulation: the memory requirements of the currently implemented boundary element technique with exact representation of the full system matrices seemed forbiddingly large. But using a particular post-processed triangulation, we were finally able to compute the nonlocal electrostatic potential for the digestion enzyme trypsin (c.f. Section 7.2). A detailed analysis of this result showed that indeed all expected features of an enhanced treatment of the electrostatic properties of water, like the enhanced visibility or a more interesting electrostatic structure of the binding pocket, were achieved. In our analysis we found that the structure of the nonlocal electrostatic potential agrees very well with the known position of the trypsin inhibitor BPTI in the trypsin – BPTI complex. In particular, it is known that three positively charged side chains in BPTI dominate the electrostatics of the complex, and these side chains fit with a very high accuracy into small "holes" of negative potential in an otherwise largely positive domain. In fact, the clouds of negative potential seem to be precisely *projected into* the positive side chains by what we call the

parabolic reflector effect. This novel feature of the nonlocal approach applied to proteins tells us that in the vicinity of clefts or pockets in the molecule, the nonlocal perturbation effect can be focused similar in spirit to the focusing of a parabolic reflector. In this way, the shielding effect of the water is significantly reduced, and thus, the potential of buried charges in the binding pocket can be projected outward of the binding site. This effect might help to explain feature of the binding process that seems mysterious in the framework of the local theory: the visibility of charges inside the binding pocket early in the binding process.

Owing to these successes we conclude that we were able to show that nonlocal electrostatics is indeed able to capture the *structural effects* inside the solvent in a nonetheless *continuum description*. Obviously, such an improvement has the potential to yield valuable theoretical insight into the behavior of electrostatically influenced biomolecular systems in an aqueous environment. This might for example lead to significant enhancement of the energetic scoring functions in use in many different fields of computational biology and computational chemistry, like in docking, folding, or structure optimization algorithms. In addition, the more accurate solvation quantities determined in the framework of nonlocal electrostatics might provide interesting descriptors for *Quantitative Structure–Activity Relationship (QSAR)* based methods, which determine correlations between structural properties of a substance and its biological activity. But apart from these applications as an ingredient for techniques requiring energetic information, the conclusions we can draw from the way the water influences electrostatic properties in our model might help us to understand several of the still unsolved questions of biomolecular interactions. The most prominent example that comes to mind is the enormous efficiency of enzymatic reactions that can not be completely understood when considering the fast decay of the fields in a *local* setting. In the nonlocal case we can not only conclude that the potential extends much farther into space than in the local description, but we also have to consider the implications of the parabolic reflector effect, which might greatly enhance the visibility of buried charges.

In order to fully explore the potential benefits of a nonlocal description, some future work in this field will have to be performed, both on the theoretical and the application side. From the numerical point of view, the most important improvement would be the application of a matrix compression scheme, leading to the so–called *fast boundary element methods.* The most popular approaches to this problem are either Wavelet–based [DPS94, DPS93, LS99] or use a hierarchical cluster decomposition [BR03, Gie97, GR87, HN89, Sau00]. This class of methods is based on the smoothness of the kernels of the boundary integral operators, which allows for an approximation of the integrals based on the property that regions on the molecular surface that are far away from each other have nearly vanishing mutual contribution to the entries in the system matrices. Neglecting sufficiently small entries, we arrive at a matrix containing many zeros, and by reordering the system it is possible to achieve a certain hierarchical matrix structure. These matrices are called $\mathcal{H}$–matrices [Hac99], can be represented in $\mathcal{O}(n \log(n))$ space and allow for efficient matrix–vector multiplication and solution of linear systems. Implementing such a scheme for our purposes would require deriving the necessary approximations for the integral kernels and the numerically stable and efficient implementation of hierarchical matrices and their operations, but the resulting advantages would clearly be worth the effort. As we have shown in Section 7.2, a suitable matrix compression scheme might reduce the required amount of RAM for a nonlocal computation for a triangulation with 10^5 triangles from approximately 670 GB to about 79 MB. This would not only enable us to consider much larger systems and much finer triangulations, it might also help with the problematic requirement of ensuring the described quality measures for the mesh.

In addition, we will assess the quality of the approximation of the boundary conditions we had to employ in order to close the system of boundary integral equations (c.f. Section 5.4.1). To achieve this, we would like to reconsider the derivation of the set of equations by studying a vector–valued

system related to the one we reduced to a scalar system in Section 4.2.2. For this system we could derive a boundary element method with exact representation of the boundary conditions, which, due to the vectorial quantities involved, would necessarily have higher memory and run–time demands than the current system but could be used for comparison with our approximate implementation.

An important advancement of the theory that can be obtained with low theoretical cost and can probably be achieved without the need for modifications of the numerical solver is the inclusion of linearized counterion effects in a Debye–Hückel like description. Apart from the theoretical insight this might yield, it would also be an important prerequisite to the application to DNA electrostatics where counterion effects are known to play a prominent role [SYYT01, YMvH89, KN00, FNvG02].

Some more down–to–earth questions that should be addressed in the future contain the parametrization of suitable radii and charges for nonlocal electrostatics. It is obvious that a determination of the radii by means of molecular dynamics simulations as described in Section 3.5.2 and the determination of the charges by quantum mechanical electronic structure computations as described in Chapter 7 is much too costly to be performed with each input structure prior to the determination of the electrostatic potential. The conventional sets of radii and charges like the PARSE parameter set on the other hand are designed to be adapted to a local description, and at least for the radii there is no reason to assume that they carry over to the nonlocal case without any modifications. Therefore, a re-parametrization of the known parameter sets for the requirements of the nonlocal theory seems desirable. Alternatively, the determination of the radii for all atom types in a given parameter set might be performed independently of the theory of nonlocal electrostatics, for example by trying to determine cut–offs in the electronic densities computed with the help of a quantum mechanics code.

On the application side, a thorough investigation of the nonlocal effects is the next logical step. As soon as a more space efficient implementation is available it will be possible to generate the electrostatic potentials for a large number of test cases, including nearly arbitrarily sized proteins. This would for example allow to systematically study the implications of nonlocal electrostatics for the visibility and binding specificity of proteins. Especially interesting in this respect seems the investigation of the question whether the parabolic reflector effect – the out–propagation of the potential of buried charges – might explain some common features of active regions of enzymes – in particular the occurrence of the well–known binding pockets. A thorough study of this effect might thus not only contribute to our knowledge of the protein binding process, but also to the elucidation of fundamental questions of the architecture of enzymes.

In our opinion, the results of this thesis have shown that the theory of nonlocal electrostatics can indeed be fruitfully employed for an improved quantitative analysis of biomolecular systems. But a more accurate prediction of electrostatic quantities in aqueous solutions than is possible in the conventional local framework would have far–reaching consequences in a wide number of fields of sciences apart from computational biology, mostly in physics and chemistry. We thus hope that the current and – hopefully – future successes will convince researchers from computational biology as well as from other fields of science to reconsider this beautiful and appealing theory that had been nearly abandoned due to its seemingly overwhelming complexity. If in this way the transition from the currently established "homogeneous continuum" approximation to what might be called a "structured continuum" – a continuum that is not blind to correlations among its "constituents" – might be advanced, our current understanding of many electrostatically dominated processes on a molecular scale might be drastically changed, and we hope that the work presented in this thesis – the reformulation of the equations of nonlocal electrostatics, the development of an efficient and accurate boundary element solver, and the first and successful application to non–trivial real–world examples from computational biology – might serve as at least a small step along this road.

A. The Fourier transform

The Fourier transform is an invaluable tool with applications in many different branches of science, including the theory of partial differential equations. Its popularity in this field is mostly due to an astonishing property: the Fourier transform allows to convert linear differential equations into algebraic equations, which are usually much more convenient to study and solve. In this chapter we will give the necessary definitions and briefly discuss those properties of the transform that are important for our application. A more detailed treatment can be found in virtually any book on integral transforms or in any monograph about mathematical methods in physics (see e.g. [CH96] or [RHB02]).

A.1. Definition

The Fourier transform is clearly the most important integral transform of mathematical physics. In a certain sense, it decomposes a signal into its frequency components, i.e. it projects onto a space of complex exponential functions $e^{i\boldsymbol{k}\boldsymbol{r}}$, or sine and cosine waves. The definition of this transform allows for a certain degree of freedom: the sign of the exponent $e^{\pm i\boldsymbol{k}\boldsymbol{r}}$ can be exchanged as long as it differs in the transform *from* and *to* Fourier space, and the product of the normalization factors from and to Fourier space must equal $\frac{1}{(2\pi)^d}$, where d is the dimensionality of the transform. For this work, we will choose the *symmetric normalization convention*, and a positive exponent for the back transform. With these conventions, our definition of the Fourier transform looks as follows:

Definition A.1.1 (The Schwartz–space of test functions). Let $\Omega \subset \mathbb{R}^n$ be a domain in $\mathbb{R}^n$, and let $\varphi : \Omega \to \mathbb{C}$ be an infinitely differentiable test function[1] $\varphi \in C_0^\infty(\Omega)$. Let

$$p_{k,r}(\varphi) := \sup_{\boldsymbol{r} \in \Omega} \left(|\boldsymbol{r}|^k + 1 \right) \sum_{|\alpha| \leq r} |\partial^\alpha \varphi(\boldsymbol{r})| \quad k, r, n \in \mathbb{N}, n \neq 0 \tag{A.1}$$

The *Schwartz–space* $\mathcal{S}(\Omega)$ is defined as the subspace of all *sufficiently fast decaying* infinitely differentiable $\varphi \in C_0^\infty(\Omega)$, in the sense that

$$p_{k,r}(\varphi) < \infty \quad \forall k, r \tag{A.2}$$

Definition A.1.2 (The Fourier transform). Let $f(\boldsymbol{r}) \in \mathcal{S}(\mathbb{R}^n)$. Then, the following integral exists for all $\boldsymbol{r} \in \mathbb{R}^n$:

$$\hat{f}(\boldsymbol{k}) := \frac{1}{\sqrt{2\pi}^d} \int\limits_V d\boldsymbol{r} f(\boldsymbol{r}) e^{+i\boldsymbol{k}\boldsymbol{r}} \tag{A.3}$$

and the resulting function $\hat{f}(\boldsymbol{k})$, the *Fourier transform* of $f(\boldsymbol{r})$ is again in $\mathcal{S}(\mathbb{R}^n)$. The transform can be inverted by the adjoint operator

$$f(\boldsymbol{r}) := \frac{1}{\sqrt{2\pi}^d} \int\limits_V d\boldsymbol{k} \hat{f}(\boldsymbol{k}) e^{-i\boldsymbol{k}\boldsymbol{r}} \tag{A.4}$$

---

1 The reasons for this nomenclature will become clear in Chapter C

the *inverse Fourier transform*. The Fourier operator

$$\mathcal{F} : \mathcal{S}(\mathbb{R}^n) \to \mathcal{S}(\mathbb{R}^n) \tag{A.5}$$

$$\mathcal{F}[f(\boldsymbol{r})] := \hat{f}(\boldsymbol{k}) \tag{A.6}$$

is a linear unitary homeomorphism.

From now on, we will only consider the case $d = 3$.

A.1.1. Radial Fourier transforms

We will often consider systems with rotational symmetry, i.e. systems that only depend on the radius $r = \|\boldsymbol{r}\|$. In these cases, we will usually use spherical coordinates, which can lead to significantly simplified integrals.

Considering a function $f(\boldsymbol{r})$ in spherical coordinates $\boldsymbol{r} = (r, \vartheta, \varphi)$ that depends only on the radius r, the Fourier transform becomes:

$$\hat{f}(k) \;=\; \frac{1}{\sqrt{2\pi}^3} \int\limits_0^{2\pi} d\varphi \int\limits_0^{\pi} d\vartheta \, \sin(\vartheta) \int\limits_0^{\infty} dr \, r^2 f(r) e^{i\boldsymbol{k}\boldsymbol{r}} \tag{A.7}$$

$$=\; \frac{2\pi}{\sqrt{2\pi}^3} \int\limits_0^{\infty} dr \, r^2 \int\limits_0^{\pi} d\vartheta \, \sin(\vartheta) f(r) e^{ikr \cos(\vartheta)} \tag{A.8}$$

$$=\; \frac{1}{\sqrt{2\pi}} \int\limits_0^{\infty} dr \, r^2 f(r) \left[\sin(\vartheta) \frac{-1}{ikr \sin(\vartheta)} e^{ikr \cos(\vartheta)} \right]_0^{\pi} \tag{A.9}$$

$$=\; \frac{1}{\sqrt{2\pi}} \int\limits_0^{\infty} dr \, r^2 f(r) \left\{ \frac{i}{kr} \left(e^{-ikr} - e^{ikr} \right) \right\} \tag{A.10}$$

$$=\; \frac{1}{\sqrt{2\pi}} \int\limits_0^{\infty} dr \, r^2 f(r) \left\{ 2\frac{\sin(kr)}{kr} \right\} \tag{A.11}$$

$$=\; \sqrt{\frac{2}{\pi}} \int\limits_0^{\infty} dr \, r^2 f(r) \frac{\sin(kr)}{kr} \tag{A.12}$$

A.1.2. Parseval's Theorem

An important property of the Fourier transform is its unitarity. This follows from the important theorem of Parseval:

$$\int\limits_{-\infty}^{\infty} d\boldsymbol{r} f(\boldsymbol{r})^* g(\boldsymbol{r}) \;=\; \int\limits_{-\infty}^{\infty} d\boldsymbol{k} \hat{f}^*(\boldsymbol{k}) \hat{g}(\boldsymbol{k}) \tag{A.13}$$

where $*$ denotes complex conjugation.

Using $f = g$ in (A.13), it follows:

$$\int\limits_{-\infty}^{\infty} d\boldsymbol{r} |f(\boldsymbol{r})|^2 \;=\; \int\limits_{-\infty}^{\infty} d\boldsymbol{k} |\hat{f}(\boldsymbol{k})|^2 \tag{A.14}$$

$$\Leftrightarrow \|f\|_{\mathcal{L}^2} \;=\; \|\hat{f}\|_{\mathcal{L}^2} \tag{A.15}$$

where $\|\|_{\mathcal{L}^2}$ denotes the $\mathcal{L}^2$-norm.

A.1.3. Convolution theorem

Let us denote the *convolution* of two functions f, g with $f * g$,

$$(f * g)(\boldsymbol{r}) := \int d\boldsymbol{r}' f(\boldsymbol{r}) g(\boldsymbol{r} - \boldsymbol{r}') = \int d\boldsymbol{r}' f(\boldsymbol{r} - \boldsymbol{r}') g(\boldsymbol{r}').$$

Using the definition of the Fourier transform (A.4), it follows:

$$
\frac{1}{\sqrt{2\pi}^3} \int\limits_{\mathbb{R}^3} d\boldsymbol{k} (f * g)(\boldsymbol{r}) e^{-i\boldsymbol{k}\boldsymbol{r}} = \frac{1}{\sqrt{2\pi}^3} \int\limits_{\mathbb{R}^3} f(\boldsymbol{r}') \int\limits_{\mathbb{R}^3} g(\boldsymbol{r} - \boldsymbol{r}') \times
$$
$$
\times e^{-i\boldsymbol{r}\boldsymbol{k}} d\boldsymbol{r} d\boldsymbol{r}' \tag{A.16}
$$

And with the substitution

$$\boldsymbol{R} := \boldsymbol{r} - \boldsymbol{r}'$$

this becomes:

$$
(\text{A.16}) = \frac{1}{\sqrt{2\pi}^3} \int\limits_{\mathbb{R}^3} f(\boldsymbol{r}') \int\limits_{\mathbb{R}^3} g(\boldsymbol{R}) \times
$$
$$
\times e^{-i(\boldsymbol{R}+\boldsymbol{r}')\boldsymbol{k}} d\boldsymbol{r}' d\boldsymbol{R} \tag{A.17}
$$
$$
= \frac{1}{\sqrt{2\pi}^3} \int\limits_{\mathbb{R}^3} d\boldsymbol{r}' f(\boldsymbol{r}') e^{-i\boldsymbol{r}'\boldsymbol{k}} \times
$$
$$
\times \frac{\sqrt{2\pi}^3}{\sqrt{2\pi}^3} \int\limits_{\mathbb{R}^3} d\boldsymbol{R} g(\boldsymbol{R}) e^{-i\boldsymbol{R}\boldsymbol{k}} \tag{A.18}
$$
$$
= \sqrt{2\pi}^3 \hat{f}(\boldsymbol{k}) \hat{g}(\boldsymbol{k}) \tag{A.19}
$$

Therefore, if we denote the Fourier transform by $\mathcal{F}$, we have:

$$\mathcal{F}(f * g) = \sqrt{2\pi}^3 \mathcal{F}(f)\mathcal{F}(g) \tag{A.20}$$

(A.20) is the important *convolution theorem* for the Fourier transform.

A.1.4. Derivatives in Fourier space

The probably most useful property of the Fourier transform which explains its importance especially in the field of physics is the fact that it relates linear differential equations in physical space to algebraic equations in Fourier space. This can easily be seen in the following way:

$$
\boldsymbol{\nabla} f(\boldsymbol{r}) = \boldsymbol{\nabla} \frac{1}{\sqrt{2\pi}^3} \int\limits_{\mathbb{R}^3} d\boldsymbol{k} \hat{f}(\boldsymbol{k}) e^{-i\boldsymbol{k}\boldsymbol{r}} \tag{A.21}
$$
$$
= \frac{1}{\sqrt{2\pi}^3} \int\limits_{\mathbb{R}^3} d\boldsymbol{k} \hat{f}(\boldsymbol{k}) \boldsymbol{\nabla} e^{-i\boldsymbol{k}\boldsymbol{r}} \tag{A.22}
$$
$$
= \frac{1}{\sqrt{2\pi}^3} \int\limits_{\mathbb{R}^3} d\boldsymbol{k} \underbrace{(-i\boldsymbol{k}\hat{f}(\boldsymbol{k}))}_{(*)} e^{-i\boldsymbol{k}\boldsymbol{r}} \tag{A.23}
$$

and from (A.23) we can conclude that $(*)$ is the Fourier transform of $\boldsymbol{\nabla} f(\boldsymbol{r})$:

$$\boldsymbol{\nabla} f(\boldsymbol{r}) \;=\; -i\boldsymbol{k}\,\mathcal{F}(f). \tag{A.24}$$

Thus, when transforming an equation into Fourier space, we can replace $\boldsymbol{\nabla}$ by $-i\boldsymbol{k}$:

$$\boldsymbol{\nabla} \overset{\mathcal{FT}}{\rightarrow} -i\boldsymbol{k} \tag{A.25}$$

A.1.5. Symmetry properties

$f(\boldsymbol{r})$	$\mathcal{F}(f)$
real and even	real and even
real and odd	imaginary and odd
imaginary and even	imaginary and even
complex and even	complex and even
complex and odd	complex and odd
real and asymmetrical	complex and asymmetrical
imaginary and asymmetrical	complex and asymmetrical
real even plus imaginary odd	real
real odd plus imaginary even	imaginary

B. Distributions as generalized functions

In this section, we will give a brief introduction to the theory of distributions. The distribution concept generalizes the function concept in a natural way, and is one of the cornerstones of the modern theory of partial differential equations. Of special importance for our treatment of nonlocal electrostatics is Dirac's δ–distribution, which we will define and investigate. For a more detailed treatment from a physicist's perspective, the reader is referred to [Vla03], while the classical rigorous discussion can be found in [GS77].

B.1. Motivation

During the advance of quantum mechanics, it became more and more apparent that the well–known classical function concept had to be extended to allow for the mathematical treatment of certain "pathological" situations in physics. When trying to define a derivative for discontinuous functions exhibiting jumps, Dirac was lead to hand–wavingly introduce a new kind of *generalized function*, which was "much more singular" than is allowed in the context of classical functions:

> "One cannot go far in the development of the theory [...] without needing a notation for that function of [...] x that is equal to zero except when x is very small, and whose integral through a range that contains the point $x = 0$ is equal to unity. We shall use the symbol $\delta(x)$ to denote this function, i.e., $\delta(x)$ is defined by
>
> $$\delta(x) = 0 \text{ when } x \neq 0, \text{ and } \int\limits_{-\infty}^{\infty} \delta(x) = 1.$$
>
> Strictly, of course, $\delta(x)$ is not a proper function of x, but can be regarded only as a limit of a certain sequence of functions. All the same one can use $\delta(x)$ as though it were a proper function for practically all the purposes of quantum mechanics without getting incorrect results. One can also use the differential coefficients of $\delta(x)$, namely $\delta'(x), \delta''(x), \ldots$, which are even more discontinuous and less 'proper' than $\delta(x)$ itself."[Dir27]

While it was obvious that such a function could not exist in the classical context[1], the enormous success and the popularity the Dirac δ–distribution gained in theoretical physics lead mathematicians to formulate a strict theory of such pathological objects. This succeeded in the 1940s, when Laurent Schwartz, building on prior work by S. L. Sobolev[Sob36], explained distributions as linear functionals over the space of "test functions"[Sch51].

B.2. Definitions

Definition B.2.1 (Operator). An *operator* $A : K \rightarrow J$ is a mapping from a vector space K into a vector space J. Usually, at least K is a *function space*.

---

1 To see this, one could e.g. consider the value of the integral in the above quote; since changing the integrand on a set of measure zero does not change the value of the integral in the theory of Lebesgue integration, setting $\delta(x = 0) = 0$ leads to a contradiction.

Definition B.2.2 (Functional). A *functional* $\mathcal{L}: V \to \mathbb{R}$ is a real– or complex–valued function on a vector space V, where V is usually a function space.

Example B.2.1 (Energy functional over the unit sphere). Let $\mathcal{S}^2$ be the unit sphere, $C^1(\mathcal{S}^2)$ the space of differentiable functions over $\mathcal{S}^2$. Then,

$$E: C^1(\mathcal{S}^2) \to \mathbb{R}$$
$$E[f] = \int_{\mathcal{S}^2} \|\boldsymbol{\nabla} f\|^2 d\boldsymbol{r}$$

is called the *energy functional* over the unit sphere.

Looking again at the hand–waving definition of the Dirac δ–distribution in [Dir27], it becomes clear that $\int_{\mathbb{R}} \delta(x) f(x)\, dx = f(0)$, i.e. the Dirac δ–distribution induces a *linear functional*

$$\delta: \mathcal{L}^1(\mathbb{R}) \to \mathbb{R}$$
$$\delta[f] \mapsto f(0) \tag{B.1}$$

where $\mathcal{L}^1(\mathbb{R})$ is the space of Lebesgue–integrable functions over $\mathbb{R}$.

Definition B.2.3 (Space of test functions). $\mathcal{D}(\Omega) := C_0^\infty(\Omega)$, the space of all infinitely differentiable complex valued functions with compact support in Ω, is called the space of *test functions*.

Definition B.2.4 (Distribution). A continuous linear functional $F: \mathcal{D}(\Omega) \to \mathbb{C}$ on the space of test functions $\mathcal{D}(\Omega)$ is called a *distribution*. The space of distributions is denoted by $\mathcal{D}'(\Omega)$.

An important special case are the so-called *regular distributions*, which are induced by continuous functions:

Definition B.2.5 (Regular Distribution). To each continuous function $f: \Omega \to \mathbb{C}$, we can uniquely assign a distribution $F \in \mathcal{D}'(\Omega)$ through the relation $F[\varphi] := \int_\Omega f\varphi\, dx \;\; \forall \varphi \in \mathcal{D}(\Omega)$. A distribution $F \in \mathcal{D}'(\Omega)$ that can be defined in such a way is called a *regular distribution*.

Remark B.2.1. Even though the Dirac δ–distribution is *not* a regular distribution, its action on a test function φ is often symbolically denoted as

$$\delta[\varphi] =: \int_\Omega \delta(x)\varphi(x)\, dx = \varphi(0) \tag{B.2}$$

Definition B.2.6 (The δ_y–Distribution). Using the notation from remark B.2.1, we generalize the Dirac δ–distribution to

$$\delta_y[\varphi] = \int_\Omega \delta(x-y)\varphi(x)\, dx = \varphi(y)$$

B.3. Derivatives of distributions

The importance of regular distributions lies in the way we generalize operations on continuous functions to distributions: usually, the operation is declared on distributions in such a way that in the special case of a regular distribution the classical operation is recovered. Most importantly for us, this allows the definition of the derivative of a distribution: let $F \in \mathcal{D}'(\Omega)$ be a regular distribution, i.e.

$F[\varphi] = \int_\Omega f\varphi\,dx$ for some continuous function $f : \Omega \to \mathbb{C}$. If a certain partial derivative $\partial^\alpha f$ of the generating function exists, then we can conclude using partial integration:

$$\int_\Omega (\partial^\alpha f)\,\varphi\,dx = (-1)^{|\alpha|} \int_\Omega f\,(\partial^\alpha \varphi)\,dx =: G[\varphi]$$

since $\varphi \in C_0^\infty(\Omega)$. Obviously, the right hand side of this equation generates a new regular distribution $G \in \mathcal{D}'(\Omega)$, which can be interpreted as the of the regular distribution F. Since in the definition of G, all derivatives are acting on the well–behaved test function φ, we can generalize this relation to regular distributions for which classically, the derivative $\partial^\alpha f$ would *not* exist. This motivates the following generalization to all distributions $F \in \mathcal{D}'(\Omega)$:

Definition B.3.1 (Derivative of a distribution). For each distribution $F \in \mathcal{D}'(\Omega)$, the partial derivative ∂^α of order $|\alpha|$ is defined as

$$(\partial^\alpha F)[\varphi] := (-1)^{|\alpha|} F[\partial^\alpha \varphi] \quad \forall \varphi \in \mathcal{D}(\Omega) \tag{B.3}$$

By virtue of definition B.3.1 each distribution possesses derivatives of arbitrary degree $|\alpha|$. Therefore, they form the ideal basis for a modern theory of partial differential equations, not troubled by the typical harsh smoothness conditions required by the classical theory. If a differential equation does not admit a classical solution, it may still possess a solution in the distributional sense[2]. This allows to describe situations that make sense from a physical point of view (e.g. non–continuous pressure fields), but could not be handled using the classical theory of partial differential equations.

B.4. Tensor product of distributions

The *tensor* or *direct product* $u \otimes v$ of two functions $u\colon \mathbb{R}^n \to \mathbb{C}$, $v\colon \mathbb{R}^m \to \mathbb{C}$, which is defined as

$$(u \otimes v)(x, y) := u(x)v(y) \quad \forall x \in \mathbb{R}^n,\, y \in \mathbb{R}^m$$

creates a new function $w\colon \mathbb{R}^{n+m} \to \mathbb{C}$ from u and v with the remarkable property that functions from two possibly different function spaces are mapped to a function in a third one. We can easily generalize this concept to regular distributions: let $F \in \mathcal{D}'(\mathbb{R}^n)$ and $G \in \mathcal{D}'(\mathbb{R}^m)$ be regular distributions with

$$F[\varphi] = \int_{\mathbb{R}^n} f(x)\varphi(x)\,dx \quad \forall \varphi \in \mathcal{D}(\mathbb{R}^n)$$

$$G[\psi] = \int_{\mathbb{R}^m} g(y)\psi(y)\,dy \quad \forall \psi \in \mathcal{D}(\mathbb{R}^m)$$

For $\varphi \in \mathcal{D}(\mathbb{R}^{n+m})$, we define the direct product of the regular distributions F and G as defined above as

$$(F \otimes G)[\varphi] := \int_{\mathbb{R}^n} f(x)\left(\int_{\mathbb{R}^m} g(y)\varphi(x, y)\,dy\right) dx \tag{B.4}$$

Looking at equation (B.4), we see that for regular distributions $(F \otimes G)[\varphi]$ is equivalent to $F[G[\varphi(x, .)]]$, where $\varphi(x, .)$ denotes the value of G for the test function $y \mapsto \varphi(x, y)$ for fixed value of x. This observation allows to define the tensor product for arbitrary distributions:

Definition B.4.1. Let $F \in \mathcal{D}'(\Omega), G \in \mathcal{D}'(\Sigma)$. The *tensor product* or *direct product* $F \otimes G \in \mathcal{D}'(\Omega \otimes \Sigma)$ is defined as

$$(F \otimes G)[\varphi] := F[G[\varphi(x, .)]] \quad \forall \varphi \in \mathcal{D}'(\Omega \otimes \Sigma) \tag{B.5}$$

---

2 This is often called the *weak* sense

B.5. Convolution of distributions

With the help of the tensor product (B.5), we can now generalize the *convolution* of two functions $f, g : \mathbb{R}^n \to \mathbb{C}$ with the property that the support of f is bounded:

$$(f * g)(x) := \int_{\mathbb{R}^n} f(x - y) g(y) \, dy \quad \forall x \in \mathbb{R}^n \tag{B.6}$$

to the space of distributions. Starting again with two regular distributions $F, G \in \mathcal{D}'(\Omega)$, F having bounded support

$$F[\varphi] = \int_{\Omega} f(x) \varphi(x) \, dx \quad \forall \varphi \in \mathcal{D}(\Omega)$$

$$G[\varphi] = \int_{\Omega} g(x) \varphi(x) \, dx \quad \forall \psi \in \mathcal{D}(\Omega)$$

the obvious definition of the convolution $F * G$ is given by

$$(F * G)[\varphi] := \int_{\Omega} \left\{ \int_{\Omega} f(\xi) g(x - \xi) \, d\xi \right\} \varphi(x) \, dx \tag{B.7}$$

Introducing the new variable $\eta := x - \xi$, this equation becomes

$$(F * G)[\varphi] := \int_{\Omega} \int_{\Omega} f(\xi) g(\eta) \varphi(\xi + \eta) \, dx \, d\xi \tag{B.8}$$

Recalling equation (B.5), we notice that (B.8) is equivalent to

$$(F * G)[\varphi] = \int_{\Omega} \int_{\Omega} f(\xi) g(\eta) \varphi(\xi + \eta) \, dx \, d\xi$$
$$= (F \otimes G)[\tilde{\varphi}] \tag{B.9}$$

with

$$\tilde{\varphi}(x, y) := \varphi(x + y)$$

This allows us to define the convolution for all kinds of distributions, when at least one of them has bounded support:

Definition B.5.1. Let $F, G \in \mathcal{D}'(\Omega)$ and let F have bounded support. Then, the *convolution* $F * G$ of F and G,

$$(F * G)[\varphi] := (F \otimes G)[\tilde{\varphi}] \quad \forall \varphi \in \mathcal{D}(\Omega) \tag{B.10}$$
$$\text{with} \quad \tilde{\varphi}(x, y) := \varphi(x + y) \quad \forall x, y \in \Omega$$

defines a distribution $(F * G) \in \mathcal{D}'(\Omega)$.

Lemma B.5.1. *From the definition of the convolution of two distributions $F, G \in \mathcal{D}'(\Omega)$, we can infer the following important properties:*

(i) $F * G = G * F$ (commutativity)

(ii) $\forall \alpha \in \mathbb{N}, |\alpha| > 0 : \partial^\alpha (F*G) = (\partial^\alpha F)*G = F*(\partial^\alpha G)$

(iii) $\delta * F = F * \delta = F$

Proof.

(i) This property follows trivially from the definition of the convolution.

(ii) $\partial^\alpha (F*G)[\varphi] \underset{\text{(B.3)}}{=} (-1)^{|\alpha|} (F*G)[\partial^\alpha \varphi(x,.)]$

$\underset{\text{(B.10)}}{=} (-1)^{|\alpha|} F[G[\partial^\alpha \varphi(x,.)]]$

$\underset{\text{(B.3)}}{=} F[(\partial^\alpha G)[\varphi(x,.)]]$

$\underset{\text{(B.10)}}{=} F*(\partial^\alpha G)$

and similarly for $(\partial^\alpha F)*G$

(iii) $(\delta * F)[\varphi] \underset{(1)}{=} (F*\delta)[\varphi]$

$\underset{\text{(B.10)}}{=} (F \otimes \delta)[\tilde\varphi]$

$\underset{\text{(B.5)}}{=} F^x[\delta^y[\tilde\varphi(x,y)]]$

$\underset{\text{(B.1)}}{=} F^x[\tilde\varphi(x,0)]$

$= F[\varphi(x+0)]$

$= F[\varphi]$

where F^x and δ^y denotes, that F is applied to φ with respect to the argument x and δ^y with respect to y.

$\square$

B.6. The Fourier transform of distributions

Generalizing the Fourier transform to the space of distributions is a more complicated task, and in fact, the common definition does not apply to arbitrary distributions, but rather to certain well–behaved subset. To characterize this subset, it is necessary to recall the definition of the Schwartz–space $\mathcal{S}(\Omega)$ in A.1.1, which we defined as the space of sufficiently fast decaying infinitely differentiable test functions. Since in the classical sense we defined the Fourier transform as a linear homeomorphism on the Schwartz space, it makes sense to restrict its generalization to distributions to the subset of distributions on $\mathcal{S}(\Omega)$. This idea is made precise in the following definition

Definition B.6.1 (Tempered distributions). A *tempered distribution* is a linear continuous functional

$$T : \mathcal{S}(\Omega) \to \mathbb{C}$$

on the Schwartz–space of test functions. The space of tempered distributions on Ω is denoted by

$$\mathcal{S}'(\Omega)$$

With the help of $\mathcal{S}'(\mathbb{R}^n)$, we can now finally give the generalization of the Fourier transform to at least an important subset of the space of distributions:

B. Distributions as generalized functions

Definition B.6.2 (The Fourier transform for tempered distrubutions). Let $T \in \mathcal{S}'(\mathbb{R}^n)$. The *Fourier transform* of T is declared by

$$(\mathcal{F}T)[\varphi] := T[\mathcal{F}\varphi] \quad \forall \varphi \in \mathcal{S}(\mathbb{R}^n)$$

Then, $\mathcal{F}T \in \mathcal{S}'(\mathbb{R}^n)$ is again a tempered distribution on $\mathbb{R}^n$, generalizing the linear operator $\mathcal{F}$ to a linear operator

$$\mathcal{F} : \mathcal{S}'(\mathbb{R}^n) \to \mathcal{S}'(\mathbb{R}^n)$$

Theorem B.6.1 (Fourier transform of a Dirac δ–distribution). *The Dirac δ–distribution is obviously a tempered distribution:*

$$\delta_y[\varphi] = \varphi(y) \quad \forall \varphi \in \mathcal{S}'(\mathbb{R}^n)$$

and can thus be Fourier transformed to yield:

$$\mathcal{F}\delta_y = \frac{1}{\sqrt{2\pi}^3} e^{i\,\boldsymbol{k}\cdot\boldsymbol{y}} \tag{B.11}$$

As an important special case,

$$\mathcal{F}\delta_0 = \frac{1}{\sqrt{2\pi}^3} \tag{B.12}$$

Proof. Let $\varphi \in \mathcal{S}'(\mathbb{R}^n)$. Then,

$$(\mathcal{F}\delta_y)[\varphi] = \delta_y[\mathcal{F}\varphi] \tag{B.13}$$

$$= \delta_y \left[\frac{1}{\sqrt{2\pi}^3} \int_{\mathbb{R}^3} d\boldsymbol{r}\,\varphi(\boldsymbol{r}) e^{i\boldsymbol{k}\boldsymbol{r}} \right] \tag{B.14}$$

$$= \frac{1}{\sqrt{2\pi}^3} \int_{\mathbb{R}^3} d\boldsymbol{r}\,\varphi(\boldsymbol{r}) e^{i\,\boldsymbol{y}\cdot\boldsymbol{r}} \tag{B.15}$$

The right hand side of this equation is no longer dependent on any free variable, since application of the Dirac δ effectively removed the dependence on $\boldsymbol{k}$. Thus, the term is a functional on the space $\mathcal{S}(\mathbb{R}^n)$, i.e. a tempered distribution. In fact, it is even a *regular distribution* with the generating function

$$\frac{1}{\sqrt{2\pi}^3} e^{i\,\boldsymbol{y}\cdot\boldsymbol{r}}$$

In the distributional sense, we can thus conclude that the Fourier transform of the distribution δ_y equals the regular distribution generated by $\frac{1}{\sqrt{2\pi}^3} e^{i\,\boldsymbol{y}\cdot\boldsymbol{r}}$. Since it typically helps our imagination to think of the Fourier transform of a distribution as of a function in Fourier space, it is more common to replace the free variable $\boldsymbol{r}$ by $\boldsymbol{k}$, which concludes our proof. $\qquad\square$

C. Fundamental solutions and Green's functions

Solving a given linear system of equations is – at least conceptually – easy: if an inhomogeneous system

$$\underline{\underline{A}} x = y$$

has a unique solution, it is sufficient to invert the matrix $\underline{\underline{A}}$ to yield the inverse $\underline{\underline{A}}^{-1}$, from which x can easily be computed as

$$x = \underline{\underline{A}}^{-1} y$$

Obviously, a generalization of this concept to the case of linear systems of *differential equations* would be very useful. To this end, we need to find an equivalent of the inverse matrix $\underline{\underline{A}}^{-1}$ for a linear differential operator $\mathcal{L}$.

C.1. The fundamental solution

Definition C.1.1. For a given linear partial differential operator $\mathcal{L}$, a solution U^* of

$$\mathcal{L} U^* = \delta$$

with $U^* \in \mathcal{D}'(\Omega)$ and δ being the Dirac δ–distribution is called a *fundamental solution* of $\mathcal{L}$.

Given a special fundamental solution U_0^* of $\mathcal{L}$, all fundamental solutions U^* of $\mathcal{L}$ can be written in the form

$$U^* = U_0^* + H$$

with $H \in \mathcal{D}'(\Omega)$ being an arbitrary solution to the homogeneous problem $\mathcal{L} H = 0$. The importance of the fundamental solution for the theory of partial differential equations can now be understood by recognizing that the inhomogeneous differential equation $\mathcal{L} U = F$ with $U, F \in \mathcal{D}'(\Omega)$ can be solved as follows:

Theorem C.1.1. *Let $\mathcal{L}$ be a linear differential operator, $U^* \in \mathcal{D}'(\Omega)$ a fundamental solution of $\mathcal{L}$, and $U, F \in \mathcal{D}'(\Omega)$. Then, the inhomogeneous linear partial differential equation*

$$\mathcal{L} U = F$$

is solved by

$$U = U^* * F$$

where $*$ denotes the convolution operator (c.f. B.5.1).

Proof. Let $U = U^* * F$. Inserting this equation into the differential equation $\mathcal{L} U = F$, it follows

$$
\begin{aligned}
\mathcal{L} U \quad &= \quad \mathcal{L}\left(U^* * F\right) \\
&\underset{B.5.1(1)}{=} \quad \left(\mathcal{L} U^*\right) * F \\
&\underset{B.5.1(3)}{=} \quad \delta * F \\
&\underset{B.5.1(3)}{=} \quad F
\end{aligned}
$$

$\square$

Therefore, the knowledge of the fundamental solution for a particular differential operator allows us to solve the corresponding inhomogeneous differential equation for *any arbitrary* inhomogeneity term $F \in \mathcal{D}'(\Omega)$.

Theorem C.1.2 (Malgrange–Ehrenpreis). *Any linear differential equation of order $|\alpha|$ with constant coefficients $a_\alpha \in \mathbb{C}$*

$$\sum_{|\alpha| \leq m} a_\alpha \partial^\alpha U = F$$

with $U \in \mathcal{D}'(\mathbb{R}^n), F \in \mathcal{D}'(\mathbb{R}^n)$, where F is a given inhomogeneity or source term, has a fundamental solution.

C.1.1. The Green's function

According to Section C.1, the fundamental solution of a given differential operator $\mathcal{L}$ is not uniquely determined due to the additivity with respect to solutions of the homogeneous equation $\mathcal{L}H = 0$. Since the $\mathcal{L}$ is considered linear, we have for $H' := \alpha H$ with arbitrary $\alpha \in \mathbb{R}$

$$\mathcal{L}H' = \mathcal{L}(\alpha H) = \alpha \mathcal{L}H = 0$$

and thus H' is a solution to the homogeneous equation as well. Thus, if one such H exists, and if U_0^* is a fundamental solution for $\mathcal{L}$, then $U_\alpha^* := U_0^* + \alpha H$ is as well, allowing us to construct infinitely many fundamental solutions to the same differential operator.

It is important to realize that this high degree of arbitrariness is not introduced by the concept of the fundamental solution, but is rather inherited from the properties of the solutions of inhomogeneous differential equations, to which we can always add any arbitrary solution of the corresponding homogeneous equation. But this seems at first glance to contradict our use of the solutions of partial differential equations in modeling physical quantities like – in our case – the electric field, which are in our experience uniquely determined, if possibly up to certain gauge factors. Resolving the non–uniqueness to yield a physically meaningful function is then achieved by requiring that the solution fulfills certain observed *boundary conditions*, which hopefully exclude all but one particular solution to the given problem.

Definition C.1.2 (The Green's function). A fundamental solution U^* to a given linear differential operator $\mathcal{L}$ that fulfills a certain set of boundary conditions on a given geometry is called the *Green's function* of $\mathcal{L}$ for that particular geometry.

Of special interest are the so–called *free–space Green's functions*, which are the Green's functions of $\mathcal{L}$ in the absence of any interfering boundaries, i. e. without any additional requirements on the boundary conditions. The Green's function for a particular geometry is then typically found by taking the free–space Green's function $\mathcal{F}$ and adding a homogeneous solution H to $\mathcal{L}$ such that $\mathcal{F} + H$ fulfills the boundary conditions on that particular geometry.

Remark C.1.1 *(Nomenclature).* In the physics literature it is common to use the terms free–space Green's function and fundamental solution interchangeably, even though according to the precise definition given above, *all* Green's functions are fundamental solutions. Typically, the distinction is irrelevant or could be easily determined from the context.

C.1.2. The fundamental solution of the Laplace operator

The clearly most important fundamental solution in mathematics and physics is that of the Laplacian, $\mathcal{G}^L$, solving

$$\Delta \mathcal{G}^L = \delta$$

Assuming that $\mathcal{G}^L$ will finally be a classical function, we can drop the general distribution notation. Since the Laplacian and the right hand side of the equation – the Dirac δ – distribution in the representation of remark B.2.1 – are then seen to be rotation invariant, we can simplify the computation using spherical coordinates where we have for the Laplacian of a spherically symmetric function $\varphi(r)$

$$\Delta\varphi(r) = \frac{1}{r^2}\frac{\partial}{\partial r}\left[r^2\frac{\partial\varphi}{\partial r}\right]$$

Expressing the Dirac δ–distribution in spherical coordinates requires a bit of thought. While it might seem that the three–dimensional $\delta(\boldsymbol{r})$ could be replaced by the one–dimensional $\delta(r)$ applied to just the radius function r since $\boldsymbol{r} = \boldsymbol{0} \Leftrightarrow r = 0$, this would yield an incorrect normalization:

$$\int_{\mathbb{R}^3}\delta(r)d\boldsymbol{r} = \int_0^{2\pi}\int_0^{\pi}\int_0^{\infty}r^2\sin(\vartheta)\delta(r)d\phi\,d\vartheta\,dr \tag{C.1}$$

$$= 2\pi\left\{\int_0^{\pi}\sin(\vartheta)d\vartheta\right\}\left\{\int_0^{\infty}r^2\delta(r)\,dr\right\} \tag{C.2}$$

$$= 2\pi\left[\cos(\vartheta)\right]_0^{\pi}\int_0^{\infty}r^2\delta(r)\,dr \tag{C.3}$$

$$= 4\pi\underbrace{\int_0^{\infty}r^2\delta(r)\,dr}_{=0} \tag{C.4}$$

but the definition of the δ–distribution requires

$$\int_{\mathbb{R}^3}\delta(\boldsymbol{r})d\boldsymbol{r} = 1$$

Therefore, expressing the three–dimensional δ–distribution in spherical coordinates[1] introduces an additional normalization factor, yielding

$$\delta(\boldsymbol{r}) = \frac{\delta(r)}{4\pi r^2}$$

With the above explanations, we see that to determine the fundamental solution of the Laplace operator we have to solve the equation

$$\Delta\varphi(r) = \delta(\boldsymbol{r}) \tag{C.5}$$

$$\Leftrightarrow \frac{1}{r^2}\frac{\partial}{\partial r}\left[r^2\frac{\partial\varphi}{\partial r}\right] = \frac{\delta(r)}{4\pi r^2} \tag{C.6}$$

$$\Leftrightarrow \frac{\partial}{\partial r}\left[r^2\frac{\partial\varphi}{\partial r}\right] = \frac{\delta(r)}{4\pi} \tag{C.7}$$

Integrating once over r yields

$$r^2\frac{\partial\varphi}{\partial r} = \int_{\mathbb{R}}\frac{\delta(r)}{4\pi}\,dr = \frac{1}{4\pi} + C_1 \tag{C.8}$$

$$\Leftrightarrow \frac{\partial\varphi}{\partial r} = \frac{1}{4\pi r^2} + \frac{C_1}{r^2} \tag{C.9}$$

---

1 The situation becomes slightly more delicate when considering $\delta(\boldsymbol{r} - \boldsymbol{\xi})$ instead of just $\delta(\boldsymbol{r})$

and integrating again over r, we arrive at

$$\varphi(r) = -\frac{1}{4\pi r} - \frac{C_1}{r} + C_2 \tag{C.10}$$

$$= -\left\{ \frac{1}{4\pi} + C_1 \right\} \frac{1}{r} + C_2 \tag{C.11}$$

The value of C_2 is an additive gauge constant, obviously fulfilling $\Delta C_2 = 0$, and can thus be set to zero for the free–space Green's function. To determine C_1, we check that the Laplacian of $\varphi(r)$ indeed behaves like a Dirac δ–distribution, by computing

$$\int_{\mathbb{R}^3} \Delta\varphi(r)\, d\boldsymbol{r} = \int_0^{2\pi} \int_0^{\pi} \int_0^{\infty} r^2 \sin(\vartheta) \Delta\varphi(r)\, d\phi\, d\vartheta\, dr \tag{C.12}$$

$$= 4\pi \int_{\mathbb{R}} r^2 \left\{ \frac{1}{r^2} \frac{\partial}{\partial r} \left[r^2 \frac{\partial \varphi}{\partial r} \right] \right\} dr \tag{C.13}$$

$$= -4\pi \int_{\mathbb{R}} \frac{\partial}{\partial r} \left[r^2 \frac{\partial}{\partial r} \left(\frac{1}{4\pi r} + \frac{C_1}{r} \right) \right] dr \tag{C.14}$$

$$= 4\pi \int_{\mathbb{R}} \frac{\partial}{\partial r} \left[r^2 \left\{ \frac{1}{r^2} \left(\frac{1}{4\pi} + C_1 \right) \right\} \right] dr \tag{C.15}$$

$$= 4\pi \left(\frac{1}{4\pi} + C_1 \right) \tag{C.16}$$

$$= 1 + 4\pi C_1 \tag{C.17}$$

$$\overset{!}{=} \int_{\mathbb{R}^3} \delta(\boldsymbol{r})\, d\boldsymbol{r} \tag{C.18}$$

$$= 1 \tag{C.19}$$

$$\Rightarrow C_1 = 0 \tag{C.20}$$

We thus conclude

Theorem C.1.3 (The fundamental solution of the Laplace operator). *The fundamental solution of free–space Green's function for the Laplace operator $\mathcal{G}^L(\boldsymbol{r})$ is given by*

$$\mathcal{G}^L(\boldsymbol{r}) = -\frac{1}{4\pi} \frac{1}{|\boldsymbol{r}|}$$

D. Sobolev spaces

For a modern theory of partial differential equations, the classical concepts of continuity and differentiability turn out to be insufficient, since they usually demand too much regularity of the functions we want to study. A classical example for this is the theory of turbulence, where the involved pressure fields are typically not even continuous, but appear in a *differential equation*. In our discussion of distributions in Appendix B we have already seen how the concept of differentiation can be generalized to a much wider class of objects, the distributions. In this chapter, we will see how the *generalized differentiability* of a function can be expressed or assessed, and how this relates to the *smoothness properties* of a given function or distribution.

D.1. The generalized derivative of locally integrable functions

In B we have seen how the concept of differentiability can be generalized to the space of distributions, which were in turn linear functionals on the space of test functions. In particular we have seen that for any regular distribution the partial derivative can be shifted from the generating function to the test function via integration by parts. But our definition of a regular distribution required the use of a *continuous* generating function $f : \Omega \to \mathbb{C}$, with associated distribution

$$F[\varphi] := \int_\Omega f(\boldsymbol{r})\varphi(\boldsymbol{r})\, d\boldsymbol{r}$$

It turns out though, that in many cases, the same technique may be used to define a generalized derivative of a *locally integrable* function, which need not necessarily be continuous.

Definition D.1.1 (Locally integrable functions). A function f on Ω is said to be *locally integrable* in Ω, if f is integrable over any compact subset $\tau \subset \Omega$. The space of integrable functions on Ω is denoted by $L_1^{\mathsf{loc}}(\Omega)$.

Definition D.1.2 (The generalized derivative of locally integrable functions). A locally integrable function $f \in L_1^{\mathsf{loc}}(\Omega)$ is said to possess a *generalized or weak derivative weak derivative* with respect to $\boldsymbol{r}$ if there exists a locally integrable function $v \in L_1^{\mathsf{loc}}(\Omega)$, with

$$\int_\Omega v(\boldsymbol{r})\varphi(\boldsymbol{r})\, d\boldsymbol{r} = -\int_\Omega f(\boldsymbol{r})\partial_{\boldsymbol{r}}\varphi(\boldsymbol{r})\, d\boldsymbol{r}$$

In that case, we say that

$$\partial_{\boldsymbol{r}} f(\boldsymbol{r}) := v(\boldsymbol{r})$$

is the generalized derivative of $f(\boldsymbol{r})$. Iterating this definition, we can define partial derivatives ∂^α of arbitrary positive order α.

Remark D.1.1. Please note that if we a interpret

$$\int_\Omega f(\boldsymbol{r})\varphi(\boldsymbol{r})\, d\boldsymbol{r}$$

as a slightly generalized regular distribution F – generalized because in our earlier definition, we demanded $f \in C^1(\Omega)$ – with

$$F[\varphi] := \int_\Omega f(\boldsymbol{r})\varphi(\boldsymbol{r})\,d\boldsymbol{r}$$

then F of course possesses generalized derivatives up to arbitrary order *in the distributional sense*. But the resulting derivative need **not** be given by a locally integrable function again, but could rather be any arbitrary kind of distribution. Thus, a locally integrable function might possess arbitrary generalized derivatives in the **distributional** sense, but **no** derivative in the locally integrable sense. A common example is the Heaviside function

$$\theta(x) := \begin{cases} 0, & x < 0 \\ 1, & x > 0 \end{cases}$$

θ is obviously integrable over each compact subset of $\mathbb{R}$, and thus locally integrable, but the generalized derivative is given by the Dirac δ–function, which can **not** be represented as a regular distribution with locally integrable generating function. Thus, θ has arbitrary derivatives in the distributional sense, but none in the locally integrable one.

With this concept, we can now introduce the Sobolev spaces:

Definition D.1.3 (The Sobolev spaces $W_p^m(\Omega)$). Let $1 \leq p < \infty$ and $m \in \mathbb{N}_0$. The *Sobolev space* $W_p^m(\Omega)$ is defined as the space of all functions f in $L_p(\Omega)$ having generalized derivatives $\partial^\alpha f \in L_p(\Omega)$ up to the order[1] $m = |\alpha|$.

An equivalent definition that also generalizes to the cases of $p = \infty$ and $m \in \mathbb{R}$ can be found by introducing the family of Sobolev norms:

Definition D.1.4 (The Sobolev norm). Let $m \in \mathbb{N}_0$. Then, the following family defines a family of norms on the spaces $W_p^m(\Omega)$:

$$\|f\|_{W_p^m(\Omega)} := \begin{cases} \left\{ \sum_{|\alpha| \leq m} \|\partial^\alpha f\|_{L_p(\Omega)}^p \right\}^{\frac{1}{p}} & 1 \leq p < \infty \\ \max_{|\alpha| \leq m} \|\partial^\alpha f\|_{L_\infty(\Omega)} & p = \infty \end{cases} \tag{D.1}$$

Inserting the definition of the $L_p(\Omega)$–norms, this can also be written as

$$\|f\|_{W_p^m(\Omega)} := \begin{cases} \left\{ \sum_{|\alpha| \leq m} \int_\Omega |\partial^\alpha f|^p d\boldsymbol{r} \right\}^{\frac{1}{p}} & 1 \leq p < \infty \\ \max_{|\alpha| \leq m} \|\partial^\alpha f\|_{L_\infty(\Omega)} & p = \infty \end{cases} \tag{D.2}$$

This family of norms is a subfamily of a broader class of norms, defined for arbitrary $s \in \mathbb{R}$:

Definition D.1.5 (The Sobolev–Slobodeckii norm). Let $0 < s \in \mathbb{R}$ with $s = m + \kappa$, such that $m \in \mathbb{N}_0$ and $\kappa \in (0,1)$, and let $\Omega \subset \mathbb{R}^n$. Then, the *Sobolev–Slobodeckii norm* $\|\cdot\|_{W_p^s(\Omega)}$ is defined as

$$\|f\|_{W_p^s(\Omega)} := \left\{ \|f\|_{W_p^m(\Omega)}^p + |f|_{W_p^m(\Omega)}^p \right\}^{\frac{1}{p}} \tag{D.3}$$

with the semi–norm

$$|f|_{W_p^m(\Omega)}^p := \sum_{|\alpha|=m} \int_\Omega \int_\Omega \frac{|\partial^\alpha f(\boldsymbol{r}) - \partial^\alpha f(\boldsymbol{\xi})|^p}{|\boldsymbol{r} - \boldsymbol{\xi}|^{d+p\kappa}}\,d\boldsymbol{r}\,d\boldsymbol{\xi} \tag{D.4}$$

---

1 Here, α should be understood as a multiindex, allowing arbitrary combinations of differentials.

Using the Sobolev–Slobodeckii family of norms will allow us to generalize the Sobolev spaces to arbitrary $m \in \mathbb{R}$ and $p = \infty$. We start this process by first extending the definition to positive $m \in \mathbb{R}$:

Definition D.1.6 (Generalization of the Sobolev spaces). For $0 < s \in \mathbb{R}$, $1 \le p \le \infty$, the Sobolev space $W_p^s(\Omega)$ is defined as the *closure* of $C^\infty(\Omega)$ under the Sobolev–Slobodeckii norm $\|\cdot\|_{W_p^s(\Omega)}$:

$$W_p^s(\Omega) := \overline{C^\infty(\Omega)}^{\|\cdot\|_{W_p^s(\Omega)}} \tag{D.5}$$

i.e. for all f in $W_p^s(\Omega)$, there is a sequence $\{f_i\}_{i\in\mathbb{N}} \subset C^\infty(\Omega)$, with $\lim_{i\to 0}\|f - f_i\|_{W_p^s(\Omega)} = 0$.

Remark D.1.2. For $s \in \mathbb{N}$, $1 \le p \le \infty$, the two alternative definitions are equivalent, and thus the spaces $W_p^s(\Omega)$ are well–defined.

In the same way, we can define an additional family of Sobolev spaces:

Definition D.1.7 (The Sobolev spaces $\mathring{W}_p^s(\Omega)$). For $0 < s \in \mathbb{R}$, $1 \le p \le \infty$, the Sobolev space $\mathring{W}_p^s(\Omega)$ is defined as the closure of $C_0^\infty(\Omega)$ under the Sobolev–Slobodeckii norm:

$$\mathring{W}_p^s(\Omega) := \overline{C_0^\infty(\Omega)}^{\|\cdot\|_{W_p^s(\Omega)}} \tag{D.6}$$

This finally allows us to give the definitions of the Sobolev spaces for the remaining cases, i.e. for $0 < s \in \mathbb{R}$:

Definition D.1.8 (General Sobolev spaces). Let $s \in \mathbb{R}$, $1 \le p \le \infty$. For $0 < s$, the Sobolev spaces $W_p^s(\Omega)$ and $\mathring{W}_p^s(\Omega)$ are defined as the closures of $C^\infty(\Omega)$ and $C_0^\infty(\Omega)$ under the corresponding Sobolev–Slobodeckii norm. For $s < 0$, $1 < p < \infty$, the Sobolev space $W_p^s(\Omega)$ is defined as the dual space of $\mathring{W}_q^{-s}(\Omega)$, with

$$\frac{1}{q} + \frac{1}{p} = 1$$

and with associated norm

$$\|f\|_{W_p^s(\Omega)} := \sum_{0 \ne w \in \mathring{W}_q^{-s}(\Omega)} \frac{|\langle f, w\rangle_\Omega|}{\|w\|_{W_q^{-s}(\Omega)}} \tag{D.7}$$

Similarly, $\mathring{W}_p^s(\Omega)$ is defined as the dual space of $W_q^s(\Omega)$ for negative s and the same definition of q as above.

D.2. The spaces $H^s(\Omega)$

Let $\varphi \in \mathcal{S}(\mathbb{R}^n)$ be an element of the Schwartz space. According to Appendix A, the Fourier transform of φ, $\mathcal{F}\varphi$ exists and is an element of $\mathcal{S}(\mathbb{R}^n)$ itself. We can then introduce a linear bounded operator $\mathcal{I}^s$ on $\mathcal{S}(\mathbb{R}^n)$ as follows:

Definition D.2.1 (The Bessel potential operator). Let $s \in \mathbb{R}$ and $\varphi \in \mathcal{S}(\mathbb{R}^n)$, and let $\hat{\varphi}(\boldsymbol{k}) := \mathcal{F}(\varphi)$ denote the Fourier transform of φ. Then, the *Bessel potential operator*, given by

$$\mathcal{I}^s : \mathcal{S}(\mathbb{R}^n) \to \mathcal{S}(\mathbb{R}^n) \tag{D.8}$$

$$(\mathcal{I}^s\varphi)(\boldsymbol{r}) := \int_{\mathbb{R}^n} \left(1 + |\boldsymbol{k}|^2\right)^{\frac{s}{2}} \hat{\varphi}(\boldsymbol{k}) e^{-2\pi i \boldsymbol{r}\cdot\boldsymbol{k}} \, d\boldsymbol{k}, \qquad \boldsymbol{r} \in \mathbb{R}^n \tag{D.9}$$

is bounded and linear.

D. Sobolev spaces

Application of the Fourier operator $\mathcal{F}$ yields

$$(\mathcal{F}\mathcal{I}^s\varphi)(\boldsymbol{k}) = \left(1 + |\boldsymbol{k}|^2\right)^{\frac{s}{2}} \hat{\varphi}(\boldsymbol{k}) \tag{D.10}$$

This can now be generalized to the space of tempered distributions by using for $T \in \mathcal{S}'(\mathbb{R}^n)$ the expression:

$$(\mathcal{I}^s T)[\varphi] := T[\mathcal{I}^s\varphi] \quad \forall \varphi \in \mathcal{S}(\mathbb{R}^n) \tag{D.11}$$

which introduces a linear and bounded operator

$$\mathcal{I}^s : \mathcal{S}'(\mathbb{R}^n) \to \mathcal{S}'(\mathbb{R}^n)$$

With the help of the Bessel potential operator we can now define another family of Sobolev spaces, the spaces $H^s(\Omega)$:

Definition D.2.2 (The Sobolev spaces $H^s(\Omega)$). Let $\mathcal{I}^s : \mathcal{S}'(\mathbb{R}^n) \to \mathcal{S}'(\mathbb{R}^n)$ denote the Bessel potential operator. The *Sobolev space* $H^s(\mathbb{R}^n)$ is defined as the space of all tempered distributions $T \in \mathcal{S}'(\mathbb{R}^n)$ with

$$\mathcal{I}^s T \in L_2(\mathbb{R}^n) \tag{D.12}$$

with the associated inner product

$$\langle T, S \rangle_{H^s(\mathbb{R}^n)} := \langle \mathcal{I}^s T, \mathcal{I}^s S \rangle_{L_2(\mathbb{R}^n)} \tag{D.13}$$

and the induced norm

$$\|\varphi\|^2_{H^s(\mathbb{R}^n)} := \|\mathcal{I}^s\varphi\|^2_{L_2(\mathbb{R}^n)} = \int_{\mathbb{R}^n} \left(1 + |\boldsymbol{k}|^2\right)^s |\hat{\varphi}(\boldsymbol{k})|^2 \, d\boldsymbol{k} \tag{D.14}$$

For a domain $\Omega \subset \mathbb{R}^n$, we define the Sobolev space $H^s(\Omega)$ by

$$H^s(\Omega) := \left\{ \varphi = \tilde{\varphi}_{|\Omega} \,\middle|\, \tilde{\varphi} \in H^s(\mathbb{R}^n) \right\} \tag{D.15}$$

with the induced norm

$$\|\varphi\|_{H^s(\Omega)} := \inf_{\substack{\tilde{\varphi} \in H^s(\mathbb{R}^n) \\ \tilde{\varphi}_{|\Omega} = \varphi}} \|\tilde{\varphi}\|_{H^s(\mathbb{R}^n)} \tag{D.16}$$

Thus, the space $H^2(\Omega)$ contains exactly those tempered distributions $T \in \mathcal{S}'(\Omega)$, for which $\|T\|_{H^s(\Omega)} < \infty$. Looking a little closer at the norm in those spaces, we find that for a function to have a finite Sobolev norm $\|\cdot\|_{H^s(\Omega)}$, its Fourier transform has to vanish faster than $(1 + |\boldsymbol{k}|^2)^s$ for $|\boldsymbol{k}| \to \infty$. Thus, the Sobolev index s can be thought of as a measure for the speed of the decay of a function's Fourier modes. Since the behaviour of the Fourier transform of a function for large $|\boldsymbol{k}|$ is intimately related with its *smoothness* – a function is considered *rough* if it varies on small length scales, which corresponds to the existence of large $|\boldsymbol{k}|$ modes in the Fourier transform – the Sobolev index s is a convenient and important measure for the smoothness of a function. This motivates the following definition:

Definition D.2.3 (Smoothness of a distribution). Let $T \in H^s(\Omega)$, $S \in H^r(\Omega)$. We call T and S *equally smooth* if $s = r$, T *more smooth* than S by a Sobolev index of k if $s = r + k$ for $k > 0$, and *less smooth* than S if $s = r - k$ for $k > 0$.

Remark D.2.1. With this notion of smoothness in mind, it is intuitively clear that

$$H^s(\Omega) \subset H^r(\Omega) \quad \text{for } s > r$$

Analogously to the definition of the spaces $\mathring{W}_p^m(\Omega)$, we define the spaces $H_0^s(\Omega)$ via

Definition D.2.4 (The Sobolev spaces $H_0^s(\Omega)$ and $\tilde{H}^s(\Omega)$). The Sobolev space $H_0^s(\Omega)$ is defined as the closure of $C_0^\infty(\Omega)$ under the $H^s(\Omega)$ norm, i.e.

$$H_0^s(\Omega) := \overline{C_0^\infty(\Omega)}^{\|\cdot\|_{H^s(\Omega)}} \tag{D.17}$$

Similarly, the Sobolev space is defined as the closure of $C_0^\infty(\Omega)$ under the full $H^s(\mathbb{R}^n)$ norm:

$$\tilde{H}^s(\Omega) := \overline{C_0^\infty(\Omega)}^{\|\cdot\|_{H^s(\mathbb{R}^n)}} \tag{D.18}$$

Theorem D.2.1 (Equivalences of Sobolev spaces). *Let $\Omega \subset \mathbb{R}^n$ be a Lipshitz domain, and let $s > 0$. Then, the following embedding holds for the Sobolev spaces $\tilde{H}^s(\Omega)$ and $H_0^s(\Omega)$:*

$$\tilde{H}^s(\Omega) \subset H_0^s(\Omega) \tag{D.19}$$

and in particular

$$\tilde{H}^s(\Omega) = H_0^s(\Omega) \quad \text{for } s \notin \left\{\frac{1}{2}, \frac{3}{2}, \frac{5}{2}, \dots\right\} \tag{D.20}$$

For the spaces $W_2^s(\Omega)$ and $H^s(\Omega)$, we have the equivalence:

$$W_2^s(\Omega) = H^s(\Omega) \quad \forall\, 0 < s \in \mathbb{R} \tag{D.21}$$

D.3. Lipshitz–domains and the spaces $\mathcal{C}^{k,\kappa}(\Omega)$ of Hölder-continuous functions

In the derivation of the boundary element method central to this thesis, we will make use of a number of distribution– and Sobolev space–related results that only hold under certain regularity conditions of the boundary of the respective domain under consideration.[2] In this section, we will provide the necessary vocabulary for a precise formulation of these geometrical requirements.

Definition D.3.1 (Hölder-continuity). Let $f : \Omega \to \mathbb{R}$, $\boldsymbol{\xi} \in \Omega$, $0 < \kappa < 1$. f is said to be *Hölder-continuous* in $\boldsymbol{\xi}$ with exponent κ, iff

$$\sup_{\boldsymbol{r} \in \Omega} \frac{|f(\boldsymbol{r}) - f(\boldsymbol{\xi})|}{|\boldsymbol{r} - \boldsymbol{\xi}|^\kappa} < \infty$$

and Hölder-continuous in Ω with exponent κ iff it is Hölder- continuous in **all $\boldsymbol{\xi} \in \Omega$** with exponent κ.

Definition D.3.2 (The space $\mathcal{C}^{k,\kappa}(\Omega)$ of Hölder-continuous functions). By $\mathcal{C}^{k,\kappa}(\Omega)$, we denote the space of all functions $f \in \mathcal{C}^k(\Omega)$ for which the k–th derivative is Hölder-continuous with exponent κ over Ω.

Remark D.3.1. According to definition D.3.2, the space $\mathcal{C}^{k,\kappa}(\Omega)$ is assigned the norm

$$\|f\|_{\mathcal{C}^{k,\kappa}(\Omega)} := \|f\|_{C^k(\Omega)} + \sum_{|\kappa|=k} \sup_{\substack{r,\xi \in \Omega \\ r \neq \xi}} \frac{|\partial^\alpha f(\boldsymbol{r}) - \partial^\alpha f(\boldsymbol{\xi})|}{|\boldsymbol{r} - \boldsymbol{\xi}|^\alpha}$$

---

2 These regularity conditions typically hold for the molecular surfaces used for biomolecular electrostatics.

Definition D.3.3 (Lipshitz-continuity). Extending the above definitions to the case of $\kappa = 1$, we arrive at the so-called *Lipshitz-continuous* functions, i.e. a function $f : \Omega \to \mathbb{R}$ for which the property from definition D.3.1 holds in a point $\boldsymbol{\xi} \in \Omega$ with $\kappa = 1$ is said to be *Lipshitz-continuous* in $\boldsymbol{\xi}$ and Lipshitz-continuous in Ω if it is Lipshitz-continuous in all $\boldsymbol{\xi} \in \Omega$. Finally, $\mathcal{C}^{k,1}(\Omega)$ is the space of functions $f \in \mathcal{C}^k(\Omega)$ with Lipshitz-continuous derivatives of order $|\alpha| = k$.

With the help of these important concepts we can finally define the requirements on the regularity of the domains for all our numerical computations:

Definition D.3.4 (The space $\mathcal{C}^{0,1}$ of piecewise smooth boundaries). Let $\Omega \subset \mathbb{R}^n$ be a domain with boundary $\partial\Omega$. $\partial\Omega$ is said to be *piecewise smooth*, iff there is a finite cover

$$\partial\Omega = \bigcup_{i=1}^{p} \Gamma_i$$

for which the following two properties of the Γ_i hold:

1. Each Γ_i can be represented by a Lipshitz-continuous function γ_i on an open box Q in $\mathbb{R}^{n-1}$: for all $\boldsymbol{\xi} \in \Gamma_i$, $\boldsymbol{\xi} = (\boldsymbol{r}, \gamma_i(\boldsymbol{r}))$ for some $\boldsymbol{r} \in \mathbb{R}^{n-1}$

2. The domain Ω lies completely "to one side of Γ_i", i. e. for some $\gamma > 0$, all points $(\boldsymbol{r}, \gamma_i(\boldsymbol{r}))$ with $-\gamma < \gamma_i(\boldsymbol{r}) < 0$, $\boldsymbol{r} \in Q$ belong to Ω, while all points $(\boldsymbol{r}, \gamma_i(\boldsymbol{r}))$ with $0 < \gamma_i(\boldsymbol{r}) < \gamma$, $\boldsymbol{r} \in Q$ do **not** belong to Ω

The space of piecewise smooth boundaries is denoted by $\mathcal{C}^{0,1}$

Definition D.3.5 (Lipshitz-domain). A domain $\Omega \subset \mathbb{R}^n$ with $n \geq 2$ is said to be a *Lipshitz-domain*, iff any arbitrary cover of its boundary $\partial\Omega$ can be represented by Lipshitz-continuous functions. In particular, all domains with piecewise smooth boundary $\partial\Omega \in \mathcal{C}^{0,1}$ are Lipshitz-domains.

Remark D.3.2. While the Lipshitz-property of each covering of the boundary allows for "sensible" edges or corners, those with a zero angle are forbidden (c.f. Fig. D.1).
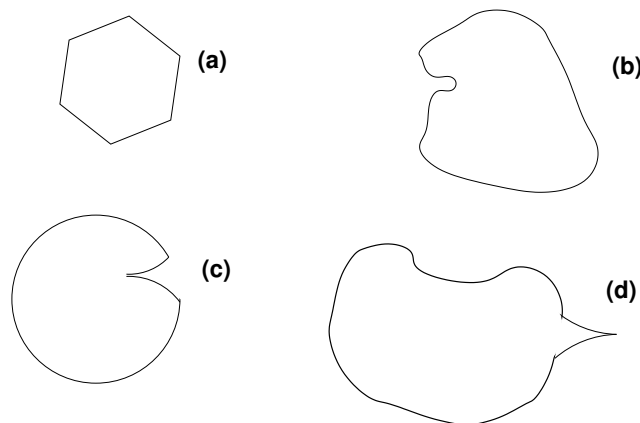
Figure D.1.: Some Lipshitz (a, b) and non-Lipshitz (c, d) domains.

E. Systems of units for electrostatics

Any researcher in electrostatics will very soon become aware of the astonishing confusion arising in this field due to the large number of different systems of units, that are still in use today. This seriously complicates the process of comparing or combining results of different authors. In this chapter, we thus want to mention the most important systems of units for the theory of electrostatics briefly and give a table for conversions from one of them to the officially recommended SI system, which is used throughout this book, and back.

E.1. Systems of units

The following table is an abbreviated version of the one found in the appendix of [Jac98]

System of units	ε_0	$\boldsymbol{D}$	Maxwell equations
SI	$\frac{10^7}{4\pi c^2}$ $\approx 8.8 \times 10^{-12} \frac{F}{m}$	$\boldsymbol{D} = \varepsilon_0 \boldsymbol{E} + \boldsymbol{P}$	$\boldsymbol{\nabla}\cdot\boldsymbol{D} = \rho$ $\boldsymbol{\nabla} \times \boldsymbol{E} = 0$
Electrostatic Units (esu)	1	$\boldsymbol{D} = \boldsymbol{E} + 4\pi\boldsymbol{P}$	$\boldsymbol{\nabla}\cdot\boldsymbol{D} = 4\pi\rho$ $\boldsymbol{\nabla} \times \boldsymbol{E} = 0$
Gaussian Units (cgs)	1	$\boldsymbol{D} = \boldsymbol{E} + 4\pi\boldsymbol{P}$	$\boldsymbol{\nabla}\cdot\boldsymbol{D} = 4\pi\rho$ $\boldsymbol{\nabla} \times \boldsymbol{E} = 0$
Heaviside- Lorentz Units	1	$\boldsymbol{D} = \boldsymbol{E} + \boldsymbol{P}$	$\boldsymbol{\nabla}\cdot\boldsymbol{D} = \rho$ $\boldsymbol{\nabla} \times \boldsymbol{E} = 0$

Please note that esu and cgs - units are equivalent for electrostatics! They only differ for the description of magnetic phenomena, which can be neglected for the scope of this work.

E.2. Unit conversions

The following table can be used to convert *electrostatic* units between the SI - and the esu and cgs (Gaussian) System of units. Conversion of a quantity Q can be achieved via:

$$Q_{\text{Gaussian}} = \kappa Q_{SI} \tag{E.1}$$

In the table, the following abbreviations have been used:

$$\alpha = 10^2 cm\, m^{-1} \tag{E.2}$$
$$\beta = 10^7 erg\, J^{-1} \tag{E.3}$$

	Physical Quantity	Gaussian unit
charge	$\sqrt{\frac{\alpha\beta}{4\pi\varepsilon_0}}$	statcoulomb
charge density	$\sqrt{\frac{\beta}{4\pi\alpha^3\varepsilon_0}}$	statcoulomb/cm^3
current	$\sqrt{\frac{\alpha\beta}{4\pi\varepsilon_0}}$	statampere
current density	$\sqrt{\frac{\beta}{4\pi\alpha^3\varepsilon_0}}$	statampere/cm^2
electric field	$\sqrt{\frac{4\pi\beta\varepsilon_0}{\alpha^3}}$	statvolt/cm
electric potential	$\sqrt{\frac{4\pi\beta\varepsilon_0}{\alpha}}$	statvolt
energy	β	erg
energy density	$\frac{\beta}{\alpha^3}$	erg/cm^3
force	$\frac{\beta}{\alpha}$	dyne
length	α	cm
mass	$\frac{\beta}{\alpha^2}$	gram
power	β	erg/sec
pressure	$\frac{\beta}{\alpha^3}$	dyne/cm^2
velocity	α	cm/sec

Bibliography

[Å90]   Johan Åqvist. Ion-water interaction potentials derived from free energy perturbation simulations. *J. Phys. Chem.*, 94:8021, 1990.

[ABB⁺99]   E. Anderson, Z. Bai, C. Bischof, S. Blackford, J. Demmel, J. Dongarra, J. Du Croz, A. Greenbaum, S. Hammarling, A. McKenney, and D. Sorensen. *LAPACK Users' Guide*. Society for Industrial and Applied Mathematics, Philadelphia, PA, third edition, 1999.

[AHU83]   A. Aho, J. Hopcroft, and J. Ullman. *The Design and Analysis of Computer Algorithms*. Addison–Wesley, Reading MA, 1983.

[AM97]   C. Amovilli and B. Mennucci. Self–consistent–field calculation of Pauli repulsion and dispersion contributions to the solvation free energy in the polarizable continuum model. *J. Phys. Chem. B*, 101:1051–1057, 1997.

[Ame01]   Mohammed Ameen. *Boundary Element Analysis – Theory and Programming*. Narosa Publishing House, New Dehli, 2001.

[AP95]   R. Aldrovandi and J.G. Pereira. *An Introduction to Geometrical Physics*. World Scientific, 1995.

[Arf85]   G. Arfken. *Mathematical Methods for Physicists*. Academic Press, Orlando, FL, 3rd edition, 1985.

[BHW00]   N. Baker, M. Holst, and F. Wang. Adaptive multilevel finite element solution of the Poisson–Boltzmann equation II: Refinement at solvent accessible surfaces in biomolecular systems. *J. Comp. Chem.*, 21:1343–1352, 2000.

[BJH83]   Ph. A. Bopp, G. Jancsó, and K. Heinzinger. An improved potential for non-rigid water molecules in the liquid phase. *Chem. Phys. Lett.*, 98:129, 1983.

[BK04]   Mario Botsch and Leif Kobbelt. A remeshing approach to multiresolution modeling. In R. Scopigno and D. Zorin, editors, *Eurographics Symposium on Geometry Processing*. The Eurographics Association, 2004.

[BKS96]   P. A. Bopp, A.A. Kornyshev, and G. Sutmann. Static nonlocal dielectric function of liquid water. *Phys. Rev. Lett.*, 76:1280–1283, 1996.

[BN87]   Arieh Ben-Naim. *Solvation Thermodynamics*. Plenum Press, New York, 1987.

[BNDS97]   R.E. Bruccoleri, J. Novotny, M.E. Davis, and K.A. Sharp. Finite difference Poisson–Boltzmann electrostatic calculations: Increased accuracy achieved by harmonic dielectric smoothing and charge antialiasing. *J. Comp. Chem.*, 18(2):268–276, 1997.

[Boe73]   C.J.F. Boettcher. *Theory Of Electric Polarization, Volume I: Dielectrics In Static Fields*. Elsevier, second edition, 1973.

[BP96] Mikhail V. Basilevsky and Drew F. Parsons. An advanced continuum medium model for treating solvation effects: Nonlocal electrostatics with a cavity. *J. Chem. Phys.*, 105(9):3734–3746, 1996.

[BP98a] Mikhail V. Basilevsky and Drew F. Parsons. Nonlocal continuum solvation model with exponential susceptibility kernels. *J. Chem. Phys.*, 108(21):9107–9113, 1998.

[BP98b] Mikhail V. Basilevsky and Drew F. Parsons. Nonlocal continuum solvation models with oscillating susceptibility kernels: A nonrigid cavity model. *J. Chem. Phys.*, 108(21):9114–9123, 1998.

[BPvGH81] H.J.C. Berendsen, J.P.M. Postma, W.F. van Gunsteren, and J Hermans. Interaction models for water in relation to protein hydration. *in: B. Pullman (Ed.), Intermolecular Forces, Riedel, Dordrecht, The Netherlands*, pages 331–342, 1981.

[BR98] J.O. Bockris and A.K.N. Reddy. *Modern Electrochemistry*. Plenum Press, New York, 1998.

[BR03] M. Bebendorf and S. Rjasanow. Adaptive low–rank approximation of collocation matrices. *Computing*, 70:1–24, 2003.

[BSHM01] N. Baker, D. Sept, M. Holst, and J.A. McCammon. The adaptive multilevel finite element solution of the Poisson–Boltzmann equation on massively parallel computers. *IBM Journal of Research and Development*, 45:427–438, 2001.

[BWF$^+$00] H.M. Berman, J. Westbrook, Z. Feng, G. Gilliland, T.N. Bhat, H. Weissig, I.N. Shindyalov, and P.E. Bourne. The Protein Data Bank. *Nucleic Acids Research*, 28:235–242, 2000.

[BWS$^+$95] R. Bharadwaj, A. Windemuth, S. Sridharan, B. Honig, and A. Nicholls. The fast multipole boundary element method for molecular electrostatics: An optimal approach for large systems. *J. Comput. Chem.*, 16:898–913, 1995.

[Cau74] A. Cauchy. Sur un nouveau genre de calcul analogue au calcul infinitésimal. Exercises de mathematiques 1826. In *Oeuvres complètes (Reprint)*, volume 6 of *Ser. 2*, pages 23–37. Gauthier–Villars, Paris, 1882–1974.

[CBA51] B.E. Conway, J.O.M. Bockris, and I.A. Ammar. The dielectric constant of the solution in the diffuse and Helmholtz double layers at a charged interface in aqueous solution. *Trans. Faraday Soc.*, 47:756–766, 1951.

[CC03] F. Chen and D.M. Chipman. Boundary element methods for dielectric cavity construction and integration. *J. Chem. Phys.*, 119(19):10289–10297, 2003.

[CF97a] Christian M. Cortis and Richard A. Friesner. An automatic three-dimensional finite element mesh generation system for the Poisson–Boltzmann equation. *J. Comp. Chem.*, 18(13):1570–1590, 1997.

[CF97b] Christian M. Cortis and Richard A. Friesner. Numerical solution of the Poisson–Boltzmann equation using tetrahedral finite-element meshes. *J. Comp. Chem.*, 18(13):1591–1608, 1997.

[CH96] Richard Courant and David Hilbert. *Methods of Mathematical Physics*. Wiley–Interscience, 1996.

[CHCT96]   C.C. Chambers, G.D. Hawkins, C.J. Cramer, and D.G. Truhlar. Model for aqueous solvation based on class iv atomic charges and first solvation shell effects. *J. Phys. Chem.*, 100:16385–16398, 1996.

[CLRS01]   T.H. Cormen, C.E. Leiserson, R.L. Rivest, and C. Stein. *Introduction to Algorithms*. MIT press, 2nd edition, 2001.

[CMJW02]   R. Chen, J. Mintseris, J. Janin, and Z. Weng. A protein–protein docking benchmark. *Proteins: Structure, Function, and Genetics*, 52(1):88–91, 2002.

[Con]   M.L. Connolly. Molecular surfaces: A review. `http://www.netsci.org/Science/Compchem/feature14.html`.

[Con81a]   M.L. Connolly. Molecular surface program. *QCPE Bull.*, 1:75, 1981.

[Con81b]   M.L. Connolly. *Protein surfaces and interiors*. PhD thesis, University of California at Berkeley, 1981.

[Con83]   M.L. Connolly. Analytical molecular surface calculation. *J. Appl. Crystallogr.*, 16:548–558, 1983.

[Con85]   M.L. Connolly. Molecular surface triangulation. *J. Appl. Crystallogr.*, 18:499–505, 1985.

[Cru69]   T.A. Cruse. Numerical solutions in three–dimensional elastostatics. *Int. J. Solids & Strucs.*, 5:1259–1274, 1969.

[Cru74]   T.A. Cruse. An improved boundary integral equation method for three–dimensional elastic stress analysis. *Computers & Strucs.*, 4:741–754, 1974.

[CT99]   Christopher J. Cramer and Donald G. Truhlar. Implicit solvation models: Equlibria, structure, spectra, and dynamics. *Chem. Rev.*, 99:2161–2200, 1999.

[Dav62]   N. Davidson. *Statistical Mechanics*. McGraw–Hill, New York, 1962.

[DDCDH90a]   J.J. Dongarra, J. Du Croz, I.S. Duff, and S. Hammarling. Algorithm 679: A set of level 3 basic linear algebra subprograms. *ACM Trans. Math. Soft.*, 16:18–28, 1990.

[DDCDH90b]   J.J. Dongarra, J. Du Croz, I.S. Duff, and S. Hammarling. A set of level 3 basic linear algebra subprograms. *ACM Trans. Math. Soft.*, 16:1–17, 1990.

[DDCHH88a]   J.J. Dongarra, J. Du Croz, S. Hammarling, and R.J. Hanson. Algorithm 656: An extended set of FORTRAN basic linear algebra subprograms. *ACM Trans. Math. Soft.*, 14:18–32, 1988.

[DDCHH88b]   J.J. Dongarra, J. Du Croz, S. Hammarling, and R.J. Hanson. An extended set of FORTRAN basic linear algebra subprograms. *ACM Trans. Math. Soft.*, 14:1–17, 1988.

[Deb54]   P. Debye. *The Collected Papers of Peter J. W. Debye*. Interscience, New York, 1954.

[Del34]   B. Delaunay. Sur la sphère vide. *Izvestia Akademii Nauk SSSR, Otdelenie Matematicheskikh i Estestvennykh Nauk*, 7:793–800, 1934.

[DH23a]   P. Debye and E. Hückel. Zur Theorie der Elektrolyte. I. Gefrierpunkts–Erniedrigung und Verwandte Erscheinungen. *Phys. Z.*, 24:185, 1923.

[DH23b]   P. Debye and E. Hückel. Zur Theorie der Elektrolyte. II. Das Grenzgesetz für die elektrische Leitfähigkeit. *Phys. Z.*, 24(305), 1923.

Bibliography

[Dir27]   P.A.M. Dirac. The physical interpretation of quantum dynamics. *Proc. Royal Soc. London, Ser. A*, 113:625, 1927.

[DKKU85]   Revaz R. Dogonadze, Erika Kálmán, Alexei A. Kornyshev, and Jens Ulstrup. *The Chemical Physics of Solvation, Part A: Theory of Solvation*. Elsevier Science Ltd., 1985.

[DKM81]   O. V. Dolgov, D.A. Kirzhnits, and E.G. Maksimov. On an admissible sign of the static dielectric function of matter. *Rev. Mod. Phys.*, 53(81), 1981.

[DM90]   L. Debnath and P. Mikusinski. *Introduction to Hilbert Spaces with Applications*. Academic Press, San Diego, CA, 1990.

[DM91]   M.E. Davis and J.A. McCammon. Dielectric boundary smoothing in finite difference solutions of the Poisson equation: An approach to improve accuracy and convergence. *J. Comp. Chem.*, 12(7):909–912, 1991.

[DPS93]   W. Dahmen, S. Prößdorf, and R. Schneider. Wavelet approximation methods for pseudodifferential equations II: Matrix compression and fast solution. *Adv. Comput. Math.*, 1:259–335, 1993.

[DPS94]   W. Dahmen, S. Prößdorf, and R. Schneider. Wavelet approximation methods for pseudodifferential equations I: Stability and convergence. *Math. Z.*, 215:583–620, 1994.

[DS92]   N.A. Dumont and R.M. Souza. *Boundary Elements XIV (A simple unified technique for the evaluation of quasi–singular, singular and strongly–singular integrals.)*, pages 619–632. Computational Mechanics Publications, Southampton, Boston, 1992.

[Dum94]   N.A. Dumont. On the efficient numerical evaluation of integrals with complex singularity poles. *Engineering Analysis with Boundary Elements*, 13:155–168, 1994.

[FNvG02]   C. Fleck, R.R. Netz, and H.H. von Grünberg. Poisson–Boltzmann theory for membranes with mobile charged lipids and the pH–dependent interaction of a DNA molecule with a membrane. *Biophys. J.*, 82:76–92, 2002.

[Fra04]   Theodore Frankel. *The geometry of physics: an introduction*. Cambridge University Press, 2nd edition, 2004.

[Fre03]   I. Fredholm. Sur un classe d'equations fonctionelles. *Acta Math.*, 27:365–390, 1903.

[GG90]   M. Guiggiani and A. Gigante. A general algorithm for multidimensional Cauchy principal value integrals in the boundary element method. *ASME Journal of Applied Mechanics*, 57:906–915, 1990.

[Gie97]   K. Giebermann. *Schnelle Summationsverfahren zur numerischen Lösung von Integralgleichungen für Streuprobleme im $\mathbb{R}^3$*. PhD thesis, Universität Karlsruhe, 1997.

[GKW03]   L. Gaul, M. Kögl, and M. Wagner. *Boundary Element Methods for Engineers and Scientists – An Introductory Course with Advanced Topics*. Springer–Verlag Berlin Heidelberg, 2003.

[GR87]   L. Greengard and V. Rokhlin. A fast algorithm for particle simulations. *J. Comput. Phys.*, 73:325–348, 1987.

[GR00]   I.S. Gradshteyn and I.M. Ryzhik. *Tables of Integrals, Series, and Products*. Academic Press, San Diego, CA, 6th edition, 2000.

[GS77]   I.M. Gel'fand and G.E. Shilov. *Generalized Functions.* Academic Press, 1977.

[Hac99]   W. Hackbusch. A sparse matrix arithmetic based on $\mathcal{H}$–matrices. I. introduction to $\mathcal{H}$–matrices. *Computing*, 62:89–108, 1999.

[Has73]   J.B. Hasted. *Aqueous Dielectrics.* Chapman and Hall, London, 1973.

[HBR⁺04] A. Hildebrandt, R. Blossey, S. Rjasanow, O. Kohlbacher, and H.-P. Lenhof. Novel formulation of nonlocal electrostatics. *Phys. Rev. Lett.*, 93(10):108104, 2004.

[HBW00]   M. Holst, N. Baker, and F. Wang. Adaptive multilevel finite element solution of the Poisson–Boltzmann equation I: Algorithms and examples. *J. Comp. Chem.*, 21:1319–1342, 2000.

[HC72]   Marie-José Huron and Pierre Claverie. Calculation of the interaction energy of one molecule with its whole surrounding. I. method and application to pure nonpolar compounds. *J. Phys. Chem.*, 76(15):2123–2133, 1972.

[HCT97]   G.D. Hawkins, C.J. Cramer, and D.G. Truhlar. Parametrized model for aqueous free energies of solvation using geometry–dependent atomic surface–tensions with implicit electrostatics. *J. Phys. Chem. B*, 101:7147–7157, 1997.

[HCT98]   G.D. Hawkins, C.J. Cramer, and D.G. Truhlar. Universal quantum mechanical model for solvation free energies based on gas–phase geometries. *J. Phys. Chem. B*, 102:3257–3271, 1998.

[Hil86]   T.L. Hill. *An Introduction to Statistical Mechanics*. Dover, New York, 1986.

[Hil02]   Andreas Hildebrandt. An algorithm for the efficient and reliable computation of the electrostatic contribution to the free energy of solvation using nonlocal electrodynamics. Master's thesis, Computers Science faculty of Saarland University, Saarbrücken, 2002.

[HKBL02] Andreas Hildebrandt, Oliver Kohlbacher, Ralf Blossey, and Hans-Peter Lenhof. Using nonlocal electrostatics for solvation free energy computations: ions and small molecules. *http://www.arxiv.org/physics/0212074*, 2002.

[HN89]   W. Hackbusch and Z.P. Nowak. On the fast matrix multiplication in the boundary element method by panel clustering. *Numer. Math.*, 54:463–491, 1989.

[Hol94]   M.J. Holst. *The Poisson–Boltzmann Equation – Analysis and Multilevel Numerical Solution*. PhD thesis, Department of Computer Science, University of Illinois, Urbana–Champaign, 1994.

[Hun04]   Peter Hunter. *FEM/BEM Notes*. Department of Engineering Science, The University of Auckland, New Zealand, 2004. `http://www.esc.auckland.ac.nz/teaching/ Engsci450FC/FEModule/fembemnotes_2up.pdf`.

[Isr98]   Jacob Israelachvili. *Intermolecular & Surface Forces*. Academic Press, Harcourt Brace & Company, Publishers, second edition, 1998.

[Jac98]   John David Jackson. *Classical Electrodynamics*. John Wiley & Sons, Inc, third edition, 1998.

[Jas63]   M.A. Jaswon. Integral equation methods in potential theory I. *Proc. Royal Soc. London*, A275:23–32, 1963.

Bibliography

[JBH84]   G. Jancsó, Ph. A. Bopp, and K. Heinzinger. Molecular dynamics study of high-density liquid water using a modified central force potential. *Chem. Phys.*, 85:377, 1984.

[JBvK+91]   Andre H. Juffer, Eugen F. F. Botta, Bert A. M. van Keulen, Auke van der Ploeg, and Herman J.C. Berendsen. The electric potential of a macromolecule in a solvent: A fundamental approach. *J. Comp. Phys.*, 97(1):144–171, 1991.

[JCM+83]   W.L. Jorgensen, J. Chandrasekhar, J.D. Madura, R.W. Impey, and M.L. Klein. Comparison of simple potential functions for simulating liquid water. *J. Chem. Phys.*, 79:926, 1983.

[Jos02]   J. Jost. *Partial Differential Equations*, volume 214 of *Graduate Texts in Mathematics*. Springer–Verlag, 2002.

[JS94]   R.M Jackson and M.J.E Sternberg. Application of scaled particle theory to model the hydrophobic effect: implications for molecular association and protein stability. *Protein Eng.*, 7:371–383, 1994.

[JS95]   R.M Jackson and M.J.E Sternberg. A continuum model for protein–protein interactions: Application to the docking problem. *J. Mol. Biol.*, 250:258–275, 1995.

[JV98]   A.H. Juffer and H.J. Vogel. A flexible triangulation method to describe the solvent–accessible surface of biopolymers. *J. Comp.–Aided Mol. Design*, 12(3):289–299, 1998.

[KN00]   K.K. Kunze and R.R. Netz. Salt–induced DNA-histone complexation. *Phys. Rev. Lett.*, 85:4389, 2000.

[Kno96]   K. Knopp. *Theory of Functions Parts I and II, Two Volumes Bound as One, Part I*. Dover, New York, 1996.

[Koh]   O. Kohlbacher H. P. Lenhof et al. Ball – Biochemical Algorithms Library. `http://www.bioinf.uni-sb.de/OK/BALL`.

[Kra26]   H.A. Kramers. *Nature*, 117:775, 1926.

[Kra99]   S.G. Krantz. *Handbook of Complex Variables*. Birkhäuser, Boston, MA, 1999.

[Kri67]   V.I. Krilov. *Priblizhennoe vichislenie integralov*. Nauka, Moskva, 1967.

[Kro26]   R. de L. Kronig. *J. Opt. Soc. Am.*, 12:547, 1926.

[KRV78a]   A. A. Kornyshev, A. I. Rubinshtein, and M. A. Vorotyntsev. Model nonlocal electrostatics: I. *J. Phys. C: Solid State Phys.*, 11:3307–3321, 1978.

[KRV78b]   A. A. Kornyshev, A. I. Rubinshtein, and M. A. Vorotyntsev. Model nonlocal electrostatics: II. spherical interface. *J. Phys. C: Solid State Phys.*, 11:3323–3331, 1978.

[KS97]   A.A. Kornyshev and G. Sutmann. Nonlocal dielectric saturation in liquid water. *Phys. Rev. Lett.*, 79:3435–3438, 1997.

[KS99]   A.A. Kornyshev and G. Sutmann. Nonlocal dielectric function of water: how strong are the effects of intramolecular charge form factors? *J. Mol. Liquids*, 82:151–160, 1999.

[Kup65]   O.D. Kupradze. *Potential Methods in the Theory of Elasticity*. Daniel Davy, New York, 1965.

[Lam03]   Gene Lamm. *Reviews in Computational Chemistry (edited by Kenny B. Lipkowitz, Raima Larter, Thomas R. Cundari)*, volume 19, chapter 4 – The Poisson–Boltzmann Equation, pages 147–365. Wiley–VCH, John Wiley & Sons, Inc., 2003.

[Law77]   C.L. Lawson. *Mathematical Software III, Rice, J.R. (ed.)*, chapter "Software for $\mathcal{C}^1$ surface interpolation", pages 161–194. Academic Press, New York, 1977.

[Lea94]   AR Leach. Ligand docking to proteins with discrete side–chain flexibility. *J. Mol. Biol.*, 235(1):345–356, 1994.

[LG98]   R.M. Levy and E. Gallicchio. Computer simulations with explicit solvent: recent progress in the thermodynamic decomposition of the free energies and in modeling electrostatic effects. *Annu. Rev. Phys. Chem.*, 49:531–567, 1998.

[LHKK79]   C.L. Lawson, R.J. Hanson, D. Kincaid, and F.T. Krogh. Basic linear algebra subprograms for FORTRAN usage. *ACM Trans. Math. Soft.*, 5:308–323, 1979.

[LHM85]   H.-B. Li, G.-M. Han, and H.A. Mang. A new method for evaluating integrals in stress analysis of solids by the boundary element method. *International Journal for Numerical Methods in Engineering*, 21:2071–2098, 1985.

[LL84]   L.D. Landau and E.M. Lifshitz. *Course of Theoretical Physics, Vol. 8: Electrodynamics of Continouos Media.* Translated from the Russian. Pergamon, Oxford, 1984.

[LL87]   L.D. Landau and E.M. Lifshitz. *Course of Theoretical Physics, Vol. 2: The Classical Theory of Fields.* Translated from the Russian, Pergamon, Oxford, 1987.

[LR71]   B. Lee and F.M. Richards. The interpretation of protein structures: Estimation of static accessibility. *J. Mol. Biol.*, 55:389–400, 1971.

[LR96]   H.C. Lee and B. Rosenstein. Phase diagram of a dusty plasma. *Phys. Rev. E*, 55(6):7805–7808, 1996.

[LS99]   C. Lage and C. Schwab. Wavelet Galerkin algorithms for boundary integral equations. *SIAM J. Sci. Comput.*, 20:2195–2222, 1999.

[LSJBI02]   M.S. Lee, F.R. Salsbury Jr., and C.L. Brooks III. Novel generalized Born methods. *J. Chem. Phys.*, 116(24):10606–10614, 2002.

[LW76]   J.C. Lachat and J.O. Watson. Effective numerical treatment of boundary integral equations: a formulation for three–dimensional elastostatics. *International Journal for Numerical Methods in Engineering*, 10:991–1005, 1976.

[Mag83]   M. Magini. *Ions and Molecules in Solution, N. Tanaka, H. Ohtaki, and R. Tamamushi (Eds.)*, page 97. Elsevier, 1983.

[Mar85]   Y. Marcus. *Ion Solvation.* Wiley, New York, 1985.

[Max64]   James Clerk Maxwell. A dynamical theory of the electromagnetic field. *Philosophical Transactions of the Royal Society of London*, 155:459–512, 1864.

[McQ76]   D.A. McQuarrie. *Statistical mechanics.* Harper & Row, New York, 1976.

[ME84]   E.L. Mehler and G. Eichele. Electrostatic effects in water-accessible regions of proteins. *Biochemistry*, 23(17):3887–3891, 1984.

Bibliography

[MF53]   P.M. Morse and H. Feshbach. *Methods of Theoretical Physics, Part I*. McGraw–Hill, New York, 1953.

[MJ00]   M.W. Mahoney and W.L. Jorgensen. A five-site model for liquid water and the reproduction of the density anomaly by rigid, nonpolarizable potential functions. *J. Chem. Phys.*, 112:8910–8922, 2000.

[Mun93]   J. R. Munkres. *Elements of Algebraic Topology.*, chapter 1.2: Simplicial Complexes and Simplicial Maps., pages 7–14. Perseus Press, 1993.

[Mus97]   Oleg R. Musin. Properties of the delaunay triangulation. In *Proceedings of the thirteenth annual symposium on Computational Geometry*, pages 424–426. ACM Press, New York, NY, USA, 1997.

[ND99]   M. Noronha and N.A. Dumont. A numerical procedure for the evaluation of singular and quasi–singular integrals that occur in the three–dimensional boundary element analysis. In Brazilian Society of Mechanical Sciences, editor, *6th Pan American Conference on Applied Mechanics, Rio de Janeiro*, 1999.

[Net99]   Roland Netz. *Field–theoretic Approaches to Classical Charged Systems*. Habilitation Thesis Universität Potsdam, 1999.

[NO00]   R.R. Netz and H. Orland. Beyond Poisson–Boltzmann: Fluctuation effects and correlation functions. *Euro. Phys. J. E*, 1:203–214, 2000.

[Pau60]   Linus Pauling. *The nature of the Chemical Bond and the Structure of Molecules and Crystals; An Introduction to Modern Structural Chemistry.* Cornell University Press, Ithaca, NY, USA, 1960.

[PCC⁺95]   D.A. Pearlman, D.A. Case, J.W. Caldwell, W.S. Ross, T.E. Cheatham, S.E. DeBolt, D.M. Ferguson, G.L. Seibel, and P.A. Kollman. AMBER, a package of computer programs for applying molecular mechanics, normal mode analysis, molecular dynamics and free energy calculations to simulate the structural and energetic properties of molecules. *Comp. Phys. Let.*, 1995.

[Pea]   S Popinet et al. Gts – GNU Triangulated Surface Library. `http://gts.sourceforge.net/`.

[PFvG01]   J. W. Pitera, M. Falta, and W. F. van Gunsteren. Dielectric properties of proteins from simulation: The effects of solvent, ligands, pH, and temperature. *Biophysical Journal*, 80(6):2546–2555, 2001.

[PPL96]   J.-T. Pan, W.-J. Peng, and T.-H. Lin. A novel charge distribution method for the numerical solution of the Poisson–Boltzmann equation. *J. Chinese Chem. Soc.*, 43:7–16, 1996.

[Rad48]   J. Radon. Zur mechanischen Kubatur. *Monatshefte für Mathematik*, 52(4):286–300, 1948.

[Ras90]   A. A. Rashin. Hydration phenomena, classical electrostatics, and the boundary element method. *J. Phys. Chem.*, 94(5):1725–1733, 1990.

[Ras93]   Alexander A. Rashin. Aspects of protein energetics and dynamics. *Prog. Biophys. Mol. Biol.*, 60(2):73–200, 1993.

[Rei80]   L. E. Reichel. *A modern course in statistical physics*. Edward Arnold Ltd., Texas, 1980.

[RH85]   A. A. Rashin and B. Honig. Reevaluation of the Born model of ion hydration. *J. Phys. Chem.*, 89(26):5588, 1985.

[RHB02]   K.F. Riley, M.P. Hobson, and S.J. Bence. *Mathematical Methods for Physics and Engineering*. Cambridge University Press, second edition, 2002.

[Ric77]   F.M. Richards. Areas, volumes, packing and protein structure. *Annu. Rev. Biophys. Bioeng.*, 6:151–176, 1977.

[Ric01]   S.W. Rick. Simulation of ice and liquid water over a range of temperatures using the fluctuating charge model. *J. Chem. Phys.*, pages 2276–2283, 2001.

[Riz67]   F.J. Rizzo. An integral equation approach to boundary value problems of classical elastostatics. *Q. Appl. Maths*, 25:83–95, 1967.

[Rja90]   S. Rjasanow. *Vorkonditionierte iterative Auflösung von Randelementgleichungen für die Dirchlet–Aufgabe*. Wissenschaftliche Schriftenreihe der TU Chemnitz, 1990.

[RN61]   S.A. Rice and M. Nagasawa. *Polyelectrolyte Solution*. Academic Press, New York, 1961.

[RWRG92]   U. Ritschel, L. Wilets, J.J. Rehr, and M. Grabiak. Non–local dielectric functions in classical electrostatics and QCD models. *J. Phys. G: Nucl. Part. Phys.*, 18:1889–1900, 1992.

[San91]   G. Sansone. *Orthogonal Functions: Integral properties of spherical harmonics and the addition theorem for Legendre polynomials.*, chapter 3.19, pages 253–272. Dover, New York, 1991.

[Sau00]   S.A. Sauter. Variable order panel clustering. *Computing*, 64(223–261), 2000.

[SB96]   Steven J. Stuart and B.J. Berne. Effects of polarizability on the hydration of the chloride ion. *J. Phys. Chem.*, 100:11934–11943, 1996.

[SBB+93]   M.W. Schmidt, K.K. Baldridge, J.A. Boatz, S.T. Elbert, M.S. Gordon, J.J. Jensen, S. Koseki, N. Matsunaga, K.A. Nguyen, S. Su, T.L. Windus, M. Dupuis, and J.A. Montgomery. GAMESS. *J. Comput. Chem.*, 14:1347–1363, 1993.

[Sch51]   Laurent Schwartz. *Théorie des distributions I/II*. Hermann, Paris, 1950/51.

[SGG]   J. Schöberl, H. Gerstmayr, and R. Gaisbauer. Netgen – automatic mesh generator. `http://www.hpfem.jku.at/netgen/`.

[Sha76]   R.D. Shannon. Revised effective ionic radii and systematic studies of interatomic distances in halides and chalcogenides. *Acta Cryst.*, 32:751–767, 1976.

[Sib78]   R. Sibson. Locally equiangular triangulations. *Comput. J.*, 21(3):243–245, 1978.

[Sim01]   T. Simonson. Macromolecular electrostatics: continuum models and their growing pains. *Curr. Op. Struct. Biol.*, 11:243–252, 2001.

[SMNM92]   S. Sirtori, G. Maier, G. Novati, and S. Miccoli. A Galerkin symmetric boundary–element method in elasticity: formulation and implementation. *International Journal for Numerical Methods in Engineering*, 35:255–282, 1992.

Bibliography

[Sob36]   S.L. Sobolev. Méthode nouvelle à résoudre le problème de Cauchy pour les équations hyperboliques normales. *Mat. Sb.*, 1(43):39–72, 1936.

[Som85]   C. Somigliana. Sopra l'equilibio di un corpo elastico isotropo. *Il nuovo cimento*, 3:17–20, 1885.

[SP69]   R.D. Shannon and C.T. Prewitt. Effective ionic radii in oxides and fluorides. *Acta Cryst. B*, 25(925–946), 1969.

[SP92]   T. Simonson and D. Perahia. Internal and interfacial dielectric properties of cytochrome c from molecular dynamics in aqueous solution. *Proc. Natl. Acad. Sci. U.S.A.*, 4:1082–1086, 1992.

[SP99]   T. Sulea and E.O. Purisima. Desolvation free energy field derived from boundary element continuum dielectric calculations. *Quant. Struct.–Act. Relat.*, 18:154–158, 1999.

[SPSP03]   M. Shirts, J.W. Pitera, W.C. Swope, and V.S. Pande. Extremely precise free energy calculations of amino acid side chain analogs: Comparison of common molecular mechanics force fields for proteins. *J. Chem. Phys.*, 119(11):5740–5761, 2003.

[SSH94]   Doree Sitkoff, Kim A. Sharp, and Barry Honig. Accurate calculation of hydration free energies using macroscopic solvent models. *J. Phys. Chem.*, 98:1978–1988, 1994.

[Ste02]   Olaf Steinbach. *Stability estimates for hybrid coupled domain decomposition methods*. Springer–Verlag, Berlin Heidelberg, 2002.

[Ste03]   Olaf Steinbach. *Numerische Näherungsverfahren für elliptische Randwertprobleme – Finite Elemente und Randelemente (in German)*. Advances in Numerical Mathematics. Teubner Verlag/GWV Fachverlage GmbH, Wiesbaden, 2003.

[Str69]   V. Strassen. Gaussian elimination is not optimal. *Numerische Mathematik*, 14:354–356, 1969.

[Str03]   S. Strobel. Robust and fast computation of molecular surfaces. Master's thesis, Fachbereich Informatik, Universität des Saarlandes, 2003.

[Sut99]   Godehard Sutmann. *Die nichtlokale dielektrische Funktion von Wasser*. PhD thesis, Forschungszentrum Jülich, Institut für Werkstoffe und Verfahren der Energietechnik, 1999.

[Sym63]   G.T. Symm. Integral equation methods in potential theory II. *Proc. Royal Soc. London*, A275:33–46, 1963.

[SYYT01]   T. Sakaue, K. Yoshikawa, S.H. Yoshimura, and K. Takeyasu. Histone core slips along DNA and prefers positioning at the chain end. *Phys. Rev. Lett.*, 87:078105, 2001.

[TA01]   Maxim Totrov and Ruben Abagyan. Rapid boundary element solvation electrostatics calculations in folding simulations: Successful folding of a 23–residue peptide. *Biopolymers*, 60:124–133, 2001.

[Tay96a]   M.E. Taylor. *Partial Differential Equations, Vol. 1: Basic Theory*. Springer–Verlag, New York, 1996.

[Tay96b]   M.E. Taylor. *Partial Differential Equations, Vol. 2: Qualitative Studies of Linear Equations*. Springer–Verlag, New York, 1996.

[Tay96c]   M.E. Taylor. *Partial Differential Equations, Vol. 3: Nonlinear Equations*. Springer–Verlag, New York, 1996.

[TCdS01]   O. Teschke, G. Ceotto, and E.F. de Souza. Interfacial water dielectric–permittivity–profile measurements using atomic force microscopy. *Phys. Rev. E*, 64:011605, 2001.

[Tel87]   J.C.F. Telles. A self–adaptive coordinate transformation for efficient numerical evaluation of general boundary element integrals. *International Journal for Numerical Methods in Engineering*, 24:959–973, 1987.

[THH93]   A.D. Trokhymchuk, M.F. Holovko, and K. Heinzinger. Static dielectric properties of a flexible water model. *J. Chem. Phys.*, 99(4):2964–2971, 1993.

[TJE87]   O. Teleman, B. Jönsson, and S. Engström. A molecular dynamics simulation of a water model with intramolecular degrees of freedom. *Mol. Phys.*, 60:193–203, 1987.

[Uhl37]   H.H. Uhlig. The solubilities of gases and surface tension. *J. Phys. Chem.*, 41(9):1215–1226, 1937.

[vGB87]   W. F. van Gunsteren and H. J. C. Berendsen. *Groningen Molecular Simulation (GROMOS) Library Manual*. Biomos, B.V., Nijenborgh 16, Groningen, The Netherlands, 1987.

[VGS92]   Y.N. Vorobjev, J.A. Grant, and H.A. Scheraga. A combined iterative and boundary-element approach for solution of the nonlinear Poisson-Boltzmann equation. *J. Amer. Chem. Soc.*, 114(9):3189–3196, 1992.

[Vla03]   V.S. Vladimirov. *Methods of the Theory of Generalized Functions (Analytical Methods and Special Functions)*. CRC Press, 2003.

[VS96]   Yury N. Vorobjev and Harold A. Scheraga. A fast adaptive multigrid boundary element method for macromolecular electrostatic computations in a solvent. *J. Comp. Chem.*, 18(4):569–583, 1996.

[WACS81]   R. Wolfenden, L. Andersson, P.M. Cullis, and C.C.B. Southgate. Affinities of amino acid side chains for solvent water. *Biochemistry*, 20(4):849–855, 1981.

[WD97]   R. Clint Whaley and Jack Dongarra. Automatically Tuned Linear Algebra Software. Technical Report UT-CS-97-366, University of Tennessee, December 1997. `http://www.netlib.org/lapack/lawns/lawn131.ps`.

[WD98]   R. Clint Whaley and Jack Dongarra. Automatically tuned linear algebra software. In *SuperComputing 1998: High Performance Networking and Computing*, 1998. `http://www.cs.utk.edu/~rwhaley/papers/atlas_sc98.ps`.

[WD99]   R. Clint Whaley and Jack Dongarra. Automatically Tuned Linear Algebra Software. In *Ninth SIAM Conference on Parallel Processing for Scientific Computing*, 1999. CD-ROM Proceedings.

[Wea]   R. Clint Whaley et al. Atlas. `http://math-atlas.sourceforge.net/`.

[WFF90]   J. Weber, P. Flueckiger, and M.J. Field. Computer–animated chemical models. In *Computer Animation '90 (Second workshop on Computer Animation)*. Springer–Verlag, 1990.

Bibliography

[Whi60] E. Whittaker. *A History of the Theories of Aether and Electricity*, volume 1. Harper, 1960.

[WJD91] A.-P. Wang, Y.-J. Jin, and Q.-H. Du. A numerical method for Cauchy principal value of singular integral under parametric transformation in BEM. *Acta Mechanica Solida Sinica (English Edition)*, 4:39–47, 1991.

[WM90] J. Weber and P.Y. Morgantini. *Scientific visualization and graphics simulation: "Visualization techniques in chemistry"*, pages 203–215. Wiley, New York, 1990.

[WMFR89] J. Weber, Y.P. Morgantini, P. Flueckiger, and M. Roch. Molecular graphics modeling of organometallic reactivity. *Computers & Graphics*, 13:229–235, 1989.

[WPD01] R. Clint Whaley, Antoine Petitet, and Jack J. Dongarra. Automated empirical optimization of software and the ATLAS project. *Parallel Computing*, 27(1–2):3–35, 2001. Also available as University of Tennessee LAPACK Working Note #147, UT-CS-00-448, 2000 (`www.netlib.org/lapack/lawns/lawn147.ps`).

[YMvH89] T.D. Yager, C.T. McMurray, and K.E. van Holde. Salt–induced release of DNA from nucleosome core particles. *Biochemistry*, 28:2271–2281, 1989.

[Zau95] R. J. Zauhar. Smart: a solvent–accessible triangulated surface generator for molecular graphics and boundary element applications. *J. Comput. Aided Mol. Des.*, 9:149–159, 1995.

[Zei95] E. Zeidler. *Applied Functional Analysis: Applications to Mathematical Physics*. Springer Verlag, New York, 1995.

[ZM88] R. J. Zauhar and R.S. Morgan. The rigorous computation of the molecular electric potential. *J. Comput. Chem.*, 9:171–187, 1988.

[ZM90] R.J. Zauhar and R.S. Morgan. Computing the electric potential of biomolecules: Application of a new method of molecular surface triangulation. *J. Comp. Chem.*, 11:603–622, 1990.

[ZYY95] X. Zhexin, S. Yunyu, and X. Yingwu. A simple method for molecular surface triangulation. *J. Comp. Chem.*, 16:512–516, 1995.

Index